Cell biology and biochemical studies of ovine batten disease

A thesis

submitted in partial fulfilment

of the requirements for the Degree of

Doctor of Philosophy in Biochemistry

at

Lincoln University

by

Janet Boyu Xu

Lincoln University

2018

Declaration

Parts of this thesis have been submitted and accepted for publication and/or presented in advance of submission of the thesis.

Publications

- Hughes SM, Hope KM, **Xu JB**, Mitchell NL, Palmer DN. (2014) Inhibition of storage pathology in prenatal CLN5-deficient sheep neural cultures by lentiviral gene therapy. *Neurobiology of Disease*, 62: 543-550.
- Hughes SM, Palmer DN, Schoderboeck L, Mitchell NL, Mclntyre K, Haskell RE, Anderson RD, Wicky HE, **Xu JB**. (2014) New antibodies predict an interaction between CLN5 and CLN6. 14th International Conference on Neuronal Ceroid Lipofuscinoses (Batten disease). Hotel Sheraton, Cordoba, Argentina, 22 Oct 2014 - 26 Oct 2014, *Medicina, 74* (Supl II, O-49), 23.
- **Xu JB**, Mitchell NL, Palmer DN. Allelic variations in exon 1 of genes causing CLN5 Batten disease are not disease associated. Submitted to *Journal of Animal Science*.

Presentations

- **Xu JB**. (2009) Allelic variation in exon 1 of CLN5 is not disease associated. ComBio Conference in convention centre, 5-12 December 2009, Christchurch, New Zealand. (Poster)

Abstract of a thesis submitted in partial fulfilment of the
requirements for the Degree of Doctor of Philosophy.

Cell biology and biochemical studies of ovine batten disease

by

Janet Boyu Xu

The neuronal ceroid lipofuscinoses (NCLs, Batten disease) are a group of fatal inherited neurodegenerative lysosomal storage diseases of humans, which result in severe cortical atrophy, blindness, seizures, and the accumulation of fluorescent lysosome-derived organelles in neurons and most other cells throughout the body. Two naturally occurring of forms of NCL in sheep, CLN5 and CLN6, are used to study human disorders. A mutation in a soluble lysosomal protein (CLN5) causes NCL in Borderdale sheep and the South Hampshire sheep have a defective intracellular endoplasmic reticulum membrane protein (CLN6). The functions of these proteins are still unclear. Generation of highly specific and sensitive antibodies to these proteins would be very useful for biological and functional studies. Studies described in this thesis used ovine CLN5 and CLN6 NCL models to establish the full length coding sequences of the genes and expression of the encoded proteins. Antibodies against ovine CLN5 and CLN6 were generated and used for characterisation studies of both proteins *in vitro*.

The full length ovine *CLN5* gene sequence was amplified using a two-step PCR and ligation strategy with internal overhanging primers. Ovine *CLN5* exon 1 has an allelic variant, but it was not associated with the CLN5 sheep mutation. Recombinant ovine CLN5 and CLN6 proteins were not expressed in *Escherichia coli* (*E. coli*) prokaryotic systems, perhaps because the gene sequences may be toxic to the host.

Recombinant ovine CLN5 and CLN6 proteins were expressed successfully in eukaryotic mammalian cells using lentiviral vectors. The adenoviral antibodies against ovine CLN5 and

CLN6 specifically recognized ovine CLN5 and CLN6 as shown by immunocytochemistry, Western blotting and mass spectrometry. The rabbit anti-CLN5 antibodies specifically identified the ovine mature CLN5 glycosylated form with a molecular weight of 60 kDa in media and cells and a molecular weight of 35 kDa when deglycosylated by PNGase F. The rabbit anti-CLN6 antibodies specifically detected overexpressed ovine CLN6 at molecular weight of 27 kDa in cells by Western blotting. Mass spectrometry revealed that the CLN5 N-signal sequence is cleaved off when it is mature. The deglycosylation study confirmed that CLN5 is a soluble glycosylated protein, containing high-mannose or complex type glycans at six out of eight predicted N-glycosylation sites.

A lysosomal localisation of ovine CLN5 study was confirmed by rabbit anti-CLN5 antibodies labelling of the cells that also expressed the lysosomal associated membrane protein LAMP1, while ER intracellular localisation of ovine CLN6 was revealed by co-staining with rabbit anti-CLN6 antibodies and an ER marker. The CLN5 antibodies also detected endogenous CLN5 expression throughout the normal sheep and human brains. This study also provides evidence for the hypothesis of interactions between CLN5 and CLN6 in cultured and virally transduced neural cell lines using the anti-CLN5 and anti-CLN6 antibodies. Co-expression of CLN6 and CLN5 up-regulated CLN5 expression in CLN5 affected cells.

In conclusion, the work described in this thesis elucidates the capability of lentiviral system expression of CLN5 and CLN6 proteins, and proved the reliability of the generated adenoviral CLN5 and CLN6 antibodies.

Keywords: Batten disease, neuronal ceroid lipofuscinosis, lysosomal storage disease, animal models, sheep, brain, CLN5, CLN6, proteins, antibodies.

Acknowledgements

To complete a PhD is a bit like a battle. Without the support, assistance, and motivation provided by the following amazing people around me, this study would not have been accomplished.

Firstly, I would like to express my sincere gratitude to my supervisor Professor David Palmer, for providing this exciting research opportunity and always having an open door to guide me through the intricate world of Batten disease, for all of his support and encouragement through the journey of completing this PhD study. His guidance helped me during all the time of research and writing of this thesis. It has not been easy to live and work in a foreign country, and so I certainly had quite a few ups and downs over the past years, but he has been a great mentor and even a warm friend, supporting me in every way, encouraging me when I felt lost, sharing his funny stories. I really appreciated the time and positive effort he has put into helping me, especially in the past couple of years when so many other unexpected events have been going on. I could not imagine having a better supervisor and advisor for my PhD study.

I whole-heartedly thank our Batten Animal Research Network (BARN) colleague, particularly Dr Stephanie Hughes for offering me almost a one-year lab work opportunity in the Neural Development and Disease Lab, at the Department of Biochemistry, University of Otago. She opened up my eyes in the different fields of biochemical science, and introduced an alternative method of recombinant protein expression, which occupied me for more than two years. With her help, my PhD work was lifted to another level and to a very satisfying conclusion. Thanks for warmly accommodating me in her house, when I was working in University of Otago. I had a wonderful time there as she is more like a friend to me, sharing her experience on cooking, playing with her four “children” and shopping… it was nice to be able to share our love for Chinese food! It was a pleasure to spend time there with the great people in her lab.

Thanks to my associated supervisor, Assoc Prof Jim Morton, who helped me with my study and the write-up of this thesis. He always made time to answer my questions and give advice, and I really appreciated it. Thanks to Dr Nadia Mitchell for being the most organised, helpful, efficient and generous researcher a PhD student could ask for. She has been there

since the beginning of my research, warmly introducing me into this Batten lab work. I really appreciate the time that she has spent teaching me techniques, discussing ideas and experiments.

Thanks to the people who helped me at some stage through my studies. Thanks to Dr Martin Kennedy for kindly providing human oral samples, putting me up in his laboratory at Christchurch Hospital and working on the genotyping of human CLN5. Thanks to Dr Imke Tammen (University of Sydney) who kindly provided bovine DNA samples and Prof Jon Hickford (Lincoln University) who kindly provided sheep DNA samples for my genotyping study. I also would like to thank all the lab members in Dr Stephanie Hughes' group. It was a pleasure to spend time with them, sharing experiences in cell culture technique at work and all the delicious desserts from the "Friday Bakery". Thanks to our Head of Department, Assoc Prof Roland Harrison, for his insightful comments and encouragement, and support in the final stage of my studies. And thanks to Assoc Prof Rainer Hofmann for advice on statistical analysis of the interactions of CLN5 and CLN6 proteins.

Many thanks to the following funding organisations: Neurological Foundation of New Zealand; the John W and Carrie McLean Trust for my PhD scholarship; Faculty of Agriculture and Life Sciences, Lincoln University for financial support for this study and my conference travel grants. I would not be here today without all of my family and friends outside of work. My deepest gratitude goes to my parents, Xu and Ji Hong Zhai, and to my little man, Alex, for their continuous love, support and never ending belief in me. Thanks to all my friends, particular Jie and Mike, for always standing beside me, sharing the wonderful moments and hugely supporting me. You are my best friends.

Table of Contents

List of Tables

List of Figures

List of Abbreviations

Only abbreviations that appear more than once and in more than one chapter are displayed.

AAV	adeno-associated virus
Ab	antibody
ANCL	adult NCL
APS	ammonium persulphate
BARN	Batten Animal Research Network
BBB	blood brain barrier
bp	base pair
BSA	bovine serum albumin
cDNA	complementary DNA
CDS	coding DNA sequence
CLN/CLN	NCL causing gene/protein
CMV	cytomegalovirus promoter
CNS	central nervous system
CSF	cerebrospinal fluid
CTSD	cathepsin D
DAB	3, 3'-diaminobenzadine
ddH_2O	sterilized water
DDM	n-dodecyl-β-D-maltoside
DMEM	Dulbecco's Modified Eagle Medium
DMEM/12	Dulbecco's Modified Eagle Medium: Nutrient mixture F12
DMSO	dimethylsulphoxide
DNA	deoxyribonucleic acid
dNTP	deoxynucleotide triphosphate
DPX	p-xylene-bis(pyridinium bromide)
DTT	dithiothreitol
ECL	enhanced chemiluminescence

EDTA	ethylenediaminetetraacetic acid
Endo H	endoglycosidase H
EPA	Environmental Protection Agency (NZ)
ER	endoplasmic reticulum
ERMA	Environmental Risk Management Authority
ERT	enzyme replacement therapy
FBS	fetal bovine serum
gDNA	genomic deoxyribonucleic acid
GFAP	glial fibrillary acidic protein
GFP	green fluorescent protein
HEK293	human embryonic kidney 293 cells
HIV-1	human immunodeficiency virus 1
HRP	horseradish peroxidase
ICC	immunocytochemistry
INCL	infantile NCL
JNCL	juvenile NCL
kDa	kiloDalton(s)
kb	kilobase
LAMP 1	lysosome-associated membrane protein-1
LB	Luria-Bertani
LINCL	late infantile NCL
LSD(s)	lysosomal storage disease(s)
LV	lentiviral
L2000	Lipofectamine 2000
MND (U3)	myeloid sarcoma virus (U3 element)
mRNA	messenger ribonucleic acid
NCBI	National Centre for Biotechnology Information
NCL	neuronal ceroid lipofuscinosis
NGS	normal goat serum

OD	optical density
OptiMEM	reduced serum medium
PAGE	polyacrylamide gel electrophoresis
PBS	phosphate buffered saline solution, pH 7.4
PBST	phosphate buffered saline, pH 7.4, containing 0.3% Triton X-100
PCR	polymerase chain reaction
PFA	paraformaldehyde
PMSF	phenylmethylsuphonyl fluoride
PNGase F	peptide-N-glycosidase F
PPT1	palmitoyl protein thioesterase 1
RNA	ribonucleic acid
SDS	sodium dodecyl sulphate
SNP	single nucleotide polymorphism
SSCP	single strand conformational polymorphism
sub c	subunit c of the mitochondrial ATP synthase
TBS	Tris buffered saline solution
TBST	Tris buffered saline solution with Tween 20
TE	Tris-EDTA
TEMED	N,N,N',N'-tetramethylethylenediamine
TPP1	tripeptidyl peptidase I
WT	wild type

Chapter 1
Literature Review

1.1 Overview of the neuronal ceroid lipofuscinoses

The neuronal ceroid lipofuscinoses (NCLs, Batten disease) are a group of fatal neurodegenerative lysosomal storage diseases (LSD) of humans and other animals. Most are autosomal recessively inherited diseases. All forms share two definitive hallmarks; severe brain atrophy (progressive loss of neurons) and the accumulation of fluorescent lysosome-derived organelles (storage bodies) in neurons and most other cells throughout the body (Palmer et al., 2015). Retinal degeneration is also a common feature. Affected children start life normally but then develop personality and behavioural changes, progressive visual failure, and mental and motor deterioration. They suffer nightmares, fits and seizures, and die between 7 years old and adulthood (Goebel et al., 1999; Mole et al., 2005; Mole et al., 2011). The traditional estimate of incidence of 1 in 12,500 live births (Rider and Rider, 1988) was once thought to be pessimistic, but now seems realistic as a higher frequency becomes apparent with improved diagnosis. The causes and development of these devastating neuropathies are still poorly understood, and current treatment options mostly are limited to alleviating the symptoms.

1.2 History of human NCLs

The first clinical description of the NCLs was made by Dr. Otto Christian Stengel in 1826 (Stengel, 1982). His article in the Norwegian Medical Journal reported a singular illness in four siblings, who were healthy until the age of six. Starting with sight decline, the disease course led to blindness, gradual loss of intellect and speech, followed by epileptic fits and death in the twenties. After almost a century of being undocumented, the disease was reported again by Batten in 1903 and by Vogt in 1905 (Hoffman, 1956). A number of reports of further childhood forms with progressive vision loss and mental retardation followed (Haltia, 2006). Despite the variation in the molecular genetics and clinical features, all the forms share unifying pathomorphological features, and for a long time were grouped as “amaurotic family idiocy” along with Tay-Sachs disease, before being recognised as a separate disease.

The field remained unclear until Zeman and Dyken introduced the new term neuronal ceroid-lipofuscinosis (NCL) in 1969, according to the histochemical and electron microscopic features of the storage material (Zeman and Dyken, 1969). The NCLs were then divided into four subtypes based on the ages of onset, the clinical features and the ultrastructure of the storage material (Haltia, 2003). These four types are infantile NCL (INCL), late-infantile NCL (LINCL), juvenile NCL (JNCL) and adult NCL (ANCL). In the late 1980s and 1990s, two major hydrophobic proteins were found to be specially stored in the NCL storage cytosomes: either subunit c of mitochondrial ATP synthase (Palmer et al., 1989; Palmer et al., 2015) or the sphingolipid activator proteins, SAPs A and D (Tyynelä et al., 1993). Since the first gene responsible for the INCL form was identified in 1995 (Vesa et al., 1995), a number of different genes have been discovered which underlined the different human NCLs. Currently, mutations in a total of 13 different genes are known to cause human NCLs and each gene is responsible for a form designated as *CLNs 1-8 and 10-14* (NCL mutation database; http://www.ucl.ac.uk/ncl/mutation.shtml, 2017). There may be more yet to be discovered.

1.3 Lysosomes and lysosomal storage diseases

Lysosomes are acidic membrane bound organelles found in many eukaryotic cells (Vellodi, 2005), and they contain different soluble digestive enzymes (Futerman and van Meer, 2004; Sleat et al., 2013). Over 60 lysosomal proteins were identified in earlier studies (Sleat et al., 1996, 2005, 2007, 2008a), and more than 165 murine proteins may be lysosomal proteins (Sleat et al., 2013). Lysosomes break down macromolecules in the cells (i.e. proteins, carbohydrates, nucleic acids and lipids) to subunits such as sugars and amino acids that the cell can either utilize or excrete (Luzio et al., 2007). They act as a waste disposal system for the cell by digesting unwanted materials from the cytoplasm, and from outside the cells. Therefore the lysosome is a key organelle in the regulation of cellular homeostasis. All the lysosomal enzymes are optimally active at an acidic pH of 4.5-6 (Marshansky and Futai, 2008). Abnormal lysosomal functions consequent to loss of acidity or mutations in the lysosomal enzyme related genes can result in failures to fully catabolize or process macromolecules, which then accumulate in lysosomes; hence the description lysosomal storage diseases (LSDs) (Futerman and van Meer, 2004).

The LSDs are a group of 50 inherited diseases (Futerman and van Meer, 2004; Platt et al., 2012; Bailey, 2017) with a combined incidence estimated at around 1:5,000 live births (Fuller et al, 2006). The NCLs are LSDs, as they are recessively inherited and characterized by the

abnormal accumulation of material in lysosomes. NCLs are divided into two groups based on the composition of the storage bodies (Table 1.1): those storing sphingolipid activator proteins (saposins or SAPs A and D), including CLN1, CLN4 and CLN10; while storage of subunit c of mitochondrial ATP synthase is found in CLNs 2-3 and 5-8 (Palmer et al., 1992, 2015; Haltia, 2006), where gene mutations result in specific subunit c accumulation. The reasons for these specific protein storage disorders remain unclear.

1.4 Molecular genetic classification of NCLs

The NCLs were historically classified into four types, INCL, LINCL, JNCL and ANCL, based on the ages of onset of clinical symptoms. Since then, extensive human molecular genetics and biochemical studies have increased our knowledge of the different genetic variants (Mole et al., 2004). Mutations in different NCL genes can cause a similar clinical phenotype, such as the LINCL-like forms, caused by deficiencies in CLN5, CLN6, CLN7 or CLN8 (Warrier et al., 2013). Mutations in the same gene can also cause different disease courses (Kousi et al., 2012; Warrier et al., 2013). In light of this, recent information on the NCL related genes and mutations, a new classification of the human NCLs has been developed that includes 13 genes whose deficiencies result from a current total of 446 mutations (http://www.ucl.ac.uk/ncl/mutation.shtml, 2017). These classifications are based on the defective genes as well as the age of onset (Table 1.1). More mutations may be discovered. However, the more recently discovered variants (CLN11-14) do not always meet all the classification criteria (Palmer et al., 2013).

Cases of this disorder are also classified into two groups based on the types of gene products (Table 1.1); soluble lysosomal proteins (CLN1, CLN2, CLN5, CLN10, and CLN13) or putative membrane bound proteins (CLN3, CLN6, CLN7, CLN8, CLN12 and CLN14).

Table 1.1 Genetic classification of the human NCLs

(From Kousi et al., 2012; Cotman et al., 2013; Kollmann et al., 2013; Warrier et al., 2013)

Gene/ NCL form	Locus	Major subtype	NCL Gene product	Protein type/ cellular localisation	Storage proteins
CLN1	1p32	Classic infantile	PPT1	Soluble/lysosomal matrix	SAP A and D
CLN2	11p15	Classic late Infantile	TPP1	Soluble/lysosomal matrix	Subunit c
CLN3	16p12	Classic juvenile	CLN3	Membrane bound/lysosomal membrane	Subunit c
CLN4/ DNAJC5	20q13.33	Adult (Parry disease)	CSP	Membrane bound/synaptic vesicles	SAP A and D
CLN5	13q21-32	Variant late infantile	CLN5	Soluble/lysosomal matrix	Subunit c
CLN6	15q23	Variant late infantile	CLN6	Membrane bound/ER membrane	Subunit c
CLN7	4q28.1-28.2	Variant late infantile	MFSD8	Membrane bound/lysosomal membrane	Subunit c
CLN8	8p23	Late infantile, Northern epilepsy	CLN8	Membrane bound/ER-Golgi membrane	Subunit c
CLN10 (CTSD)	11p15.5	Congenital	Cathepsin D	Soluble/lysosomal matrix	SAP A and D
CLN11/ GRN	17q21	Adult	Progranulin	Extracellular	
CLN12/ ATP13A2	1p36	Juvenile	P-type ATPase	Membrane bound/lysosomal membrane	
CLN13/ CTSF	11q13	Adult Kufs type B	Cathepain F	Soluble/lysosomal matrix	
CLN14	7q11.21	Infantile	KCTD7	Membrane bound/cytosolic membrane associated	

Abbreviations: **CLN1** etc, ceroid lipofuscinosis, neuronal 1 etc; **CSP**, cysteine string protein; **DNAJC5**, DnaJ (Hsp40) homolog, subfamily C, member 5; **ER**, endoplasmic reticulum; **KCTD7**, potassium channel tetramerization domain-containing protein 7; **MFSD8**, major facilitator superfamily domain containing 8; **PPT1**, palmitoyl protein thioesterase I; **SAP**, sphingolipid activator protein; **SCAR7**, autosomal recessive spinocerebellar ataxia type 7; **TPP1**, tripeptidyl peptidase I.

CLN1

The gene *CLN1* was first localised to human chromosome 1p32 (Järvelä et al., 1991), and found to encode a functional enzyme, palmitoyl protein thioesterase 1 (PPT1) (Vesa et al., 1995). PPT1 is a small glycoprotein postulated to be involved in the catabolism of lipid-modified proteins during lysosomal degradation (Vesa et al., 1995). The crystal structure of PPT1 indicates that the CLN1 mutations affect catalysis, substrate binding or cause improper folding of the core, resulting in enzyme dysfunction (Bellizzi et al., 2000). Studies have suggested that the CLN1 protein is localised in synaptosomes and synaptic vesicles in neuronal cells, while it also acts as a soluble lysosomal protein targeted to lysosomes (Hellsten et al., 1996).

A major founder effect has caused a high incidence of a particular mutation of the *CLN1* gene in Finland, the cause of classical infantile NCL (INCL) (Vesa et al., 1995; Bellizzi et al., 2000). Development of affected children is normal until 3-18 months of age, and they die between 6 and 15 years of age (Siintola et al., 2006). In addition, other mutations in the *CLN1* gene are associated with LINCL, JNCL and ANCL variants (Das et al., 1998; Diggelen et al., 2001). A total of 67 disease-causing mutations have been described in the *CLN1* gene (NCL Mutation Database, http://www.ucl.ac.uk/ncl/CLN1mutationtable.htm, 2017).

CLN2

CLN2, localised to chromosome 11p15 by homozygosity mapping, encodes the lysosomal enzyme tripeptidyl peptidase (TPP1) (Sleat et al., 1997). Mutations in it lead to a severe deficiency in TPP1 (Sleat et al., 1997; 2008b). Loss of TPP1 activity is associated with the specific accumulation of subunit c of ATP synthase (Palmer et al., 1992). Affected children show clinical symptoms from the age of 2-4 years. They suffer seizures, ataxia, developmental and mental retardation, visual impairment and speech loss before death in mid-childhood. Most of the published 116 mutations (http://www.ucl.ac.uk/ncl/CLN2mutationtable.htm, 2017) lead to the classical LINCL phenotype but a few cases with a juvenile NCL phenotype have been also reported (Sleat et al., 1997; Bessa et al., 2008).

CLN3

Mutations in *CLN3* cause juvenile CLN3 disease, the most common subtype of NCL. First described were two separate mutations and a point mutation in the *CLN3* gene (Lerner et al., 1995). *CLN3,* mapped to chromosome 16p12 (Mitchison et al., 1994), encodes a putative lysosomal transmembrane protein with 6 transmembrane domains, both the N- and C-termini being in the cytosolic (Mao et al., 2003). Affected patients show progressive visual failure from the age of 5-10 years, followed by seizures and complete motor deterioration, with death occurring in the third decade or earlier (Munroe et al., 1997). Over 67 disease associated mutations have been reported, and most of the cases share prematurely truncated protein products (http://www.ucl.ac.uk/ncl/CLN3mutationtable.htm, 2017).

CLN4

CLN4 is autosomal-dominant adult onset NCL, first described in the 1970s, that is named Parry disease (Boehme et al., 1971). Following genetic analyses of affected ANCL families,

researchers identified a unique heterozygous mutation in *DNAJC5* encoding cysteine-string protein alpha (CSPα), and found a reduced amount of CSPα in neuronal cells of affected cases (Noskova et al., 2011). Another subtype, the autosomal recessive of ANCL, referred to as Kufs disease, affects individuals aged between 25 and 46 years, starting with progressive epilepsy, behaviour changes, and movement disorders (Noskova et al., 2011). The main clinical symptom is dementia, and patients die about 10 years after onset (Siintola et al, 2006; Noskova et al., 2011). The CLN4/*DNAJC5* gene was localised in 20q13.33, and two mutations in exon 3 have been reported from ANCL affected cases so far (Noskova et al., 2011).
2008).

CLN5

See section 1.6.

CLN6

See section 1.7.

CLN7

A variant form of LINCL originally detected in Turkish patients was referred as CLN7 (Wheeler et al., 1999). Patients show clinical features from the age of 2 to 7 years, with rapid visual loss, mental and motor regression, seizures, and all die prematurely (Kousi et al, 2012). The CLN7 protein is encoded by *MFSD8* (major facilitator superfamily domain 8-containing gene), localised on chromosome 4q28.1-q28.2 (Siintola et al., 2007). CLN7 patients have been diagnosed in many populations since then, including Pacific Islanders (Kousi et al., 2012) and a total of 38 mutations have been reported so far (http://www.ucl.ac.uk/ncl/CLN7mutationtable.htm, 2017).

CLN8

CLN8 which maps to chromosome 8p23 is the causative gene for Northern epilepsy, also called progressive epilepsy with mental retardation (EPMR) (Ranta et al., 1999). It encodes a putative membrane protein predicted to have five transmembrane domains, and to reside in the ER and ER-Golgi intermediate compartments in non-neuronal cells, while localized outside the ER in neurons (Lonka et al., 2000). The function of the CLN8 protein remains unclear. A total of 31 mutations identified in *CLN8* (http://www.ucl.ac.uk/ncl/CLN8mutationtable.htm, 2017) cause two distinct diseases, EPMR

and late infantile variant NCL (Kousi et al., 2012). The CLN8 vLNCL form has an earlier onset (from 2-7 years) and more a rapid disease course than the EPMR form (from 5-10 years).

CLN10 (CTSD)

A mutation in the well-known cathepsin D gene (*CTSD*) was found to cause a naturally occurring ovine congenital NCL disease (Tyynelä et al., 2000) and a similar disease was later reported in humans (Siintola et al., 2006). The *CTSD* gene is localised to chromosome 11p15.5, and mutations that entirely abolish CTSD activity result in the most severe NCL, congenital NCL, CLN10 (Tyynelä et al., 2000; Siintola et al., 2006b). CTSD is an aspartyl protease, a soluble lysosomal protein. A total of 10 mutations have been reported in patients (Siintola et al., 2006b; Hersheson et al., 2014; Doccini et al., 2016; http://www.ucl.ac.uk/ncl/CLN10CTSDmutationtable.htm, 2017). The onset in new born babies includes respiratory insufficiency and seizures that may have begun before birth. Death occurs within hours to weeks of birth. Patients have smaller brains and a firmer gyral pattern than normal following a developmental delay occurring between the 30th and 32nd week of gestation (Kousi et al., 2012). Patients with later onset forms (early school age or even later) present with ataxia, blindness, loss of speech, and motor dysfunction (Kousi et al., 2012).

CLN 11-14

The recently identified CLNs 11-14 do not meet all the clinical or neuropathological criteria for NCL classification and mutations in some of the genes implicated are associated with other diseases. Thus, there is less certainty about their inclusion into the NCL family (Palmer et al., 2013).

CLN11: CLN11 disease, caused by a mutation in the progranulin gene (*GRN*), was reported to cause an adult onset NCL in a single -family (Smith et al., 2012). The affected patients presented with rapidly progressive visual failure and seizures. *GRN* is on chromosome 17q21.32, and encodes progranulin, a secretory glycoprotein of unknown function.

CLN12: Mutations in *ATP13A2* have been found to cause Kufor-Rakeb syndrome, a rare Parkinsonism disorder (Dehay et al., 2012), and also a juvenile onset NCL (CLN12) in a single family with learning difficulties (Bras et al., 2012). *ATP13A2* encodes a lysosomal type 5 P-type ATPase predicted to have 10 transmembrane domains (Dehay et al., 2012).

CLN13: Mutations in the cathepsin F (*CTSF*) gene have been discovered to cause an autosomal recessive dementia with adult onset NCL (CLN13), Kufs Type B (Smith et al., 2013).

CLN14: The *CLN14/KCTD7* gene encodes the potassium channel tetramerization domain – containing protein 7 (Kousi et al., 2012; Farhan et al., 2014), a highly conserved protein that is located in the cytoplasm and expressed in the brain. Mutations in *KCTD7* have been described in INCL as well as in infantile progressive myoclonic epilepsy (Van Bogaert et al., 2007; Kousi et al., 2012).

1.5 Animal models of NCL

The first description of an animal form of NCL was from English setters (Koppang, 1962, 1970). Since then spontaneous forms of NCL were discovered in other breeds of dogs (Jolly et al., 1994; Melville et al., 2005; Palmer et al., 2011), as well as in cats (Bildfell et al., 1995), sheep (Jolly and West, 1976; Jolly et al., 1980; Cook et al., 2002; Jolly et al., 2002), goats (Fisk and Storts, 1988), cattle (Harper et al., 1988; Hafner et al., 2005), horses (Url et al., 2001), pigs (Cesta et al., 2006), ferrets (Nibe et al., 2011) and mice (Bronson et al., 1998; Ranta et al., 1999; Gao et al., 2002; Cooper et al., 2006; Shacka, 2012).

Colonies of animal models in which all affected individuals have the same mutation are particularly valuable tools for determining the pathophysiology of disease and for validating therapeutic strategies. The work described in this thesis is based on the natural occurrence of the two forms of NCL in sheep, CLN5 and CLN6. Sheep have a large human-like brain and human-like physiology, and their longer life expectancy than rodent have allows for investigations of the long-term effects of treatments. Because of their relevance to humans, the findings of studies in sheep have been world leading. There is a rapidly growing demand for large animal model studies. For instance these have recently become mandatory for the US Federal Drug Agency approval of therapeutic drugs. Being domestic production animals, sheep are bred for easy care and are used to human handling, making them ideal for this purpose and remarkably cost effective compared with the alternatives, particularly when managed in a New Zealand pastoral environment. An initiative is underway to ensure that the strategies, skill-sets and facilities developed in these studies become available for other investigations, as this utilisation of pastoral sheep is a growing niche area for research.

1.6 CLN5

1.6.1 Human CLN5

CLN5 NCL first described as a Finnish variant late infantile neuronal ceroid lipofuscinosis, was mapped to chromosome 13q22 (Savukoski et al., 1998). Later studies identified *CLN5* mutations in a variety of populations and also causative of juvenile and adult forms (Cannelli et al., 2007; Xin et al., 2010; Kousi et al., 2012). The gene consists of four exons, spanning over 13 kb of genomic DNA. The human *CLN5* coding sequence contains four possible ATG initiation sites. Initially, the first ATG was suggested as the initiator of translation which would yield a 407 amino acid protein (about 47 kDa) containing two transmembrane domains (Savukoski et al., 1998). In subsequent protein expression experiments, CLN5 was expressed as a 60 kDa glycoprotein that was shifted to 38 KDa after deglycosylation with PNGase F (Isosomppi et al., 2002). It was then concluded that the fourth ATG in humans is the major initiation site. A SignalP V2.0 program (http://www.cbs.dtu.dk/) predicted that the human CLN5 polypeptide undergoes proteolysis of the N-terminal signal peptide, resulting in a theoretical molecular weight of 36.6 kDa protein (Isosomppi et al., 2002).

So far, 36 different *CLN5* mutations are known to occur in humans. The most common mutation among patients with Finnish vLINCL is a 2 bp deletion in exon 4 (c.1175delAT), resulting in a truncated protein (http://www.ucl.ac.uk/ncl/CLN5mutationtable.htm, 2017). As the mutant protein showed defective intracellular lysosomal targeting, Isosomppi et al. (2002) suggested that the pathogenesis of this type of *CLN5* may be associated with defective lysosomal trafficking and prevention of its normal biological function.

The CLN5 protein does not share significant homology with other known proteins and its function is still unclear. *CLN5* encodes a soluble lysosomal glycoprotein with eight putative N-glycosylation sites (Isosomppi et al., 2002; Sleat et al., 2006a). Localisation studies have suggested that various N-glycosylation sites of CLN5 have different effects on folding, trafficking and the lysosomal function of CLN5 (Moharir et al., 2013).

1.6.2 CLN5 animal models

Naturally occurring CLN5 NCLs have been found in cattle (Houweling et al., 2006), sheep (Jolly et al., 2002), Border Collie dogs (Melville et al., 2005) and Golden Retriever dogs (Gilliam et al., 2015), with disease courses matching human CLN5. A CLN5 knock-out mouse

model has been generated by deletion of exon 3 (Kopra et al., 2004). However, these mice are not characterised by the severe brain atrophy seen in humans, sheep and dogs.

Studies on sheep models of NCLs offer significant benefits. The clinical progression in sheep is more similar to that of human NCL patients than that in mice. Domestic sheep are easy to maintain and manage. In New Zealand, Borderdale sheep have been found with a naturally occurring NCL (Jolly et al., 2002). The affected sheep present with blindness from 10 months of age, have a tendency to walk in circles when disturbed, and move toward humans rather than away from them (Jolly et al., 2002). The causes of blindness are atrophy of the occipital cortex and loss of photoreceptors from the retina.

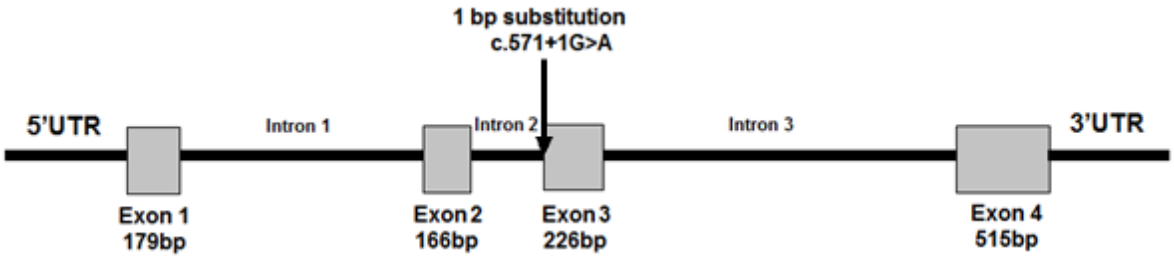

Figure 1.1 A schematic diagram of ovine *CLN5* with the location of the known mutation indicated by the black arrow

The naturally occurring form of CLN5 in Borderdale sheep results from a single substitution at a consensus splice site, causing a deletion of exon 3 and a truncated putative protein (Frugier et al. 2008).

The accumulation of subunit c of mitochondrial ATP synthase was detected in the affected Borderdale sheep and the cause of disease traced to a mutation in *CLN5* (Frugier et al., 2008). A flock of these sheep has been established for research, which is particularly relevant to the human CLN5 late infantile form but also soluble enzyme forms of NCLs in general. The ovine *CLN5* cDNA has been sequenced (NM_001082595), and has a single start codon that aligns best with the third ATG of the human *CLN5* sequence (Frugier et al., 2008). *CLN5* is located on sheep chromosome 10, contains four exons (Figure 1.1), and encodes a predicated 361 amino acid protein. The mutation in Borderdale sheep causes a nucleotide substitution at a consensus splice site in the ovine *CLN5* gene (c.571+1G>A) with subsequent excision of exon 3 (Figure 1.1) yielding a truncated putative protein (Frugier et al., 2008).

1.7 CLN6

1.7.1 Human CLN6

Human *CLN6* is located on chromosome 15q21-q23 (Wheeler et al., 2002), and has a predicted open reading frame of 933 nucleotides in seven exons which span a genomic region of approximately 23 kb (Gao et al, 2002). It encodes a highly conserved non-glycosylated, 311 amino acid protein, with a putative N-terminal cytoplasmic domain, seven predicted transmembrane domains, followed by a C-terminus (Gao et al., 2002; Heine et al, 2004; Mole et al., 2004). It is thought to be localised in the ER (Mole et al., 2004).

Raising antibodies against peptide fragments of the CLN6 sequence has proved to be problematic but it has been reported that antisera raised against CLN6 detected a 27-30 kDa band (Heine et al, 2004; Mole et al., 2004). The *CLN6* sequence has not been assigned to any family of proteins. It is highly conserved across mammalian species, human *CLN6* being 92% identical to the sheep gene (Tammen et al., 2006), and 90.3% to the mouse gene (Gao et al., 2002). The majority of the differences were in exon 1. No function has yet been assigned for the CLN6 protein, and it is still unclear how defects in, or absence of, CLN6 leads to lysosomal dysfunction (Heine et al, 2004; Mole et al., 2004). However, it has been suggested that CLN6 plays a role in endocytosis of lysosomal proteins. A number of mutant CLN6 polypeptides are transported to lysosomes, may be via the endosomal compartment. The endocytic pathway is reduced in cultured CLN6 deficient fibroblasts (Heine et al, 2004). It has also been reported that mutant CLN6 proteins are degraded 3-20 fold faster that wild type ones (Kurze et al., 2010).

The majority of mutations in *CLN6* result in variant late infantile NCLs (vLINCL; MIM# 601780). To date, 71 disease-causing mutations have been identified from 20 countries (http://www.ucl.ac.uk/ncl/CLN6mutationtable.htm, 2017). Ages of onset range from 18 months to 8 years, the majority being between 3 and 5 years (Mole et al., 2005). Symptoms are developmental mental retardation followed by speech impairment, seizures, ataxia, motor delay and visual loss. After deteriorating rapidly, most affected children die between the ages of 5 and 12 years.

CLN6 mutations have also been reported in NCLs with teenage and juvenile onsets (Andrade et al., 2012; Faruq et al., 2013) and Kufs disease Type A (Arsov et al., 2011). The teenage onset patients showed progressive myoclonus epilepsy; whereas the juvenile onset patients

presented with cerebellar ataxia with seizures. The CLN6 Kufs disease Type A patients are quite different from the other CLN6 patients (Arsov et al., 2011). The age of onset is between 30 and 50 years with progressive myoclonus epilepsy and loss of intellect, but not visual loss. It is unclear why different mutations in *CLN6* lead to different disease phenotypes and there are no effective treatments for CLN6 patients.

1.7.2 CLN6 animal models

Naturally occurring NCLs have been diagnosed in animals and localized to *CLN6*, including the *nclf* mouse (Bronson et al., 1998; Gao et al, 2002; Wheeler et al., 2002), the New Zealand South Hampshire (SH) sheep, and the Australian Merino sheep (Jolly and West, 1976; Jolly et al., 1980; Tammen et al., 2001, 2006; Cook et al., 2002). Both affected sheep breeds have also been called OCL sheep, and provide excellent large animal models for studies of CLN6 disease progression and for testing treatments.

CLN6 affected SH sheep develop clinical symptoms between 10 and 14 months of age, notably blindness. The course of the disease is similar to the CLN5 form in Borderdale sheep, but brain atrophy is less severe and the sheep die by the age of 2 years (Jolly et al., 1982, 1989, 2002). *CLN6* affected Merino sheep develop clinical symptoms between 7 and 12 months of age, with similar disease progression to that seen in SH sheep (Tammen et al., 2001; Cook et al., 2002; Palmer et al., 2011). The accumulated storage material, subunit c of mitochondrial ATP synthase was first identified in the SH sheep model (Palmer et al., 1989) and proved to be a major descriptor of this disorder in humans and other animal models (Palmer, 2015).

Linkage studies positioned the genetic lesion in the SH sheep to ovine chromosome 7q13–15, homologous to the human *CLN6* location on chromosome 15q21–23 (Broom et al., 1998). The Merino NCL has also been linked to the same region on chromosome 7 (Tammen et al., 2001). Ovine *CLN6* (NM_001109984) contains seven exons (Figure 1.2). A missense mutation (c.184C>T) causes CLN6 disease in Merino sheep, whereas affected South Hampshire sheep have a large 5'UTR exon 1 deletion (see comments on Figure 1.2) and reduced levels of *CLN6* mRNA (Tammen et al., 2006). A silent polymorphism (c.822G>A) was also found in both New Zealand SH and Australian Merino sheep (Tammen et al., 2006).

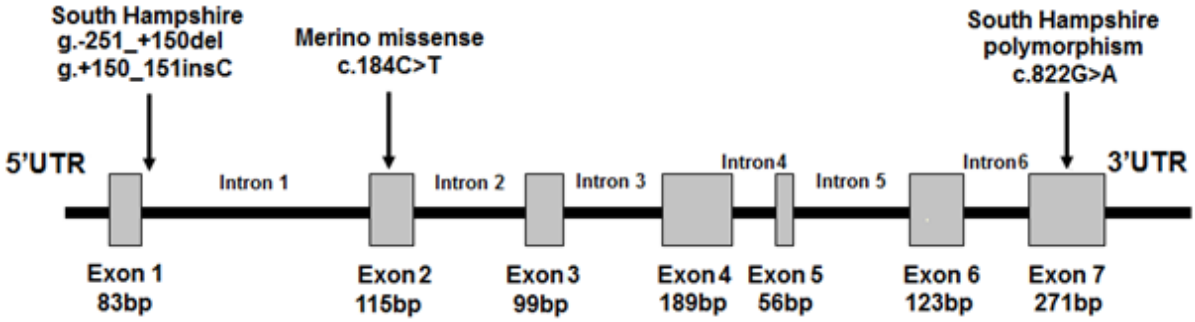

Figure 1.2 A schematic diagram of the ovine *CLN6* with the locations of the known mutations and polymorphism indicated by black arrows

The naturally occurring form of CLN6 in South Hampshire sheep results from a single base insertion and a major 401 base deletion from the 5' UTR of the gene to intron 1 (Mohd Ismail, 2014). A single substitution in exon 2 (c.184C>T) results in ovine CLN6 in Australian Merino sheep (Tammen et al., 2006).

1.8 N-glycosylation and lysosome protein trafficking pathways

Proteins can be post-translationally modified by the addition of oligosaccharides to form glycoproteins, in a process called glycosylation. N-linked glycosylation refers to the attachment of oligosaccharides (known as glycans) to the amide nitrogen on the side chain of asparagine (Asn). Both secreted and membrane-bound proteins in eukaryotes can undergo N-glycosylation. Addition of an N-glycan to a protein has several roles (Imperiali and O'Connor, 1999; Shental-Bechor and Levy 2009; Sinclair and Elliott, 2005). Firstly, adding glycans can enhance the solubility and stability of proteins in the ER-Golgi membranes and on the outside of cell membrane. Secondly, N-glycans can signal trafficking. They can determine when to transport a protein to the Golgi apparatus or to target it for degradation, for instance, in case of major folding defects.

N-linked glycosylation begins in the ER and continues in the Golgi apparatus in eukaryotes (Stanley et al., 2009). Biosynthesis starts with the addition of a large oligosaccharide precursor from dolichol to which it is attached by a diphosphate linkage (Figure 1.3). Dolichol is a lipid molecule, embedded in the phospholipid bilayer of the ER membrane and acts as a carrier for the oligosaccharide. The transferred glycan is a branched oligosaccharide, containing three glucose (Glc), nine mannose (Man), and two *N*-acetylglucosamine (GlcNAc) residues (Figure 1.3, in the red rectangle). Five of its 14 residues are essentially core in the structures of all *N*-linked oligosaccharides, being two GlcNac and three Man residues (Figure 1.3, in the purple rectangle).

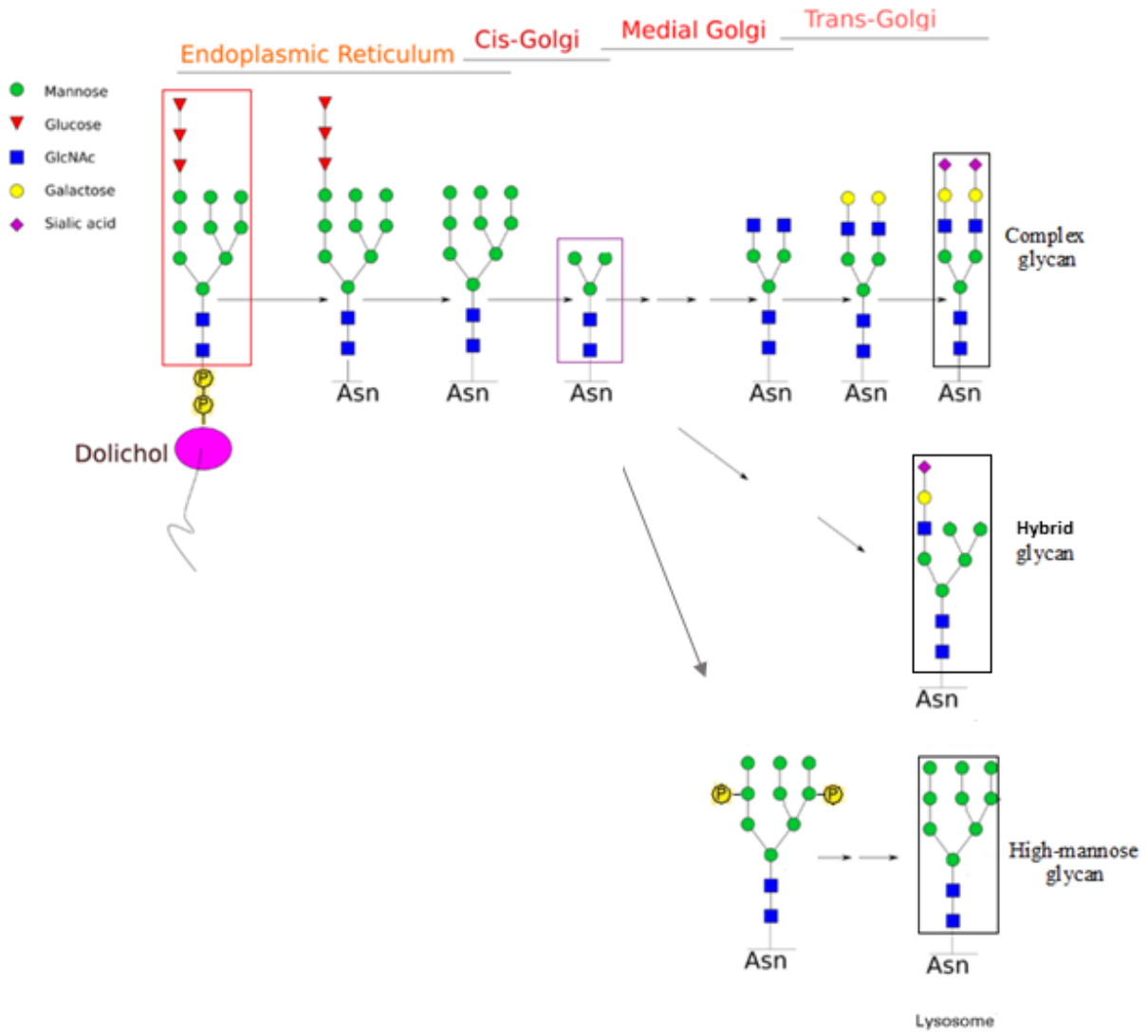

Figure 1.3 Glycan processing in ER and Golgi membranes

Modified from Drickamer and Taylor (2006).

As a nascent polypeptide moves into the lumen of the ER, the entire glycan is transferred from the dolichol carrier to an asparagine residue on the polypeptide (Figure 1.3). The asparagine must be located within the consensus sequence, Asn-X-Ser/Thr where X is any amino acid except proline (Drickamer and Taylor, 2006). Not all Asn-X-Ser/Thr sequences become glycosylated. For instance, the rapid folding of a segment of a protein containing an Asn-X-Ser/Thr sequence may prevent the transfer of a glycan to it.

After attachment the glycan is used as a label molecule in the folding process (Drickamer and Taylor, 2006). The majority of glycoproteins require at least one glycosylated residue in order to achieve proper folding in the ER. Once the protein is folded correctly, three glucose and one mannose residues are removed from the oligosaccharide chains. This initial

trimming process acts as a quality control step to monitor folding. Without proper folding the glucose residues are not removed and the glycoprotein does not leave the ER.

Properly folded glycoproteins are transferred from the ER to the *cis*-Golgi network where the glycans are modified to three mature types: high mannose, complex and hybrid (Drickamer and Taylor, 2006) (Figure 1.3). High mannose glycans have just two GlcNac with many mannose residues, often almost as many as in the precursor oligosaccharides before attachment. Complex type glycans contain almost any number of the other types of saccharides (mainly combinations of mannose, GlcNac, N-acetylgalactosamine, fucose and sialic acid residues). Hybrid type glycans contain mannose residues on one side of the branch, while on the other side a GlcNac initiates a complex branch. The structure of each type is different in different proteins and only some examples of the process are depicted in Figure 1.3.

The high-mannose glycans (Figure 1.3, in the black square) can have one or more mannose residues that are phosphorylated on their 6-carbon atoms, forming mannose-6-phosphate residues (M6P). These phosphorylated glycans bind to M6P receptors in the *trans*-Golgi at a slightly acidic pH (≈ 6.5 – 7) and are trafficked via the M6P-dependent pathway (Figure 1.4). They are then collected via the cytosolic tails of the M6P receptors and transferred by clathrin-coated vesicles to late endosomes (LE), where the M6P receptors disassociate as the pH decreases (5.5) and are then dephosphorylated. Lysosomal membrane proteins (Figure 1.4, labelled with black arrows) are not phosphorylated. Instead their cytosolic tails bind as do the tails of M6P receptors. These glycoproteins are transported to the lysosomes, while the M6P receptors recycle back to the trans-Golgi network. M6P receptors are also found on the plasma membrane.

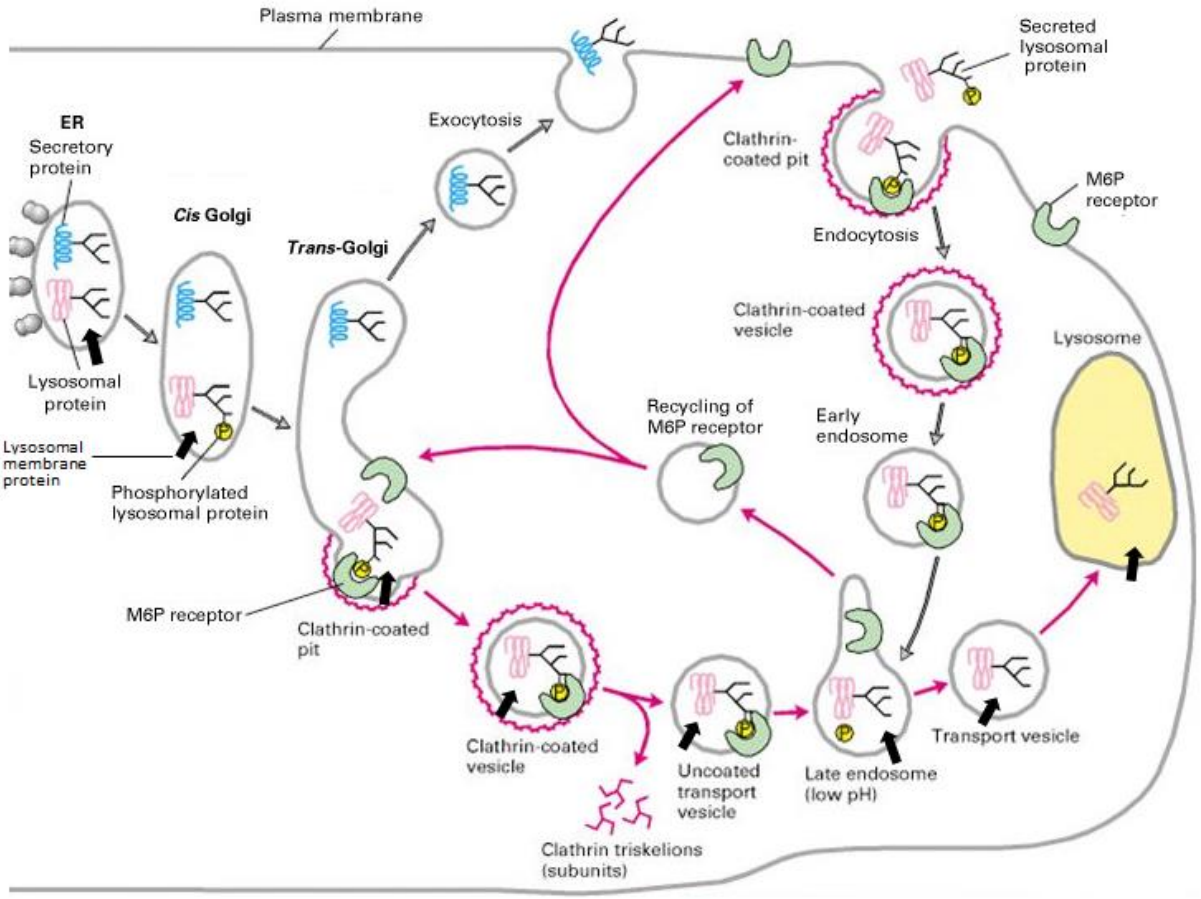

Figure 1.4 The mannose 6 phosphate (M6P) pathway, a major route for lysosomal proteins to lysosomes
Lysosomal proteins migrate from the ER to the cis-Golgi apparatus where mannose residues are phosphorylated. The phosphorylated proteins bind to M6P receptors in the trans-Golgi, and form vesicles that fuse with late endosomes, where the proteins dissociate from the M6P receptors and are then dephosphorylated. The receptors are recycled back to the Golgi apparatus or transferred to the plasma membrane. The cargo proteins fuse with a lysosome. Some of secreted lysosomal proteins are taken up into the cells by M6P receptors on the plasma membrane and transported to the early endosome, the late endosome and finally to the lysosome (used with permission from D. Palmer).

1.9 Production of polyclonal antibodies

Highly specific and sensitive antibodies are invaluable for biological studies and clinical diagnoses. They are traditionally produced by immunization of a suitable animal, such as a mouse, rabbit or goat, with an antigen. This induces B-lymphocytes (antigen-binding cells) to produce antibody-secreting plasma cells specific for the antigen via the injected host's humoral immune response. In general, polyclonal antibodies are produced from a range of B-cells that show heterogeneity in the amino acid sequences of the antigen-binding immunoglobulin and bind to different epitopes on the antigen. Monoclonal antibodies arise from specific B-cell clones in culture.

1.9.1 Expression of recombinant protein via *Escherichia coli* (*E. coli)* prokaryotic systems

The immunizing antigen can be a peptide, a purified recombinant protein, or a semi-purified cell homogenate injected together with a highly immunogenic adjuvant. In this study, the planned antigens were to be recombinant proteins. The first choice for the expression of recombinant proteins is typically an *E. coli* prokaryotic system. Production of proteins in this bacterial strain is well established, simple and usually provides high yields. The progressive fundamental understanding of transcription, translation, and protein folding in *E. coli* have made the bacterium more user-friendly than eukaryotic protein expression systems. However, it is not always possible to generate appropriate antigens, and it is time consuming to do so.

1.9.2 Expression of protein in eukaryotic mammalian cells by using lentiviral vectors

An alternative production method is to use eukaryotic mammalian cell expression systems, which have the ability to perform comprehensive post-translational modifications and to secrete glycoproteins. One of the most popular stable mammalian cell lines is from human embryonic kidney (HEK293) cells. HEK293 cells produce biologically functional proteins with native structures and similar post-translational modifications to those in the human body.

Vectors derived from lentiviruses, a family of complex retroviruses derived from the human immunodeficiency virus (HIV-1), are commonly used to transfer genes of interest for expression in mammalian cells (Brooks et al., 2002). Recombinant lentiviral vectors have transferred genes under tightly controlled promoters to a variety of tissues, including the brain (Jakobsson et al., 2003). Safety is important when using these viruses and the vectors are highly modified so as to be unable to cause virulent infections or to self-replicate.

A recombinant lentiviral vector is generated using four plasmids (Figure 1.5). The first plasmid functions as a packaging signal and promoter, and integrates the transgene into the host genome. The gene of interest (ovine *CLN5*, or *CLN6* coding sequence in the current study) is inserted into the plasmid and replaces the structural viral genes (such as *gag*, *pol*, and *env*). The structural genes responsible for virus assembly, infection into host cells, and regulation of promoter transgene expression are supplied separately in another three plasmids. Since about 60% of the HIV-1 genome has been removed, the HIV-1 virus is not able to be reconstituted, ensuring that it is safe to use (Trono, 2000). This mature lentiviral

package uses receptor-mediated cell entry and once it is inside the host cell (e.g. human embryonic kidney cell, HEK293), the transgene plasmid is transcribed to two single strand RNAs (ssRNA) that assemble with the three viral proteins (Figure 1.5). Post transfection, the mature viruses (lentiviral CLN5 and CLN6) are exported into the cell culture media, and then extracted and purified.

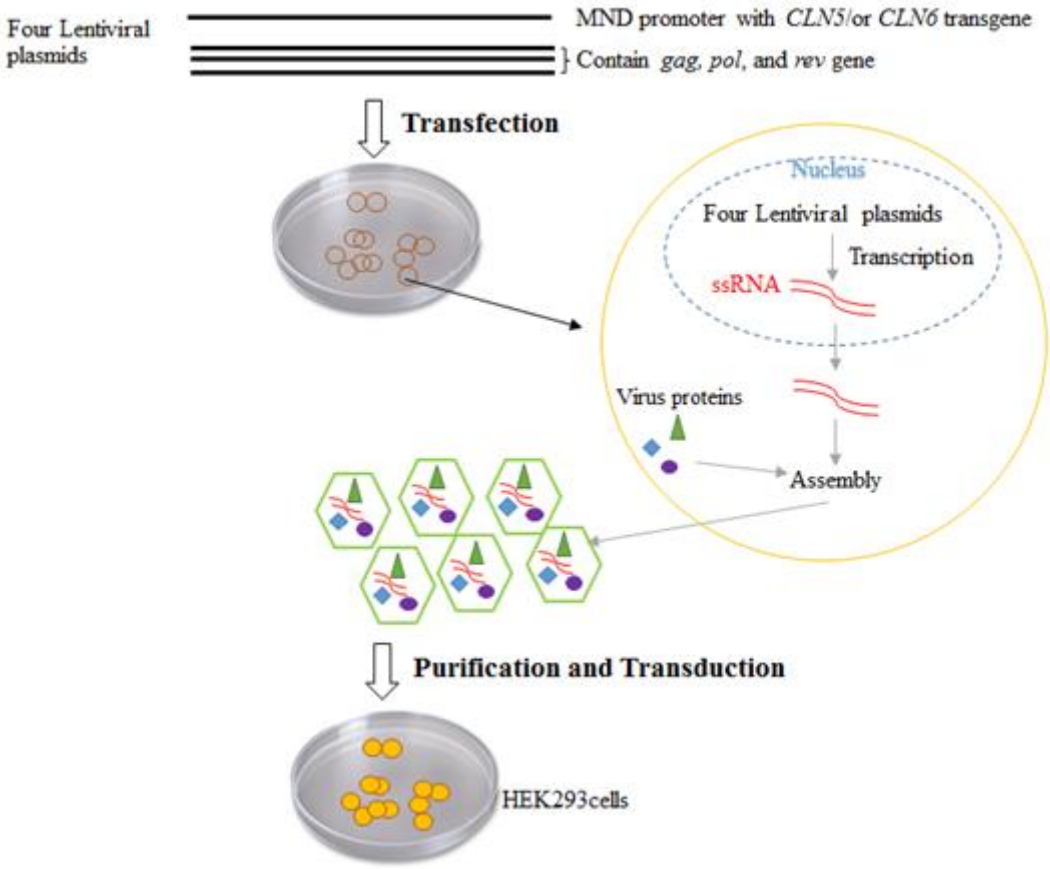

Figure 1.5 Recombinant lentiviral vector production and transduction of HEK293 cells

The lentiviral plasmids are transfected in cultured HEK293 cells. Each cell that receives all four plasmids will transcribe the promoter transgene plasmid from the LTRs. This creates two copies of ssRNA that assemble with the viral proteins. The assembled mature virus particles bud off from the cell surface and are exported to the cell culture supernatant from which they can be extracted and purified by centrifugation. Purified virus is pipetted directly onto cells of interest, such as sheep neural cells, and are taken up in a process known as transduction.

Advantages of lentiviral vectors are their ability to mediate potent transduction of large cloning sequences, up to 10 kb, and their efficient integration into chromosomes to allow stable and prolonged transgene expression in dividing and non-dividing cells (Vodicka, 2001; Palfi et al., 2014). The major use of lentiviral vectors is to infect non-dividing cells, such as

neurons. Several animal model studies have shown that lentiviruses are able to transduce different cell types in the brain, resulting in high and long term transgene expression *in vivo*, suggesting their suitability in gene therapy studies (Kordower et al., 1999; Brooks et al., 2002; Haskell et al., 2003; Dahl et al., 2015). Lentiviruses are utilized in the laboratory to transfer genes into dividing cells *in vitro* to express target proteins for functional analysis.

1.9.3 Specific antibody generation using adenoviral vectors

Adenoviruses are medium-sized (90–100 nm) naked viruses consisting of a nucleocapsid and a linear double-stranded DNA genome. Over 51 different types are found in humans. When these viruses infect a host cell, they introduce their DNA into the host. The genetic material of adenoviruses is not incorporated into the host genetic material, but is left free in the nucleus, and the instructions in this extra DNA molecule are transcribed just like any other gene. The only difference is that these extra genes are not replicated when the cells undergo division so daughter cells do not have the extra gene.

Adenoviral vectors are widely used gene transfer tools to promote targeted gene expression in many tissues, such as muscle, eye, brain, liver and lung (Daly, 2004; Rein et al., 2006). They have several advantages (Danthinne and Imperiale, 2000). Firstly they can infect a wide range of dividing and non-dividing cells. Secondly, they are easily purified in high titres. Thirdly, they can accommodate up to 37 kb of foreign genomic DNA. Fourthly, their genome rarely integrates into the host chromosome. In addition, it has been suggested that adenoviral vectors could be a good adjuvant for antibody generation. They shuttle the target gene to overexpress an antigen *in vivo*, overcoming the frustrating process of protein generation, purification and multiple injections into hosts *(*Anderson et al., 2000). This is a simple, rapid way to generate antibodies without the need for preparation of the protein or peptide of interest, for instance TPP1 antibodies (Haskell et al., 2003). In this thesis, the coding sequences of the target genes (ovine *CLN5* and *CLN6*) were cloned into adenoviral shuttle plasmids (pVQAd CMV K-NpA) by colleagues at the Unviersity of Otago (Dr. Stephanie Hughes, Dunedin, New Zealand) using standard techniques (Figure 1.6) and the shuttle plasmids transfected into HEK293 packing cells. Adenoviruses were amplified by cell passaging and purified adenoviral vectors were then injected into rabbits and mice.

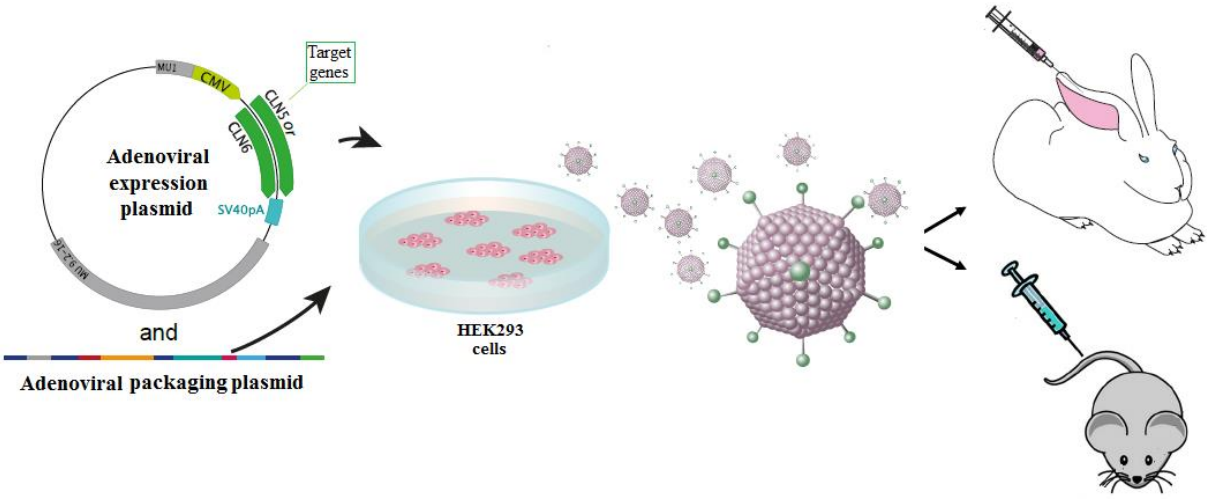

Figure 1.6 Generation of antibodies using adenoviral vectors

The cDNA encoding the protein of interest is cloned into an adenoviral shuttle plasmid which is transfected into HEK293 cells together with an adenoviral packaging plasmid. Adenovirus containing the target sequencing is amplified by serial passaging of HEK293 cells and purified. Adenoviral particles are injected into the host animals via a single injection into a rabbit or a mouse. Sera containing antibodies are collected (modified from Hughes et al., 2014b).

1.10 Neural cells in the central nervous system

The central nervous system (CNS) consists of a wide range of cell types that work together to receive, transmit and react to information and to coordinate the activities of body parts. Neurons, or nerve cells, localized in the brain and spinal cord of the CNS, process and transmit information via electrical and chemical signals, and connect to form neural networks. A typical neuron has three main structures; a soma (the cell body), dendrites and an axon. The cell body contains the nucleus which stores the genes of the cell. Dendrites are thin structures that start from the soma, are highly branched, and receive signals from other neurons. Axons are long cables extending from the soma that carry electrical signals away from the cell body toward other neurons. Neurons vary in size, shape and length.

There are many possible sub-classifications of neurons. Researchers have categorized neurons by function (Kandel, 2000). Sensory neurons collect information from sensory organs (such as the skin, eyes and nose) and send signals to the CNS (Figure 1.7 A). Motor neurons send signals from the CNS and form synapses with muscles to transmit commands for muscle contractions (Figure 1.7 B). Interneurons form neuron-neuron interconnections in the nervous system (Figure 1.7 C).

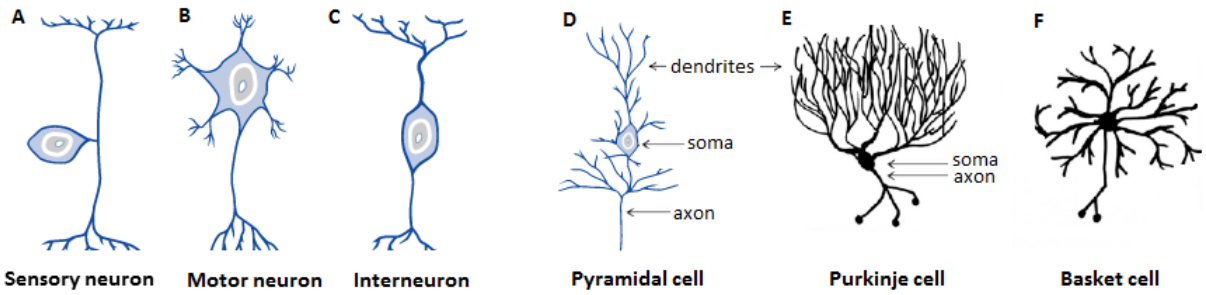

Figure 1.7 Overview of some neuron types

(A) Sensory neurons transform physical stimuli into electrical activity in cells. (B) Motor neurons carry commands from the brain to muscles and glands. (C) Interneurons convey signals from one brain region to another. (D) Pyramidal cells with somata like pyramids constitute the majority of neurons in the cerebral cortex. (E) Cerebellar Purkinje cells have extensively ramified dendritic trees. (F) Cortical basket neurons are inhibitory interneurons with extensive dendritic trees for contacting other neurons (modified from Stahl et al., 2008).

Neuronal cells are also classified based on location, shape and the pattern of dendrites (Stahl, 2008). Pyramidal cells have triangular shaped somata (Figure 1.7 D). Most neurons in the cerebral cortex are pyramidal neurons, especially those in the frontal cortex. Purkinje cells, located in the cerebellum, have extensively branched dendrites (Figure 1.7 E). A specific, recognizable feature of Purkinje neurons is the expression of calbindin (Whitney et al., 2008). Basket cells contain highly ramified dendritic trees. They are interneurons present in the cortex, hippocampus and cerebellum (Figure 1.7 F) (Wang et al., 2002; Stahl, 2008). The hippocampal basket cells are also parvalbumin-expressing cells.

1.11 Experimental rationale

1.11.1 Research objectives

The neuronal ceroid lipofuscinoses are the most common group of inherited neurodegenerative diseases that affect children. Naturally occurring animal models, e.g. sheep, are used to study human neurological disorders, and supply more reliable information than small animal models (Pinnapureddy et al., 2015). Two NCL proteins, CLN5 and CLN6, have been studied for two decades, but their functions are still unclear. Generation of highly specific and sensitive antibodies to these proteins would be very useful for biological and functional studies. In the studies described in this thesis, the naturally occurring ovine models of CLN5 and CLN6 NCL were used to establish the full length coding sequences of the genes and expression of the encoded proteins. Antibodies against ovine

CLN5 and CLN6 were generated and used for characterisation studies of both proteins *in vitro*.

1.11.2 Research aims

The first aim of this study was to clone full length ovine *CLN5* and *CLN6* gene sequences into an expression vector (e.g. pRUN vector or Gateway cloning vectors), and attempt recombinant protein expression in *E. coli*. The *CLN5* exon 1 allelic variants were also tested. These results are described in Chapter 2.

The second aim was to use lentiviral vectors expressing full length *CLN5* and *CLN6* coding sequences under the control of the MND promoter. These vectors were packaged and transduced into HEK293FT cells, and the over-expressed recombinant CLN5 and CLN6 proteins produced from these cell lines used to test the specificity of antibodies. Adenoviral anti-CLN5 and CLN6 antibodies were generated and characterised by immunocytochemistry, Western blotting and mass spectrometry, described in Chapter 3.

The third aim was to visualise cellular and regional CLN5 and CLN6 expressions in the ovine CNS, and to examine the correlations between these two proteins, described in Chapter 4.

Chapter 5 provides a general discussion and conclusion, as well as suggesting future directions for this research.

Chapter 2
Generation of full length ovine CLN5 and CLN6 constructs for recombinant protein expression

2.1 Introduction

Two unique sheep models of Batten disease are being used to develop gene therapy strategies for these devastating neurodegenerative diseases of children. CLN5 Batten disease in Borderdale (BD) sheep is caused by a defect in a soluble lysosomal protein, whereas the CLN6 form in South Hampshire (SH) sheep is caused by a defect in a membrane protein. Despite the two proteins having quite different cellular residences and presumed functions, the clinical developments of these two forms of Batten disease are similar. However, the functions of the CLN5 and CLN6 proteins are still unclear. They have not been purified and generation of the two proteins would be very useful for biological and functional studies. This study aimed to clone full length ovine *CLN5* and *CLN6* gene sequences into an expression vector (e.g. pRUN or Gateway cloning vectors) for recombinant protein expression in *E. coli*.

The pRUN vector is a high copy number expression plasmid closely related to the pET vector family. It was modified from a pMW172 plasmid with more restriction sites in the polylinker. The pMW172 expression vector was generated based on the original pET vector containing a modified polylinker and has been used to express segment 1 of gelsolin (Way et al., 1990). In the present study, *CLN5* and *CLN6* sequences were initially cloned into pRUN vector, and overexpression in the host *E. coli* strain C43 (DE3) was attempted. C43 (DE3) is a mutant strain of BL21 (DE3) (Miroux and Walker, 1996), frequently used to overcome toxicity associated with overexpressing some recombinant proteins using the bacteriophage T7 RNA polymerase expression system (Dumon-Seignovert L et al., 2004). An alternative Gateway cloning expression system was also used in attempts to generate ovine CLN5 and CLN6 recombinant proteins. Recombinant transcripts are also controlled by the T7 polymerase promoter.

2.2 Animal samples and methods

2.2.1 Animal samples

CLN5 BD and CLN6 affected SH sheep have been developed and are maintained under standard New Zealand pastoral conditions on Lincoln University farms. All animal procedures were carried out in compliance with the New Zealand Animal Welfare Act (1999) and were approved by the Lincoln University Animal Ethics Committee.

For the CLN5 exon 1 study, ~~six BD~~ genomic DNAs (genotyped by Dr. Nadia Mitchell) were obtained from 2 affected (*CLN5*$^{-/-}$), 1 heterozygote (*CLN5*$^{+/-}$) and 3 controls (*CLN5*$^{+/+}$). For the ovine CLN5 genotyping study, a total of 351 sheep genomic DNA samples were investigated, including 42 *CLN5*$^{-/-}$, 82 *CLN5*$^{+/-}$ and 80 *CLN5*$^{+/+}$ Borderdale samples, and 69 from *CLN5*$^{+/+}$ South Hampshire sheep. Blood samples from Merino, Kelso ranger, Kelso maternal, Coopdale, Romney and Coopworth sheep on FTA paper matrix cards (Whatman, Middlesex, UK) were kindly donated by Professor Jon Hickford, Lincoln University.

For the bovine CLN5 study, a total of 30 Devon cattle DNA samples, including 2 *CLN5*$^{-/-}$, 12 *CLN5*$^{+/-}$ and 16 *CLN5*$^{+/+}$ controls, were kindly provided by Dr. Imke Tammen, University of Sydney, Australia. For the human CLN5 study, 53 anonymous mixed age human oral DNA samples were kindly provided by Professor Martin Kennedy, University of Otago, Christchurch. The two normal human brain tissues used were obtained from Professor Richard Faull, the Huntington Brain Bank, University of Auckland, Auckland.

2.2.2 Genomic DNA extraction

2.2.2.1 Genomic DNA extraction from brain

DNA was extracted from brain frontal lobes using an Axyprep Multisource Genomic DNA Miniprep Kit (Axygen, USA). Brain tissues were frozen in liquid nitrogen prior to processing. Tissue (20 mg) was processed through the Axyprep spin column. The OD_{260} and the 260/280 ratio of each sample were measured spectrophotometrically (Nano Drop, Germany). The concentration of DNA (ng/µl) was calculated from 50 × OD_{260} of each sample. Purified DNA samples were stored at -20°C until required for PCR.

2.2.2.2 Genomic DNA exaction from blood on FTA cards

DNA from each blood sample was purified using a two-step washing procedure (Zhou et al. 2006). A 1.2 mm blood disc was punched from an FTA card (Whatman), placed into a PCR

tube, washed with 200 µl of 20 mM NaOH, 30 min, and equilibrated in 200 µl TE buffer, 5 min. After removal of the TE buffer, the disc containing genomic DNA was air-dried overnight, and placed in 500 µl of ddH_2O at 4°C.

2.2.2.3 RNA extraction and complementary DNA synthesis of ovine CLN5

Borderdale RNA from each blood sample was exacted by Dr. Nadia Mitchell using a PureLink Total RNA blood kit (Invitrogen, NZ). Single stranded cDNA was synthesised from (450 ng) of total RNA in 20 µl PCR reactions using Superscript III reverse transcriptase (Invitrogen, NZ).

2.2.3 PCR

2.2.3.1 Primers

The design of all the primers used here were based on the sequence information in the National Centre for Biotechnology Information (NCBI) GenBank using the DNAMAN 4 programme (©fLynnon Biosoft). The published mRNA sequences used were ovine *CLN5* (NM_001082595), ovine *CLN6* (NM_001040289.1), bovine *CLN5* (NM_001046299.1) and human *CLN5* (NM_006493). The information for each specific primer pair and their generated PCR products is shown in Table 2.1 and Table 2.2, and the locations of the designed primers on their mRNA sequences are provided in Appendix, A.1. All specific primers were synthesised and supplied lyophilized (Invitrogen, NZ). Each primer was diluted with TE (10 mM Tris-HCl, pH 8.0, 1 mM EDTA) to a stock concentration of 50 µM and stored at -20°C.

2.2.3.2 PCR using Platinum Pfx Taq DNA polymerase

Platinum pfx *Taq* DNA polymerase (Invitrogen, NZ) was used to generate full length *CLN5* and *CLN6* coding sequences. A standard 50 µl PCR reaction was performed with template DNA (~100ng), 0.25 µM of each primer, 200 µM of each dNTP, 1.5 mM $MgSO_4$, 2.5 units of Platinum pfx *Taq* DNA polymerase (Invitrogen, NZ), 2× PCR enhancer solution, and 1× the amplification buffer supplied with the polymerase. Amplifications were carried out in a Thermo cycler (Eppendorf, Hamburg, Germany). The PCR cycles were: 94°C for 2 min, 35 cycles of 94°C, 15 sec, 55°C, 30 sec and 68°C, 1 min, followed by 72°C, 5 min. Ovine *CLN5* exon 1 sequence was generated using primer sets of CLN5_TOPO_For 2 (forward) and CLN5_GSP2 (reverse) and the full ovine *CLN5* sequence using primer sets of CLN5_TOPO_For 2 (forward) and CLN5_3'UTR-R5 (reverse) (Table 2.1).

Table 2.1 CLN5 primer sequences and PCR product information

PCR product names	Primer names	Primer sequences 5'- 3'	Product sizes
Sheep CLN5 exon 1	F: CLN5_TOPO_For2 R: CLN5_GSP2	CACC**ATG**GCGCAGGCGGGGGGTGCCGG ACAGTCACTTTGGAACTGGCCAACG	430bp
Sheep CLN5 exons 2-4 stop	F: CLN5_Ex2F R: CLN5_TOPO_Revstop	ACGCTTCTCCTTCCGTCCGGAAC **TTA**TAAACCAGAGAGTGTTCTG	907bp
Sheep CLN5 exons 2-4	F: CLN5_Ex2F R: CLN5_3'UTR-R5	ACGCTTCTCCTTCCGTCCGGAAC TGTTAGCTTTCTGCCCCAAGG	1012bp
Sheep CLN5 exon 1 (fragment A)	F: CLN5_TOPO_For2 R: CLN5_Exons 1-2Rlong	CACC**ATG**GCGCAGGCGGGGGGTGCCGG CGGAAGGAGAAGCGTTTGTAGGGCACCGGCCACT	205bp
Sheep CLN5 exon 2-4 (fragment B)	F: CLN5_Exons 1-2Flong R: CLN5_3'UTR-R5	GCCGGTGCCCTACAAACGCTTCTCCTTCCGTCCGGAAC TGTTAGCTTTCTGCCCCAAGG	1021bp
Sheep CLN5	F: CLN5_TOPO_For2 R: CLN5_3'UTR-R5	CACC**ATG**GCGCAGGCGGGGGGTGCCGG TGTTAGCTTTCTGCCCCAAGG	1199bp
Sheep CLN5his	F: CLN5_TOPO_For2 R: CLN5_His_R	CACC**ATG**GCGCAGGCGGGGGGTGCCGG **TTA**GTGGTGGTGGTGGTGGTGTAAACCAGAGAGTGTTCT	1104bp
Sheep CLN5his *Bam*H I/*Hin*dIII	F: CLN5_F_*Bam*H I R: CLN5_R_*Hin*dIII_his	TATTATCGGGATCC**ATG**GCGCA AGCCCAAGCTT**TTA**GTGGTGGT	1129bp
Sheep CLN5his exons 2-4 *Bam*H I/ *Hin*dIII	F: CLN5_ex2-4F_*Bam*H I R: CLN5_R_*Hin*dIII_his	GGTTATCGGGATCCAAACGCTT AGCCCAAGCTT**TTA**GTGGTGGT	952bp
Sheep CLN5$_{151-207}$	F: CLN5_F151-207 R: CLN5_R151-207	CACCATATCCCGGCGCCAGT C**CTA**ATCTGGTTCCGGACGG	68bp
Sheep CLN5$_{656-717}$	F: CLN5_F656-717 R: CLN5_R656-717	CACCATAAGCCCGAAAAAGGAG CCCGC**CTA**CCTTAACACAAAT	78bp
Sheep CLN5myc	F: CLN5_TOPO_For2 R: CLN5_mycR	CACC**ATG**GCGCAGGCGGGGGGTGCCGG **TCA**CAGATCCTCTTCTGAGATGAGTTTTTGTTCTAAACCAG AGAGTGTTCT	1120bp
Cattle CLN5 exon1	F: 5'UTRF7 R: I1R2	AGCCGAGTGGATCGAGCGCT GCCAGGACGCAACTTCCTAC	437bp
Human CLN5 exon1	F: H1F2 R: H1R1	CATAAAAGATGACGCCCCAGGTC GACCCCAACCCCGACAGTGC	470bp

Table 2.2 CLN6 primer sequences and PCR product information

PCR product names	Primer names	Primer sequences 5'- 3'	Product sizes
Sheep CLN6	F: CLN6_OF R: CLN6_WTOR	CACC**ATG**GAGGCTGCGGCGCGGAG TTGGCTGCTGACGTGGAGGGTG	972bp
Sheep CLN6his	F: CLN6_OF R: CLN6_His_R	CACC**ATG**GAGGCTGCGGCGCGGAG **TCA**GTGGTGGTGGTGGTGGTGTATTGGCTGCTGACGTG	951bp
Sheep CLN6his *Bam*H I/*Hin*dIII	F: CLN6_F_*Bam*H I R: CLN6_R_*Hin*dIII_his	TATATCGGGATCC**ATG**GAGGCT ATCCCAAGCTT**TCA**GTGGTGGT	978bp
Sheep CLN6 exon 2-7	F: CLN6_Ex207F R: CN6_Ex2-7R	CACCCACAGCTCCGTCAAGGC **TCA**GTGGTGGTGGTGGTGG	874bp

Notes: Start and stop codons are in bold. Bases highlighted in grey refer to enzyme cutting sites: *Bam*H I (GGATCC) and *Hin*dIII (AAGCTT). The 6× His tags are in boxed, and the myc tag is underlined.

The full ovine *CLN6* coding sequence was also amplified with Platinum pfx *Taq* DNA polymerase, using CLN6 genomic DNA from normal SH sheep for the DNA template (~100 ng), and primer sets, CLN6_OF (forward) and CLN6_WTOR (reverse) (Table 2.2) in a 50 µl PCR reaction. The PCR cycles were 2 min at 94°C, followed by 35 cycles of 94°C, 15 sec; 68°C and 2 min, with a final extension of 72°C, 5 min.

2.2.3.3 PCR using Taq DNA polymerase

Qiagen *Taq* DNA polymerase (Qiagen, Hilden, Germany) was used for most sequence amplifications. A standard 20 µl PCR reaction was performed with template DNA (~100ng), 0.25 µM of each primer, 125 µM of dNTPs, 2.5 mM $MgCl_2$, 1 unit of *Taq* DNA polymerase (Qiagen) and 2 µl 10× PCR buffer. The cycles consisted of 95°C, 5 min, followed by 35 cycles of 95°C, 30 sec; 55°C, 30 sec, and 72°C, 90 sec, and a final extension of 72°C, 5 min. This PCR programme was used to generate the ovine *CLN5* exons 2-4 sequence (section 2.3.6.3), the bovine *CLN5* exon 1 sequence (2.3.6.4) and the target insert of *CLN6* exons 2-7 for cloning (2.2.6.1). The specific primer sets used to generate each PCR product are listed in Table 2.1 and Table 2.2.

2.2.3.4 Agarose gel electrophoresis

Agarose gel electrophoresis was used to analyse PCR products and plasmid DNAs. Unless otherwise specified, 1.5 % (w/v) agarose gels were used. Electrophoresis was performed in Tris acetate EDTA (TAE) buffer (40 mM Tris base, 20 mM acetate, 1 mM EDTA, pH 8.0) with ethidium bromide dye (0.2 µg/ml), 100 V, 20 min. DNA was visualised under UV light and photographed with a GelDoc XR (Bio-Rad, USA) imaging system.

2.2.3.5 Purification of PCR products

Amplified PCR products were gel-purified using an AxyPrep DNA gel extraction kit (Axygen, NZ).

2.2.3.6 Direct sequencing of DNA fragments

Mixtures containing 6 ng of PCR product and 5 pmol of forward or reverse primers were diluted in ddH_2O to 15 µl and sent to the Allan Wilson Centre Genome Service, Massey University, NZ, for sequencing on a Big Dye terminator v3.1 sequencer. The resulting sequences were analysed using GeneScan (http://genes.mit.edu/GENSCAN.html) and aligned to the specific target sequences published on NCBI using GeneDoc 2.6.02 from the GeneDoc HomePage (http://www.psc.edu/biomed/genedoc/).

2.2.3.7 PCR – single strand conformational polymorphism (SSCP)

PCR-SSCP was used to genotype ovine *CLN5* genomic DNA sequences. PCR amplification was performed in a 50 µl PCR reaction containing the extracted genomic DNA, generated in section 2.2.3.2, with Platinum pfx *Taq* DNA polymerase, previously described in section 2.2.3.3. Directly after PCR, a 0.7 µl aliquot of each amplicon was mixed with 7 µl of loading dye (98% formamide, 10 mM EDTA, 0.025% bromophenol blue, 0.025% xylene) for SSCP analysis. After denaturation at 95°C, 5 min, samples were cooled on ice and loaded onto 16 ×

18 cm, 14% acrylamide vertical gels (acrylamide: bis-acrylamide 37.5:1, Bio-Rad) which were polymerized with 0.01% (v/v) N,N,N'N'-tetramethylethylenediamine (TEMED) and 0.05% (w/v) ammonium persulphate. Gels were run in Protean II cells (Bio-Rad), 390 V, 19 h, 12°C, in TBE buffer (45 mM Tris, 45 mM boric acid, 1 mM EDTA), then fixed and stained in 10% ethanol, 0.5% acetic acid and 0.2% silver nitrate for 5 min (Byun et al., 2009). They were rinsed with ddH_2O, 3 min, then developed with a warm solution (55°C) of 3% NaOH and 0.1% formaldehyde until dark bands appeared on a yellow background (5 - 10 min). Development was terminated with a solution of 10% ethanol and 0.5% acetic acid, and gels were kept in ddH_2O.

2.2.4 Cloning ovine *CLN5* and *CLN6* coding sequences into pRUN vector

An empty pRUN plasmid (2587 bp) was kindly provided by Mike Runswick and Professor John Walker, MRC, Mitochondrial Biology Unit, Cambridge, UK. Purified *CLN5* and *CLN6* PCR fragments containing a 6× Histidine (His) tag at C-terminus were cloned into *Bam*H I-*Hin*dIII cleaved pRUN vector, and overexpression of CLN5 and CLN6 proteins in the host *E. coli* strain C43 (DE3) attempted as follows. The 6× His tag was cloned into the target gene sequence to allow purification of expressed recombinant proteins by binding to Ni affinity chromatography columns.

2.2.4.1 Generation of full length CLN5, full length CLN6 and CLN5 exons 2-4 sequences with a 6× His tag as target inserts

The full *CLN5* target insert was amplified from the *CLN5*$^{+/+}$ cDNA (as described in section 2.2.2.3), using Platinum *Taq* polymerase (Invitrogen) and the primer sets of CLN5_Topo_For 2 (forward) and CLN5_His_R (reverse) which contained a 6× His in-frame tag sequence at the C terminus, named as CLN5his (Figure 2.1). To allow directional cloning of the target insert into pRUN, two restriction enzyme cutting sites with 5-8 extra bases were introduced onto the 5' (*Bam*H I, GGTACC) and 3' (*Hin*dIII, AAGCTT) of the CLN5his sequence by a second PCR with CLN5_F_*Bam*H I (forward) and CLN5_R_*Hin*dIII_his (reverse) primers (Table 2.1) using the reaction programme and cycles described in section 2.2.3.2.

The full CLN6 target insert of was generated in the same manner. It was amplified from the *CLN6*$^{+/+}$ cDNA, using Qiagen *Taq* polymerase and the primers CLN6_OF (forward) and CLN6_His_R (reverse (Table 2.2) which contained a 6× His in-frame tag sequence at the C terminus, named as CLN6his (Figure 2.1). Two enzyme cutting sites were then added into the

CLN6his sequence by a second PCR with CLN6_*Bam*H I (forward) and CLN6_R_*Hin*dIII_his (reverse) primers (Table 2.2) as described in section 2.2.3.3.

An alternative CLN5 target insert (excluding exon 1) was also amplified using CLN5his as the template and the primers CLN5_ex2-4F_*Bam*H I (forward) and CLN5_R_*Hin*dIII_his (reverse) as described in section 2.2.3.2. All three PCR products were gel purified and sequenced prior to cloning.

2.2.4.2 DNA ligation and bacterial transformation

The three purified target insert DNAs, encoding the full length *CLN5* and *CLN6* genes, and the *CLN5* gene excluding exon 1, were cloned into linearized pRUN and transformed into C43 (DE3) competent *E. coli* cells as follows. All steps were carried under sterile conditions.

Double restriction enzyme digestions were carried out on the target inserts and the pRUN vector, to generate sticky ligation sites. The DNAs (~350 ng), were digested in a 25 µl solution containing 1.5 µl of *Hin*dIII enzyme (New England Biolabs, UK), 3 µl of digestion buffer and ddH_2O, 37°C, 1 h; followed by digestion in 1.5 µl of *Bam*H I enzyme (New England Biolabs, UK) and 3 µl of digestion buffer for another 1.5 h. All the digested DNAs were confirmed by agarose electrophoresis. For DNA ligation, each enzyme-digested target insert (10 µl) was added to 5 µl of 10× ligation buffer, 1 µl T4 ligase (New England Biolabs, UK), 5 µl of linearized vector at a molar ratio of PCR product: vector of 2:1, and the finial volume adjusted to 25 µl with ddH_2O. This ligation reaction was mixed gently and incubated at room temperature, 1 h. The generated plasmid DNAs were named as pRUN CLN5his, pRUN CLN6his and pRUN CLN5his exons 2-4 (Figure 2.1). A reference reaction containing only pRUN vector was included as a negative control.

For *E. coli* transformation, the full ligation reaction was added to a vial of *E. coli* TOP10 competent cells (Invitrogen, NZ), incubated on ice, 1 h, heat-shocked at 42°C, 45 sec, and immediately chilled on ice, 1 min. Room temperature SOC medium (Super Optimal Broth, 250 µl, Invitrogen, NZ) was added to the vial containing DNA and *E. coli* cells, and incubated, with horizontal shaking, 37°C, 200 rpm, 1 h. The transformation mixture (50 µl) was spread on an LB-agar plate (1% w/v tryptone, 0.5% w/v yeast extract, 1% w/v NaCl, 1.5% w/v agar, pH 7.5) supplemented with 100 µl/ml ampicillin, which was incubated overnight, 37°C, to produce colonies. A reference plate spread with 50 µl of component cells was included as a negative control.

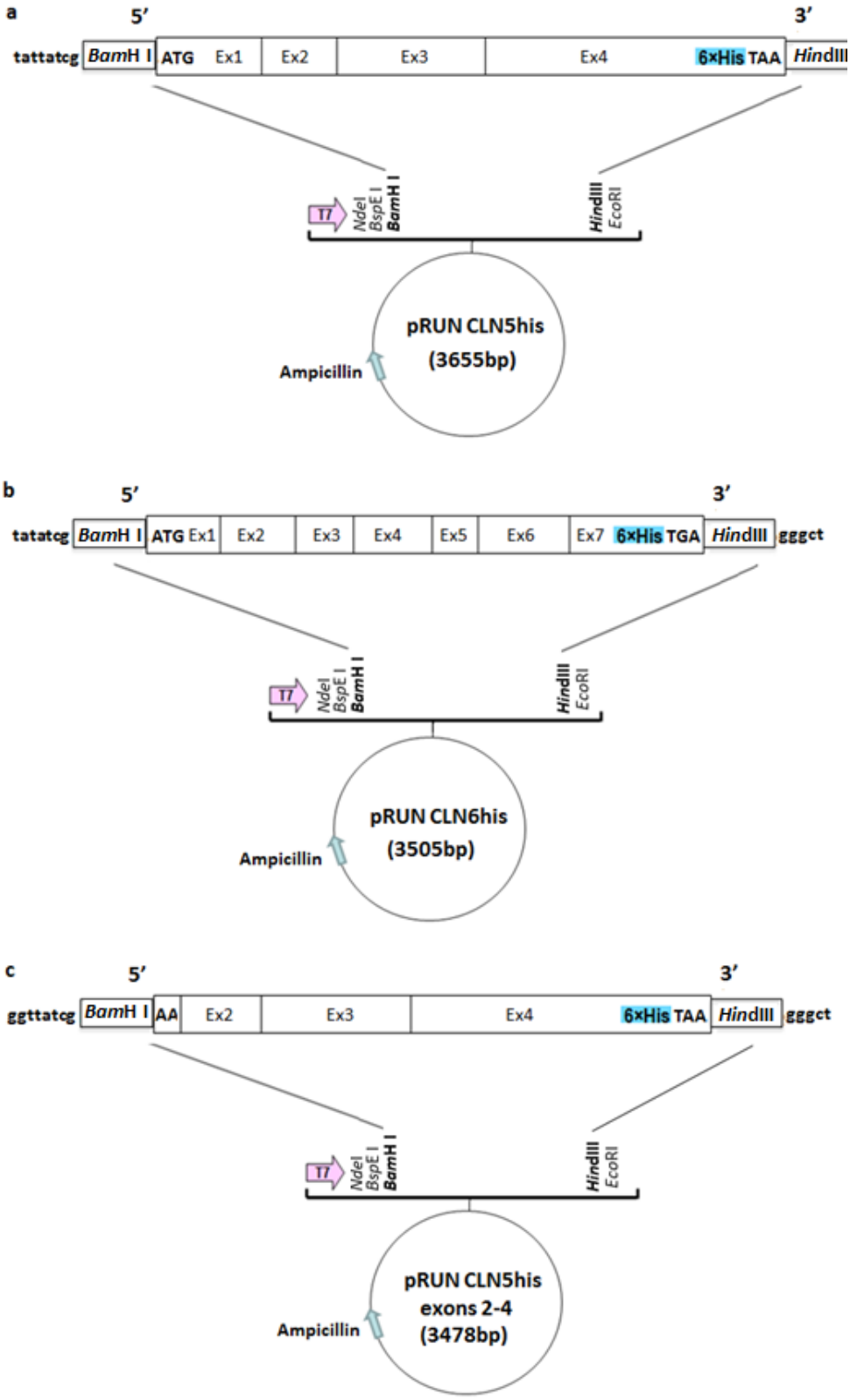

Figure 2.1 pRUN constructs for recombinant protein expression

(a) pRUN CLN5his, (b) pRUN CLN6his and (c) pRUN CLN5his exons 2-4

2.2.4.3 Plasmid DNAs purification

Single colonies of *E. coli* TOP 10 cells transformed with the different plasmid DNAs were inoculated into 3 ml of LB medium (Sigma, NZ) containing 100 µg/ml of ampicillin, followed by vigorous shaking, 250 rpm, overnight, 37°C. The cells were harvested by centrifugation, 1 min, 12,000 *g*, 4°C, and the plasmid DNAs purified from the cell pellets using Axygen Plasmid Mini kits (Axygen, NZ). The concentrations of plasmid DNA were tested using a Nano Drop spectrophotometer (ND-1000, 3.3.0, USA) and the size of the plasmid DNA was checked by restriction endonuclease digestion and agarose gel electrophoresis as described in section 2.2.4.4. The purified plasmid DNAs were labelled as pRUN CLN5his, pRUN CLN6his and pRUN CLN5his exons 2-4 (Figure 2.2).

2.2.4.4 Restriction endonuclease digestion of plasmid DNA

*Apa*I (New England Biolabs, UK) restriction endonuclease was used to digest the purified pRUN CLN5his plasmid DNA, *Bgl*II was used to digest the purified pRUN CLN6his and *Bam*H I was used to digest pRUN CLN5his exons 2-4. Plasmid DNAs (1 µg) were digested in 20 µl reactions containing digestion buffer (2 µl) and 10 units of the restriction enzyme, 37°C, overnight, then inactivated by incubation at 65°C, 15 min. The digested plasmid DNAs were analysed on agarose gels as previously described in section 2.2.3.4.

2.2.5 Recombinant protein expression in *E. coli*

2.2.5.1 Protein expression

The successful constructs, pRUN CLN6his and pRUN CLN5his exons 2-4 , were subsequently expressed in the *E. coli* strain C43 (DE3). LB medium, 3 ml, supplemented with ampicillin (100 µg/ml) was inoculated with a single colony and incubated in an orbital incubator, 250 rpm, overnight, 37°C. A 25 µl aliquot was added to 50 ml of fresh LB medium containing ampicillin (100 µg/ml), and the cells grown at 37°C until the OD_{600nm} = 0.6. Expression of recombinant protein was induced by adding isopropyl β-D-1-thiogalactopyranoside (IPTG, 1 M stock solution) to a final concentration of 1 mM. The cells were then incubated with vigorous shaking at 37°C for an additional 5.5 h. Half ml samples from each of the bacterial cells were collected and harvested before induction and 5.5 h after induction. The remaining bacterial cells were pelleted and stored at -20°C. Alternative protein expression conditions were also tested, including lower cell growth temperatures, 30°C or 25°C, and a decrease in the IPTG concentration to 0.5 mM.

Cell samples were harvested by centrifugation 10 min, 5000 rpm, 4°C. Each cell sample pellet was treated with 200 µl of 2× protein sample buffer (4% SDS, 300 mM mercaptoethanol, 20% glycerol, 0.004% bromophenol blue, 500 mM Tris-HCl pH 6.8), boiled, 10 min, and particulates pelleted, 5 min, 14,000 rpm, 4°C. Supernatants were transferred to fresh tubes. As CLN6 is an insoluble protein, it may be in the inclusion bodies in the CLN6 cells. An extra step was performed for cells transformed with pRUN CLN6his clones. Pellets were treated with 5 ml of 8 M urea, 10 mM sodium phosphate, pH 8.0 and centrifuged again, 5 min, 14,000 rpm, 4°C to pellet insoluble cellular debris. The resulting supernatant was collected. To test protein expression, the solubilised fractions from each clone were subjected to SDS-PAGE electrophoresis.

2.2.5.2 SDS-PAGE electrophoresis

Prior to SDS-PAGE, BCA protein assays were used to determine protein concentrations using Biorad DC protein assay kits (Bio-Rad, NZ). Sample fractions and the corresponding pre-induced samples of each construct were separated by SDS-PAGE in a Bio-Rad Mini cell electrophoresis system (Bio-Rad laboratories, Hercules, CA, USA). Protein samples (30 µg) were loaded onto 10% acrylamide gels, and electrophoresis was carried out at 80 V, 20 min, followed by 120 V for another 1.5 h. Apparent molecular weights of proteins were determined by comparison with the visible blue bands of Precision plus protein standard markers (7 µl, Bio-Rad, NZ). Immediately following electrophoresis, gels were stained with a solution of 42% methanol, 16% acetic acid containing 0.1% Commassie blue R250 overnight and destained with several changes of 40% methanol and 10% acetic acid until the backgrounds were clear.

2.2.6 Generation of CLN5 and CLN6 recombinant proteins using the Gateway cloning expression system

An alternative cloning system was also tested. Usually, the generation of a recombinant protein expression construct via Gateway technology involves two steps. First, the gene of interest is inserted into an “entry” vector, pENTR™//D-TOPO (Invitrogen, NZ). Secondly, the resultant constructs are re-cloned into a “destination” vector, pDEST17 (Invitrogen, NZ), which contains an N-terminal 6× His tag used for protein purification.

2.2.6.1 Generation of protein expression constructs

To generate *CLN5* target inserts, two small polypeptide cDNAs corresponding to ovine CLN5 amino acids 51-69 (named as $CLN5_{151\text{-}207}$) and 218-239 (named as $CLN5_{656\text{-}717}$) were

generated by separate PCRs (Figure 2.2 a and b) using the standard processes described in sections 2.2.3.2 and 2.2.4.1. The full length *CLN6* target insert was amplified from *CLN6*$^{+/+}$ cDNA by PCR (Figure 2.2 c). All target inserts contained 'CACC' at the N terminus for directional cloning. The specific primer sets used were shown in Table 2.1 and Table 2.2.

PCR amplicons of the target inserts were purified and sub-cloned into pENTR/D/TOPO (Figure 2.2) and transformed into TOP10 competent *E. coli* cells as described in section 2.2.4.2, except that the transformation mixture was spread onto LB-agar plates supplemented with 50 µl/ml kanamycin (Invitrogen, NZ). Plasmid DNA from randomly selected clones for each gene were extracted and analysed by direct sequencing. The chosen constructs were re-cloned from pENTR/D/TOPO into the His tag containing pDEST17 vector (Figure 2.2) using Gateway LR Clonase II Enzyme Mix (Invitrogen, NZ), and transformed into C43 (DE3) cells. Plasmid DNA for the three constructs pDEST17 $CLN5_{151-207}$, pDEST17 $CLN5_{656-717}$ and pDEST17 CLN6 exons 2-7 (Figure 2.2) was extracted, confirmed by restriction digestion and glycerol stocks of C43 (DE3) bacterium containing positive clones were prepared and stored frozen.

2.2.6.2 Expression of CLN5 polypeptides and CLN6 protein

The general processes were as described in section 2.2.5.1. To generate CLN6 protein, *E. coli* C43(DE3) clones containing the pDEST CLN6 exon 2-7 construct were grown at 37°C. When the cell densities reached an OD_{600nm} = 0.6, IPTG was added to a final concentration of 1 mM or 0.5 mM and cells incubated at 37°C for an additional 4 h. Each bacterial cell sample was collected and harvested before induction and 1 h, 2 h, 3 h and 4 h after induction. Cells were also inducted by 1 mM IPTG and incubated at 20°C for an additional 23 h and cells samples harvested before induction, and 6 h and 23 h after induction.

To generate two small CLN5 polypeptides, both of the expression constructs pDEST17 $CLN5_{151-207}$ and pDEST17 $CLN5_{656-717}$ were transformed into one C43 (DE3) cell, and grown at 37°C. The cells containing the CLN5 polypeptide sequences were induced by 1 mM IPTG and incubated at 37°C for additional 5 h. Cell samples were collected before induction, and 2 h and 5 h after induction. Solubilized fractions were analysed by SDS-PAGE as described in sections 2.2.5.1 and 2.2.5.2.

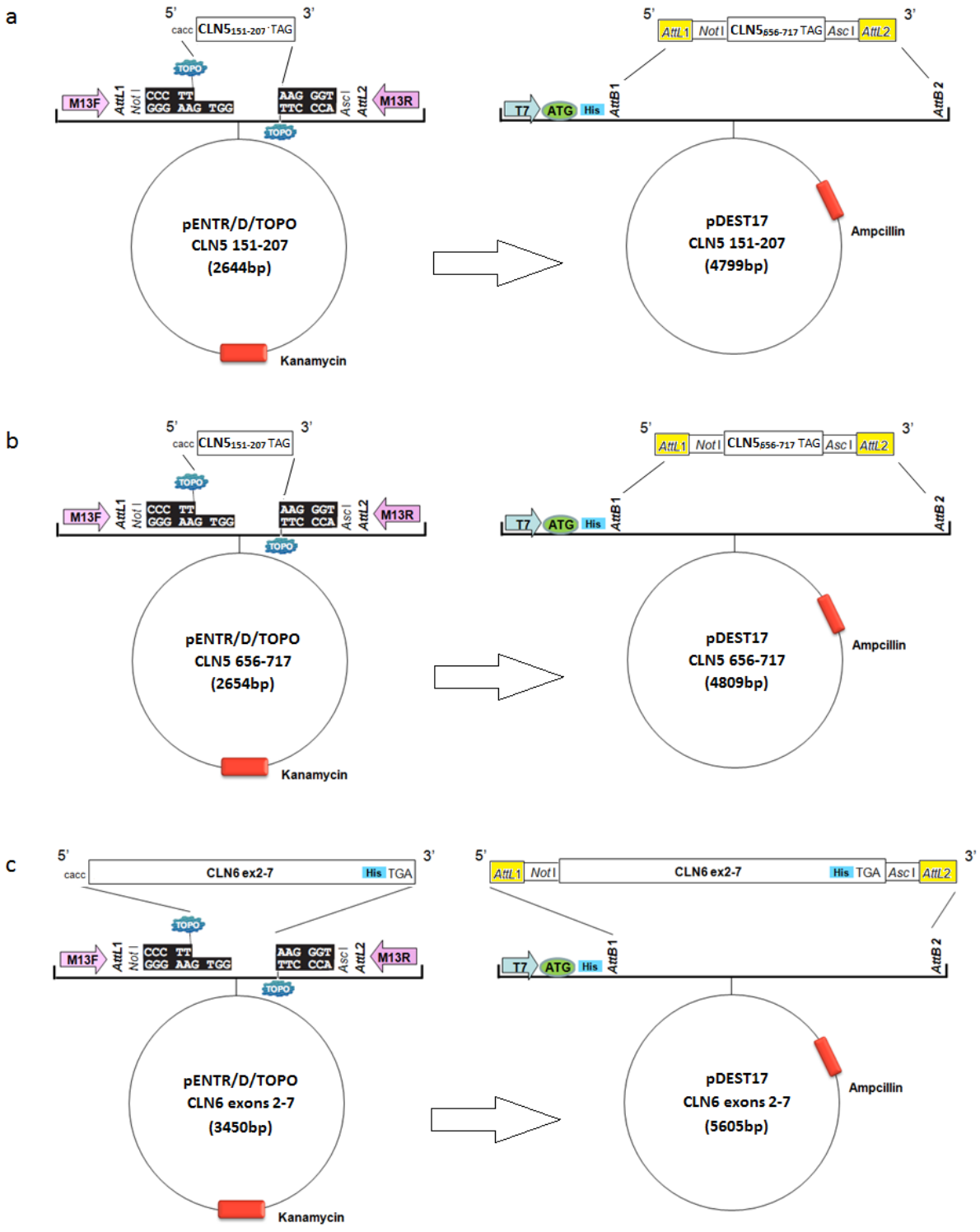

Figure 2.2 Gateway constructs for recombinant protein expression

(a) pDEST17 CLN5$_{151-207}$, (b) pDEST17 CLN5$_{656-717}$ and (c) pDEST17 CLN6 exons 2-7. Genes of interest were PCR-amplified using forward primers containing a 5'-CACC-overhang and their specific reverse primers (Table 2.1 and Table 2.2). The resulting PCR products were cloned directionally into a pENTR/D/TOPO and subsequently re-cloned into pDEST17 expression vectors.

2.2.7 Clone the *CLN5* coding sequence into pCR4-TOPO vector

The full length ovine *CLN5* coding sequence, both with and without a myc tag, was cloned into pCR4-TOPO (Invitrogen, Carlsbad, CA, USA), and used to generate lentiviral vectors which express CLN5 protein in HEK293FT cells (described in Chapter 3)

2.2.7.1 Addition of a myc tag to the CLN5 coding sequence

The full *CLN5* sequence with a myc tag (CLN5myc) was generated by PCR using Platinum *Taq* polymerase (Invitrogen) with the primers CLN5_Topo_For 2 (forward) and CLN5_mycR (reverse) (Table 2.1) containing a C-terminal myc tag sequence (section 2.2.3.2). The product, CLN5myc, was gel purified and sequenced using the CLN5_mycR reverse primer.

2.2.7.2 Generation of CLN5 protein expression constructs

The two purified PCR products, encoding full length CLN5 (1199 bp, Appendix A.2.1) and CLN5myc (1120 bp, Appendix A.2.2), were cloned into pCR4-TOPO (3957 bp) and transformed into TOP10 *E. coli* cells as follows. All steps were carried under sterile conditions. For each PCR product, 5 µl, was first added to 0.2 µl of 10 mM dATP, 1 µl 10× PCR buffer, 5 units of *Taq* DNA polymerase (Qiagen), and incubated at 70°C, 30 min to generate a poly-A tail. For DNA ligation, the poly-A-tailed PCR products (2 µl) were added to 1 µl of salt solution and 1 µl of TOPO vector at a molar ratio of PCR product: vector of 1:1, and the final volume was adjusted to 6 µl with ddH_2O. This ligation reaction was mixed gently and incubated, room temperature, 30 min, then subsequently transformed to *E. coli* as previously described (section 2.2.4.2). Positive clones of pCR4-TOPO CLN5 (Figure 2.3 a) and pCR4-TOPO CLN5myc (Figure 2.3 b) were selected. The plasmid DNAs were extracted, and confirmed by *Eco*RI (New England Biolabs, UK) restriction digestion as previously described (section 2.2.4.5).

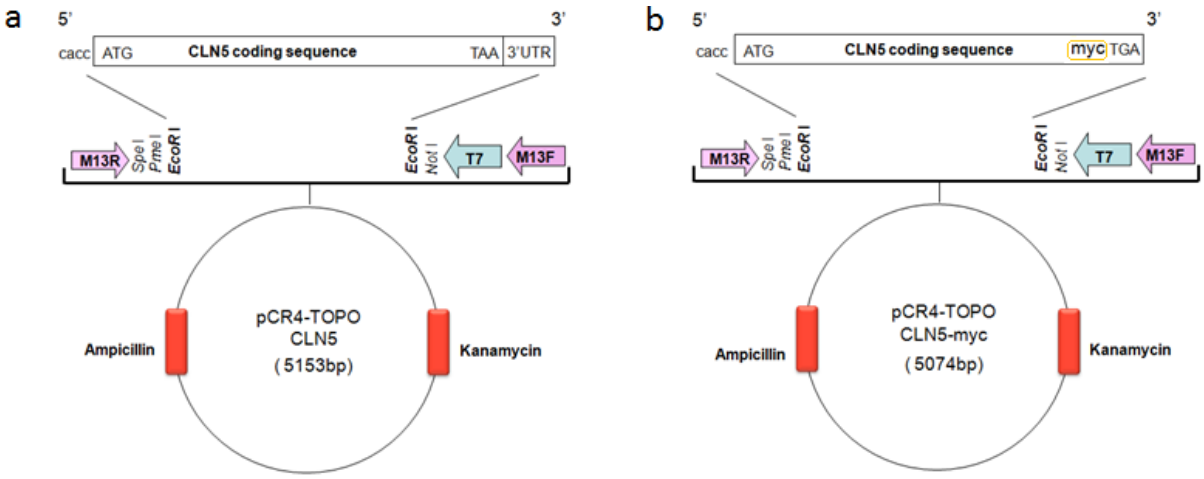

Figure 2.3 pCR4-TOPO CLN5 constructs

(a) pCR4-TOPO CLN5, (b) pCR4-TOPO CLN5myc

2.3 Results

2.3.1 Generation of full length ovine *CLN5* and *CLN6* coding sequences

Attempts to clone the full length cDNA of ovine *CLN5* in one reaction were unsuccessful, possibly due to the disjunction in GC/AT ratios. Ovine *CLN5* exon 1 sequence contains a much higher percentage of G/C bases (around 80%) compared with exons 2-4. To overcome this, a two-step PCR and ligation strategy was used to generate full length ovine *CLN5*. In brief, the *CLN5* exon 1 (section 2.2.3.2) and exons 2-4 (section 2.2.3.3) were amplified separately and then the isolated gene fragments joined using a two-step hybrid PCR with internally overhanging primers. Full length ovine *CLN6* cDNA was successfully generated in one amplification reaction (section 2.2.3.3).

2.3.1.1 The presence of allelic variants in exon 1 of ovine CLN5

Amplifications of exon 1 in genomic DNA from a number of sheep produced two distinct PCR products, 426 bp (the predicted size) and a smaller 406 bp product (Figure 2.4). The 426 bp band was obtained from both affected (*CLN5*$^{-/-}$) and control (*CLN5*$^{+/+}$) sheep samples, while the 406 bp band was detected from one control and a heterozygote (*CLN5*$^{+/-}$) sheep. Each amplified PCR product was gel purified and sequenced (sections 2.2.3.4- 2.2.3.6) to determine which sequence was the published sheep *CLN5* exon 1.

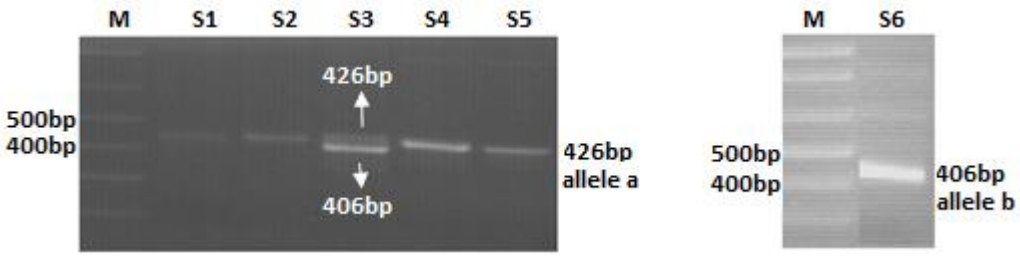

Figure 2.4 PCR products of the ovine *CLN5* exon 1

PCR products were run on 1.5% agarose gels and examined under UV-light. The primers used in the reactions are listed in Table 2.1. A 426 bp PCR product (allele a) was observed in samples S1, S2, S4 and S5; while a 406 bp PCR product (allele b) was revealed in sample S6. Sample 3 had both PCR products (alleles a and b). M refers to the 1 kb Plus DNA ladder (Invitrogen, NZ).

The two nucleotide sequences were aligned with the published sequence of ovine *CLN5* exon 1 and the first part of intron 1 (NM_001082595). The 426 bp fragment (allele a) was identical to the published ovine *CLN5* sequence (Figure 2.4 and Figure 2.5 a). The 406 bp allele variant (allele b) had five changes compared to the published sequence; two polymorphisms, one deletion and two non-sense changes (Figure 2.5 a, indicated in black or green arrows). Protein sequence alignment of the a and b alleles revealed three amino acid differences (Figure 2.5 b, indicated in green arrows), which arose from the two polymorphisms and one deletion shown in the nucleotide sequence alignment. The first replacement in the allele b sequence (Pro23Leu) resulted from a C to T transition at nucleotide 68, the second (Ala44Thr) from a G to A transition at nucleotide 130 and the deletion of an Arg (Arg47del) from a GGC deletion at nucleotide position 138.

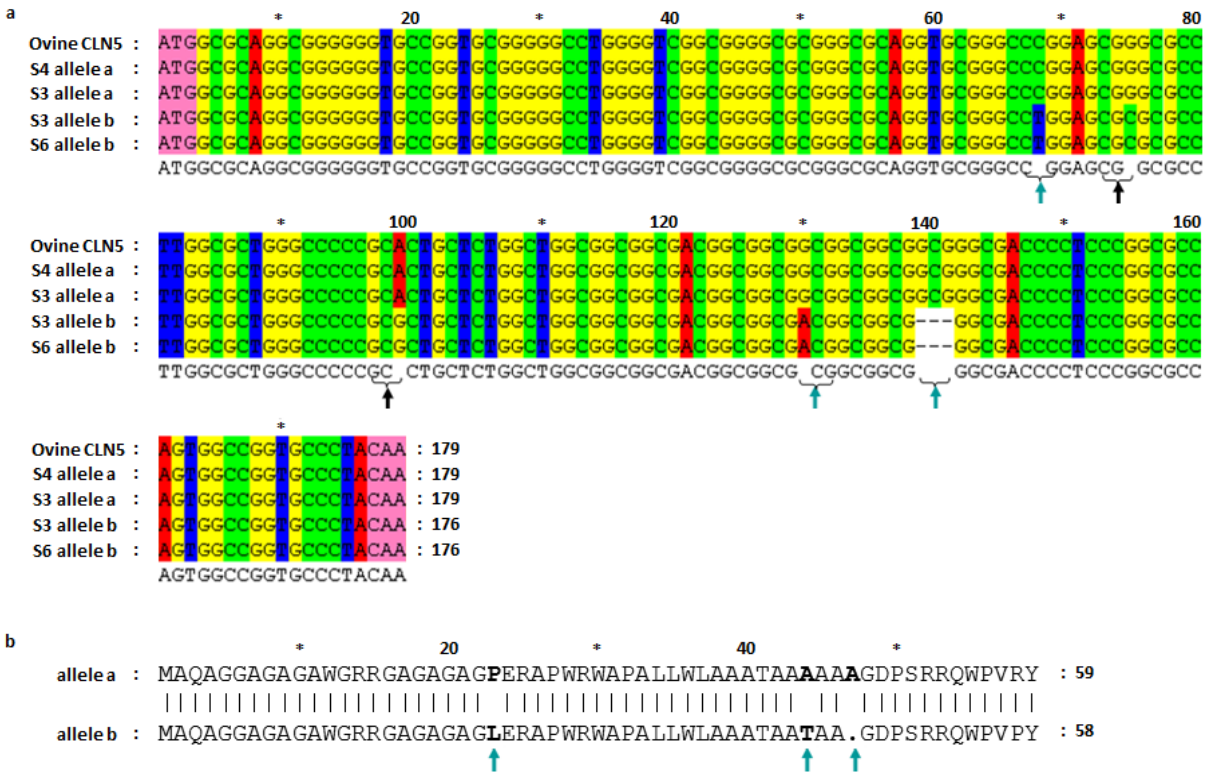

Figure 2.5 Sequence alignment of published ovine *CLN5* exon 1 and two allelic variants a and b.

(a) DNA sequence (NM_001082595). ATG is the start codon of exon 1, and CAA is the stop codon of the exon 1.

(b) Protein sequence. Black arrows indicate silent changes in nucleotides. Green arrows indicate changes in both nucleotides and amino acids**.**

2.3.1.2 Generation of the ovine CLN5 exons 2-4 sequence

Amplification of exons 2-4 from genomic DNA templates produced a single band with the expected size of 1012 bp (Figure 2.6). The sequence aligned 100% with the published *CLN5* coding sequence (NM_001082595).

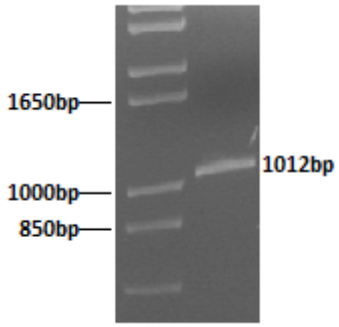

Figure 2.6 PCR product of the ovine *CLN5* exons 2-4

5 µl PCR product run on a 1.5% agarose gel and examined under UV light. A 1021 bp PCR product was generated from the CLN5_Ex2F and CLN5_3'UTR_R5 primer sets (Table 2.1). M refers to the 1 kb Plus DNA ladder (Invitrogen).

2.3.1.3 Generation of the full length ovine CLN5 coding sequence

The full length ovine *CLN5* coding sequence was generated by a two-step hybrid PCR (Figure 2.7). Two DNA fragments with internal overlaps of the exon 1-exon 2 boundaries (A and B) were amplified separately, then the two isolated fragments joined in a second PCR (Figure 2.7). After the first PCR, a single 205 bp band (Figure 2.8 a) of the *CLN5* exon 1 sequence fragment (A) and a single 1021 bp band (Figure 2.8 b) of the *CLN5* exons 2-4 sequence fragment (B) were revealed by agarose gel electrophoresis. After the second PCR, a sequence fragment with expected size of 1199 bp (Figure 2.8 c) was observed. Each PCR product was sequenced, and aligned 100% with the published *CLN5* coding sequence (NM_001082595).

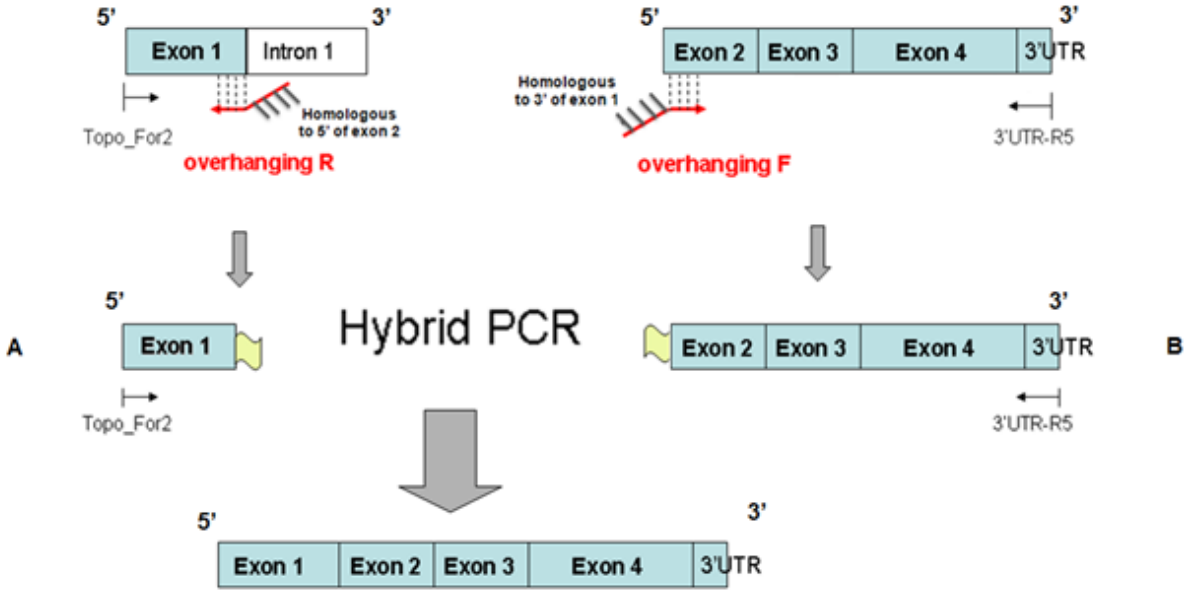

Figure 2.7 Generation of the full length ovine *CLN5* coding sequence using a two-step hybrid PCR

The first cycle consisted of two separate PCRs. Fragment A was amplified using *CLN5* exon 1 (generated as in section 2.2.3.2) as a DNA template, Platinum *Taq* polymerase (Invitrogen) and primer sets of CLN5_TOPO_For 2 (forward) and CLN5_Exon 1-2R long (reverse, overhanging R), designed from the 3' end sequence of exon 1, followed by a corresponding overhanging sequence homologous to the 5' end sequence of exon 2 (Table 2.1 and section 2.2.3.2). The fragment B was amplified with *CLN5* exons 2-4 (generated as in section 2.2.3.3), Qiagen *Taq* polymerase and primer sets of CLN5_Exon 1-2F long (forward, overhang F), generated with an overhanging sequences homologous to the 3' end sequence of exon 1, and the 5' end sequence of exon 2 and CLN5_3'UTR-R5 (reverse) (section 2.2.3.3). A second PCR ligated the two separate PCR products (A and B, containing internal overlaps over the exon 1-exon 2 boundaries) and amplified the resultant product using the primer sets of CLN5_TOPO_For 2 (forward) and CLN5_3'UTR-R5 (reverse) to obtain the full length coding sequence (section 2.2.3.2)

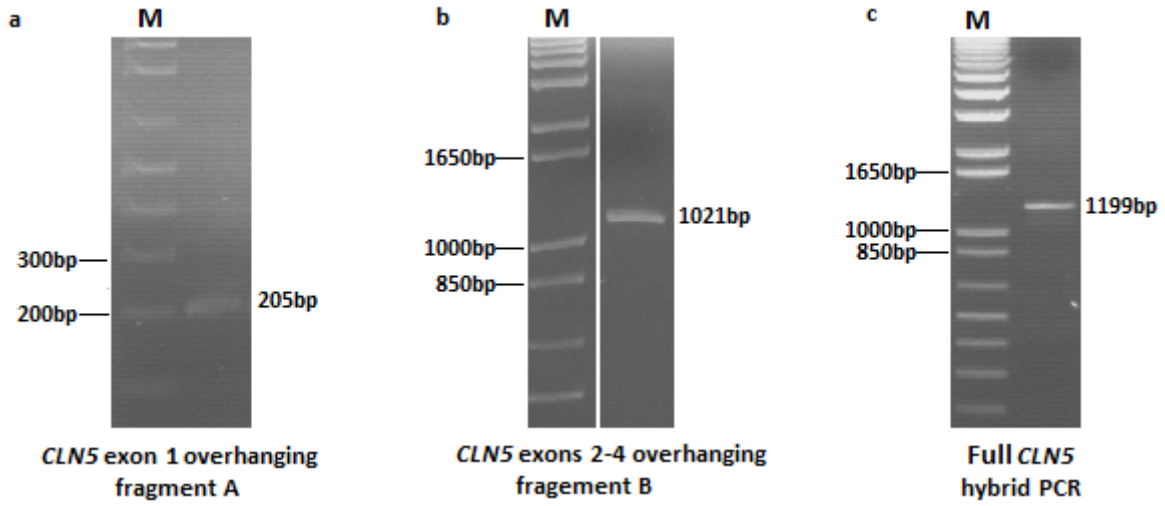

Figure 2.8 PCR amplifications of ovine *CLN5*

(a) *CLN5* exon 1 with overhanging 205 bp, (b) *CLN5* exons 2-4 with overhanging 1021 bp, and (c) full length *CLN5* 1199 bp. PCR products were run on 1.5% agarose gels and examined under UV light. The primers used in the reactions are listed in Table 2.1. M refers to the 1 kb Plus DNA Ladder.

2.3.1.4 Generation of the full ovine CLN6 coding sequence

The full length of ovine *CLN6* sequence was amplified using forward CLN6_OF and reverse CLN6_WTOR primers (Figure 2.1) and using *CLN6* complementary DNA from normal South Hampshire sheep as a template. A single PCR fragment of the expected size of 972 bp was apparent (Figure 2.9).

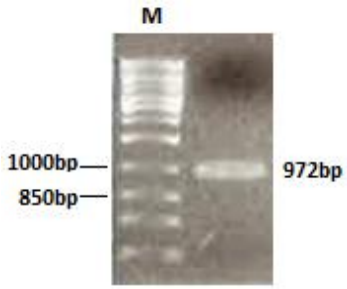

Figure 2.9 The full length ovine *CLN6* PCR products

PCR products were run on a 1.5% agarose gel and examined under UV light. The primers used are listed in Table 2.2. A 972 bp PCR product was observed. M refers to the 1 kb Plus DNA ladder.

2.3.2 Cloning ovine *CLN5* and *CLN6* coding sequences into pRUN for recombinant protein expression

The *CLN6* coding sequence containing a 6×His tag was easily generated and cloned into pRUN. However, sequencing of the CLN5his clones showed some random nucleotide base changes in exons 2 to 4 (Figure 2.10, indicated with underlines), which result in changes to two amino acids (Figure 2.10, indicated by black arrows). The change in the CLN5his clones 1

and 2 (Val87Met) resulted from a G to A transition at nucleotide 259. Another change in the CLN5his clones 2 and 3 (Leu1140Pro) resulted from a T to C transition at nucleotide 419. These changes could arise because the ovine *CLN5* gene sequences are toxic to the host during *E. coli* replication, causing mutated *CLN5* gene sequences to be amplified instead of normal ones. Other studies involving toxic proteins in *E. coli* are discussed in section 2.4.2. Sequencing showed that only one of the 8 CLN5his exons 2-4 clones had an identical protein sequence to the published ovine CLN5 (NP_001076064). Subsequently, these clones of pRUNCLN5his exons 2-4 and the pRUNCLN6his were transformed into C43 (DE3) *E. coli* cells specifically selected for protein expression.

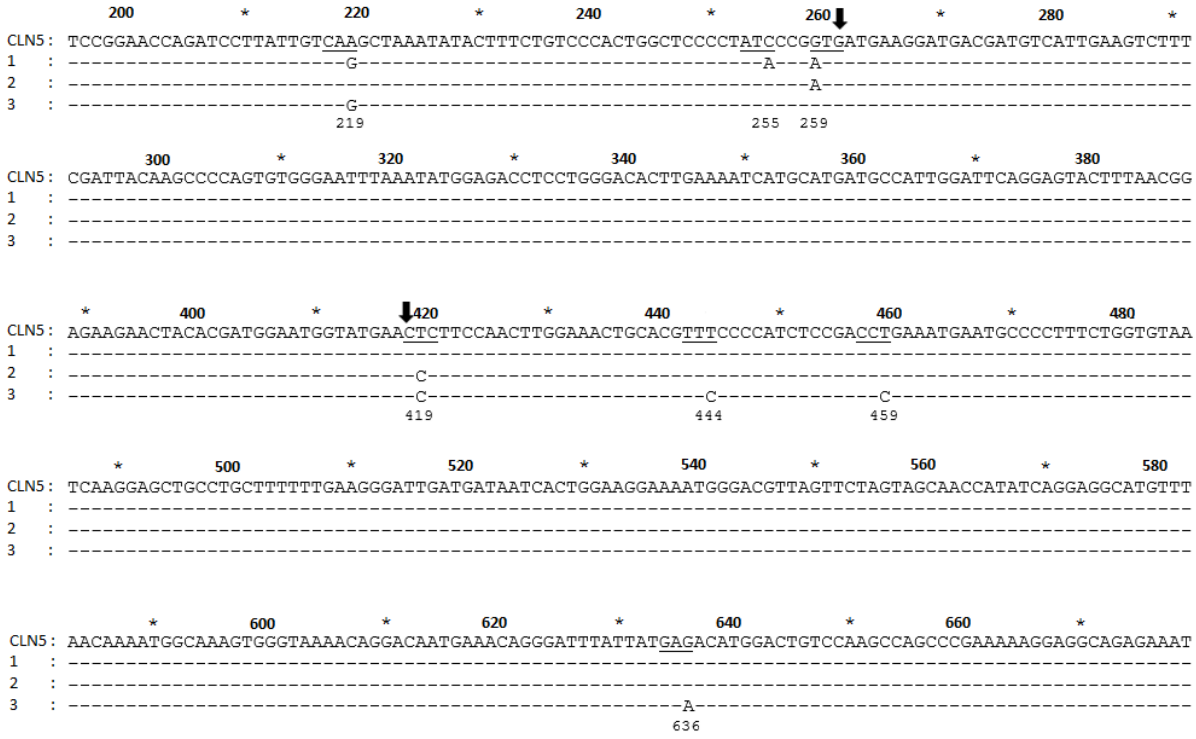

Figure 2.10 Sequence alignment of different pRUN CLN5his clones

Only the variable regions are shown in the three CLN5his clones (1, 2 and 3). A dash indicates identity with the 'true' pRUNCLN5his construct sequence (top). Silent changes in nucleotides are underlined, and arrows indicate changes in both nucleotides and amino acids. All the changed nucleotides are labelled with the numbers below referring to their positions.

2.3.3 pRUN-driven CLN5 and CLN6 protein expression was not successful

SDS-PAGE electrophoresis did not reveal any differences between all samples collected before and after induction (Appendix A.3.1), indicating that the target recombinant CLN5 and CLN6 proteins were not expressed in detectable quantities. Alternative protein

expression conditions were also tested, including a decrease in the cell growth temperature down to 25°C or 30°C after IPTG induction, and a decrease in the IPTG final induction concentration to 0.5 mM. Again no exogenous protein expression was detected by SDS-PAGE.

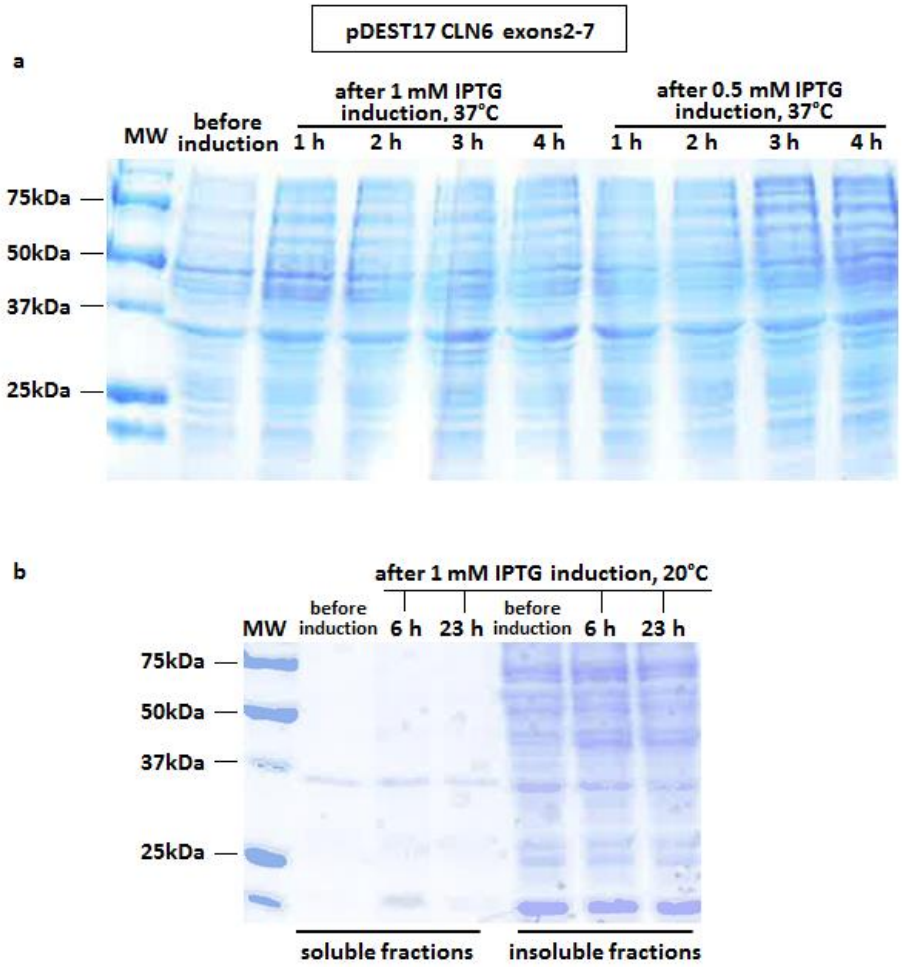

Figure 2.11 SDS-PAGE gel analysis of recombinant CLN6

For each protein sample, 30 µg, was run on a 12% acrylamide gel which was stained with Commassie blue. C43 (DE3) cells containing the CLN6 protein expression construct pDEST17 CLN6 exons 2-7 were grown at 37°C and then induced with 0.5 mM or 1 mM IPTG and incubated at (a) 37°C for 5 h or (b) 20°C for 23 h. The samples for analysis were collected just before the induction and (a) 1 h, 2 h, 3 h and 4 h post-induction or for (b) 6 h and 23 h post-induction incubation. MW refers to Precision plus protein standard.

2.3.4 Expression of the ovine CLN5 and CLN6 proteins by the Gateway expression system

Similar protein bands were visible on Coomassie stained polyacrylamide gels from CLN6his ex2-7 sample fractions from before and after IPTG induction (Figure 2.11), indicating that recombinant CLN6 protein was not expressed in detectable amounts. Any expression of

recombinant CLN5 proteins was minimal, as exogenous bands of the expected molecular weights of peptides were not detected on the gels. (Appendix A.3.2).

2.3.5 Cloning the full length *CLN5* coding sequence into a pCR4-TOPO vector

Successful cloning of the full length ovine *CLN5* sequence with and without a myc tag into pCR4-TOPO vector was confirmed by *Eco*RI restriction digestion. Two DNA fragments of the expected size of 3936 bp (vector) and 1217 bp (insert) (Figure 2.12) were observed from *Eco*RI digested pCR4-TOPO CLN5 plasmid DNA (5153 bp, generated as in section 2.2.7.2). Two DNA fragments with expected sizes of 3936 bp and 1238 bp (Figure 2.12) were revealed from *Eco*RI digested pCR4-TOPO CLN5myc plasmid DNA (5074 bp, generated as in section 2.2.7.2). Each plasmid DNA aligned 100% with the published *CLN5*, with and without myc sequences.

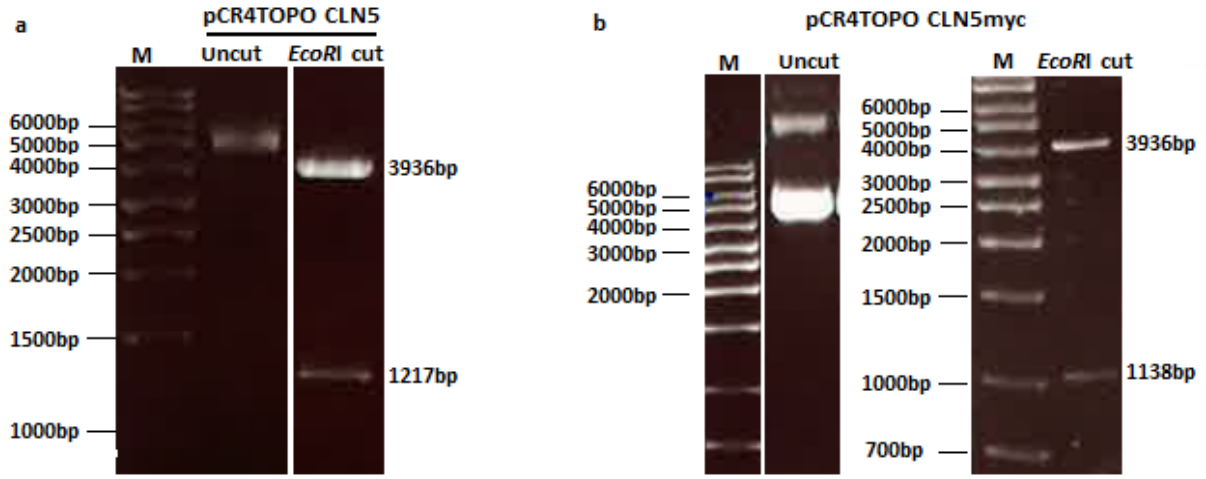

Figure 2.12 *Eco*RI digested pCR4-TOPO CLN5 and pCR4-TOPO CLN5myc plasmid DNAs

Undigested and *Eco*RI digested plasmid DNA were run on 1% agarose gel and examined under UV light. (a) Two bands of 3936 bp and 1217 bp were generated from pCR4-TOPO CLN5 DNA (5153 bp) after *Eco*RI digestion. (b) Two bands of 3936 bp and 1138 bp were generated from pCR4-TOPO CLN5myc DNA (5074 bp) after *Eco*RI digestion. M refers to the 1 kb DNA ladder (Axygen, NZ).

Subsequently, these successful clones were used for protein expression in a eukaryotic system (described in Chapter 3). The plasmid DNA of constructs pCR4-TOPO CLN5 and pCR4-TOPO CLN5myc were sent to Dr. Stephanie Hughes (Viral Vector Facility, University of Otago) for cloning into lentiviral vectors, which were then used to produce CLN5 proteins (see Chapter 3).

2.3.6 Genotyping the *CLN5* exon 1

2.3.6.1 PCR-SSCP analysis of ovine CLN5 exon 1

Amplification of the sheep exon 1 revealed two alleles (a and b) (see section 2.3.1.1). The b allelic sequence (406 bp) have five bases changes compared with the published a allele (426 bp) sequence (NM_001082595). PCR amplification of exon 1 of ovine *CLN5* from affected (n = 42), heterozygotes (n = 82) and unrelated control (n = 227) sheep blood genomic DNA also generated these two amplicons (426 bp and 406 bp) shown on agarose gels (Figure 2.13 a). The resultant three allelic patterns were revealed as follows. The aa alleles contained the 426 bp fragment, the bb alleles contained the 406 bp fragment, and the ab alleles contained both. No other bands were detected. Subsequently these PCR products were subjected to single strand conformation polymorphism (SSCP) analyses for DNA polymorphism detection. Because different ssDNAs fold differently, any base changes will be detected by the appearance of new bands, revealed by silver staining. Three SSCP patterns were observed, representing the three allele possibilities, aa, bb and ab (Figure 2.13 b). Variant aa had three dense bands, while variant bb had one major dense band.

Frequencies of the observed allele patterns were calculated across the sheep genotypes (Figure 2.13 c). All 42 affected sheep $CLN5^{-/-}$ PCR amplicons revealed only a single band of 426 bp in agarose gels (Figure 2.13 a) and a reproducible aa band pattern on SSCP analysis (Figure 2.13 b). Allele a aligned 100% with the published ovine *CLN5* sequence (Figure 2.5 a). Thus, all the affected sheep samples contained only aa alleles. The bb allele was not found in the 82 heterozygotes tested (Figure 2.13 c). All three allele possibilities were detected in 227 controls, aa, bb or ab, the overall control allele ratio being 17: 53: 30. Thus the aa alleles were present in the affected sheep samples, and in controls (38 out of the 227 normal sheep), therefore these allelic variations are not associated with the CLN5 disease.

a

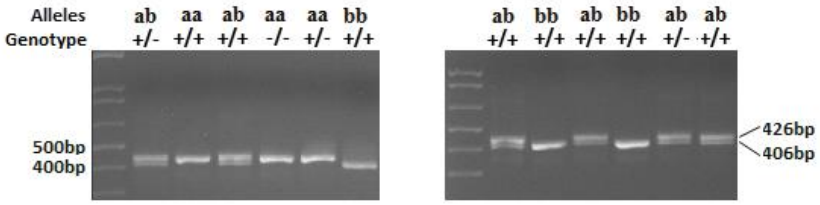

b

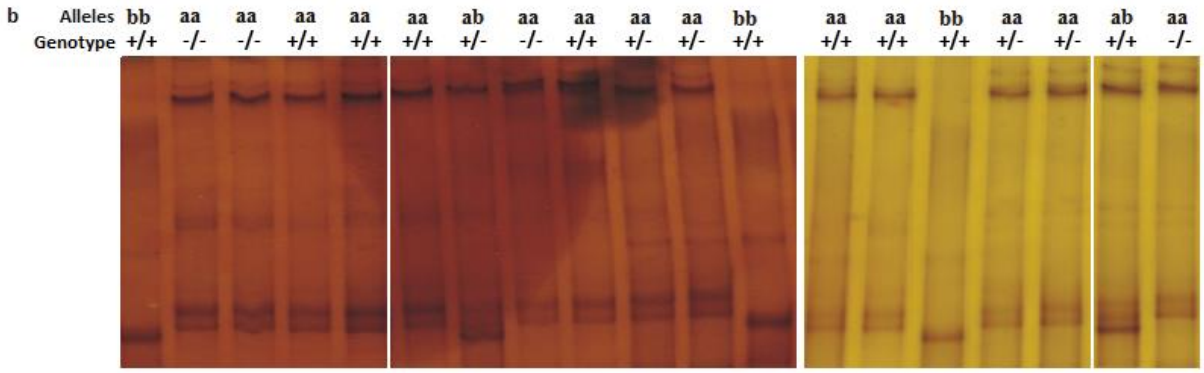

c

	Affected (-/-)		Carrier (+/-)		Normal (+/+)	
	Numbers	Ratio	Numbers	Ratio	Numbers	Ratio
Allele aa	42	100%	28	34%	38	17%
Allele bb	0	0%	0	0%	120	53%
Allele ab	0	0%	54	66%	69	30%
Total numbers	42		82		227	

Figure 2.13 Genotyping the PCR product of the ovine *CLN5* exon 1

(a) PCR of ovine *CLN5* exon 1. Three allelic variants in ovine *CLN5* exon 1 were detected - a 426 bp PCR product (aa allele), a 406 bp PCR product (bb allele) and a PCR product containing alleles a and b. **(b) Single strand conformational polymorphism of the ovine *CLN5* exon 1 gene.** Sheep DNA samples representative of the three unique SSCP patterns corresponding to three allelic sequences, aa, bb and ab, are shown. Amplicons were separated on 14% SSCP gels at 390 V, 19 h, 12°C. **(c) The percentages of different *CLN5* exon 1 alleles in New Zealand sheep.**

2.3.6.2 Sequencing the ovine CLN5 exons 2-4

Since allelic variations were found in ovine *CLN5* exon 1, the rest of the *CLN5* coding sequence (exons 2-4) was also examined. The *CLN5* exons 2-4 were amplified from nine genomic DNA samples containing exon 1 alleles aa, bb or ab. A single 907 bp band was present in all the tested samples (Figure 2.14). All these PCR products were sequenced and found to be the same as the published ovine *CLN5* coding sequence.

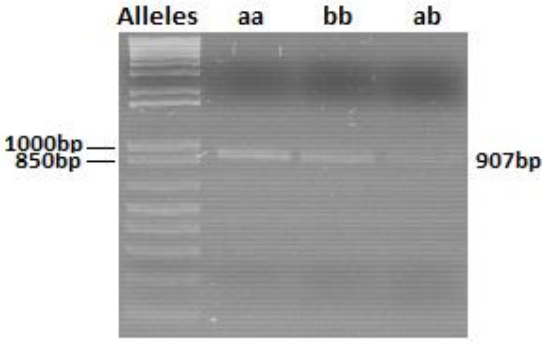

Figure 2.14 PCR amplification of the ovine *CLN5* exons 2-4

5 µl of each PCR product was run on 1.5% agarose gels and examined under UV-light. A 907 bp PCR product resulted from the use of the CLN5_Ex2F and CLN5_TOPO_Revstop primers from animals containing exon 1 alleles aa, bb and ab.

2.3.6.3 Examination of the bovine CLN5 exon 1

The unexpected occurrence of allelic variants in exon 1 of ovine CLN5 led to an examination of other species. PCR amplifications of bovine *CLN5* exon 1 from CLN5 affected Devon cattle (n = 2), heterozygotes (n = 12) and controls (n = 16) DNA generated a single expected fragment (437 bp) (Figure 2.15), which aligned 100% with the published bovine *CLN5* coding sequence (NM_001046299). Unlike ovine *CLN5* exon 1, direct sequencing of random bovine samples did not reveal any sequence variant changes in exon 1.

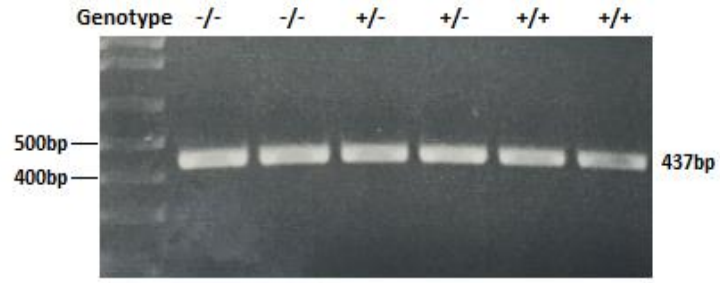

Figure 2.15 PCR amplification of the bovine *CLN5* exon 1

PCR products were run on 1.5% agarose gels. A 437 bp PCR product was amplified by using of the 5'UTRF7 and I1R2 primers.

2.3.6.4 Examination of the human CLN5 exon 1

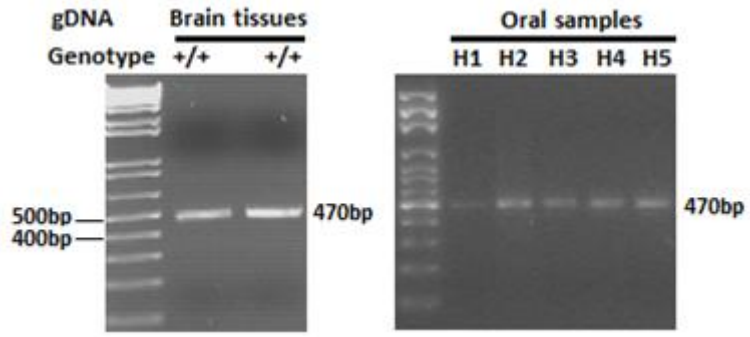

Figure 2.16 PCR amplification of human *CLN5* exon 1

PCR products were run on 1.5% agarose gels. A 470 bp PCR product was amplified by using the H1F2 and H1R1 primers.

The possibility of allelic variation in human CLN5 was also explored. A single band of the expected size (470 bp) was detected in all the *CLN5* exon 1 PCR amplicons from human samples; 53 anonymous human oral samples and 2 normal human brain tissue samples

(Figure 2.16). Direct sequencing confirmed that all amplified sequences aligned with the published human *CLN5* sequence (NM_006493), and revealed nucleotide substitutions in four locations (Figure 2.17, indicated by black underlines). The first involved a C to T substitution at nucleotide 4, resulting in an Arg to Cys change. The second also involved a C to T substitution at nucleotide 61, resulting in a change of Pro to Ser. The others substitutions were silent. However, all were located before the third ATG, which has been identified as the true start codon of the human *CLN5* (Isosompii et al., 2002, Frugier et al., 2008). There were no sequence variants present in the human *CLN5* exon 1 coding regions from all the tested samples, if the initiation site of human *CLN5* is the third ATG.

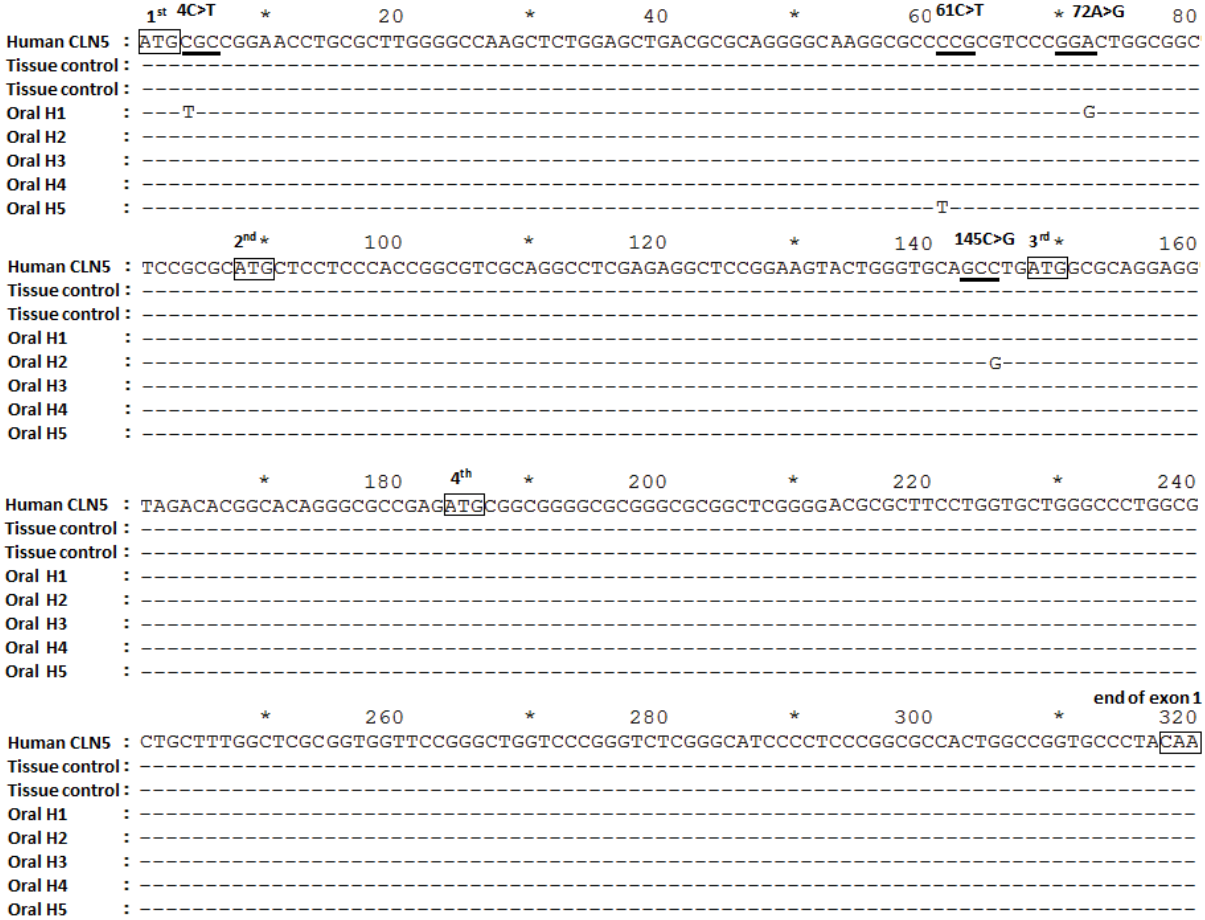

Figure 2.17 DNA sequence alignment of the human *CLN5* exon 1

Only variable regions are shown. A dash indicates identity with the top sequence, which is the published human *CLN5* coding sequence (NM_006493). The third ATG is the start of exon 1, and CAA is the end of exon 1.

2.3.7 Bioinformatics of the CLN5 interspecies comparison

The published *CLN5* ovine protein sequence (NM_001082595) was aligned to human (NM_006493), cattle (NM_001046299), dog (NM_00001011556), mouse (NM_001033242), predicted pig (XP_005668529), partial rabbit (XP_002712979) and chicken (XP_417005) sequences published on NCBI using Genedoc software (Figure 2.18). An inter-species

comparison showed that the GC-rich exon 1 is highly variable between species (in the pink box), whereas the rest of the coding sequence (starting from WPVPY…) is strongly homologous. Alignment of ovine CLN5 protein sequences also revealed a very high degree of homology to bovine (96%), and less homology to the pig (88%), dog (87%), human (84%), rabbit (80%), mouse (77%) and chicken (72%) *CLN5* sequences.

All the above species had an N-terminal hydrophobic region corresponding to amino acids 75-91 of the human CLN5 polypeptide (Holmberg et al., 2004), marked by a green line (Figure 2.18). The human CLN5 polypeptide is predicted to contain an N-terminal signal sequence, which is cleaved between amino acids 95 and 96 after entering the ER (Isosompii et al., 2002; Vesa et al., 2002). Mouse CLN5 also contains a signal sequence (Holmberg et al. 2004). A signal peptide prediction program SignalP V4.1 (http://www.cbs.dtu.dk/services/SignalP/) was used to predict the signal sequence cleavage sites (Figure 2.18, highlighted in yellow) in all the eight species. These were observed at almost the end of exon 1. The above predicted N-terminal signal sequences mediate targeting proteins to the ER in a signal recognition particle (SRP)-dependent manner. Signal sequences have a tripartite structure, consisting of a hydrophobic core region (h-region or single alpha-helix, Figure 2.18, marked by a green line) flanked by an n- (containing short positively charged amino acids) and a c-region that contains a signal peptidase (named cleavage site, Figure 2.18, marked by yellow highlight).

2.4 Discussion

2.4.1 Difficulties associated with cloning the full length ovine *CLN5*

Amplification of the full length ovine *CLN5* cDNA in one PCR reaction had not been done before. Previous studies relied on several pairs of primers which amplified the exons and introns separately to produce the ovine *CLN5* sequence (Frugier et al, 2008). All CLN5 mutation studies of other species, including humans (Bessa et al., 2006), cattle (Houweling et al, 2006), and dogs (Melville et al, 2005), also used several short PCR reactions to produce sequences.

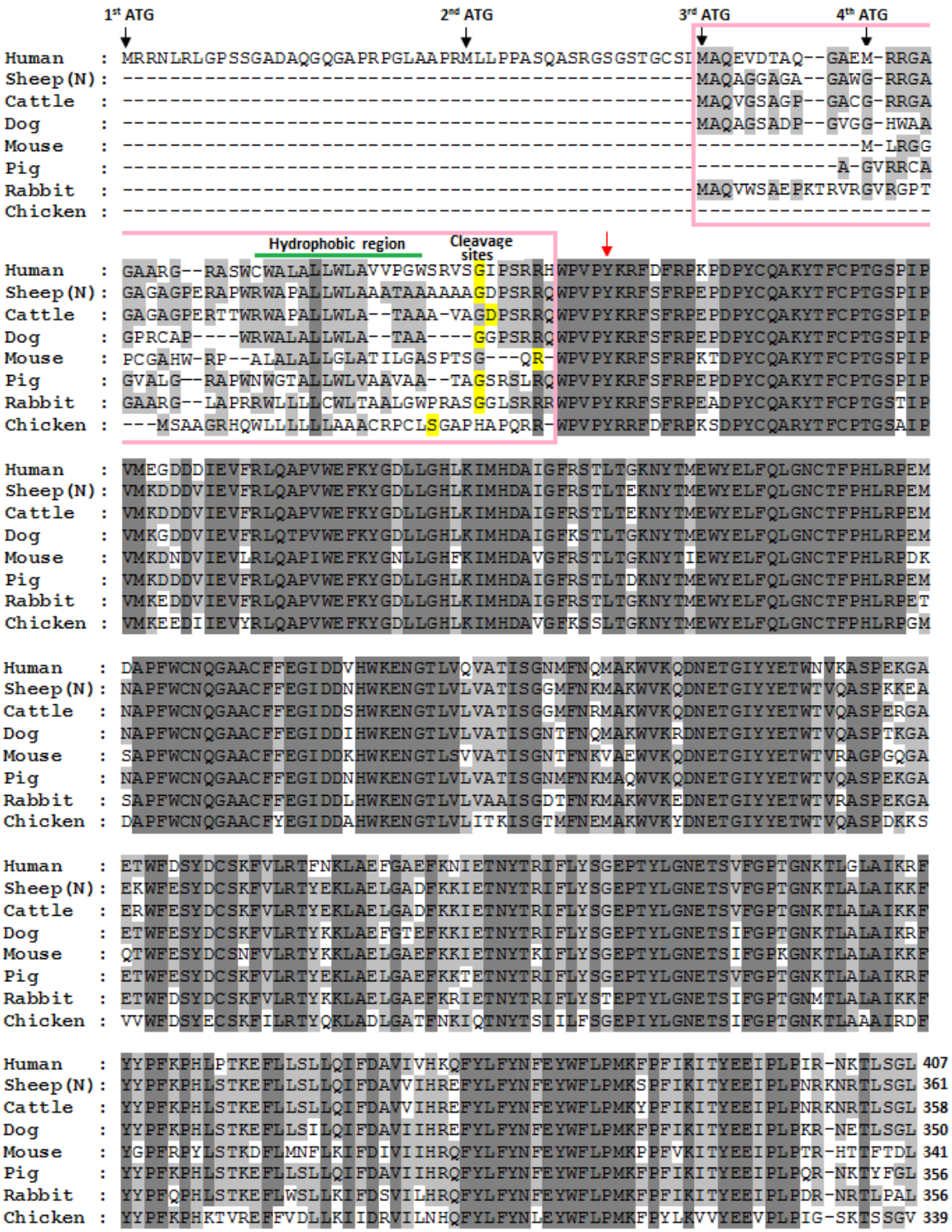

Figure 2.18 Alignment of human, sheep, cattle, dog, mouse, pig, rabbit and chicken CLN5 polypeptides

Black arrows indicate the four possible human initiation sites (M), the third of which has been identified as the actual initiation site (Isosompii et al., 2002), being the start codon of exon 1 of the other seven protein sequences. The end of exon 1 (Y) of all eight fragments is indicated by a red arrow. Pink regions indicate exon 1 of all species. Black or grey backgrounds indicate amino acids conserved in all or several species. The hydrophobic region of the predicted signal sequence is marked by a green line. The amino acids N-terminal to the predicted cleavage sites are highlighted in yellow. The predicted cleavage sites of human, sheep, dog, pig and rabbit protein sequences were glycine (G), aspartic acid (D) in cattle, arginine (R) in mouse and serine (S) in chicken. Modified from Frugier et al. (2008).

Difficulties in obtaining the full length cDNA in one PCR are likely caused by the disjunction in GC/AT ratios. *CLN5* exon 1 sequence contains a much higher percentage of G/C bases (around 80% in ovine) compared with exons 2-4. GC-rich DNA sequences are more stable for PCR than sequences with a low GC content; the higher the GC content, the higher the melting point of the DNA. Increasing the melting temperature could separate the GC rich regions, but results in very low product yields or even no PCR product (Strien et al., 2013), especially for whole coding sequence amplification perhaps, because the *Taq* enzyme begins to denature more rapidly after several of cycles.

To overcome this, a two-step PCR and ligation strategy was used here to generate the full length ovine *CLN5*. First, the GC rich *CLN5* exon 1 and the lower GC content exons 2-4 sequences were amplified separately (Figure 2.4, Figure 2.6 and Figure 2.7). Two separate PCRs were used to ensure that the two parts of the ovine *CLN5* coding sequence amplified correctly, and to produce adequate amounts DNA for templates for the next PCR. Second, the complementary internal overhanging forward primer (38 bp) and the internal overhanging reverse primer (34 bp) were quite long, which would assist annealing. The forward one was generated with an overhanging sequence homologous to the 3' end sequence of exon 1, followed by the 5' end sequence of exon 2; whereas the reverse one was designed from the 3' end sequence of exon 1, followed by a corresponding overhanging sequence homologous to the 5' end sequence of exon 2. After the exon 1 and exons 2-4 products were amplified separately using these overhanging primers, the two resultant fragments contained sequences with complementary ends at 3' end of the exon 1 fragment and 5' end of the exons 2-4 fragment (Figure 2.7), which helped *Taq* and primers to amplify the full coding sequence successfully in the final PCR reaction.

2.4.2 Attempted expression of recombinant proteins with pRUN and Gateway vectors

None of the attempts to produce recombinant proteins in prokaryotic systems were successful. These failures to express either CLN5 or CLN6 recombinant proteins may have been because of the toxicity of the target proteins, which might have caused bacterial cell death. The C43 (DE3) stain used in this study is originally a mutant strain of *E. coli* BL21 (DE3), and was developed to overcome the toxicity associated with overexpressing recombinant proteins using the T7 RNA polymerase expression system (Miroux and Walker,

1996). It has previously been shown to improve the stability of plasmids in culture during the expression of toxic proteins (Dumon-Seignovert and Vuillard, 2004).

In this study, the CLN5 clones produced only a few colonies on the agar plates, and all contained mutant *CLN5* sequences (Figure 2.10). This may result from the *CLN5* messenger RNA being toxic for C43 (DE3) cells causing growth inhibition. Previous studies also suggested that protein toxicity may arise when the recombinant protein performs an unnecessary function, which interferes with the normal proliferation and homeostasis of the host, resulting in a slower growth rate and cell death (Dong et al., 1995). However, the CLN5 mutant amplified messenger RNAs were clearly not too toxic to C43 (DE3) cells, as mutated CLN5 colonies were generated.

To help overcome this problem, an alternative method, expression of the full length CLN5 and CLN6 proteins in a eukaryotic expression system using mammalian cells (human embryonic kidney, HEK293) was attempted. Protein expression in bacteria can result in higher yields and lower costs, but the lack of chaperones, specific co-factors and post-translational modifications may cause loss of function, mis-folding, and thus affect protein-protein interactions (Wurm, 2004). Using a mammalian cell expression system could address these drawbacks. The details of protein expression using full length *CLN5* and *CLN6* coding sequences transfected into HEK293 cells are described in Chapter 3.

2.4.3 *CLN5* exon 1 allelic variants are not disease associated

PCR-SSCP analysis detected variants in the ovine *CLN5* exon 1 (Figure 2.13), but not in exons 2-4 (Figure 2.14). One allelic variant sequence (allele b) was only observed in heterozygote and control sheep. All the affected sheep had the published sequence (allele a), but this was also found in 38 unaffected sheep. Thus, this allelic variation is not associated with the CLN5 disease. This was the only variant detected in the current tested samples, but more variants may be found in other sheep.

In order to gain some idea of exon 1 variants in other species, bovine and human *CLN5* exon 1 sequences were also tested for possible allelic variations, and their association with NCL (Figure 2.15 and Figure 2.16). Naturally occurring CLN5 in cows (Houweling et al., 2006) presents with a disease course matching that of ovine CLN5, the causative mutation being a single base duplication (662dupG) in bovine *CLN5*. This mutation causes a frame-shift and a premature truncated protein (Arg221GlyfsX6). There are no *CLN5* exon 1 sequence changes

reported in cattle, and the random bovine samples tested in the current research did not have any variants in exon 1.

Human *CLN5* shows 84% sequence similarity to the sheep gene, the greatest difference being in exon 1 (Figure 2.18). The human *CLN5* coding sequence contains four possible ATG initiation sites. Initially, the first ATG was suggested as the initiator (Savukoski et al., 1998), and then the fourth ATG was considered the major initiation site, leading to a 38 kDa protein (Isosompii et al., 2002). Later studies suggested that the human CLN5 polypeptide has an N-terminal signal sequence, which is cleaved off between amino acids 95-96 (Isosompii et al., 2002; Vesa et al., 2002). After the full alignment of human, mouse, canine, bovine and ovine *CLN5* cDNA sequences, it was concluded that the third human ATG is the conserved start codon (Frugier et al., 2008). Previously, variants have been reported in the human *CLN5* exon 1. Only one silent nucleotide change (72A>G) in exon 1 was found in a JNCL patient who had a mutation in exon 4 which caused a Phe361Leufs (Xin et al., 2010). Direct sequencing of 55 random human samples in this study revealed nucleotide substitutions in four locations in exon 1, two of which involved translation changes (Figure 2.17, Arg11Cys and Pro33Ser), however all the changes are located before the real start of the human *CLN5*.

Naturally occurring CLN5 in dogs (Melville et al., 2005) have a mutation which results in a frame-shift and prematurely truncated protein (Arg221GlyfsX6). The disease in affected Border Collie dogs (Melville et al., 2005) and Australian Cattle Dogs (Kolicheski et al., 2016) is caused by a single nucleotide change at 619 bp in exon 4 of the *CLN5* coding sequence. This transition results in replacement of Gln209 with a stop codon. No other sequence changes have been reported in dog *CLN5* exon 1.

2.4.4 The relationship between *CLN5* exon 1 allelic variants and mutant CLN5 clones

Inter-species comparison revealed that the *CLN5* exon 1 is highly variable between species, whereas the rest of the coding sequence is highly conserved (Figure 2.18). All of the species studied have a predicted N-terminal signal sequence, which typically directs the newly synthesized protein to the endoplasmic reticulum and is cleaved off either during or after completion of translocation to generate a free signal peptide and a mature protein. Signal sequences are variable in length and amino acid composition, and variability of the signal sequence affects interactions with the translocon or efficiencies of the targeting protein insertion into the ER membrane (Hegde and Bernstein, 2006). In this study, all the CLN5

clones generated had DNA sequences containing only the aa allele variant in exon 1, and PCR-SSCP analysis found that all the affected sheep samples contained only aa alleles, not bb or ab alleles (Figure 2.13 c). Signal sequence binding is mediated primarily by the signal recognition particle and the hydrophobic region, then further translation directs the signal sequence-ribosome-mRNA complex to the SRP receptor. This study found that the differences between the a and b alleles were three amino acid changes in this hydrophobic region (Figure 2.18).

2.5 Conclusion

Successful expression of full length recombinant ovine CLN5 and CLN6 proteins in an *E. coli* prokaryotic system is unlikely. Without the expressed proteins, the originally planned study could not be carried out. The plan of the study was to generate CLN5 and CLN6 antibodies by inoculation of recombinant proteins as antigens into chickens, to subsequently produce IgY antibodies. Therefore, CLN5 and CLN6 protein expression experiments were attempted in eukaryotic systems (Chapter 3).

Chapter 3
Expression of CLN5 and CLN6 proteins in mammalian cells and characterisation of polyclonal antibodies raised against these proteins

3.1 Introduction

Highly specific and sensitive antibodies are critical tools for biological research and diagnostics, however this is a time-consuming and often frustrating process. Traditionally, polyclonal antibodies that are raised against proteins are generated by injection of a peptide or purified protein (as antigen) together with an immunogenic adjuvant (e.g. Freund's adjuvant) into a host animal. Antigens are commonly generated by synthesising antigenic peptides or by purifying recombinant proteins or fragments from *E. coli*. Even when this is possible some putative antigens remain difficult, particularly ones like lysosomal proteins that are often highly conserved and have a close association with the MHC II- antigen presentation system. One way around this has been to clone the sequences for the antigens of interest into the mycobacterium, Bacillus of Calmette–Guérin (BCG), which acts as an inbuilt adjuvant and vehicle for *in vivo* protein expression. This system has been used to produce immunity against many antigens, including the endosome-dwelling parasite, *Leishmania major* (Abdelhak et al 1995).

However, neither of the CLN5 or CLN6 proteins could be expressed in prokaryotic *E. coli* systems (Chapter 2). Bacterial expression systems have no capacity to perform eukaryotic post-translational modifications such as glycosylation and proper folding (Palomares et al., 2004). As an alternative, recombinant protein expression in mammalian cells has been developed. Human embryonic kidney (HEK293) cells provide a popular mammalian heterologous expression system with reliable growth and transfection characteristics (Graham et al., 1977, Thomas and Smart, 2005). HEK293FT cell lines, suitable hosts for lentiviral production, are derived from HEK293 cells, and can bind to the SV40 large T antigen which can increase protein production (ThermoFisher Scientific, growth and maintenance of the 293FT cell line guide).

Lentiviruses, a family of complex retroviruses, are often used to derive vectors for gene therapy. Use of lentiviral vectors has been considered one of the most efficient methods of

gene delivery for lysosomal disorders, showing persistent transgene expression in mouse models (Brooks et al., 2002; Haskell et al., 2003; Linterman et al., 2010). Lentiviral vectors can generate recombinant target proteins quickly and efficiently, under tight promoter control (Brooks et al., 2002; Sands and Davidson, 2006). Strong CLN6 expression resulted from using a lentiviral vector containing the ovine *CLN6* coding sequence fused with a myc tag at the C-terminus into sheep neural cell cultures (Linterman et al., 2011).

Adenoviral vectors provide another widely used gene transfer tool, and can produce a good adjuvant for antibody generation, when used to overexpress the target antigen *in vivo* (Rein et al, 2006). This is a straightforward method for generating antibodies against soluble and membrane proteins, as the protein purification step can be eliminated. Rabbits and mice are the most widely used animals. Previous studies have used adenoviral-based techniques to generate CLN2 (TPP1) antibodies by injecting a recombinant adenovirus into rabbits (Haskell et al., 2003) and similarly CLN3 antibodies have been raised in mice (Tecedor et al, 2013).

In the study described in this chapter, lentiviral vectors expressing the full length *CLN5* and *CLN6* coding sequences under the control of the MND promoter were packaged and transduced into HEK293FT cells, and the over-expressed recombinant CLN5 and CLN6 proteins with no tags produced from these stable cell lines were used to test the specificities of antibodies. Full length *CLN5* and *CLN6* sequences without tags were packed into adenoviral expression vectors, transduced in HEK293FT cells for protein expression, and used as antigens injected into rabbits and mice to raise antibodies. The specificities and sensitivities of these antibodies were characterised by immunocytochemistry, Western blotting and mass spectrometry.

3.2 Methods

3.2.1 Generation of stable HEK293FT cell lines by lentiviral transduction for CLN5 and CLN6 recombinant protein expression

3.2.1.1 Lentiviral constructs

Four plasmids, pCR4-TOPO CLN5 and pCR4-TOPO CLN5myc (generated as in section 2.3.5), pcDNA3.1D TOPO CLN6 and pcDNA3.1D TOPO CLN6myc (generated by Dr. Nadia Mitchell), were used to generate lentiviral vectors. Lentiviral vectors expressing these transgenes were produced with Batten Animal Research Network (BARN) collaborators, led by Dr. Stephanie

Hughes at the Otago Viral Vector Facility, University of Otago, under approval from ERMA New Zealand (GMD03091).

In short, HIV-1 derived lentiviral plasmids (Meyerrose et al., 2008) expressing ovine *CLN5* (NM001082595) and ovine *CLN6* (NM001040289), fused with, or without C-terminal myc tags under the control of the myeloid sarcoma virus U3 element (MND), were packaged (Zufferey et al., 1998). HEK293FT cells (Life Technologies, Carlsbad, CA, USA) were transfected with plasmids containing the NCL transgenes, packaging and VSV-G envelope genes (Zufferey et al., 1998) in serum-free OptiMEM serum media (OptiMEM, GIBCO, Invitrogen, NZ) containing Lipofectamine-2000 (Invitrogen, NZ) (Linterman *et al*., 2011). The medium was recovered 48 hours post-transfection, concentrated, resuspended in PBS containing 40 mg/ml lactose, and viral vectors were stored at -80°C in cryogenic vials. These functional viral vectors were named LVMNDCLN5myc, LVMNDCLN5, LVMNDCLN6myc and LVMNDCLN6. A viral vector, called LVMNDGFP, encoding a GFP (green fluorescent protein) reporter gene was used as a positive control for transduction.

3.2.1.2 HEK293FT cell culture

The lentiviral vectors (3.2.1.1) were used to generate stable cell lines in HEK293FT cells. A cryovial of HEK293FT cells was transferred into a T25 flask (Nunc, NZ) containing 5 ml of pre-warmed Dulbecco's modified Eagle medium (DMEM, GIBCO, Invitrogen, NZ), and incubated at 37°C in a humidified atmosphere containing 5% CO_2. Once cells reached 70-80% confluence the culture medium was removed and the cells were rinsed with Dulbecco's phosphate buffered saline solution (dPBS, GIBCO, Invitrogen, NZ). Cells were disassociated from the bottom of the flask with 0.05% trypsin EDTA (1.5 ml, Tryple E, Invitrogen, NZ), 5 min, 37°C, followed by 3.5 ml of pre-warmed DMEM complete medium to terminate the trypsin reaction. Cell counts were determined using a haemocytometer after the addition of trypan blue dye (Sigma Aldrich, NZ) at a 1:1 ratio. Healthy live cells were round and clear, whereas the dead cells were filled with the blue dye. The HEK293FT cells were then passaged into either flasks or plates at the desired density.

3.2.1.3 Transduction of lentiviral vectors and generation of HEK293FT cell lines

To obtain stable, long-term CLN5 and CLN6 expression, HEK293FT cells were transduced with the lentiviral vectors generated in 3.2.1.1. The cells were grown in T75 flasks (Nunc, NZ) until 40% confluence, and maintained in half changed media. Each vial of the five concentrated viruses was removed from the freezer and thawed to room temperature. Transduction was

achieved by direct administration of virus to the media at an estimated multiplicity of infection (MOI) of 100 (viral transduction units/cell), followed by gentle mixing, and a further 24 h incubation, 37°C. The five generated cells lines were named as 293FT LVMNDCLN5myc, 293FT LVMNDCLN5, 293FT LVMNDCLN6myc, 293FT LVMNDCLN6, 293FT LVMNDGFP. When 70% confluence was reached, the generated cells were dislodged (as described in section 3.2.1.1). Half of the cell suspensions were frozen in DMEM containing 10% DMSO (Sigma, NZ) and aliquoted into several vials (2×10^6 cells/vial), stored at -80°C overnight, and then transferred to liquid nitrogen for long term storage as stocks. The remaining cells were repeatedly passaged in DMEM, and incubated for 24 h in OptiMEM media before immunocytochemistry, Western blotting and mass spectrometry.

3.2.1.4 Immunolocalisation of myc tagged CLN5 and CLN6 proteins

Cells of 293FT LVMNDCLN5myc and 293FT LVMNDCLN6myc (3.2.1.3) were plated onto poly-L-lysine treated 6-well plates (Nunc, NZ) at 9×10^5 cells/well and maintained until 70% confluence. 293FT LVMNDGFP cells were used as a transduction control, allowing detection of virus transduction success by the detection of GFP under the fluorescent microscope. The cells were washed briefly in dPBS, and fixed in 4% paraformaldehyde (PFA), 15 min. The plates were used immediately or sealed with Parafilm (Sigma Aldrich, NZ), wrapped in foil and stored at 4°C.

After a brief wash in dPBS, the cells were incubated with 300 µl/well blocking buffer, 3% normal goat serum (NGS, Sigma, NZ) in PBST (PBS, pH7.4, containing 0.2% Triton X-100), 30 min, room temperature, followed by incubation with mouse anti-myc (ab18185, Abcam, Cambridge, UK) diluted 1:1000 in blocking buffer, 4°C, overnight. Cells were washed, 3 × 30 min, with PBST before incubation with the secondary antibody, goat anti-mouse Alexa 594 conjugated antibody (A11005, Invitrogen, NZ) diluted 1:1000 in blocking buffer, room temperature, 4 h. Unbound antibody was removed with another 3 × 30 min washes with PBST, and the cells were refreshed in 0.1 M sodium phosphate buffer (PB) pH 7.2. Cells were mounted on glass, with ProLong Gold antifade reagent (P36930, Invitrogen, NZ), cover-slipped, and images taken with an Olympus IX71 inverted fluorescent microscope fitted with a DP71 camera using the 40× and 60× objectives. For long term storage, the borders of coverslips and slides were sealed with nail varnish and the slides stored at 4°C in a lightproof slide box.

3.2.1.5 Extraction of CLN5 and CLN6 proteins, with or without myc tag, from HEK293FT cells

All the generated cells (3.2.1.3) were plated as previously described in section 3.2.1.4. The cells were incubated until 70% confluence in DMEM, then for 24 h in serum-free OptiMEM. Proteins were extracted from both media and cells for Western blot analysis. To extract CLN5myc and CLN5 proteins, media generated from 293FT LVMNDCLN5myc and 293FT LVMNDCLN5 cells were collected and concentrated 25- fold through a 10 kDa cut-off centrifugal filter device (Amicon Ultra 0.5, Millipore, Thermo Fisher) by centrifugation, 30 min, 17,000 *g*, 4°C. To test for CLN5 in cells, the cells were lysed with 100 µl of protein lysis buffer (4% w/v SDS, 20% v/v glycerol, 100 mM Tris pH 6.8) on ice, 20 min, boiled, 5 min, then gently homogenised by passing 5-10 times through a 25 gauge needle on a 1ml syringe. 293FT LVMNDGFP cells, as a negative control, were lysed as above.

Media generated from 293FT LVMNDCLN6myc and 293FT LVMNDCLN6 cells were collected, and centrifuged as above. The stable cells were lysed using ice-cold 1% n-dodecyl-β-D-maltoside (DDM, Glycon Biochemicals, Luckenwalde, Germany) in 0.5 M Tris pH 7.4 and kept on ice, 20 min. The supernatant was collected by centrifugation, 30 min, 17,000 *g*, 4°C. Protease inhibitors, phenylmethyl-sulphonyl fluoride (PMSF 1 mM, Sigma, NZ) and EDTA (1 mM) were added to all media and cell lysis buffers. Aliquoted samples for Western blotting and immunocytochemistry were stored at -80°C.

3.2.1.6 SDS-PAGE electrophoresis and Western blotting

The general process of SDS-PAGE is described in section 2.2.5.2. To prepare protein samples for loading, 30 µg of lysed cells or 10 µl of concentrated media were dissolved in protein sample buffer (protein lysis buffer with freshly added 200 mM DTT and 200 mM bromophenyl blue) and denatured at 70°C, 10 min. The proteins were separated on 10% poly acrylamide gels (80 V, 20 min, followed by 120 V, 1.5 h) and then transferred to Hybond PVDF membranes (GE Healthcare, UK), 100 V, 1 h, in a BioRad Mini Trans-Blot on ice using ice-cold transfer buffer and a cooling unit. The membranes were blocked in TBST (TBS, 0.1 M Tris-HCl, pH 7.2, 0.05% Tween 20), containing 5% skim milk powder, 1 h. This and all subsequent steps were carried out on a shaking platform, 40 rpm, followed by 3×10 min washes in TBST. Membranes were incubated in the primary antibody (1:2000 diluted in TBST) overnight, 4°C, washed, then incubated in the secondary antibody (sheep anti-mouse HRP, NXA931, GE Healthcare, UK, 1:10,000 diluted in TBST), 2 h. After washing in TBST, 3×10 min, antigens were detected by chemiluminescence (ECL), 5 min, using ECL-Plus reagents

(GE Healthcare, UK) and protein bands visualised using a Fujifilm LAS-3000 imager (Fuji, Valhalla, NY).

3.2.2 Optimisation of CLN5 and CLN6 antibodies generated from adenoviral vectors in stable cell lines

3.2.2.1 Generation of polyclonal CLN5 and CLN6 antibodies

The rabbit and mouse sera raised against CLN5 and CLN6 were produced by the laboratory of Dr Stephanie Hughes at University of Otago and ViraQuest Inc., North Liberty, USA, under approval from ERMA New Zealand (GMD 200732). In summary, the coding sequences of full length ovine *CLN5* and *CLN6* (sourced as in section 3.2.1.1) were cloned into adenoviral shuttle plasmids under the control of the CMV promoter. The shuttle plasmids containing the target genes were then transfected into HEK293FT packing cells. Adenoviruses containing CMVCLN5 and CMVCLN6 were amplified by serial passages on HEK293FT cells and purified, then injected into New Zealand white rabbits in a single ear vein injection or into Swiss Webster mice with a single injection into the tail vein. The rabbits were pre-bled before inoculation and blood collected 30 and 50 days post-injection. Mice were bled two months post-injection. Sera prepared post-coagulation were stored at -20°C.

3.2.2.2 Characterisation of anti-CLN5 and anti-CLN6 sera by Immunocytochemistry

The general methods for characterisation of anti-CLN5 and anti-CLN6 sera are described in section 3.2.1.4. 293FT LVMNDCLN5 and 293FT LVMNDCLN6 cells were plated onto poly-L-lysine treated 24-well plates (Nunc, NZ) at 4×10^4 cells/well and maintained until 70% confluent. The cells were fixed, blocked, and treated with primary rabbit anti-CLN5/CLN6 or mouse anti-CLN5/CLN6 antibodies at dilutions of 1:500 and 1:1000 in blocking buffer overnight, 4°C. Cells were washed 3 × 30 min with PBST before incubation with goat anti-rabbit Alexa 488 (green, A11008, Invitrogen, NZ) or goat anti-mouse Alexa 488 (green, A11001, Invitrogen, NZ) conjugated secondary antibodies, diluted 1:1000 in blocking buffer, 4 h. Following immunolabelling, cell nuclei were stained with 4', 6-diamidino-2-phenylindole (DAPI, 1 mg/ml stock, Sigma Aldrich, NZ), diluted to 1:10,000 in PBS, 5 min, and washed with PBS. Cell media were then replaced with 0.1 M PB before the cells were mounted onto glass, cover-slipped with ProLong Gold antifade reagent, and imaged with a fluorescence microscope. The green (488 nm) or red (594 nm) fluorescence channels were used to compare the staining intensities at each dilution, thus to determine the optimal antibody concentrations. Appropriate negative controls (without primary antibodies) were included in all staining methods.

3.2.2.3 Western blot analysis of anti-CLN5 and anti-CLN6 antibodies

The general processes for Western blot analysis of anti-CLN5 and anti-CLN6 antibodies are described in section 3.2.1.6. CLN5 and CLN6 protein samples from the 293FT LVMNDCLN5 and 293FT LVMNDCLN6 cells (3.2.1.3) were extracted and quantified. Two 10% SDS gels were prepared. One gel was loaded with 30 µg of CLN5 lysed cells and 10 µl of CLN5 concentrated media, and the other gel was loaded with 30 µg of CLN6 cells dissolved in DDM. Each set of samples was duplicated on each gel and transferred to PVDF membranes. Each membrane was blocked, and cut in half vertically. The halves were incubated separately overnight, 4°C, in one of the four primary antibodies (1:500 dilution of rabbit anti-CLN5, mouse anti-CLN5 and mouse anti-CLN6; 1:1000 dilution for rabbit anti-CLN6). Following 3 × 10 min washes with TBST, each blot was incubated with donkey anti-rabbit HRP (NXA934, GE Healthcare, UK) or donkey anti-mouse HRP (NXA931, GE Healthcare, UK) (1:5000 dilution for CLN5 and 1:10,000 dilution for CLN6), 2 h. Washing steps were carried out as above, before 5 min ECL detection.

3.2.2.4 Mass spectrometry analysis of ovine CLN5 and CLN6 proteins using anti-CLN5 and anti-CLN6 antibodies raised in rabbits

Mass spectrometry was used to identify the ligands to which the rabbit anti-CLN5 and anti-CLN6 adenoviral antibodies bound to the SDS-gel bands from stably transduced HEK293FT cell lines. SDS-PAGE gels of proteins from these cells were stained with colloidal Coomassie blue G-250 (Sigma Aldrich, St. Louis, MO, USA). However, the yields of proteins at the anticipated molecular weights were too low to result in clearly stained bands. In order to cut the correct spot of the gels for mass spectrometry, protein bands were identified by Western blotting of parallel gel lanes and the equivalent areas cut from the Coomassie stained gel.

Concentrated CLN5 media, 50 µl and 170 µg of CLN6 cell samples (as used in section 3.2.2.3) along with the protein marker were loaded onto half of a 10% SDS-PAGE gel for colloidal Coomassie blue G staining (Figure 3.6). Concentrated CLN5 media, 10 µl and 30 µg of CLN6 lysed cells were similarly loaded onto the other half of this gel for Western blotting. Immediately following electrophoresis, the gel was cut in half. The half with the protein marker was fixed overnight in 50% (v/v) ethanol and 3% phosphoric acid (v/v). After 3× 30 min washes with distilled water, the gel was equilibrated in 34% methanol (v/v), 3% phosphoric acid (v/v) and 17% (w/v) ammonium sulphate, 1 h, before the addition of 0.025 g Coomassie blue G-250 powder. Equilibrium staining was achieved after 1 day, and

terminated with three 3× 30 min washes with distilled water. The second half of the gel was Western blotted, and bands were detected with rabbit antisera raised as described in section 3.2.2.3.

Areas were cut out from the Coomassie stained gels at the appropriate sites of CLN5 and CLN6 as indicated from the Western blotting and processed for mass spectrometry at the Centre for Protein Research, University of Otago. Briefly, the gel areas were digested with sequencing grade modified trypsin (Promega, Madison, WI, USA) using a robotic workstation for automated protein digestion (DigestPro Msi, Intavis AG, Cologne, Germany). Eluted and dried peptides were analysed by liquid chromatography-coupled LTQ-Orbitrap mass spectrometry (Thermo Scientific, San Jose, CA, USA). Raw data were processed through Proteome Discoverer software v1.3 (Thermo Scientific, San Jose, CA, USA) and a Mascot search engine (Matrix Science; http://www.matrixscience.com/), searching against the SwissProt amino acid sequence database, which contains the predicted ovine CLN5 and CLN6 sequences.

3.2.2.5 Post-translational CLN5

To study CLN5 glycosylation, CLN5 protein was deglycosylated by two enzymes; endoglycosidase H (Endo H, New England Biolabs, Ipswich, MA, USA) and peptide N-glycosidase F (PNGase F, New England Biolabs). Concentrated CLN5 protein media, 2 µl, was mixed with 1 µl of 10× glycoprotein denaturation buffer and 9 µl of water. Each reaction mix was denatured at 100°C, 10 min, before incubation with 50 units of Endo H or 125 units of PNGase F according to the instructions, 37 °C, 1 h. Control samples were similarly incubated in appropriate buffers without the addition of the glycosidases. Digested protein samples and controls were separated by SDS-PAGE and visualised by immunoblotting for mass spectrometry.

3.3 Results

3.3.1 Lentiviral-mediated expression of ovine CLN5myc and CLN6myc proteins

In an initial experiment, recombinant lentiviral expression vectors containing ovine *CLN5* and *CLN6* cDNA sequences fused to a C-terminal myc tag were used to generate transduced HEK293FT cell lines and express the proteins for molecular analyses. Expressions of CLN5myc

and CLN6myc were indicated by immunocytochemistry for the myc-tag. Molecular masses of the expressed myc tagged proteins were confirmed by Western blotting.

3.3.1.1 Immunocytochemistry of expressed CmvLN5myc and CLN6myc proteins

A GFP control virus was transduced into HEK293FT cells to check transduction efficiency. Fluorescence microscopy detected GFP expression and confirmed transduction (Figure 3.1 a). Anti-myc antibody staining of transduced HEK293FT cells containing myc tagged CLN5 (Figure 3.1 b) or CLN6 (Figure 3.1 c) was revealed by red immunofluorescence in the cytoplasm. Anti-myc staining was not visible in non-transduced HEK293FT cells. These results indicated that the cell lines transduced with the CLN5myc and CLN6myc lentiviral expression vectors expressed recombinant protein within the cells.

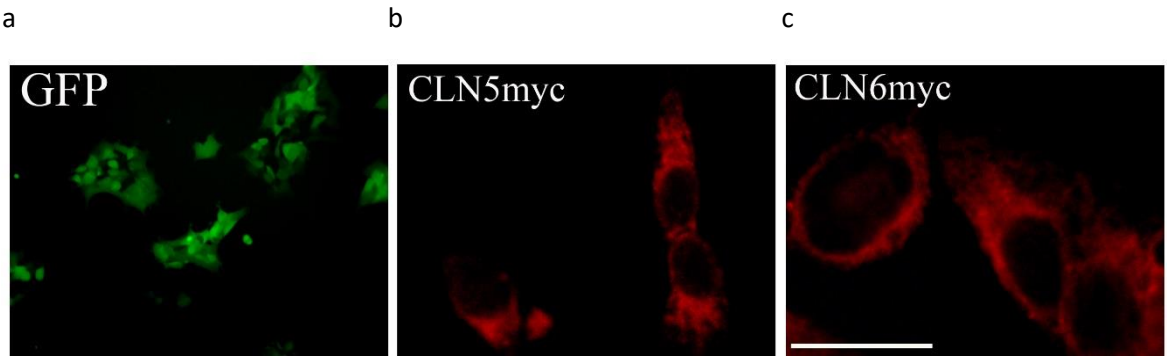

Figure 3.1 Immunofluorescent images of proteins expressed in transduced HEK293FT cells
(a) GFP expression (b) CLN5myc and (c) CLN6myc expression. Lentiviral transduction was detected with anti-GFP (green, 1:500) or mouse anti-myc (red, 1:1000). The scale bar represents 200 µm for CLN5myc (b) and 100 µm for CLN6myc (c) and GFP (a) cells.

3.3.1.2 Western blotting of expressed CLN5myc and CLN6myc proteins

The protein samples used for Western blotting of expressed CLN5myc and CLN6myc proteins were CLN5myc from cells and concentrated media, CLN6myc from cells and concentrated media, and GFP from cells (as a negative control). Western blotting using the mouse anti-myc antibody revealed a single prominent immunoreactive band of 29 kDa in cell extracts from CLN6myc transduced cells (Figure 3.2). The size of this band is similar to that of the human CLN6myc protein transiently expressed in BHK21 cells (Mole et al. 2004). However, no such band was evident in the CLN6myc media indicating that the CLN6myc protein was not secreted. CLN5 was detected by the anti-myc antibody in both CLN5myc media (secreted fractions) and CLN5myc cell extracts at apparent molecular weights of approximately 60 kDa

(Figure 3.2), similar to the full length human CLN5 protein found in media of overexpressing BHK cells (Isosomppi 2002). This size is consistent with the anticipated mass of the CLN5myc tag construct, and also similar to that of the mature human CLN5 protein (Sleat et al. 2006) A strongly stained CLN5myc band was observed in the media, but the band from the solubilized CLN5myc cells was faint, indicating that most of the synthesised CLN5myc was secreted into the media.

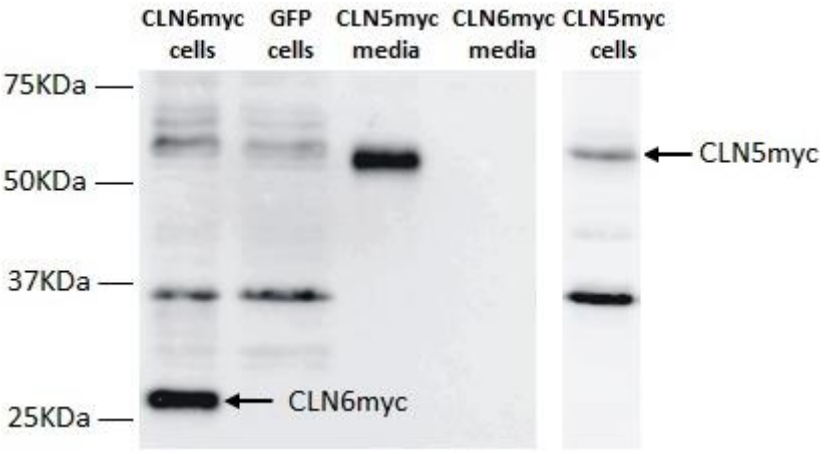

Figure 3.2 Western blot of LVMNDCLN5myc, LVMNDCLN6myc and LVMNDGFP expressing HEK293FT cells
Thirty microgram protein aliquots of each cell sample and 10 µl of CLN5myc and CLN6myc media samples were resolved on a 10% SDS-PAGE; proteins were transferred to a PVDF membrane and subsequently treated with 1:2000 mouse anti-myc and 1:10,000 donkey anti-mouse HRP. A pre-stained Precision Plus protein marker (2.2.5.2) was used to determine molecular weight.

The negative control cells, expressing GFP, did not contain bands with molecular masses of either 60 kDa or 29 kDa, as expected, since they were not transduced with either *CLN5myc* or *CLN6myc*. However, an endogenous myc band was observed around 35 kDa in all of the cell samples indicating that HEK 293FT host cells may contain a myc endogenous tag immune-reactive protein.

3.3.2 Detection of CLN5myc and CLN6myc using antisera generated from adenoviral viral vectors

Packaged adenoviral viral vectors containing *CLN5* and *CLN6* cDNAs were injected into rabbits in an attempt to raise antibodies, and sera were collected from their blood (3.2.2.1). Western blotting was used to test these putative anti-CLN5 and CLN6 antisera by determining if they stained the recombinant CLN5 and CLN6 myc tagged proteins

characterised above. The putative sheep CLN5 sera raised in rabbits detected protein bands of approximately 60 kDa in the CLN5myc media (Figure 3.3 a), similar to that previously found by mouse anti-myc staining of the CLN5myc samples (Figure 3.2). The putative sheep CLN6 antisera raised in rabbits strongly stained a 29 kDa band in CLN6myc cell extracts (Figure 3.3 b), the same sized band as observed in the same cell extracts by staining with the anti-myc (Figure 3.2). These results indicated that the sheep CLN5 and CLN6 antisera detected the CLN5myc and CLN6myc proteins.

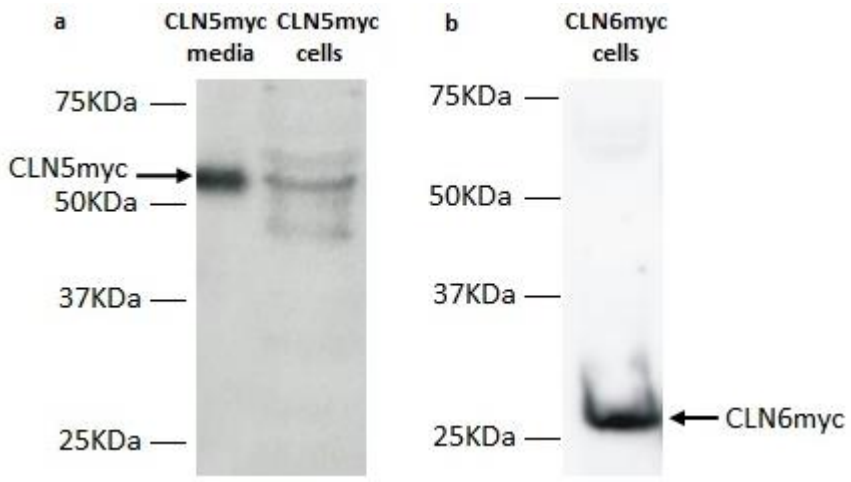

Figure 3.3 Western blots of rabbit anti-CLN5 and anti-CLN6 antibodies in LVMNDCLN5myc and LVMNDCLN6myc expressing HEK293FT cells

Protein samples and markers were loaded as for in Figure 3.2. The blot containing CLN5myc proteins was treated with 1:500 CLN5 antisera and 1:5,000 donkey anti-rabbit HRP, and the CLN6myc blot was treated with 1:1000 CLN6 antisera and 1:10,000 donkey anti-rabbit HRP.

3.3.3 Detection of CLN5 and CLN6 proteins without myc tags using antibodies generated from adenoviral vectors

The ovine CLN5 and CLN6 proteins without myc tags were also expressed in the generated 293FT LVMNDCLN5 and 293FT LVMNDCLN6 cell lines (generated as described in section 3.2.1.3). The expressed CLN5 and CLN6 proteins were used to examine the specificity of ovine CLN5 and CLN6 antisera raised in rabbit and mouse by immunocytochemistry and Western blotting.

3.3.3.1 Optimisation of immunocytochemistry

It is important that immunocytochemistry staining is of high quality, to enable detection in antiserum positive cells clear of background fluorescence. In this study, dilutions of 1:500

and 1:1000 were tested for each of the primary antibodies; rabbit anti-CLN5, rabbit anti-CLN6, mouse anti-CLN5 and mouse anti-CLN6. Cells that received antibodies at a dilution factor of 1:500 stained clearly; while the 1:1000 dilutions required higher exposure times, increasing background which impaired the clarity of the cells (Appendix A.4). Cells incubated with only secondary antibodies (as a negative control) did not show any staining. Subsequently the 1:500 dilution factor was chosen as the optimal antibody dilution for further immunochemistry experiments.

3.3.3.2 Immunocytochemical analysis of adenovirally derived anti-CLN5 and anti-CLN6 antibodies

A study was conducted to detect untagged CLN5 and CLN6 protein using the adenoviral antibodies raised in rabbits and mice. LVMNDCLN5 cells showed bright and clear punctuate green staining with both rabbit anti-CLN5 (RαCLN5) and mouse anti-CLN5 (MαCLN5) antibodies at a dilution of 1:500 (Figure 3.4 i and iii) and the LVMNDCLN6 cells also stained clearly with both the rabbit anti-CLN6 (RαCLN6) and mouse anti-CLN6 (MαCLN6) antibodies at this dilution (Figure 3.4 ii and iv). DAPI stained the nuclei of all the cells. Merged images showed that most of the cells stained by DAPI were also labelled by the individual primary antibodies, indicating a high efficiency of transduction of the generated 293FT LVMNDCLN5 and 293FT LVMNDCLN6 cells. These results indicate that all of the antibodies identified the target cells containing CLN5 or CLN6 proteins. Since much more antisera were obtained from rabbits than mice, the anti-rabbit antibodies were used for most of the subsequent immunochemistry tests.

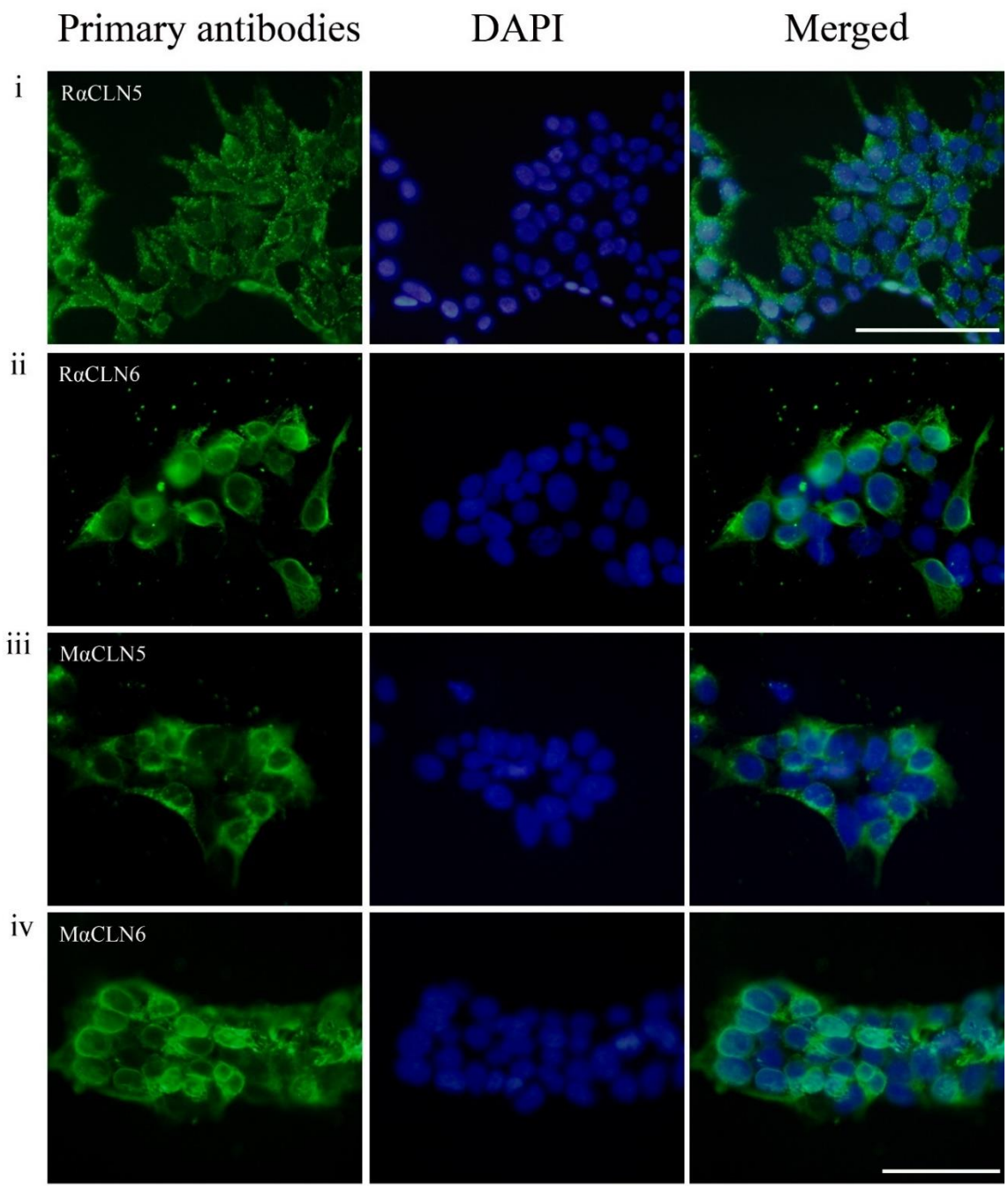

Figure 3.4 Immunofluorescent images of CLN5 and CLN6 protein expression in HEK293FT cells

CLN5 proteins were detected with (i) rabbit anti-CLN5 (RαCLN5) or (iii) mouse anti-CLN5 (MαCLN5) antibodies; CLN6 proteins were detected with (ii) rabbit anti-CLN6 (RαCLN6) or (iv) mouse anti-CLN6 (MαCLN6) antibodies. Green: anti-CLN5 or anti-CLN6, blue: DAPI stained cellular nuclei, merged images: right column. The scales bars represent 200 µm for i and 100 µm for ii, iii and iv.

3.3.3.3 Western blotting with adenovirally derived anti-CLN5 and anti-CLN6 antibodies raised in rabbits

A band with a molecular weight of 60 kDa was detected by Western blotting with rabbit anti-CLN5 (1:500) of CLN5 transduced cells and concentrated media, a size consistent with that of the mature protein (Figure 3.5 a) (Sleat et al., 2006b). This indicated that the rabbit anti-CLN5 antibodies recognise the full CLN5 protein. Two extra bands of slightly lower molecular weights were also revealed, which could be truncated forms of CLN5. The same pattern of CLN5 protein bands was detected with the mouse anti-CLN5 antibody (1:500), but the staining was not as intensive as with rabbit anti-CLN5. No staining was detected in GFP cells samples (negative control) or in CLN6-transduced cells (not shown).

Similarly, both rabbit and mouse anti-CLN6 antibodies detected a protein in CLN6-transduced cells with a molecular weight of 27 kDa (Figure 3.5 b) demonstrating the utility of the antibodies for ovine CLN6 proteins. Again, no signal was detected in GFP cells or in CLN5-transduced cells (not shown). Both blots using mouse anti-CLN5 and anti-CLN6 antibodies had darker backgrounds and two extra bands from lysed cell membrane samples.

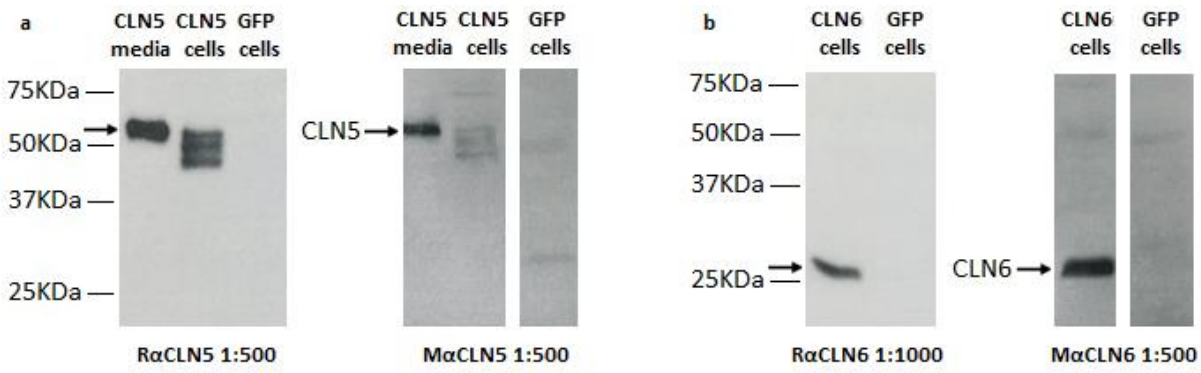

Figure 3.5 Western blot of (a) LVMNDCLN5 and (b) LVMNDCLN6 expressing HEK293FT cells

Protein bands were detected using rabbit anti-CLN5 and CLN6 or mouse anti-CLN5 and CLN6 antibodies by enhanced chemiluminescence exposed for 100 sec. Cell samples (30 µg) and CLN5 concentrated media (10 µl) were resolved by 10% SDS-PAGE. Proteins were then transferred to a PVDF membrane, treated with primary antibodies and donkey anti-rabbit/mouse HRP (1:5000 for CLN5 blot; 1:10,000 for CLN6 blot).

3.3.4 Mass spectrometry

Identity of protein exacted from gel fragments was confirmed by mass spectrometry. Coomassie blue staining from either the CLN5 or CLN6 transduced cells did not reveal bands

at the anticipated molecular weights, suggesting that the amount of the protein expressed was too little to stain with Coomassie (Figure 3.6).

To overcome this, the CLN5 and CLN6 proteins samples were also detected with either rabbit anti-CLN5 or anti-CLN6 antibodies on Western blotting. A single band of each protein was identified by Western blotting, indicating the likely location of the protein on the Coomassie blue stained gels (Figure 3.6, in red rectangles) which were subsequently cut for trypsin digestion and mass spectrometry. Trypsin specifically cleaves proteins at the carboxyl side of arginine and lysine residues that are not followed by a proline, resulting in small tryptic fragments. The tryptic peptide fragments were analysed by mass spectrometry (MS) using MS/MS ion search.

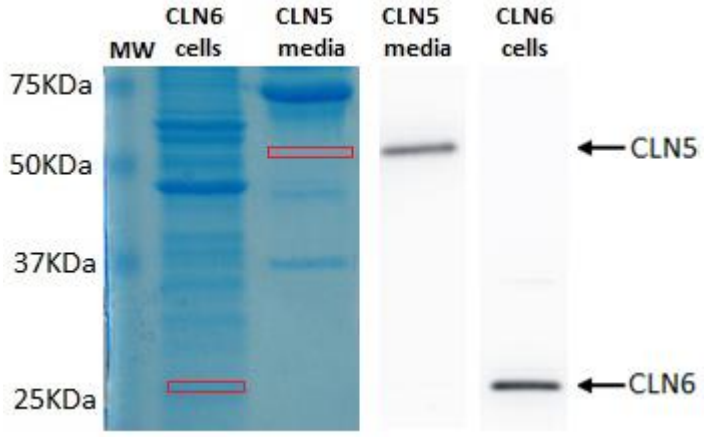

Figure 3.6 Coomassie blue staining and Western blotting of LVMNDCLN5 and LVMNDCLN6 expressing HEK293FT cells

Proteins were separated by SDS electrophoresis. Half of each gel was stained with Coomassie blue (left) and the other half was labelled with rabbit anti-CLN5 or rabbit anti-CLN6 for Western blot analysis (right). The equivalent areas on the Coomassie blue stained gel at the expected molecular weights for CLN5 and CLN6 (in the red squares) were cut and submitted for mass spectrometry.

3.3.4.1 CLN5 sequence

In silico, digestion of ovine CLN5 by trypsin using the online peptide analysis of ExPASy (http://web.expasy.org/peptide_mass/) resulted in 27 peptide sequences of four or more amino acids (Table 3.1, T1-T27 and Figure 3.8, marked in orange lines). The mass spectrometry analysis identified 13 tryptic peptides, all of which were consistent with the predicted ovine CLN5 sequences, at an expected protein coverage of 42.2% (Table 3.1,

labelled with “Yes” and Figure 3.8, highlighted in grey). The longest identified fragment (RQWP……IGFR) matched the predicted peptides from T5 to T11, which includes all of exon 2, several amino acids from the C terminus of exon 1 and the N terminus of exon 3. The remainder of the identified fragments matched the peptides T16, T18, T19, T22, T23 and T27, located in exon 4. The identified sequences in mass spectrometry started from the 53rd amino acid, but not at the predicted signal sequence (Figure 3.8, marked in a green box, amino acids 1-46, peptides T1-T4). Thus, the ovine CLN5 protein includes residues 53-361, producing a 308 amino acid mature protein.

Table 3.1 The predicted trypsin digested ovine CLN5 peptide sequences

	Mass	Position	Predicted trypsin digested peptide sequences	Identified peptide sequences (MS)
T1	1260.5902	1-14	MAQAGGAGAGAWGR	
T2	842.4115	16-25	GAGAGAGPER	
T3	529.2881	26-29	APWR	
T4	2222.1716	30-52	WAPALLWLAAATAAAAAAGDPSR	
T5	917.4879	54-60	QWPVPYK	Yes
T6	1684.7788	62-75	FSFRPEPDPYCQAK	Yes
T7	1540.7538	76-89	YTFCPTGSPIPVMK	Yes
T8	1107.5316	90-98	DDDVIEVFR	Yes
T9	1117.6040	99-107	LQAPVWEFK	Yes
T10	1015.5571	108-116	YGDLLGHLK	Yes
T11	1059.5404	117-125	IMHDAIGFR	Yes
T12	678.3668	126-131	STLTEK	
T13	5670.4685	132-178	NYTMEWYELFQLGNCTFPHLRPEMNAPFWCNQG AACFFEG IDDNHWK	
T14	1850.9680	179-196	ENGTLVLVATISGGMFNK	
T15	2230.0298	203-221	QDNETGIYYETWTVQASPK	
T16	1164.4666	227-235	WFESYDCSK	Yes
T17	534.3398	236-239	FVLR	
T18	540.2664	240-243	TYEK	Yes
T19	963.5145	244-252	LAELGADFK	Yes
T20	896.4472	254-260	IETNYTR	
T21	2591.2664	261-284	IFLYSGEPTYLGNETSVFGP TGNK	
T22	729.4869	285-291	TLALAIK	Yes
T23	1527.7994	293-304	FYYPFKPHLSTK	Yes
T24	2013.1531	305-321	EFLLSLLQIFDAVVIHR	
T25	2237.0452	322-337	EFYLFYNFEYWFLPMK	
T26	591.3500	338-342	SPFIK	
T27	1344.7158	343-353	ITYEEIPLPNRKNRTLSGL	Yes

A search of the identified CLN5 fragment peptides against the universal data base using protein blast software (https://blast.ncbi.nlm.nih.gov/Blast.cgi?PAGE=Proteins) revealed that the peptide sequence of KEAEKWFESYDCSK (Figure 3.8, T16) did not align with any other confirmed protein sequence. The other identified peptide fragments were observed in bovine CLN5 sequence (NP_001039764.1), except that the first peptide fragment

(RQWP……IGFR) (T5-11) also found in pig (XP_005668529) CLN5. Thus, the rabbit anti-CLN5 antibodies bind to the ovine CLN5 sequence specifically, after the CLN5 signal sequence has been cleaved off to produce a mature protein.

The inferred molecular mass of the sheep CLN5 was 41.3 kDa from mass spectrometry, smaller than the 60 kDa stained band in Western blotting. That the size difference could arise from cleavage of the signal peptide and post-translational N-glycosylation is explored below.

3.3.4.2 Post-translational modification of ovine CLN5

CLN5 is heavily glycosylated and cleaved into a mature soluble protein (Sleat et al., 2006a). In this study, CLN5 secreted from 293FT CLN5 cells was subjected to deglycosylation with Endo H and PNGase F. Endo H releases high-mannose type oligosaccharides bound to Asn by cutting after the first N-acetylglucosamine (GlcNAc) residue of the oligosaccharide chain, leaving one sugar moiety on Asn (Figure 3.7 a) (Leonard et al, 1990). Endo H treatment resulted in the single 60 kDa band becoming three bands with molecular weights of approximately 46 kDa, 42 kDa and 38 kDa (Figure 3.8, bands 1, 2, and 3). PNGase F removes complex type N-linked oligosaccharides by cutting immediately after the Asn, and does not leave a sugar moiety (Figure 3.7 b). The modification converts the asparagine to aspartic acid. Therefore, the PNGase F treated CLN5 samples migrated faster than Endo H treated samples. The PNGase F deglycosylation resulted in a single band (Figure 3.7 c, band 4) of approximately 35 kDa, consistent with the deglycosylated protein with the signal sequence removed. The size reduction from 60 kDa to 35 kDa confirms that the ovine CLN5 was glycosylated.

A search of the ovine CLN5 protein using NetNGlyc 1.0 Server software (http://www.cbs.dtu.dk/services/NetNGlyc/) indicated eight potential N-glycosylation sites as recognized by the sequence Asn – X – Ser/Thr. These were located at Asn (N) 132, 145, 180, 205, 257, 273, 283 and 355 of ovine CLN5 (Figure 3.8, highlighted in blue). To determine which of the these eight N-glycosylation sites are utilized, the four Endo H and PNGase F deglycosylated protein bands (Figure 3.7 c, SDS gel in red squares) were excised and analysed separately by mass spectrometry. All the deglycosylated tryptic peptides (Figure 3.8, purple lines) were then mapped individually with ovine CLN5 peptide fragments (highlighted in grey). The six putative N-glycosylation sites (indicated by pink arrows), N 180, 205, 257, 273, 283 and 355 were identified from Endo H and PNGase F treated peptides, but

not from untreated CLN5 peptide fragments. This implies that those six potential glycosylation sites of the ovine CLN5 protein are N-glycosylated. The other two N residues (N132 and N145, indicated by question marks) were not identified in any peptide sequences. Whether or not those two are real N-glycosylation sites and function in CLN5 post-translation modification is still not clear.

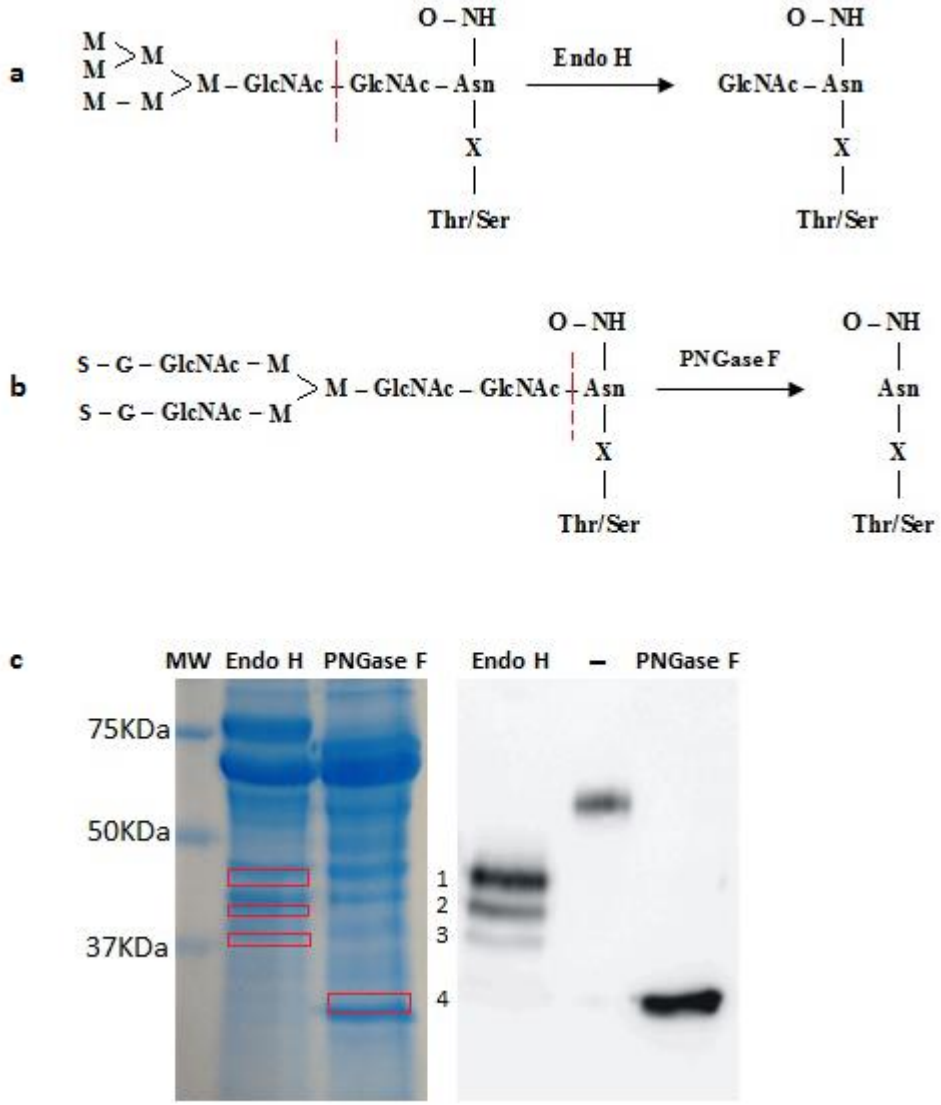

Figure 3.7 CLN5 deglycosylation

(a, b) Structures of N-linked oligosaccharide deglycosylated with Endo H or PNGase F. The abbreviations used are: M=mannose, G=galactose, GlcNAc=acetylglucosamine, Asn= asparagine, Thr=threonine, Ser=serine, and S=sialic acid. The red dashed lines indicate the enzyme cutting positions. **(c) Coomassie blue stain and Western blot of EndoH or PNGase F deglycosylated LVMNDCLN5 expressing HEK293FT cells.** As before protein bands were separated on an SDS gel, half of which was stained with Coomassie blue, and the other half labelled by Western blotting with the rabbit anti-CLN5 antibodiesfor Western blotting. The Coomassie blue stained bands at the molecular weights expected for CLN5 and CLN6 in the red rectangles were excised and submitted for mass spectrometry analysis.

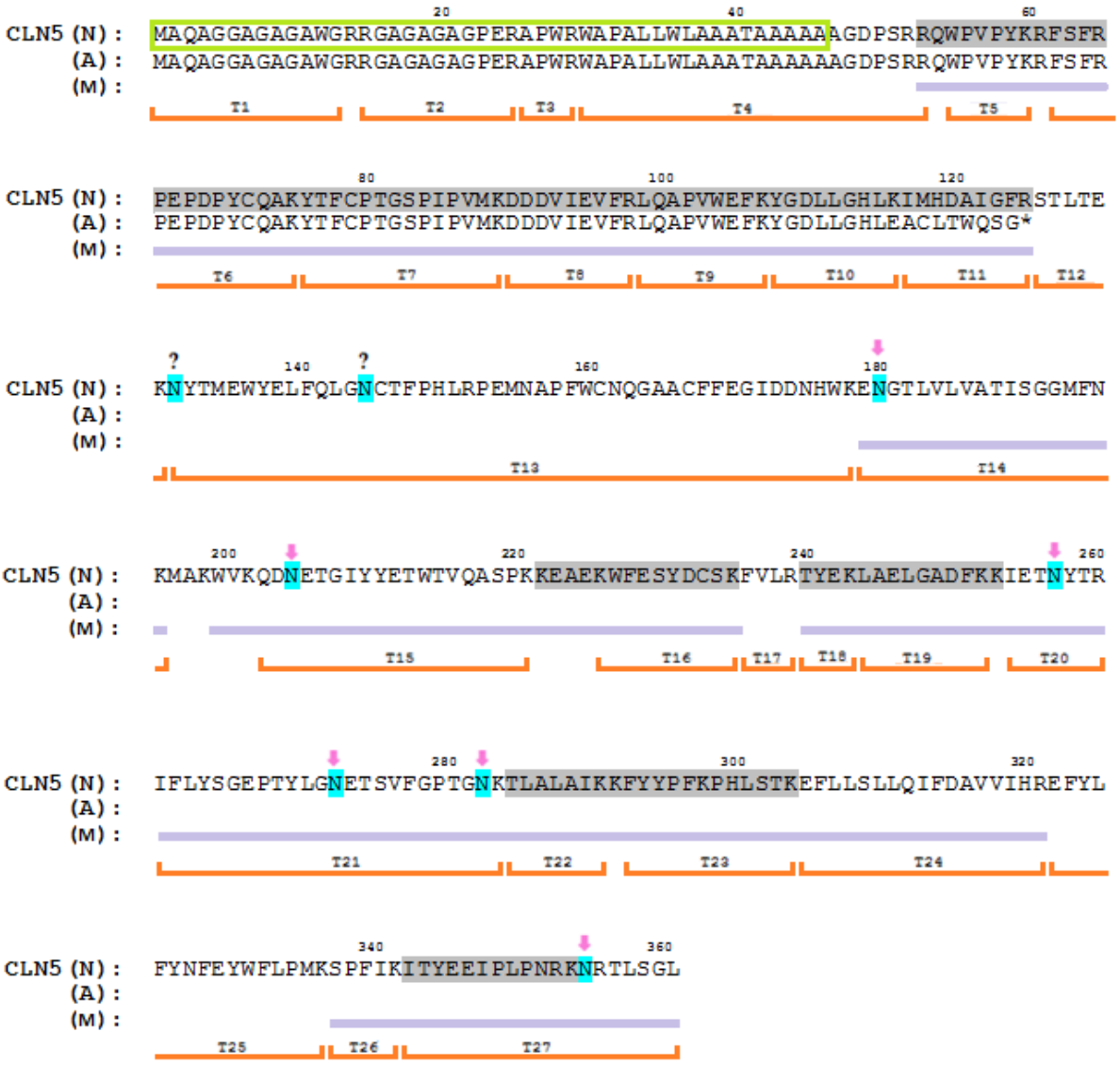

Figure 3.8 Alignment of the normal sheep (N), affected Borderdale (A) and deglycosylated (M) CLN5 protein sequences

The predicated signal sequence (residues 1-46) is marked in a green box. The asparagine residues of the eight predicated glycosylation sites are highlighted in blue. All the trypsin digested fragments from the sheep CLN5 sequence identified by mass spectrometry are highlighted in grey, while those from Endo H or PNGase F deglycosylation are marked with purple lines. The 27 trypsin digest fragments (T1-T27) predicted by ExPASy are marked in orange lines. The *CLN5* mutation in affected Borderdale sheep is a splice site mutation causing a frame shift which changes residue 116 through to a premature termination at triplet 126 (*).

3.3.4.3 CLN6 sequence

In silico trypsin digestion of the ovine CLN6 sequence using the online peptide analysis, ExPASy (http://web.expasy.org/peptide_mass/) resulted in 12 possible peptide fragments (Table 3.2, T1-T12 and Figure 3.9, marked by pink lines). Two matching peptide sequences were identified by mass spectrometry in the current study. One was LIFSGYQNHLSVR (Figure 3.9, in grey background), which matched the predicted tryptic T7 peptide sequence (Table 3.2), and the other, HPGAAGGSGARPGASFLQAR, matched the predicted T2 tryptic peptide sequence (Table 3.2 and Figure 3.9, in grey background). The identified matched peptide sequences started from amino acid 9 (H), suggesting that CLN6 is unlikely to contain a signal sequence.

Table 3.2 The predicted trypsin digested ovine CLN6 peptide sequences

Mass	Position	Predicted trypsin digested peptide sequences	Identified peptide sequences (MS)
648.3133	1-6	MEAAAR	
1864.9524	9-28	HPGAAGGSGARPGASFLQAR	Yes
557.3042	29-33	HSSVK	
7716.9398	34-99	ADEAAGTAPFHLDLWFYFTLQNWVLDFGRPIAMLVFPLEWFPLNKPS VGDYFHMAYNIITPFLLLK	
530.3296	100-103	LIER	
2842.5283	111-136	SLIYVSIITFIMGASIHLVG DSVNHR	
1533.8172	137-149	LIFSGYQNHLSVR	Yes
713.4192	150-155	ENPIIK	
5655.7321	156-201	NLKPETLIDSFELLYYYDEY LGHSMWYIPFFLILFMYFSG CFTPTK	
5347.8592	202-249	AESSMPGAALLLVVPSGLYYWYLVTEGQLFILFIFTSFAMLALVLHQK	
4096.2502	253-287	LFLDSNGLFLFYSFALALLLVALWVAWLWNDPVLR	
2616.2809	290-311	YPGVIYVPEPWAFYTLHVSSQY	

A search of the identified CLN6 fragment peptides against the universal database using protein blast software (https://blast.ncbi.nlm.nih.gov/Blast.cgi?PAGE=Proteins) revealed that the peptide sequence of HPGAAGGSGARPGASFLQAR is unique, as it did not align with any other sequence. The other identified peptide LIFSGYQNHLSVR also aligned with pig CLN6 (NP_001230543.1) and bovine CLN6 (NP_001103454.1) only. These results establish that the area of the gel where the CLN6 antibody binds contains the CLN6 protein, thus confirming that the rabbit anti-CLN6 antibodies specifically bind to ovine CLN6.

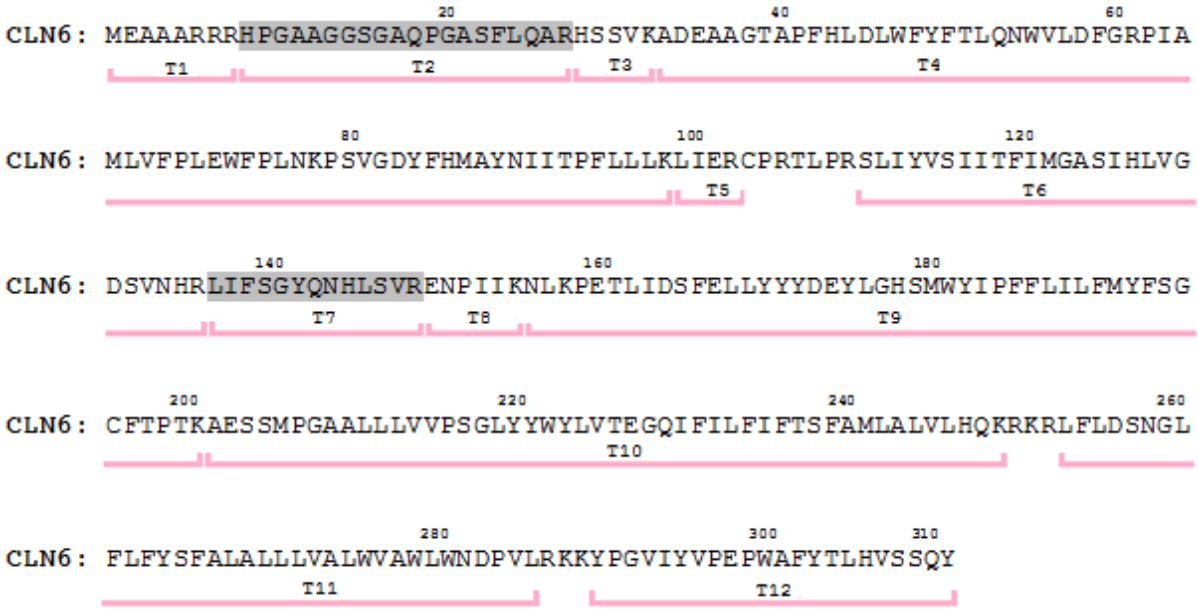

Figure 3.9 Sheep CLN6 protein sequence

The peptide sequences determined by mass spectrometry have a grey background. All the trypsin digested fragments (T1-T12) from sheep CLN6 sequence are marked with pink lines. Trypsin cuts the C-terminal side of K and R unless the next residue is P.

3.4 Discussion

3.4.1 Lentiviral-mediated expression of CLN5 and CLN6 recombinant proteins

Several expression systems are used for the generation of recombinant proteins. The expression of some proteins, such as secreted glycosylated proteins, in prokaryotic systems can be challenging, as some are toxic to the bacterial host cells. To overcome this, lentiviral vectors have been developed to generate recombinant proteins in mammalian cells (Gaillet et al., 2010; Tang et al., 2015). In this study, lentiviral vectors expressing *CLN5* and *CLN6* coding sequences fused with a C-terminal myc tag under the control of the MND promoter were used to transduce HEK293FT cells for protein expression. The immunocytochemistry (Figure 3.1) and Western blotting (Figure 3.2) results indicate the effectiveness of lentiviral-mediated over-expression of recombinant CLN5myc and CLN6myc.

3.4.2 Adenoviral antibodies

As mentioned above, the original plan for generation of antibodies was inoculation of the expressed recombinant proteins fused to myc tags into chickens and subsequent production of IgY antibodies. However, the C-terminal myc used here, along with CLN5 modifications, is

unstable within the lysosome (Pelham, 1988). As myc tagged proteins are different from untagged proteins in their protein folding and glycosylation, full length ovine CLN5 and CLN6 recombinant proteins without tags were deemed more appropriate sources for antibody generation (Figure 3.4 and Figure 3.5). In addition, even though production of IgY antibody from egg yolk has been well developed, successfully generating chicken CLN5 and CLN6 antibodies could be difficult because of the limitation of the antigens. Traditionally, to raise an antibody from one chicken would require two injections of total 200-400 μg of antigens (Brunda et al., 2006), and at least two or three chickens. Here, lentiviral vector mediated recombinant ovine CLN5 and CLN6 proteins have been expressed, but the amounts of the proteins were too low to be visible on SDS-PAGE gels (Figure 3.7 c). Therefore, producing enough antigen for injection into chickens would be problematic. Further more extensive protein purification and multiple boosting would be required, and it would take several months to raise antibodies.

Hence, an alternative method was to produce sheep antibodies by injection of adenoviral vectors expressing CLN5 and CLN6 proteins into rabbits and mice. These adenoviral antibodies were well characterised on overexpressed ovine CLN5 and CLN6 cells by immunocytochemistry (Figure 3.4) and Western blotting (Figure 3.5).

3.4.2.1 CLN5

The adenoviral CLN5 antibodies successfully recognised ovine CLN5. A mass spectrometric study using the antibody identified 13 tryptic ovine CLN5 peptides out of the 27 peptide fragments predicted by online peptide analysis (Table 3.1 and Figure 3.8). One of the identified peptide sequences (KEAEKWFESYDCSK) did not align with any other sequence among the universal data. This confirmed that these anti-CLN5 antibodies raised in rabbit were able to identify the ovine CLN5 sequence specifically. In addition, the other identified peptide sequences were found only in CLN5 sequences from cows and pigs, but not in any other proteins.

It is not surprising that not all potential tryptic digest fragments were detected by mass spectrometry. Some of these peptides (Figure 3.8, T13, T14, T15, T20 and T21) contain asparagine residues, which are potential glycosylation sites. It is possible that the carbohydrate moieties interfere with the action of trypsin, therefore they are not being recognized (Leonard et al., 1990). Some others might be either too small to be identified (i.e. T17, FVLR) or likely to be extremely hydrophilic and poorly resolved from the salt fraction

during the digestion process (i.e. T12, STLTEK). The likelihood of insufficient amount of the protein sample also needs to be taken into account.

CLN5 is a soluble lysosomal protein (Sleat et al., 2006a), synthesised as a pre-pro-protein with an N-terminal signal sequence, which translocates the precursor protein into the lumen of the ER. The signal peptide is removed and initial protein glycosylation takes place in the ER and Golgi apparatus. The mature protein is then recognized and bound by M6P receptors in the trans-Golgi network, and subsequently trafficked to lysosomes. The predicated mass of ovine CLN5 from online peptide analysis of ExPASy was 41.3 kDa. However, the peptide from the signal peptide of secreted CLN5 protein is not expected to be in the mature protein, so this part of the theoretical sequence (4.5 kDa, ProtParam tool, http://web.expasy.org/protparam/) should be excluded, and thus the mature CLN5 cDNA sequence mass reduces down to 36.8 kDa. The current study using sheep specific CLN5 antibodies detected a band matched the observed molecular weight (60 kDa) in Western blot analysis (Figure 3.5). Treatment of the secreted CLN5 samples with PNGase F, which removes complex type oligosaccharides modified in the Golgi membranes, reduced the mass to around 35 kDa (Figure 3.7 c), close to the predicted mature CLN5 mass (36.8 kDa), confirming that sheep CLN5 is glycosylated. Deglycosylation studies on CLN5 from other species have produced similar results. A 60 kDa human CLN5 polypeptide reduced to 35 kDa after PNGase F digestion (Larkin et al., 2013). These results fit well with the third human ATG site being the initiation codon and cleavage of signal sequence. In contrast, Vesa and his colleagues (2002) observed one 47 kDa band from PNFase F treated CLN5 protein, as they used CLN5 antibodies which started from an incorrect codon. The deglycosylation study using Endo H treatment produced three bands of 46 kDa, 42 kDa and 38 kDa (Figure 3.7 c).

The current deglycosylation study also found that the sheep CLN5 polypeptide contains eight predicted N-glycosylation sites, six of which (180, 205, 257, 273, 283 and 355) were confirmed, suggesting they function in CLN5 post-translation (Figure 3.8). A similar study on human CLN5 N-glycosylation sites determined seven of eight N residues were utilized *in vivo* (Vesa et al., 2002, Moharir et al., 2013), even though there was a confusion start on the human start codon.

3.4.2.2 CLN6

The mass spectrometry study using the rabbit anti-CLN6 antibodies identified 2 tryptic ovine CLN6 peptides out of the 12 peptide sequences predicted by online peptide analysis (Table

3.2 and Figure 3.9). It is clear that the abundance of expressed CLN6 on the gel is minimal (Figure 3.6), thus the amounts of trypsin digested CLN6 peptides were limited. Apart from ovine CLN6, a number of other co-migrating proteins were also present in that region (molecular weight of 27 kDa). When the CLN6 gel block was digested by trypsin, other co-migrating proteins (including human peroxiredoxin 1 and several triosephosphate isomerases) were also digested and yielded fragments detected by mass spectrometry. Subsequently, the low level of trypsin digested CLN6 peptide fragments were difficult to identify by mass spectrometry analysis. However, a Blast search proved that one of the identified CLN6 fragments (HPGAAGGSGARPGASFLQAR) was unique to sheep, and the other identified peptide sequence was found only in CLN6 sequences from cow and pig, but not in any other proteins. Further, the raised sheep specific-CLN6 antibodies detected ovine CLN6 even from such limited amounts of antigen on Western blotting.

3.5 Conclusion

In summary, recombinant ovine CLN5 and CLN6 protein expressions were obtained from use of lentiviral vectors containing the coding sequences in HEK293FT cell cultures. Adenovirally derived antibodies of ovine CLN5 and CLN6 specifically detected both native and denatured proteins.

Chapter 4
Cellular and regional localisations of the ovine CLN5 and CLN6 proteins and characterisation of their interactions

4.1 Introduction

Correlations between locations and disease progression can give clues to the functions of proteins. The specificities of the full ovine CLN5 and CLN6 antibodies raised in rabbits in (described in Chapter 3) have been confirmed in overexpressed cells. The CLN5 and CLN6 antibodies used previously in other studies are not generally as reliable as they were reported to be. The commercial antibodies were raised against CLN5 starting from an incorrect codon of human CLN5 sequence, and none of the reported CLN5 (Jules et al. 2015, 2017; Silva et al., 2015; Vesa et al., 2002) and CLN6 (Heine et al., 2004; Mole et al., 2004) antibodies were able to detect the endogenous ovine CLN5 and CLN6 proteins. In this chapter, the adenoviral generated rabbit antibodies (Chapter 3) are used to visualise cellular and regional CLN5 and CLN6 protein expression in the ovine CNS, and to determine the correlation between the two proteins.

Lysosome-associated membrane protein-1 (LAMP1) is a lysosomal marker, commonly used to study the localisation and function of lysosomal proteins (Falcón-Pérez et al., 2005; Saftig and Klumperman, 2009; Akasaki et al., 2014). It is a highly glycosylated lysosomal protein, synthesized in the ER, transported via a Golgi network, and delivered to lysosomes. Localisation of the human CLN5 protein to the lysosome has been confirmed by several studies using LAMP1 antibodies in cells overexpressing CLN5 (Vesa et al., 2002; Holmberg et al., 2004; Lyly et al, 2009). In the present study, a construct consisting of the human LAMP1, fused at its cytoplasmic carboxyl terminus to GFP, was transfected into 293FT LVMNDCLN5 cells (3.2.1.1) to express LAMP1-GFP and CLN5 proteins. The rabbit anti-CLN5 antibodies (3.2.2) were then used to determine any co-localisation between ovine CLN5 protein expression and the lysosomes (LAMP1-GFP, visualised in green).

Protein disulphide isomerase (PDI) is a resident enzyme of the endoplasmic reticulum (ER), and often used as an ER marker. Previously, the human CLN6 protein has been located as an ER resident protein using antibodies from the middle of *CLN6* sequence (Mole et al., 2004;

Heine et al., 2007). In the present study, the rabbit anti-CLN6 antibodies (3.2.2) were used to determine co-localisation of the ovine CLN6 and PDI proteins.

Previous studies have found CLN5 gene expression in neuronal cells and microglial cells in human and mouse brains (Holmberg et al., 2004). Northern blot analyses revealed CLN5 mRNA expression in mouse brain and peripheral organs; liver, heart, kidney, lung, skeletal muscle, spleen and testis (Holmberg et al., 2004). Immunohistochemical staining of mouse brain sections detected CLN5 in Purkinje cells, hippocampal pyramidal cells and cortical neurons (Holmberg et al., 2004). One aim of the present work was to test the ability of the rabbit anti-CLN5 antibodies to detect endogenous CLN5 protein in sheep and human brain tissues by DAB staining.

Neurons in the CNS are generally classified into primary sensory neurons and motor neurons. They can also be classified according to the cell shapes and patterns of dendrites into categories such as pyramidal cells, Purkinje cells and basket neurons. Most neurons in the CNS forming neuron-neuron connections are called interneurons (Kandel, 2000). Antibodies to the calcium binding ligands; calbindin, parvalbumin and calretinin are commonly used to identify specific γ-aminobutyric acid (GABAergic) interneuron subtypes. Co-localisation of GABAergic interneuron markers with other markers for specific neuronal cell types were studied in mice brain sections (Zhao et al., 2013; Molgaard et al., 2015). In the present work, the types of ovine neural cells which express CLN5 proteins were studied by double fluorescent labelling with the CLN5 antibodies (3.2.2) and GABAergic interneuron markers or a neuron-specific Nissl stain.

Similar pathology and common symptoms shared by the NCL diseases have led to the theory that the NCL proteins do not function by themselves, but through interactions, and that they may operate via in a common pathway (Margraf et al., 1999). This study revealed that *CLN2*, *CLN3* and *CLN5* mRNAs were co-expressed during mouse brain development, and all three proteins are strongly expressed in the hippocampus of the postnatal brain (Fabritius et al., 2014). A co-localisation study reported that CLN2, CLN5, CLN6 and CLN8 proteins co-immunoprecipitate (Persaud-Sawin et al., 2007). A pull-down study suggested that CLN5 possibly interacts with many other NCL proteins, including CLN1/PPT1, CLN2/TPP1, CLN3, CLN6 and CLN8 (Lyly et.al, 2009). Other studies concluded that CLN3 expression is reduced in CLN5 patients, and the expression of both CLN3 and CLN5 was reported to be down-

regulated in CLN2 deficient human patients (Bessa et al., 2006, 2008). Together, these findings suggest that CLN5 acts as a binding partner to the other NCL proteins.

CLN5 is a lysosomal protein (Isosompii et al., 2002) and CLN6 an ER resident protein (Heine et al., 2004), however the functions of CLN5 and CLN6 are still unknown. Thus the possible mechanisms of these interactions remain unclear, but are likely to occur in the ER. The specific CLN5 and CLN6 antibodies generated in Chapter 3 have been used in immunohistochemical interaction studies that show reduced CLN5 expression in the CLN6 affected South Hampshire and Merino sheep brains (Kristi McIntyre, personal communications and Russell, 2017). These data suggest a cross regulation of the expression of these two proteins. The present study also investigates potential interactions in the CLN5 and CLN6 ovine models and any effects on protein expression by transduction with single lentiviral CLN5 (LV CLN5) or lentiviral CLN6 (LV CLN6) viruses, or both, in control and affected CLN5 and CLN6 secondary neural cells *in vitro*.

4.2 Materials and Methods

4.2.1 Co-localisation of CLN5 protein to the lysosome

4.2.1.1 Isolation of LAMP1-GFP plasmid DNA

A CMV pLAMP1-GFP plasmid DNA, encoding the complete open reading frame of human LAMP1 generated by Dr. Falcon-Perez, Department of Human Genetics, University of California, USA (Falcón-Pérez, 2005), was acquired by Dr Stephanie Hughes's laboratory at the University of Otago. Top 10 competent *E. coli* cells (Invitrogen, NZ) were transformed with this plasmid and a glycerol stock prepared. The bacterial glycerol stock was used to inoculate 300 ml of LB medium (Sigma Aldrich, NZ) containing 50 μg/ml kanamycin. The culture was grown with vigorous shaking, 225 rpm, overnight, 37°C, until the $OD_{600} \geq 0.9$.

Cells were harvested by centrifugation, 1 min, 12,000 *g*, 4°C and the resultant pellets processed through Maxiprep Qiagen-tip 500 low-copy plasmid purification kits (Macherey GmbH, Germany) to isolate plasmid DNA. The concentration of plasmid DNA was determined using Nano Drop spectroscopy as described in section 2.2.2.1.

4.2.1.2 Transfection with CMV LAMP1-GFP plasmid DNA

293FT LVMNDCLN5 cells (3.2.1.3) were plated onto poly-L-lysine treated 24-well plates at 5×10^4 cells/well and maintained until 60% confluence, then transfected with the LAMP1-GFP plasmid DNA at a ratio of Lipofectamine 2000 (Invitrogen, NZ): plasmid DNA = 3:1. Plasmid

DNA, 0.5 µg, was incubated with 1.5 µg of L2000 in 300 µl OptiMEM, 20 min. This plasmid-L2000 transfection mixture was applied drop-wise onto cells containing OptiMEM media. Six hours post-transfection, media were refreshed with complete OptiMEM, and the cells cultured for a further 18 h. Untransfected HEK293FT cells were the negative control.

4.2.1.3 Immunocytochemistry

LAMP1-GFP transfected cells were fixed and blocked as described above (section 3.2.1.4). Cells were treated with the primary rabbit anti-CLN5 antibodies diluted 1:500 (3.2.2.1) in blocking buffer (PBS containing 0.2% Triton X-100 and 3% normal goat serum, NGS), 4°C, overnight. Cells were washed, with PBST, 3 × 30 min, before incubation with goat anti-rabbit Alexa 594 (red, A11012, Invitrogen, NZ) conjugated secondary antibody diluted 1:1000 in blocking buffer, 4 h. Cells were washed another 3 × 30 min with PBST and 1 × PB, mounted onto glass with ProLong Gold antifade, coverslipped, and images taken with a fluorescent microscope under the 40× objective as described above (section 3.2.1.4).

4.2.2 Co-localisation of CLN6 protein and an ER marker by immunocytochemistry

The general steps were the same as outlined above. 293FT LVMNDCLN6 cells (3.2.1.3) were plated onto a poly-L-lysine treated 24-well plate at 5×10^4 cells/well, maintained until 30% confluence and fixed with 4% PFA. To localise CLN6, co-immunocytochemistry was performed using rabbit anti-CLN6 (diluted 1 in 500, 3.2.2.1) and mouse anti-PDI (diluted 1: 100, ab2792, Abcam, Australia) primary antibodies, and subsequent incubation with goat anti-rabbit Alexa 488 (green, A11008, Invitrogen, NZ) and goat anti-mouse Alexa 594 (red, A11005, Invitrogen, NZ) secondary antibodies respectively. The mounted cells were imaged under the 60× objective lens.

4.2.3 Detection of endogenous ovine CLN5 by immunohistochemistry

4.2.3.1 Ovine brain sections

Sagittal sheep brain sections (50 µm) from level 5 (Figure 4.1 A) (Oswald et al., 2005), were obtained from 6 month old normal Coopworth and 9 month old affected Borderdale sheep. All the sections were prepared by Dr. Nadia Mitchell. A dorsal view of a whole sheep brain and a level 5 sagittal section are displayed in Figure 4.1.

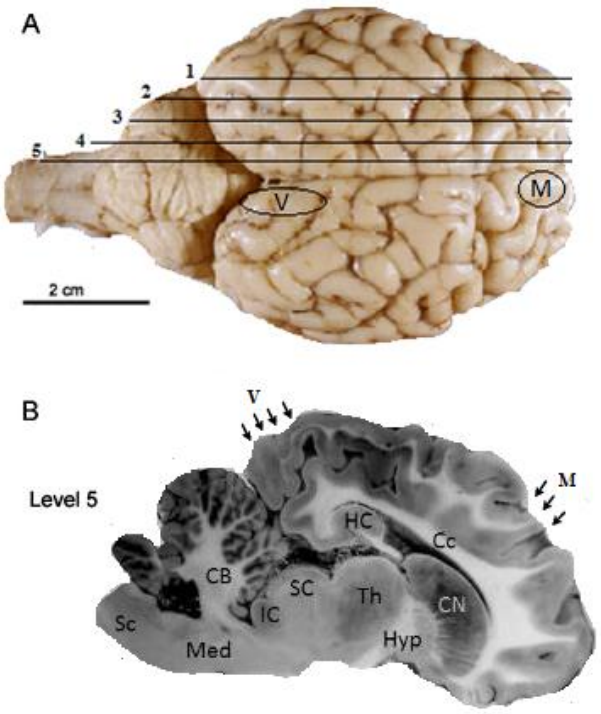

Figure 4.1 Anatomical structure of a normal sheep brain

(A) Dorsal view. (B) A Level 5 sagittal section. CB = cerebellum, Cc = corpus callosum, CN = caudate nucleus, HC=hippocampus, Hyp = hypothalamus, IC = caudal colliculus, M = motor cortex, Med = medulla, S c= spinal cord, Th = thalamus, V = visual cortex (Modified from Oswald et al., 2005)

Sections stored in 96-well plates containing cryoprotectant were thawed, washed in PBS (15 ml/well), in 6-well plates on a rocking platform, 40 rpm, overnight, 4°C. On the following day sections were washed, 3 × 5 min, PBS, treated with 1% H_2O_2 in PBS for 30 min to quench endogenous peroxide activity, then incubated in 15% NGS in PBS, pH 7.4, containing 0.3% Triton X-100 (PBST), 2 h, to remove non-specific tissue antigens. All steps were followed by 3 × 30 min washes in PBS. The sections were incubated with the primary antibodies rabbit anti-CLN5 (3.2.2.1), diluted 1:500 in PBST containing 10% NGS, overnight, 4°C. Immunoreactivity was detected using the secondary antibody, biotinylated goat anti-rabbit (B7389, Sigma Aldrich, NZ, diluted 1:1000 in PBST containing 10% NGS), 2 h. The sections were then stained in ExtrAvidin peroxidase solution (E2886, Sigma Aldrich, NZ, diluted 1:1000 in PBS), 2 h. Immunoreactivity was detected by incubation with 0.05% (0.5mg/ml) 3, 3'-diaminobenzadine (DAB, D5637, Sigma Aldrich, NZ) and 0.01% H_2O_2 in PBS for 10 min in the dark. DAB reactions were terminated by 4 × 5 min washes with ice-cold PBS. Sections were mounted onto glass slides, air dried, dehydrated in 50% ethanol, 10 min, 100% ethanol, 10 min, cleared in xylene, 30 min and immediately coversliped in DPX (BDH, Poole, England). Images were captured with an Olympus IX71 microscope with an Olympus DP71 camera (Hilenski, Germany). Negative control sections in which the primary and secondary antibodies were omitted were also processed.

4.2.3.2 Chromogenic staining of paraffin-embedded human brain sections

Wax-embedded sagittal blocks of normal human brain cortex, cerebellum and hippocampus were kindly provided by Professor Hans Goebel, Charité, Berlin, Germany and 3 µm sections were cut and mounted onto glass slides. Paraffin was removed with xylene soaking, 30 min, and a series of ethanol solutions from 100% progressing down to 50%, 10 min in each grade. All the tested slides were soaked in ddH_2O, 10 min, and excess liquid drained off. A waterproof marker pen was used to draw a circle around the mounted tissues in order to make a hydrophobic barrier (Figure 4.2).

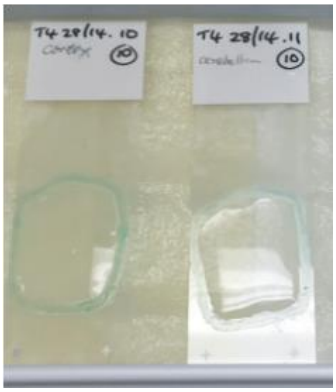

Figure 4.2 DAB staining of paraffin-embedded human brain sections within a hydrophobic barrier formed by a waterproof marker pen

The following processes were carried out in humid conditions to prevent sections drying out and without shaking. Endogenous peroxide activity was blocked with 300 µl/section of 1% H_2O_2 in PBS, 30 min, and nonspecific antibody binding blocked by incubation with 15% NGS in PBST, 300 µl/section, 2 h. Rabbit anti-CLN5 primary antibody (3.2.2.1) was diluted 1:500 in PBST containing 10% NGS and incubated on sections overnight, 4°C. Primary antibody was removed, followed by 3 × 30 min washes with PBST, before incubation in biotinylated goat anti-rabbit (1:1000 in PBST containing 10% NGS) followed by ExtrAvidin peroxidase (1:1000 in PBS), 2 h. Sections were washed 3 × 30 min with PBS, and antibody binding detected with DAB, 5-10 min in the dark (see section 4.2.3.1). Sections were then rinsed, dehydrated, air-dried, and cleared. Images were captured with an Olympus microscope and camera. Immunostainings of sections without primary or secondary antibodies provided negative controls.

4.2.4 Immunohistochemical double fluorescent labelling of ovine brain sections

Double-labelling was carried out on level 5 sagittal brain sections from a 6 month old normal Coopworth sheep. The brain sections (Table 4.1) were washed and blocked as described in

section 4.2.3.1. In preliminary studies calbindin stained the cortex, cerebellum, hippocampus, and brain stem; parvalbumin the cortex, thalamus, cerebellum, brain stem, and hippocampus; calretinin the cerebellum and hippocampus; and NeuN the cortex, cerebellum, and hippocampus. The following selected sections were used in a double labelling study following the best staining with one of the neural makers and the CLN5 antibody.

Table 4.1 Double-labelled primary and secondary antibodies

Section parts	Primary antibodies mix		Secondary antibodies mix (1: 1000)
	1st label	2nd label	
Cortex	Mouse anti-NeuN 1:1000	Rabbit anti-CLN5 1:500	Goat anti- rabbit Alex 488 Goat anti- mouse Alex 594
Cerebellum	Mouse anti-Calbindin 1:500	Rabbit anti-CLN5 1:500	Goat anti- rabbit Alex 488 Goat anti- mouse Alex 594
Thalamus	Mouse anti-Parvalbumin 1:500	Rabbit anti-CLN5 1:500	Goat anti- rabbit Alex 488 Goat anti- mouse Alex 594
Hippocampus	Rabbit anti-Calretinin 1:500	Mouse anti-CLN5 1:500	Goat anti- mouse Alex 488 Goat anti- rabbit Alex 594
Cortex	Mouse anti-GFAP 1:500	Rabbit anti-CLN5 1:500	Goat anti- rabbit Alex 488 Goat anti- mouse Alex 594
Cortex (negative control)	None	None	Goat anti- rabbit Alex 488 Goat anti- mouse Alex 594

Double primary antibody labelling was carried out with rabbit anti-CLN5 or mouse anti-CLN5, diluted 1:500 in 10% NGS in PBST, 48 h, 4°C. Sections were also co-labelled with one of the following neural markers (Table 4.1); mouse anti-NeuN (MAB3777, Millipore, USA), mouse anti-calbindin (D28K, Swant, Bellinzona, Switzerland), mouse anti-parvalbumin (PV235, Swant, Bellinzona, Switzerland), rabbit anti-calretinin (CR7697, Swant, Bellinzona, Switzerland), and mouse anti-GFAP (G3893, Sigma Aldrich, NZ). After 3 × 30 min washes in PBST, sections were incubated with secondary antibody mixes of either goat anti-rabbit Alexa 488 (green, A11008, Invitrogen, NZ) and goat anti-mouse Alexa 594 (red, A11005, Invitrogen, NZ), or goat anti-mouse Alexa 488 (green, A11001, Invitrogen, NZ) and goat anti-rabbit Alexa 594 (red, A11012, Invitrogen, NZ) (Table 4.1).

Reactions were carried out with secondary antibodies, diluted 1: 1000 in PBST, 4 h, room temperature. Sections were washed 3 × 30 min in PBST, followed by a 30 min PBS wash. Cell nuclei were stained with diamidino-2-phenylindole (DAPI, 1 mg/ml stock, Sigma Aldrich, NZ), diluted to 1:10,000 in PBS, 5 min, and washed with PBS. Sections were washed with 0.1 M PB before being mounted onto glass, and coverslips attached with ProLong Gold antifade

reagent. Fluorescent images were taken on a Zeiss LSM 710 upright confocal microscope (Zeiss, Germany), merged and processed in Photoshop.

4.2.5 Interactions of the CLN5 and CLN6 proteins

4.2.5.1 Ovine primary neural cell cultures

Approval for the use of sheep primary neural cells was obtained from EPA (approval #GMD002852). Frozen primary neural cells extracted from fetal sheep brains (Hughes et al., 2014a) at Lincoln University, were thawed rapidly in a 37°C water bath and transferred into a 50 ml tube containing 5 ml of neural culture media (DMEM, 10% FBS, 1% L-glutamine, 1% penicillin and streptomycin). After the cells were passed through a 40 µm cell strainer, they were pelleted, 1000 rpm, 5 min, in a Heraeus Multifuge3S centrifuge (Thermo Scientific, San Jose, CA). The supernatant was removed and the cell pellet re-suspended in 5 ml of neural culture media. The sheep primary neural cells were then plated onto poly-L-lysine treated 24-well plates at a density of 1×10^5 cells/1 ml well, and the cells grown at 37°C in a humidified atmosphere containing 5% CO_2. Half the neural culture media volumes were changed every three days. The neural cells were harvested at two weeks post plating.

4.2.5.2 Generation of ovine neural cell lines (secondary neural cells)

Table 4.2 Generation of secondary neural cell lines

Phenotype	ID	Generated by
CLN5$^{+/-}$	F16P3	Janet Xu
CLN5$^{+/-}$	F21P5	Dr. Hughes's lab
CLN5$^{+/-}$	F22P3	Janet Xu
CLN5$^{+/-}$	F47P3	Dr. Hughes's lab
CLN5$^{-/-}$	F14P5	Dr. Hughes's lab
CLN5$^{-/-}$	F41P5	Dr. Hughes's lab
CLN5$^{-/-}$	F43P5	Dr. Hughes's lab
CLN5$^{-/-}$	F44P3	Janet Xu
CLN6$^{+/-}$	F37P5	Dr. Hughes's lab
CLN6$^{+/-}$	F39P5	Dr. Hughes's lab
CLN6$^{+/-}$	F40P4	Dr. Hughes's lab
CLN6$^{-/-}$	F7P5	Dr. Hughes's lab
CLN6$^{-/-}$	F31P5	Dr. Hughes's lab
CLN6$^{-/-}$	F33P5	Dr. Hughes's lab

In this study, neural cell lines, referred to as secondary neural cells, were generated from ovine primary neural cells (Table 4.2). When the primary neural cells reached about 80% confluence, they were passaged and transferred to T25 flasks, until they again reached approximately 80% confluence. Cells were counted using Trypan blue, pelleted by centrifugation, and re-suspended in media for freezing. The cell suspensions were frozen as

1 ml samples at a density of 2×10^6 cells/ml at -80°C overnight then transferred to liquid nitrogen for long term storage. The control ($^{+/-}$) and affected ($^{-/-}$) CLN5 and CLN6 neural cell lines generated are shown in Table 4.2.

4.2.5.3 CLN5 lentiviral transduction of neural cell lines

Four sheep neural cell lines were used in this experiment; *CLN5*$^{+/-}$ F21, *CLN5*$^{-/-}$ F14, *CLN6*$^{+/-}$ F2 and *CLN6*$^{-/-}$ F25 (Table 4.2). Vials of frozen sheep secondary neural cells were plated and cultured in neural culture media in poly-L-lysine treated 24-well plates at 7×10^4 cells/well (4 wells/cell, 1ml/well) and refreshed with media (1ml/well) on the following day. Transduction was achieved by direct administration of LV CLN5 virus (1 µl/well, 1.1×10^{10} transducing units/ml, prepared by Dr. Stephanie Hughes's laboratory) to the media by gentle mixing followed by a further 72 h incubation at 37°C. Neural cells were then incubated for 24 h in OptiMEM neural culture media (OptiMEM, 1% L-glutamine, 1% penicillin and streptomycin, 300 µl/well). Untransduced sheep neural cell lines served as negative controls. A volume of 1.2 ml of media from each neural cell line was collected and concentrated down to 10 µl for Western blotting as described above (section 3.2.1.5). Cells were washed briefly in Dulbecco's phosphate-buffered saline solution (dPBS, GIBCO, Invitrogen, NZ), and fixed in 4% PFA (see section 3.2.1.4).

Western blots of CLN5 protein from transduced neural cells were processed as described in section 3.2.2.3. Proteins in the concentrated cultured media (3 µl) were separated on 10% SDS gels, then transferred to PVDF membranes. The membranes were blocked and incubated in 1:500 primary rabbit anti-CLN5 antibodies overnight, then treated with the 1:5000 secondary goat anti-rabbit HRP, 4 h and developed by ECL.

CLN5 protein secreted from virally transduced neural cells was also detected by immunocytochemistry. To improve the clarity of rabbit anti-CLN5 staining, a short staining protocol was performed. The fixed cells were incubated with the primary rabbit anti-CLN5 antibodies diluted 1:500 in blocking buffer with PBS, 2 h, then washed 3 × 5 min with PBST before incubation with secondary goat anti-rabbit Alexa 488 conjugated antibody diluted to 1:1000 in blocking buffer, 30 min. After another 3 × 5 min washes with PBST, cells were refreshed in 0.1 M PB, cover-slipped and imaged by fluorescent microscopy.

4.2.5.4 CLN5 expression in virally transduced control and affected neural cells

The experiment described here was aimed to detect any changes in CLN5 expression in neural cells transduced with LV CLN6 virus together with LV CLN5 virus. Four CLN5 control secondary neural cells (*CLN5*$^{+/-}$ F21, *CLN5*$^{+/-}$ F16, *CLN5*$^{+/-}$ F47, *CLN5*$^{+/-}$ F22) and four CLN5 affected secondary neural cells (*CLN5*$^{-/-}$ F14, *CLN5*$^{-/-}$ F41, *CLN5*$^{-/-}$ F43 and *CLN5*$^{-/-}$ F44) were cultured in duplicate as described in section 4.2.5.3. One well of each neural cell line was transduced with 1 µl LV CLN5 virus, and the other well was transduced with 1 µl LV CLN5 and 1 µl LV CLN6 viruses (8×10^9 transducing units/ml, prepared by Dr. Stephanie Hughes's laboratory). At 72 h post-transduction, the neural culture media were replaced with OptiMEM media (300 µl/well), and the cells incubated for another 24 h, 37°C. The media from the neural cell cultures were collected and concentrated for Western blotting (as in section 3.2.1.5). Proteins in the concentrated media from overexpressed CLN5 cells (3 µl, positive control) and the concentrated media (20 µl) from the single LV CLN5 virus and double LV CLN5 and LV CLN6 virally transduced cells were separated on a 10% SDS gel, and then transferred to a PVDF membrane. The membrane was blotted with rabbit anti-CLN5 and goat anti-rabbit HRP as described in section 3.2.2.3.

Six CLN6 secondary neural cells, three controls (*CLN6*$^{+/-}$F37, *CLN6*$^{+/-}$F39 and *CLN6*$^{+/-}$F40) and three affected (*CLN6*$^{-/-}$F7, *CLN6*$^{-/-}$F31 and *CLN6*$^{-/-}$F33), transduced with LV CLN6 or LV CLN5 plus LV CLN6 viruses, were also used to study changes of CLN5 expression. The processes were the same as described above.

4.2.5.5 CLN6 expression in virally transduced control and affected neural cells

An experiment was carried out to find any changes in CLN6 expression when LV CLN5 virus was transduced together with LV CLN6 into neural cells. Six CLN6 secondary neural cell lines (as in section 4.2.5.4), and four CLN5 secondary neural cell lines, two controls (*CLN5*$^{+/-}$ F21 and *CLN5*$^{+/-}$ F47) and two affected (*CLN5*$^{-/-}$ F14 and *CLN5*$^{-/-}$ F41), were cultured and transduced as described in section 4.2.5.4. Culture media were discarded, the cells lysed and the proteins extracted as described in section 3.2.1.5. Western blotting was performed as outlined above. The proteins from lysed cells were separated (50 µg/well) on 10% SDS gels and then transferred to PVDF membranes, which were blotted with rabbit anti-CLN6 (1:1000) and goat anti-rabbit HRP (1:10,000). Overexpressed CLN6 cells generated in section 3.2.1.5, provided the positive control and neural cells without viral transduction acted as the negative control.

β-actin was used as the loading control to determine if equal amounts of protein had been loaded into each lane. The β-actin detection was carried out after rabbit anti-CLN6 detection without stripping the blot. The antibody treatment was as described above except a primary rabbit anti-actin antibody (1:2000, A5056, Sigma Aldrich, St. Louis, MO) was used instead of the rabbit anti-CLN6 antibody.

4.2.5.6 Image analysis of Western blots

The Image J program (Rasband, National Institutes of Health USA, http://imagej.nih.gov/ij/) was used to analyse the integrated density of the protein bands detected in control and affected cell cultures. Western blotting images showing the protein bands were imported into Image J and converted to 8-bit files. Backgrounds were subtracted by setting a rolling ball radius with 50 pixels, and densities of the selected protein bands were measured and recorded automatically. All the data were collected and exported to Microsoft Excel and normalised to the densities in reference overexpressed CLN5 or CLN6 neural cells. In the CLN6 expression study, the ratios of normalised integrated densities of CLN6 to actin (loading control) from every sample were also calculated.

4.2.5.7 Statistical analysis

Normalised integrated densities data were analysed in Genstat 18 (VSN International Ltd, Hempstead, UK). This examined the interaction of protein expression and lentivirus treatments using the General Linear Model function. Means were separated by the Least Significant Difference ($P < 0.05$).

4.3 Results

4.3.1 Co-localisation of the CLN5 protein and lysosome

The subcellular localisation of the ovine CLN5 protein was studied by fluorescent microscopy after transfection of 293FT LVMNDCLN5 with LAMP1-GFP. LAMP was detected from the GFP tag as green fluorescence in the cells. Cells were labelled with the rabbit anti-CLN5 antibodies and a red fluorescent antibody tag, goat anti-rabbit Alexa 594 (Figure 4.3). Yellow fluorescence indicated overlaps of the two proteins. This co-localisation indicates that the full CLN5 antibody was able to detect ovine CLN5 in lysosomes. Not all cells were double transfected, showing signals from either LAMP1-GFP or CLN5 alone.

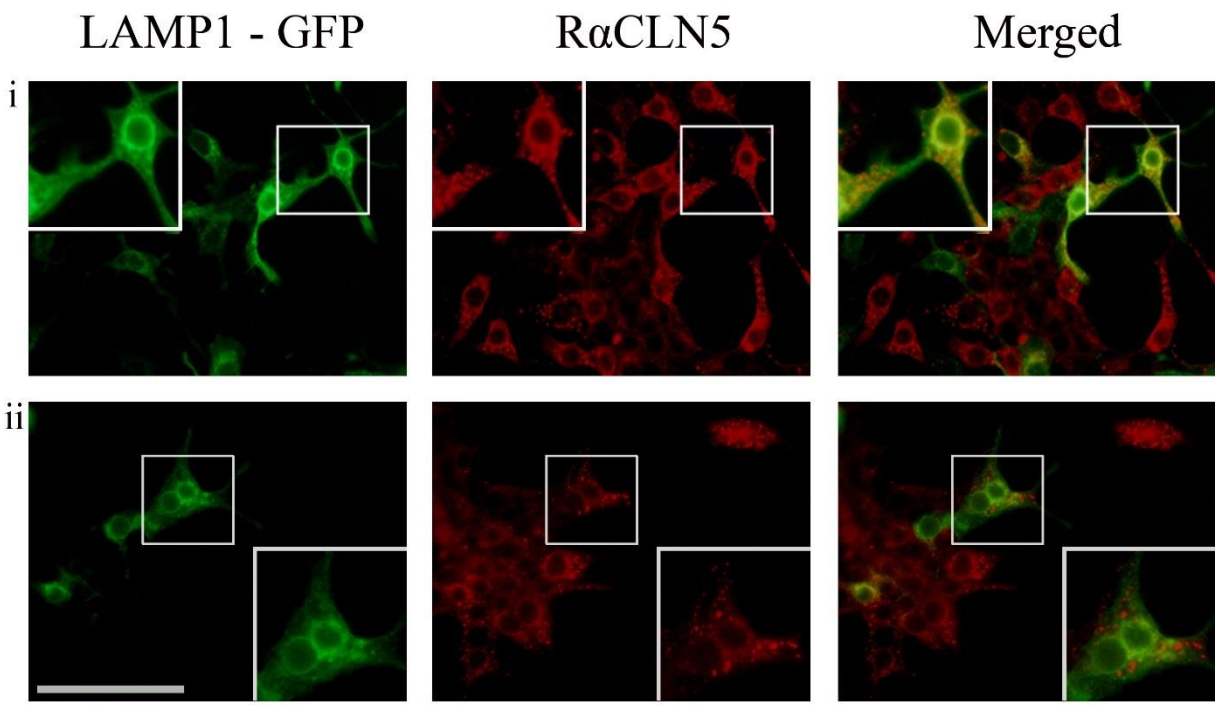

Figure 4.3 Co-localisation of a LAMP1-GFP fusion and CLN5 protein expression

Immunofluorescent images of LAMP1-GFP protein (green) and CLN5 protein (red) in the 293FT LVMNDCLN5 cells. Cell images from top (i) and bottom (ii) panels were randomly selected. RαCLN5 refers to rabbit anti-CLN5 antibodies staining. Yellow fluorescence indicates co-localisation. The scale bar represents 200 µm.

4.3.2 Intracellular co-localisation of the CLN6 protein to the ER

The 293FT LVMNDCLN6 cells were double labelled with rabbit anti-CLN6 and mouse anti-PDI antibodies. The mouse anti-PDI antibody was detected as a red signal and the CLN6 protein stained with anti-CLN6 gave a green signal. Yellow/orange fluorescence indicated co-localisation of CLN6 protein and PDI, a marker for the ER. Double immunofluorescent microscopy images taken from three randomised sites (i, ii, and iii) all demonstrated the same typical patterns of staining for both the PDI and CLN6 proteins (Figure 4.4).

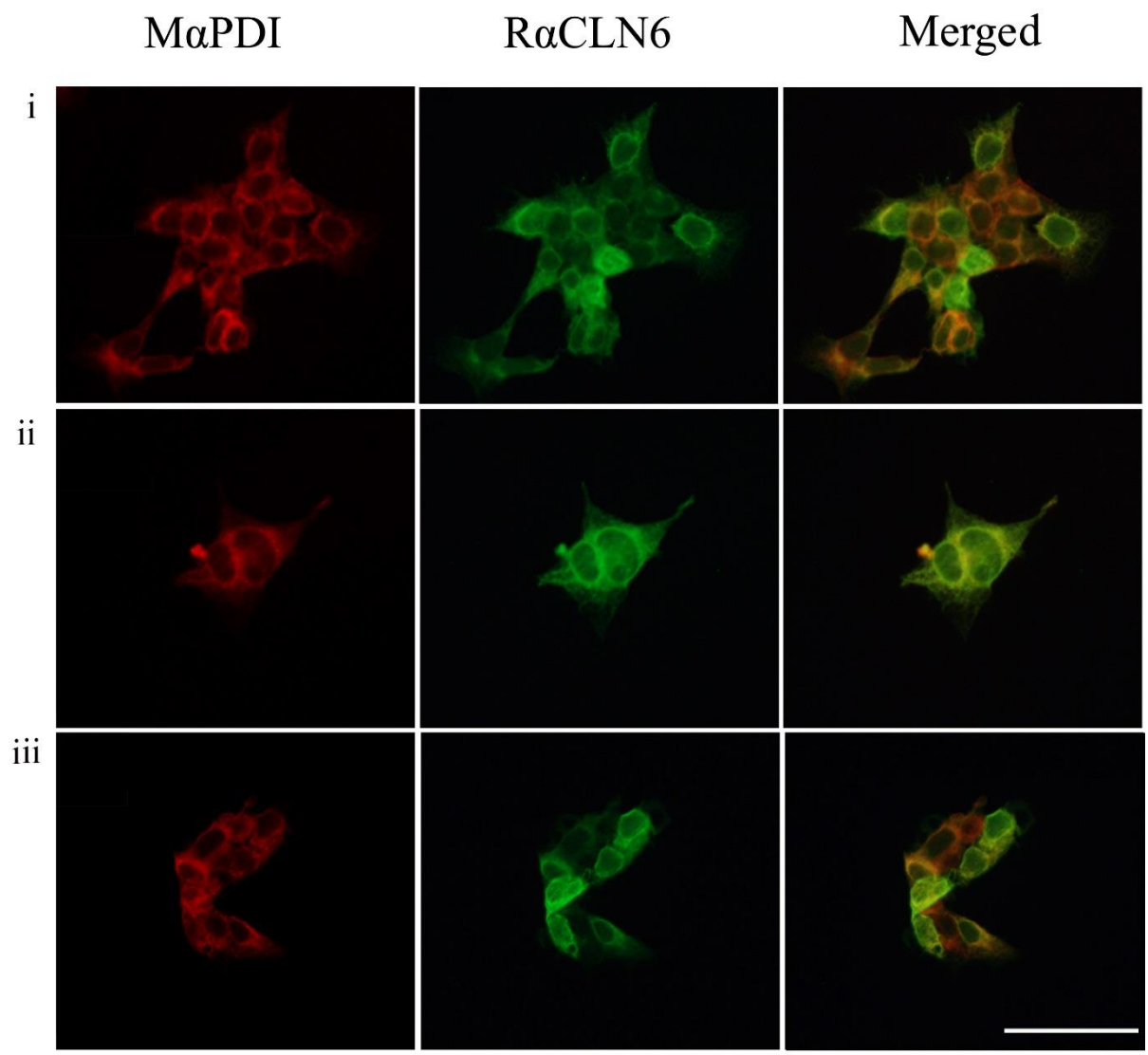

Figure 4.4 Immunofluorescent images of CLN6 and the ER marker PDI expression in 293FT LVMNDCLN6 expressing cells

293FT LVMNDCLN6 cells were fixed at 30% confluence and double-labelled with mouse anti-PDI (1:100, red) and rabbit anti-CLN6 (1:500, green). MαPDI refers to the mouse anti-PDI antibodies, RαCLN6 to the rabbit anti-CLN6 antibodies. Merged yellow and orange images indicate co-localisation. The scale bar represents 100 µm.

4.3.3 CLN5 antibodies detect endogenous protein in tissue

Results of the study described in Chapter 3 confirmed that the specific polyclonal anti-CLN5 antibody raised in rabbit detected over-expressed ovine CLN5 protein in transduced HEK293FT cells. The next step was to find out if it could detect endogenous CLN5 in ovine and human brain sections. Sections from the hippocampus, cerebellum and cortex of normal and CLN5 affected sheep, and normal human brains (obtained from Professor Hans Goebel, Berlin) were incubated with rabbit anti-CLN5. Positive staining was detected in brain sections from both sheep and humans (Figure 4.5 and Figure 4.6).

4.3.3.1 Endogenous sheep CLN5 protein expression

Light microscopy revealed intense brown punctate DAB staining in all selected regions of the control sheep brain sections (Figure 4.5). The strongest specific CLN5 punctate staining was detected in the hippocampus (Figure 4.5 A and B), the hilus, granule cells (GCL) of the dentate gyrus, pyramidal cells, particularly in the CA3 and CA2 regions (Figure 4.5 A). CLN5 immunostaining was predominantly localised to the neuronal cell soma and along the neurites of some larger cells. Endogenous CLN5 expression was also observed in the Purkinje cells layer of the cerebellum (Figure 4.5 C). CLN5 positive cells were found evenly across the all cortical layers (Figure 4.5 E), and the granular cells of the motor cortex exhibited clear CLN5 staining (not shown). No expression was seen in any of the CLN5 affected sheep tissues with the CLN5 antibody (Figure 4.5 A, insert) or negative controls from which the primary antibody was omitted (Figure 4.5 D). These results confirm the specificity of the CLN5 antibodies raised in rabbit and show that they detect endogenous CLN5 in normal sheep brains.

4.3.3.2 Endogenous human CLN5 protein expression

CLN5 protein was detected in the human brain, including the cerebellum, hippocampus and cortex (Figure 4.6). The strongest immunostaining was revealed in the cerebellar region. In particular, granular cells (small round cells) and Purkinje cell bodies and axons were noticeably stained (Figure 4.6 A and B, indicated with black arrows). This strong CLN5 immunoreactivity of human granular cells contrasts with the weaker staining of granular cells in the sheep brain samples (Figure 4.6 C). Punctate CLN5 staining of cells was also clearly detected in granular cells of the visual cortex (Figure 4.6 C), pyramidal cells in the CA3 (Figure 4.6 D) and hilus (Figure 4.6 E) of hippocampus. There was no DAB staining in sections in the absence of primary antibodies (Figure 4.6 F).

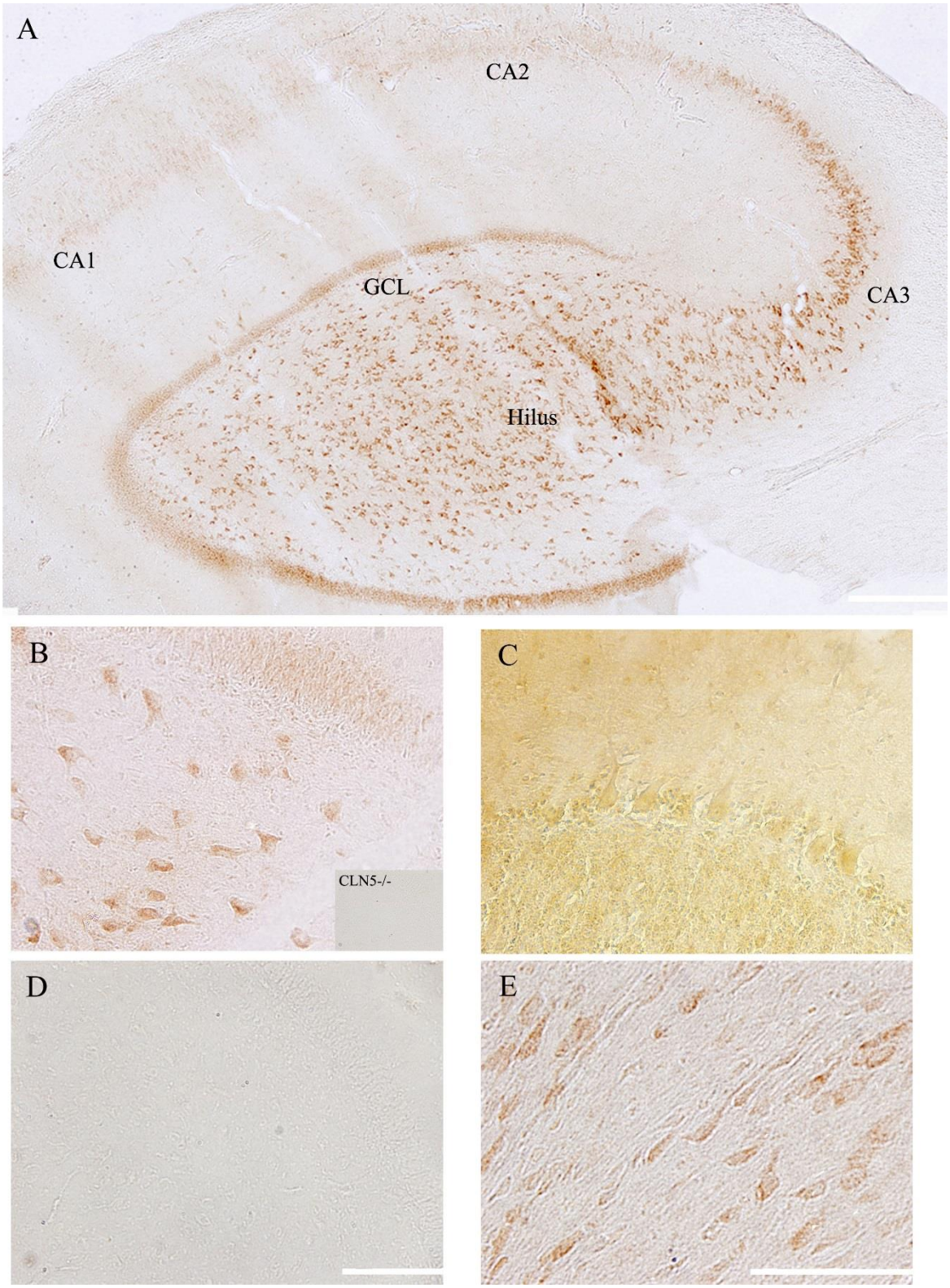

Figure 4.5 Expression of the endogenous CLN5 protein in the normal sheep brain

Positive CLN5 immunostaining in hippocampus (A, B), cerebellum (C) and visual cortex (E). The hippocampus (D) is the negative control, from which the CLN5 antibody was omitted. The insert on B shows the lack of CLN5 expression in the hippocampus of the affected brain. The scale bars represent 500 µm in A, 100 µm in B, C, E and 200 µm in D.

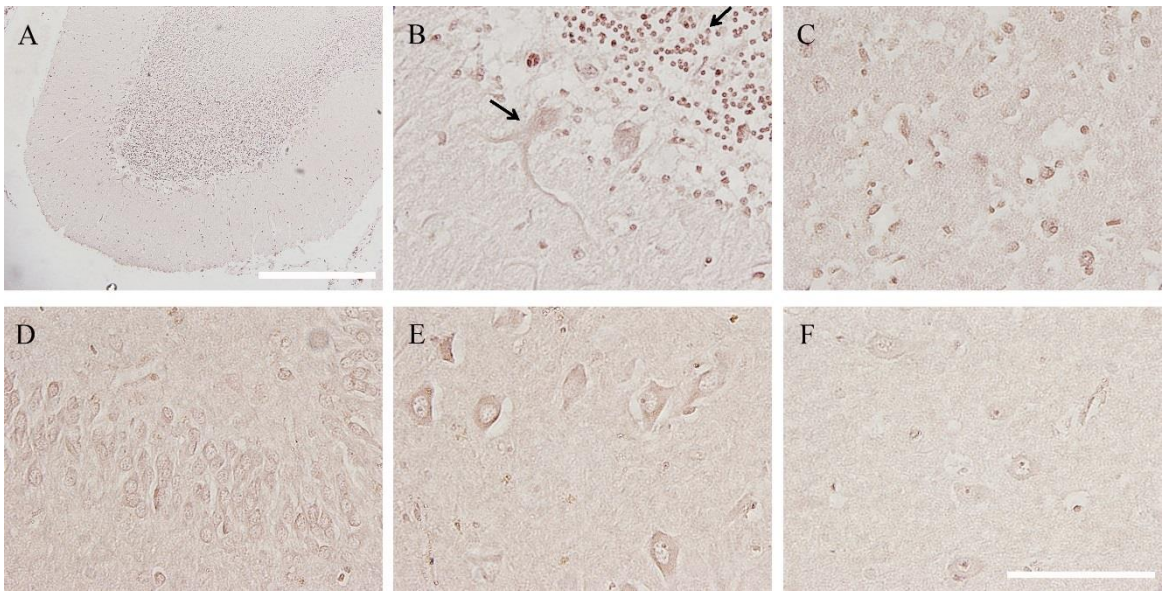

Figure 4.6 Immunohistochemistry of human brain sections

Positive staining of CLN5 in the sections of cerebellum (A, B), visual cortex (C), and hippocampus (D, E) of normal human brain. The negative control (F) is the hippocampus without primary antibody. The scale bars represent 100 µm.

4.3.4 Immunohistochemical double fluorescent labelling

Ovine CLN5 expression was detected throughout the CNS (4.2.3.1). To visualise which neural cells express CLN5, sheep brain sections were co-stained with different red fluorescent markers, including NeuN and three GABAergic interneuron markers, calbindin, parvalbumin and calretinin. All the neural markers stained red, while the rabbit (or mouse) anti-CLN5 fluorescence was green. Double labelled merged neural cells were yellow, and their nuclei were stained blue with DAPI (Figure 4.7).

Calbindin staining co-localised with CLN5 positive Purkinje and basket cells in the cerebellum (Figure 4.7 A). Calbindin/CLN5 double labelling also clearly detected big motor neurons in the brain stem (Figure 4.7 B). Parvalbumin antibodies stained GABAergic interneurons in the nervous system, shown by specific positive CLN5 co-staining in reticular cells in the thalamus (Figure 4.7 C).

Calretinin showed a similar expression pattern to CLN5 in the hippocampus, especially in the axons and dendrites of CA3 neurons, and neurons of the dentate gyrus and hilus (Figure 4.7 D). Double-labelling revealed that the neurons determined via NeuN displayed a similar CLN5 positive expression pattern. The CLN5 signal was observed in big motor neurons in the

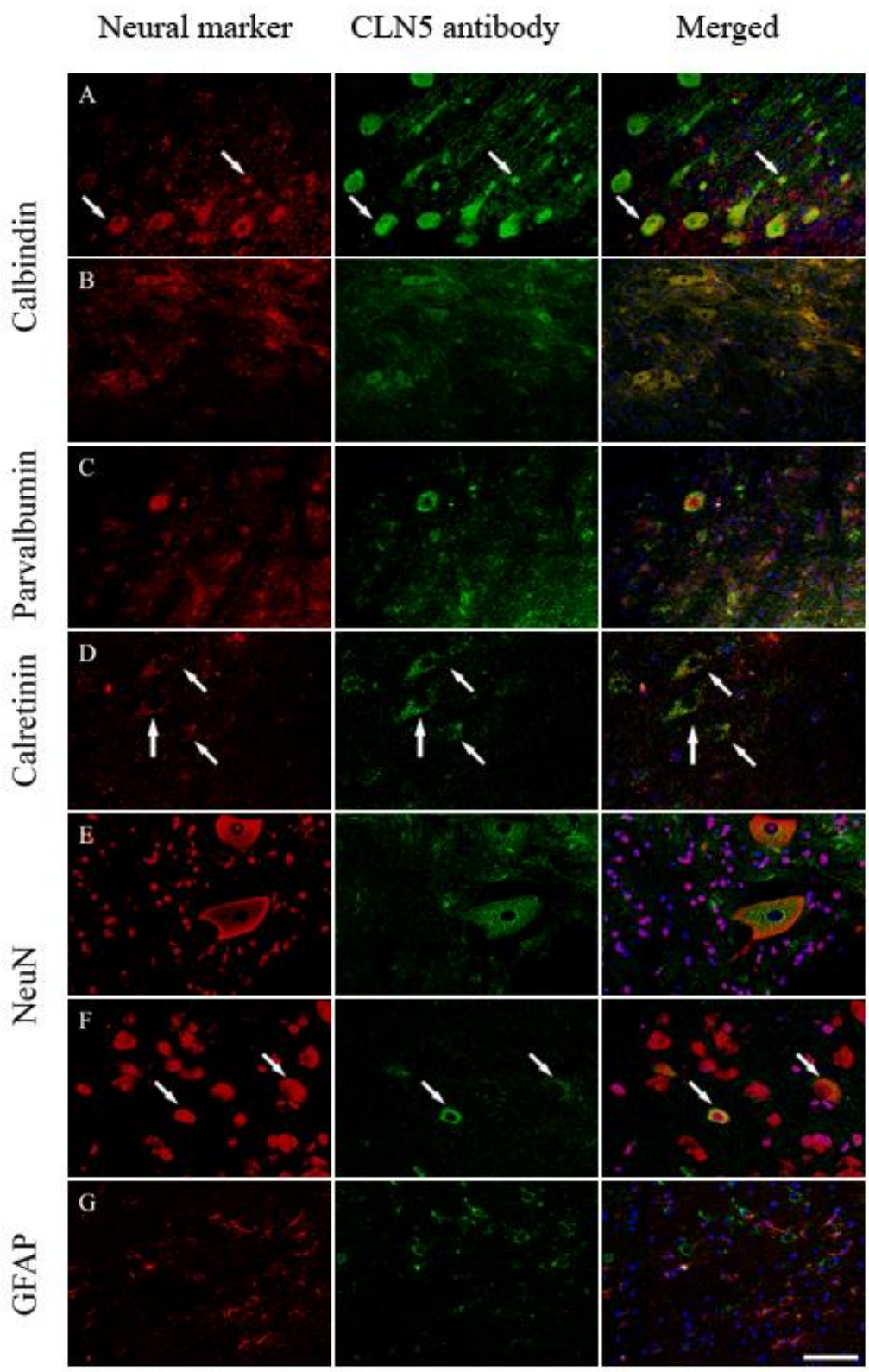

Figure 4.7 Confocal double fluorescent immunohistochemical labelling of neurons expressing CLN5 and neuron markers on ovine brain sections

Green rabbit (or mouse) anti-CLN5 co-localised with the red neural markers, calbindin in the cerebellum and brain stem (A and B), parvalbumin in the thalamus (C), calretinin in the hippocampus (D), and NeuN in the brain stem and cortex (E and F). Anti-CLN5 did not co-localise with GFAP in the cortex (G). The scale bar represents 200 µm for A, B and C and 100 µm for D, E, F and G.

brain stem (Figure 4.7 E) and pyramidal neurons in the cortex (Figure 4.7 F) by co-localisation with NeuN.

Specific staining was confirmed by comparison with glial fibrillary acidic protein (GFAP), and the omission of primary antibodies (Appendix A.4, negative control). GFAP which is found in glial cells particularly astrocytes, did not co-stain with CLN5 in the cortex (Figure 4.7 G, negative control) indicating little CLN5 expression in astrocytes. Overall, key cellular expression of CLN5 was observed in Purkinje and granular neurons in the cerebellum, hippocampal interneurons, pyramidal neurons in the cortex and motor neurons in brain stem.

4.3.5 Interactions of CLN5 and CLN6 proteins

4.3.5.1 CLN5 in culture media from CLN5 in virally transduced neural cells

Transduction of affected CLN5 and CLN6 cells with LV CLN5 was assessed by immunofluorescence and from the media by Western blotting to determine whether CLN5 protein is restored and expressed in mutated cells *in vitro*. The CLN5 band was not detectable in any of the affected non-transduced cells (negative controls), or in the control non-transduced cells (Figure 4.8a). This indicates endogenous cellular CLN5 expression is below the threshold level of detection. However, CLN5 protein, 60 kDa, was detected in all the lanes of the Western blot containing media samples from LV CLN5 transduced control and affected CLN5 and CLN6 neural cells, as well as from overexpressing CLN5 cells (positive control, section 3.2.1.5) (Figure 4.8 a). This suggests that CLN5 expression can be restored and that CLN5 secretion from these cells is detectable.

All the cells that received CLN5 viral-mediated treatment secreted CLN5 protein into the media. Immunofluorescence of LV CLN5 treated cells was carried out with the rabbit anti-CLN5 antibodies in a short staining protocol to improve the staining clarity. Both control and affected CLN5 and CLN6 secondary neural cells revealed bright and clear punctate green staining with the rabbit anti-CLN5 antibodies after transduction with LVCLN5 (Figure 4.8 B). In particular a control *CLN6*$^{+/-}$ F2 contained a large star-like cell, spreading onto the bottom of the well, typical of a secondary neural cell (Figure 4.8 B-C). The major bodies of the cells were an intense green compared with edge of the cells, suggesting that LV CLN5 transduced cells were generating CLN5 in the ER close to nuclei and then trafficking it into lysosomes

close to the plasma membrane. These results suggest that even affected neural cells (for example *CLN5*$^{-/-}$ F14 and *CLN6*$^{-/-}$ F25) are able to express and process transduced LV CLN5.

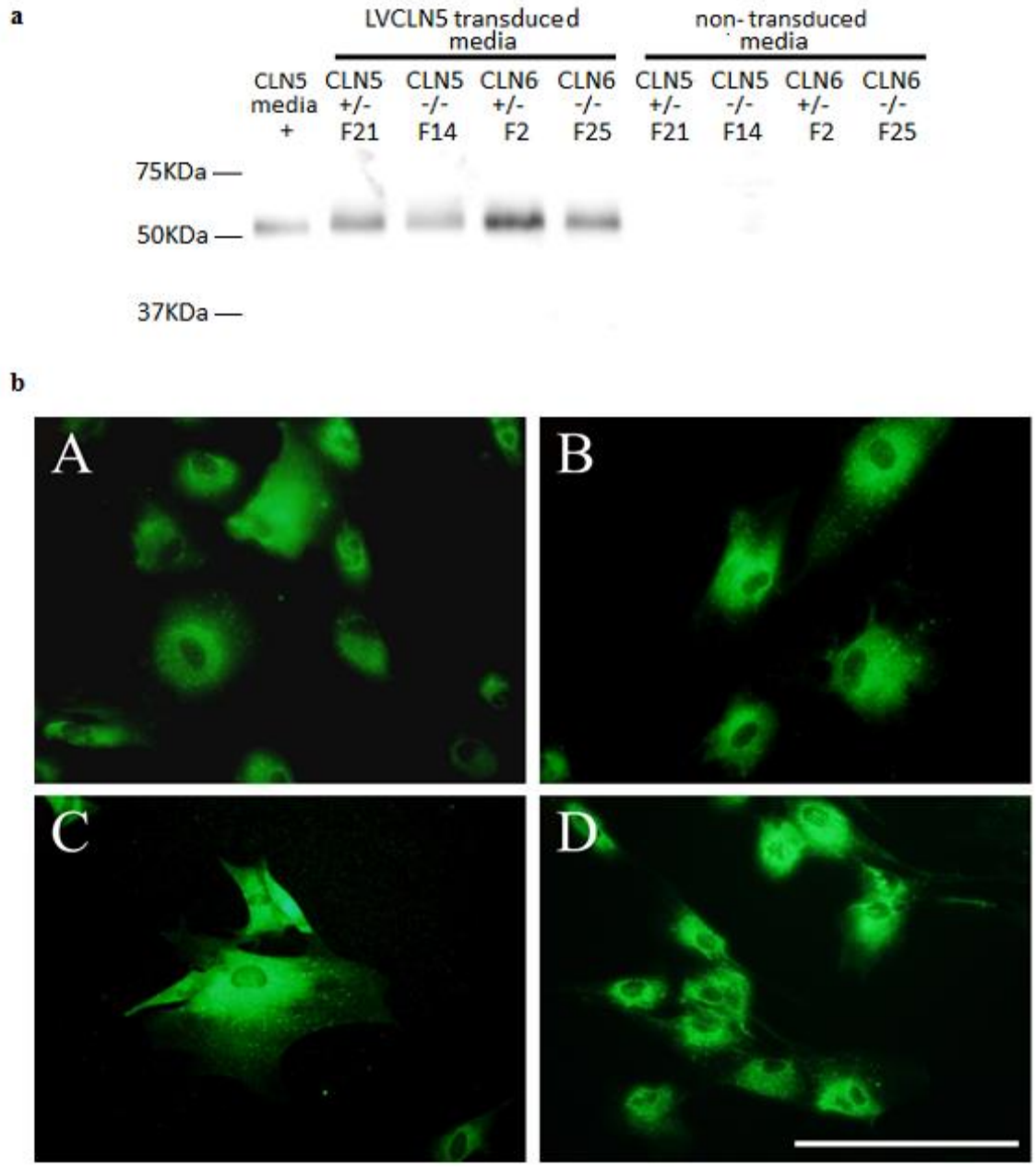

Figure 4.8 CLN5 is expressed in virally transduced CLN5 and CLN6 neural cells

Secondary ovine neural cell cultures were plated and maintained following standard protocols. (a) The media were collected and concentrated for Western blotting, then 3 µl of each concentrated media sample and the media from overexpressing CLN5 cells (positive control) were separated on a 10% SDS-PAGE, transferred to a PVDF membrane and subsequently treated with 1:5000 goat anti-rabbit HRP. A pre-stained Precision Plus protein marker was used to determine molecular weights. (b) Immunocytochemistry images of CLN5 transduced neural cells after fixing in 4% PFA: control *CLN5*$^{+/-}$ F21 (A), affected *CLN5*$^{-/-}$ F14 (B), control *CLN6*$^{+/-}$ F2 (C) and affected *CLN6*$^{-/-}$ F25 (D). CLN5 expression was detected with 1:500 rabbit anti-CLN5 and 1:1000 goat anti-rabbit Alexa 488 HRP. The scale bar represents 200 µm.

4.3.5.2 CLN5 expression in virally transduced control and affected neural cells

This particular experiment aimed to determine any effect of viral-mediated co-expression of CLN5 on cultured cells. Media were collected from control and affected CLN5 or CLN6 neural cells, which were transduced with LV CLN5 alone or both LV CLN5 and LV CLN6 and probed by Western blotting with the rabbit anti-CLN5 antibodies. CLN5 was generated in all the cell samples, detected as a single protein band at 60 kDa in all lanes (Figure 4.9 a). Integrated densities of the CLN5 protein bands in neural cells on the Western blots were measured using Image J, normalised against reference over-expressed CLN5 cells and graphed with Excel (Figure 4.9 b). Induced CLN5 expression was twice that in the *CLN5*$^{-/-}$ cells transduced with both viruses (the orange column at the right) compared with the same cells transduced with LV CLN5 alone (the blue column at the right). No significant difference was found for CLN5 expression in the *CLN5*$^{+/-}$ cells virally transduced with CLN5 or CLN5 and CLN6 vectors.

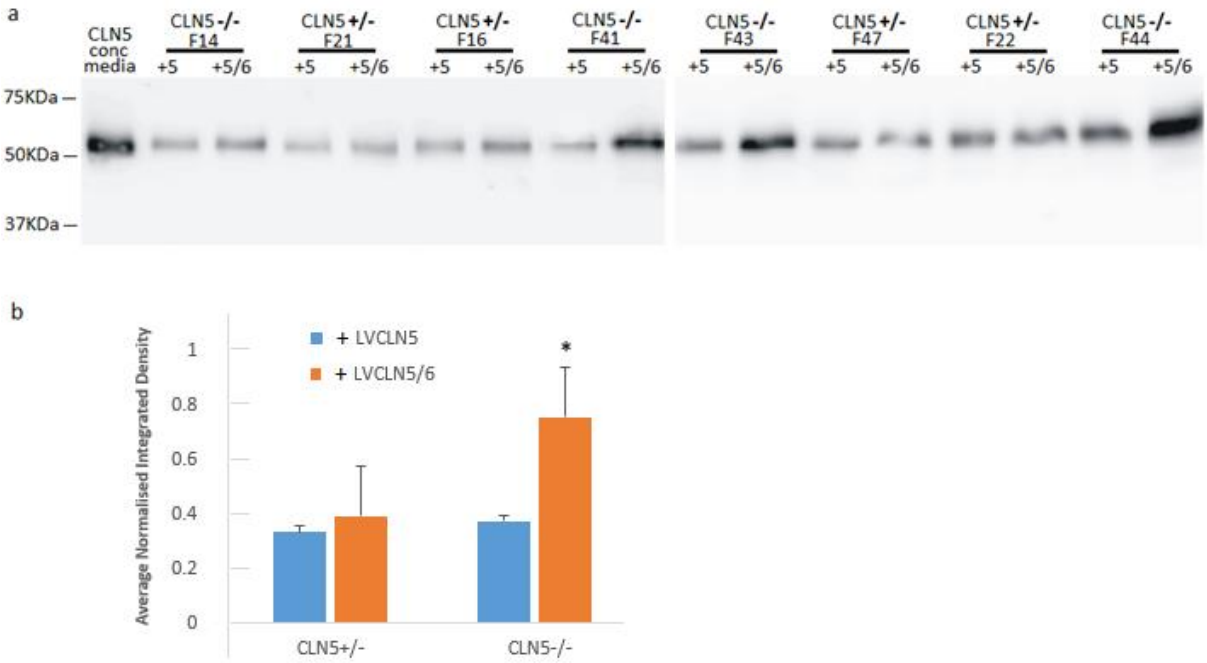

Figure 4.9 CLN5 expression in control and CLN5 affected neural cells transduced with LV CLN5 alone or both LV CLN5 and LV CLN6 virus.

(a) Western blots of the concentrated secreted CLN5 cell media. The band densities represent CLN5 expression. (b) The bands in the Western blots were measured and the average normalised integrated density of the CLN5 affected (*CLN5*$^{-/-}$, n = 4) neural cells compared with the control (*CLN5*$^{+/-}$, n = 4) neuronal cells. The blue columns refer to cells transduced with LV CLN5 alone, and the orange columns refer to cells transduced with both LV CLN5 and LV CLN6 viruses. CLN5 expression was induced 2-fold (* $P < 0.05$) in the *CLN5*$^{-/-}$ cells transduced with both viruses compared with the same cells transduced with LV CLN5 alone. The vertical error bars are $\pm$ SEM.

Western blotting also revealed a single protein band at 60 kDa in all the CLN6 neural cells transduced with either LV CLN5 or both viruses (Figure 4.10 a), suggesting that with CLN6 present, CLN5 expression was not blocked in CLN6 affected cells. The averaged normalised integrated densities of the protein bands showed CLN5 expression was not statistically different in affected cells (the blue column at the right) compared with controls after transduction with LV CLN5 alone (the blue column at the left) (Figure 4.10 b). Notwithstanding that CLN5 expression appeared to be higher in the *CLN6*$^{-/-}$ cells transduced with both LV CLN5 and LV CLN6 viruses (the orange column at the right) than those transduced with LV CLN5 alone (the blue column at the right).

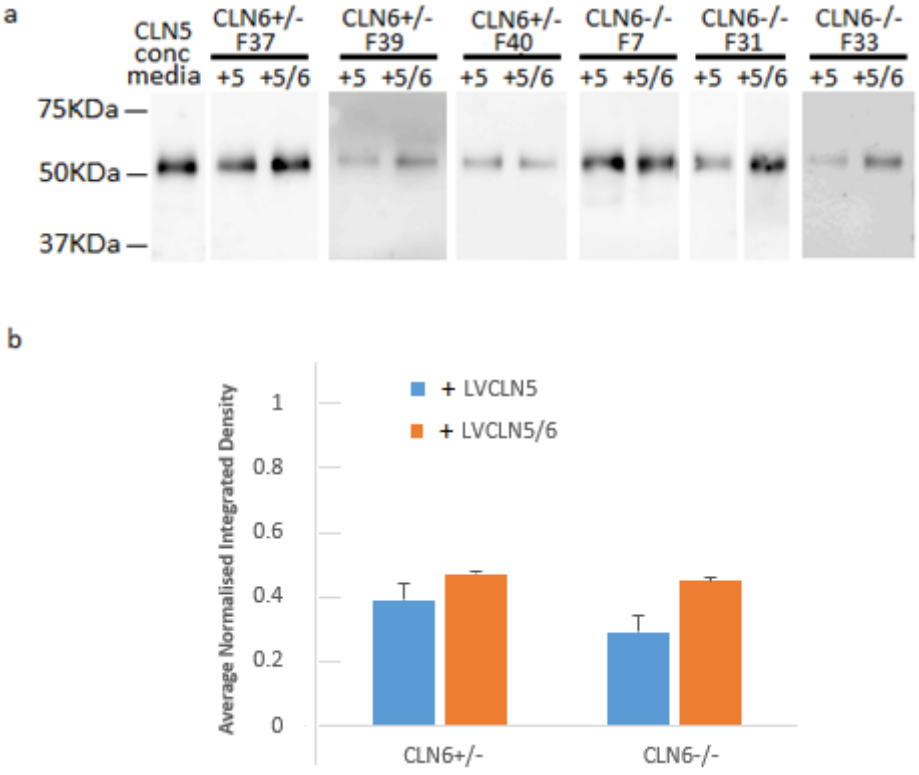

Figure 4.10 CLN5 expression in control and CLN6 affected cells transduced with LV CLN5 alone or both LV CLN5 and LV CLN6 viruses.

(a) Western blots of the concentrated secreted CLN5 cell media. (b) The bands in the Western blots were measured and the average normalised integrated density of the affected (*CLN6*$^{-/-}$, n = 3) neural cells compared with the control (*CLN6*$^{+/-}$, n = 3) neuronal cells. The blue columns refer to cells transduced with LV CLN5 alone, the orange columns refer to cells transduced with both LV CLN5 and LV CLN6 viruses. The vertical error bars are ± SEM.

4.3.5.3 CLN6 expression in virally transduced control and affected neural cells

This experiment aimed to determine the effect of viral-mediated co-expression of CLN6 on cultured cells. CLN5 and CLN6 affected neural cells transduced with LV CLN6 or LV CLN5 and LV CLN6 viruses, and the non-transduced controls were lysed for Western blotting with the rabbit anti-CLN6 antibody. CLN6 was present, as a protein band at 27 kDa in every lane (Figure 4.11 a and b). β-actin (42 kDa) was used as a loading control. No CLN6 band was detected in the blots of non-transduced cells. However, most of neural cells contained another band slightly bigger than 27 kDa, or an extra band slightly bigger than 42 kDa, while overexpressed cells showed only one band from the Western Blots.

According to the averaged normalised integrated densities of the protein bands, CLN6 protein expression was not statistically different between the affected cells (*CLN6*$^{-/-}$ and *CLN5*$^{-/-}$) transduced with both viruses compared with those cells transduced with LV CLN6 alone (Figure 4.11 c and d). However, expression appeared to be increased in the affected CLN6 cells transduced with both viruses (the orange column at the right) compared with the same cells transduced with LV CLN6 alone (the green column at the right) (Figure 4.11 c), and to be decreased in the affected cells (Figure 4.11 d).

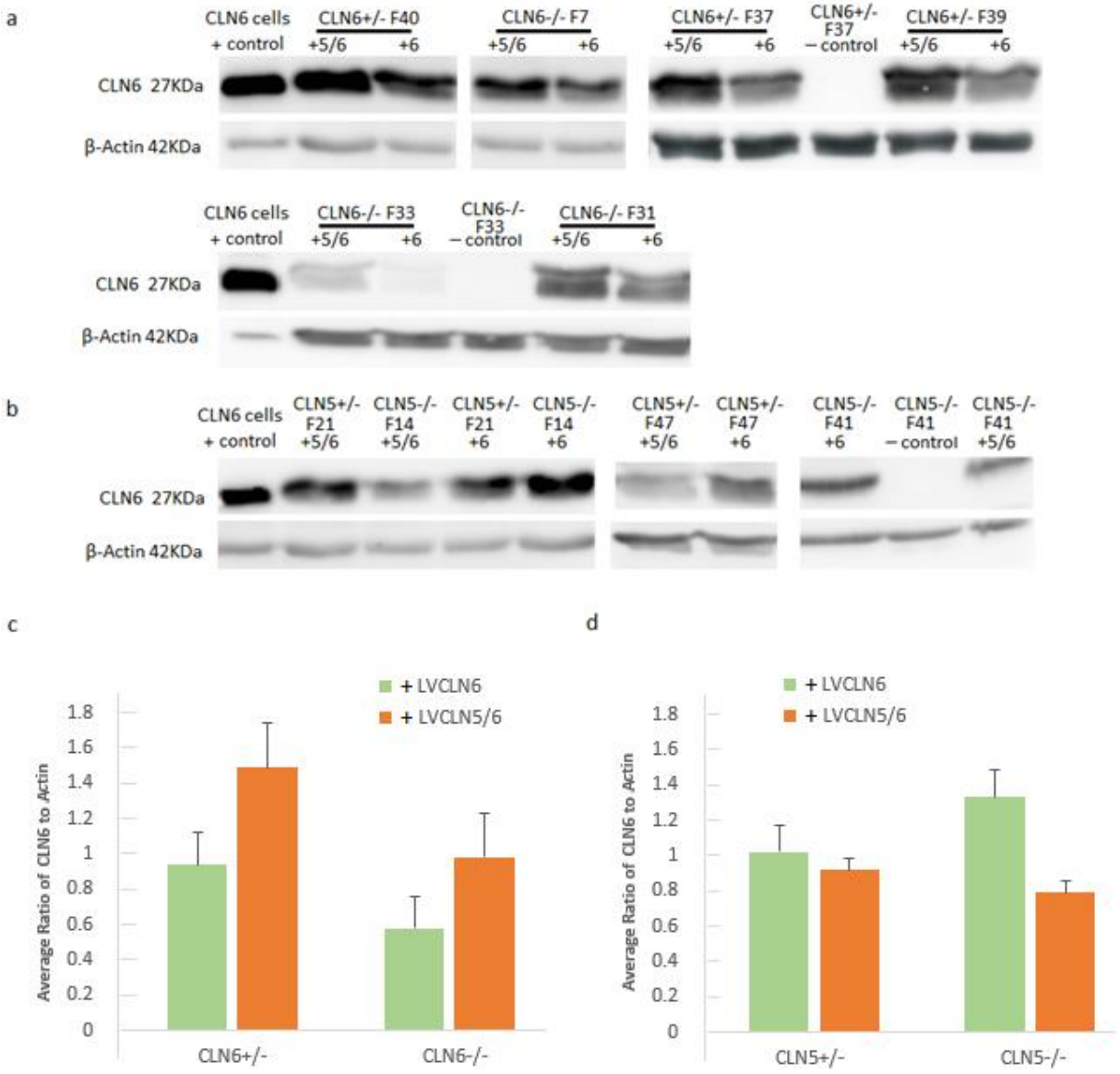

Figure 4.11 CLN6 expression in control and affected neural cells transduced with LV CLN6 alone or both LV CLN5 and LV CLN6 viruses.

(a, b) Western blots of the CLN6 expression in control, CLN6 and CLN5 affected cells. The band densities represent CLN6 expression. The averaged ratio of each normalised integrated density of CLN6 to its β-actin expression (loading control) was measured, in the CLN6 affected (*CLN6*$^{-/-}$, n = 3) neural cells compared with the control (*CLN6*$^{+/-}$, n = 3) neuronal cells (c) and the CLN5 affected (*CLN5*$^{-/-}$, n = 2) neural cells compared with the control (*CLN5*$^{+/-}$, n = 2) neuronal cells (d). The green columns refer to cells transduced with LV CLN6 alone, and the orange columns to cells transduced with both LV CLN5 and LV CLN6 viruses. The vertical error bars are ± SEM.

4.4 Discussion

The subcellular localisation and endogenous expression of both ovine CLN5 and CLN6 proteins are important for functional studies and required for understanding of the trafficking mechanisms. However, the availability and/or production of high quality

antibodies to the either protein has always been problematic. Promising specific CLN5 and CLN6 antibodies have been recently developed via adenoviral vectors (see Chapter 3). Western blotting and immunocytochemistry with these antibodies successfully detected these proteins in overexpressed cells (see Chapter 3).

4.4.1 Characterisation of the cellular localisations of ovine CLN5 and CLN6

The intracellular co-localisation of ovine CLN5 to lysosomes was revealed by specific CLN5 antibody labelling of transfected 293FT LVMNDCLN5 cells, expressing the lysosomal protein LAMP 1-GFP (lysosomal associated membrane protein) (Figure 4.3). This correlated with similar findings in the mouse brain (Holmberg et al., 2004), where the mouse CLN5 protein also co-localised with LAMP 1. Other studies on overexpressed CLN5 protein, BHK21, COS1 and HeLa cells also reported co-localisation to lysosomes (Isosomppi et al., 2002; Vesa et al., 2002; Holmberg et al., 2004; Sleat et al., 2006a). In the present study, the cells with positive CLN5 signals did not always express LAMP 1-GFP proteins, presumably because not all cells were double transfected. The HEK293FT cells were first transduced with the full ovine CLN5 DNA, and then with the LAMP 1-GFP DNA construct.

Intracellular ovine CLN6 completely co-localised with the ER marker PDI in transfected 293FT LVMNDCLN6 cells (Figure 4.4). These data confirmed previous suggestions that the CLN6 protein is localised to the ER (Mole et al., 2004; Heine et al., 2004; Kurze et al, 2010). An intracellular location of endogenous CLN6 was suggested by co-localisation of PDI and antibodies raised against synthesised peptides based on the human CLN6 sequence (Mole et al., 2004). However, this antibody was problematic and did not stain sheep sections (Dr. Lucy Barry, personal communication). Co-localisation of the CLN6 protein with PDI in BHK cells transfected with wild type CLN6 cDNA has been also reported previously (Heine et al., 2004).

4.4.2 Characterisation of antibodies for endogenous CLN5 detection

The CLN5 antibody specifically detected endogenous CLN5 expression throughout the normal sheep brain, most prominent expression being seen in the hippocampus, cortex and cerebellum, particularly in the CA3 and CA2 regions, the hilus and granule cells of the dentate gyrus (Figure 4.5). Similar CLN5 staining was seen in the mouse brain (Holmberg et al., 2004; Fabritius et al., 2014; Minye et al., 2016). Immunohistochemical staining of mouse brain sections detected CLN5 in Purkinje cells of cerebellum, hippocampal pyramidal cells and cortex (Holmberg et al., 2004).

Further analysis showed that CLN5 is expressed widely in neurons and interneurons in the normal ovine CNS (Figure 4.7). The most intense signals were detected in the Purkinje and basket cells of the cerebellum and pyramidal neurons in the hippocampus. The CLN5 protein was also expressed in some reticular cells in the thalamus and some interneurons in the striatum, frontal and visual cortices. All these data confirm earlier collaborative studies which showed that CLN5 immunoreactivity in healthy sheep brain sections co-localized with GABAergic interneuron markers and a neuronal marker (Kristina McIntyre, personal communication). The distribution of CLN5 positive cell types in the normal sheep brain is similar to the pattern reported in the normal mouse brain (Holmberg et al., 2004; Tepper et al. 2010; Minye et al., 2016). CLN5/parvalbumin and CLN5/calbindin double stainings of the normal mouse brain sections detected CLN5 in Purkinje cells of the cerebellum, hippocampal pyramidal cells and cortical neurons (Holmberg et al., 2004), while the GABAergic interneurons lost CLN5 signals in CLN5 affected cerebral cortex and cerebellum (Kopra et al., 2004). Tepper and co-workers (2010) also used these three GABAergic interneuron markers to co-label CLN5 neurons in the mouse striatum. Strong co-expression of CLN5 and calbindin (or NeuN) was revealed in motor neurons in the brain stem (Figure 4.7 B and E), suggesting CLN5 was largely expressed in motor neurons. In the late stage of human CLN5 disease, cerebella Purkinje cells and thalamic neurons are lost, as are some cortical neurons (Tyynelä et al., 1997). The ovine CLN5 protein was not detected in GFAP positive astrocytes (Figure 4.7 G), confirming a previous study showing that CLN5 and GFAP were not co-localised in sheep *in situ* (Kristina McIntyre, personal communication). On the other hand, a quantitative PCR study demonstrated murine *CLN5* mRNA expression in glial cell cultures (Holmberg et al., 2004).

The rabbit anti-CLN5 antibodies also detected CLN5 expression in the hippocampus, cortex and cerebellum of normal human brains (Figure 4.6). Human and sheep CLN5 share 84% amino acid identity (Figure 1.1), and the similarity is even higher (90%) for the mature protein without the signal sequence. Therefore, it is not surprising that rabbit anti-CLN5 is able to detect human CLN5. The granule cells and Purkinje cell bodies and axons of the human cerebellum (Figure 4.6 B) were strongly immunoreactive, compared with the slightly weaker positive signal from these cells in the sheep (Figure 4.5 C), when the same concentration of the antibodies was applied. This difference may be due to the age or

position of the samples selected. Different fixation and the dewaxed section thickness (50 µm ovine, and 3 µm human) may also have affected the staining.

Taken together, CLN5 protein shares a common distribution among sheep, human and mouse brains. In this study, CLN5 expression in sheep and human brains is concentrated in the hippocampal pyramidal cells, Purkinje cells of the cerebellum and pyramidal cells in the cortex, and this is also true for the mouse brain (Holmberg et al., 2004).

4.4.3 Interactions of the CLN5 and CLN6 proteins

Despite the very different genotypes and cellular localisation of the CLN5 and CLN6 proteins, defects in the progressive pathological changes during neurodegeneration and brain atrophy indicate that they interact closely in the CNS. An interaction between CLN5 and CLN6 was first suggested in a mouse NCL model by Lyly and co-workers (2009), but it has been difficult to substantiate, as no useful antibodies were available.

In these studies, the potential interactions between the two proteins in the CLN5 and CLN6 ovine models were examined in cultured virally transduced neural cell lines using the specific CLN5 or CLN6 antibodies. Results from Western blotting and immunofluorescence studies showed that both affected CLN5 and CLN6 cells transduced with LV CLN5 expressed CLN5 *in vitro* (Figure 4.8), indicating that the CLN5 transgene was expressed in these defective cells. It also suggested that CLN6 is not the key factor for CLN5 trafficking.

The further studies compared the effect of viral-mediated co-expression of CLN5 and CLN6 on affected CLN5 and CLN6 cells. Co-transduction of LV CLN6 with LV CLN5 significantly increased CLN5 expressions in the affected CLN5 cells transduced with both viruses compared with the cells transduced with LV CLN5 alone (Figure 4.9). These results suggest that CLN6 is involved in the correct processing of the CLN5 protein, and that CLN5 expression could be up-regulated by viral-mediated co-expression of CLN6 in CLN5 affected cells.

The amounts of CLN5 protein in affected CLN6 cells appeared to be lower than in controls (Figure 4.10), consistent with other studies of CLN6 affected brain tissues from both South Hampshire and Merino affected sheep (Mitchell, 2016; Palmer et al., 2017; Russell, 2017; Kristina McIntyre, personal communication). Surprisingly there was very little CLN5 expression in CLN6 affected sheep, and only intermediate staining in heterozygous CLN6 sheep (Hughes et al., 2014b). Further quantitative PCR studies of brain samples also implied

an interaction between CLN5 and CLN6 expression (Palmer et al., 2017). Full length *CLN5* mRNA expression was increased 3-4 fold in CLN6 affected brains at 6-months of age compared with normal, thus there are sufficient amounts of *CLN5* mRNA but this does not result in successful CLN5 expression.

Co-transduction of LV CLN5 and LV CLN6 restored CLN6 expression in CLN6 affected cells, and whilst not statistically significant, the findings merit the case for further work with higher replication to test whether the CLN5 and CLN6 proteins and gene expression may be cross-regulated. In particular, this could examine whether increased CLN6 expression occurs in the affected CLN6 cells transduced with both viruses compared with the cells transduced with LV CLN6 alone (Figure 4.11 c), as well as whether co-expression of CLN5 decreases CLN6 expression in the affected CLN5 cells (Figure 4.11 d).

Furthermore, the extra bands from the Western blots that migrated slightly slower than 27 kDa, or an extra band slightly slower than 42 kDa were detected in samples from most of the neural cells, but not from the overexpressed cells (Figure 4.11 a and b). The CLN6 proteins expressed from overexpressed cells and neural cells may be structurally different and/or artificial changing of the apparent band sizes could result from the large amount of samples loaded to the gels.

4.5 Conclusion

In summary, the newly generated specific CLN5 and CLN6 antibodies confirm that ovine CLN5 is localised to the lysosome and that ovine CLN6 is in the ER. The *in situ* study showed that endogenous CLN5 is predominantly present in Purkinje and basket cells of the cerebellum and pyramidal neurons in the hippocampus, some reticular cells in thalamus and some interneurons in the striatum, frontal and visual cortices, and motor neurons in the brain stem.

Chapter 5
General Discussion

5.1 Thesis summary

The neuronal ceroid lipofuscinoses (NCLs, Batten disease) are a group of fatal neurodegenerative human lysosomal storage disorders that are caused by mutations in any of 13 different genes (Palmer et.al., 2015). Animal models of the human diseases provide valuable tools for determining the pathophysiology of disease and for developing effective therapeutic treatments (Linterman et al., 2011; Tecedor et al., 2013; Eaton and Wishart, 2017). Two naturally occurring ovine forms, CLN5 in Borderdale (BD) and CLN6 in South Hampshire (SH) sheep, are in well-established flocks (Jolly et al., 2002; Tammen et al., 2006; Frugier et al., 2008). Mutations in *CLN5* result in the dysfunction of a soluble mannose-6-phosphate (M6P) tagged lysosomal protein (Holmberg et al., 2004; Sleat et al., 2005, 2006), which can be secreted from cells, and taken up by other cells via endocytosis. In contrast, CLN6 is considered to be an intracellular endoplasmic reticulum membrane associated protein (Gao et al., 2002; Wheeler et al., 2002; Heine et al., 2004). However, the functions of these two proteins are still unclear.

This thesis aimed to look at different cell biology and biochemistry aspects of the ovine CLN5 and CLN6 proteins, and possible interactions between them. Chapter 2 details the successful amplification of the full length ovine *CLN5* gene sequence using a two-step PCR and ligation strategy with internal overhanging primers (Figure 2.7 and Figure 2.8). This method overcomes the difficulties arising from the disjunction in GC/AT ratios between exons 1 and 2. An interesting finding is that ovine *CLN5* exon 1 has an allelic variant, with three amino acid differences arising from two polymorphisms and one deletion (Figure 2.4 and Figure 2.5), however this was not disease-associated. Unlike ovine *CLN5*, the human (Figure 2.16 and Figure 2.17) and bovine *CLN5* (Figure 2.15) genes do not contain variant sequences in their exon 1 region. Both full length ovine *CLN5* and *CLN6* sequences were cloned into expression vectors (e.g. pRUN vector or Gateway cloning vectors) for recombinant protein expression in *Escherichia coli* (*E. coli*). Unfortunately, all the CLN5 clones containing the target inserts showed random nucleotide base changes in the region from exon 2 to 4, most of which resulted in changes to two amino acids (Figure 2.10). These changes could arise because the ovine *CLN5* sequences may be toxic to the host during *E. coli* replication, which

would result in mutated *CLN5* sequences being selected instead of normal ones. Furthermore, none of the CLN5 and CLN6 clones could be used to express recombinant CLN5 and CLN6 proteins in *E. coli*. prokaryotic systems.

In Chapter 3, lentiviral vectors expressing the full length *CLN5* and *CLN6* coding sequences with or without C-terminal myc tags, under the control of the MND promoter were transduced into HEK293FT cells, and recombinant CLN5 and CLN6 proteins were successfully generated (Figure 3.1 and Figure 3.5). Adenoviral antibodies against ovine CLN5 and CLN6, produced by injection of adenoviral vectors expressing CLN5 and CLN6 proteins into rabbits and mice, were shown to recognise ovine CLN5 and CLN6 at high sensitivities. Western blotting with the rabbit anti-CLN5 antibodies specifically detected overexpressed ovine CLN5 at an apparent molecular weight of 60 kDa (Figure 3.5), and a single PNGaseF deglycosylated CLN5 product at around 35 kDa (Figure 3.7). Mass spectrometry studies confirmed that these antibodies specifically identified the ovine CLN5 protein. All of the tryptic peptides identified were consistent with the ovine CLN5 sequence and one of them was unique to ovine CLN5 (Figure 3.8). The N-signal sequence from *CLN5* exon 1 was not found in the CLN5 protein fragment of the band recognised by the rabbit anti-CLN5 antibodies. It was likely removed during processing through the ER, consistent with other soluble proteins whose signal sequences are cleaved when they mature, and consistent with the molecular weight from the gel. The deglycosylation study confirmed that CLN5 is a soluble glycosylated protein, containing both high-mannose and complex types glycans, allowing it to be trafficked to the lysosome mainly via a mannose-6-phosphate (M6P)-dependent pathway as well as secreted via exocytosis. There are eight potential N-glycosylation consensus sites (Asn – X – Ser/Thr) present in the ovine CLN5 polypeptide and six of them, at positions N180, 205, 257, 273, 283 and 355, have been confirmed (Figure 3.8). Similarly, the rabbit anti-CLN6 antibodies specifically detected a band in overexpressed ovine CLN6 at an apparent molecular weight of 27 kDa on Western blotting (Figure 3.5). Mass spectroscopy of the trypsin digested CLN6 fragments identified included a single fragment unique to ovine CLN6 (Figure 3.8).

Chapter 4 details the cellular and regional localisations of ovine CLN5 and CLN6 and the interactions between the proteins. Lysosomal localisation of ovine CLN5 was confirmed by double-labelling of transfected 293FT LVMNDCLN5 cells with rabbit anti-CLN5 antibodies and the lysosomal associated membrane protein, LAMP1 (Figure 4.3). Similarly, the ER

intracellular localisation of ovine CLN6 was revealed by co-staining with rabbit anti-CLN6 antibodies and the ER marker PDI in transfected 293FT LVMNDCLN6 cells (Figure 4.4).

The anti-CLN5 antibodies detected endogenous CLN5 expression throughout the normal sheep brain, most prominently in pyramidal cells of the cerebral cortex, Purkinje and basket cells of the cerebellum as well as the hilus, granule cells of the dentate gyrus and the pyramidal cells, particularly in the CA3 and CA2 regions of the normal sheep hippocampus (Figure 4.5). The ovine CLN5 protein was also found in motor neurons, some reticular cells in the thalamus and some interneurons in the striatum, frontal and occipital cortices. Furthermore, rabbit anti-CLN5 antibodies also detected CLN5 protein expression in normal human brain sections in the hippocampus, cortex and particularly the granule cells, Purkinje cell bodies and axons of the human cerebellum (Figure 4.6). The second part of this chapter provided evidence for the hypothesis that interactions between CLN5 and CLN6 proteins exist, using the rabbit anti-CLN5 and rabbit anti-CLN6 antibodies in cultured and virally transduced neural cell lines. Transducing CLN6 affected cells with a CLN5-containing lentivirus (LV CLN5) restored CLN5 expression (Figure 4.8), indicating that CLN6 is not a vital component of the transport of CLN5. Co-transduction of LV CLN6 and LV CLN5 restored CLN5 expression in CLN6 affected cells (Figure 4.10), and dramatically increased CLN5 expression in affected CLN5 cells transduced with both viruses compared with the cells transduced with LV CLN5 alone (Figure 4.9).

5.2 Overall discussion

5.2.1 Generation of the full ovine *CLN5*

Amplification of GC-rich sequences by PCR has been an irritant for scientists for decades and amplification of the full length ovine *CLN5* cDNA in one PCR reaction has not yet been achieved. Previous studies relied on several pairs of primers which amplified the exons and introns separately to produce the ovine *CLN5* sequence (Frugier et al, 2008). All mutation studies of *CLN5* in other species, including humans (Bessa et al., 2006), cattle (Houweling et al, 2006), and dogs (Melville et al, 2005), also used several short PCR reactions to produce the sequence data.

These difficulties are caused by the disjunction in GC/AT ratios, with a much higher percentage of G/C bases (around 80%) in the ovine *CLN5* exon 1 sequence compared with exons 2-4 (39%). GC-rich containing DNA sequences are more stable for PCR than sequences

with a low GC content; the higher the GC content, the higher the melting point of the DNA. The most common approach to overcome this problem is to increase the melting temperature, but this results in lower product yields, especially for whole coding sequence amplifications, as the *Taq* enzyme denatures more rapidly after several PCR cycles at higher temperature (Jensen et al., 2010). Substitution of dimethyl sulphoxide (DMSO) into PCR reaction mix could reduce the annealing temperature, but this also inhibits the *Taq* enzyme (Jurišić et al., 2016).

In this study, a two-step PCR and ligation strategy was developed to generate full length ovine *CLN5* (chapter 2). The key was to design pairs of complementary internal overhanging primers, which were 38 bp and 34 bp in length (at least 10 base pairs longer than standard PCR primers), so as to assist annealing. Each of the primers contained sequences with complementary ends of 5' or 3' sequences, so that the two separate *CLN5* exon 1 and exons 2-4 amplicons contained complementary sequences at the 3' end of the exon 1 fragment and the 5' end of the exons 2-4 fragment (Figure 2.7). This resulted in successful amplification of the full length coding sequence in the second PCR reaction. Doronina (2012) has also suggested increasing primers length by 10 bp as well as moving the primers 20-30 bp upstream or downstream for better annealing of difficult PCRs with GC rich substrates.

5.2.2 Failure of prokaryotic systems to express recombinant proteins

All attempts to express the ovine CLN5 and CLN6 recombinant proteins in prokaryotic systems failed, probably because of the toxicity of the target proteins, which may even cause bacterial cell death.

Expression vectors for many membrane proteins, as well as for other toxic proteins, can kill the host bacterium (Miroux and Walker, 1996). A modified C43 (DE3) strain was used in this study as it has been known to improve the stability of plasmids in cloning and culture during the expression of toxic proteins (Miroux and Walker, 1996), but only a few colonies were produced on the agar plates, and no recombinant CLN6 proteins was expressed by the clones. Similarly, only small amounts of F-ATPase b and c subunits (toxic proteins) were expressed using strain C43 (DE3), suggesting that removal of the toxic effects of an expression plasmid cannot automatically guarantee that the protein is generated in large amounts (Miroux and Walker, 1996). Based on these facts, it may be necessary to remove

the unnecessary features in the coding sequence that inhibit translation, or to prevent proteolytic degradation (Kane, 1995; Miroux and Walker, 1996).

Only a few CLN5 clones were produced in *E.coli*, and all contained mutant *CLN5* sequences (Figure 2.10), indicating that the highly toxic nature of the *CLN5* mRNA inhibited replication of any hosts containing normal *CLN5* sequences. Instead, only hosts containing mutated *CLN5* sequences were amplified. As explained above, the CLN5 toxicity may be due to the recombinant protein performing an unnecessary function, which interferes with the normal proliferation and homeostasis of the host and results in a slower growth rate and cell death (Dong et al., 1995).

In addition, many mammalian proteins are glycosylated, but CLN5 could not be glycosylated properly in *E. coli*, the N-terminal signal sequence not cleaved, and the protein may even be incapable of folding correctly without ER processing (Getty and Pearce, 2011). For example, a mouse CLN5-cDNA lacking the suggested signal sequence (aa 26-341) and fused with N-terminal GST tag construct was reportedly able to be expressed in *E. coli* (Lyly et al., 2009). However, the expressed GST-mCLN5 fusion protein was incubated with cultured cells for GST pull-down assays, but was not purified and detected by SDS-PAGE via traditional methods. Therefore whether or not enough mouse CLN5 was expressed with the correct molecular weight is not clear. Expressing a highly modified protein like CLN5 in *E. coli* does not necessarily produce a native CLN5 protein (Getty and Pearce, 2011).

5.2.3 Adenoviral derived anti-CLN5 and anti-CLN6 antibodies

Good antibodies are required for many biological analyses and clinical diagnostics. However, published research-generated or commercially available antibodies against CLN5 and CLN6 were not always as reliable as they were reported to be. This is specially so for antibodies against ovine CLN5 and CLN6. In the present studies, adenoviral antibodies against ovine CLN5 and CLN6, produced by injection of adenoviral vectors expressing CLN5 and CLN6 proteins into rabbits and mice, were shown to recognise ovine CLN5 and CLN6 at a high sensitivity. Generating antibodies using recombinant adenoviral vectors was straightforward. It required cloning of the full length *CLN5* and *CLN6* sequences into an adenoviral plasmid, packaging and purification of adenoviral particles and direct injection of the vectors into host animals, e.g. rabbits. This technique eliminated the need for purification of the protein antigens and re-administration of the antigen to enhance immune responses.

5.2.3.1 Adenoviral derived anti-CLN5 antibodies

Like most soluble lysosomal proteins, ovine CLN5 is N-glycosylated, and most of the overexpressed glycosylated CLN5 was secreted into the culture medium (Figure 3.5), indicating that it is a soluble protein. This confirmed previous reports of human CLN5 being a soluble glycoprotein based on the fact that it is secreted (Isosompppi et al., 2002; Sleat et al., 2006a; Palmer et al., 2015). Mouse CLN5 has also been identified as a soluble lysosomal glycoprotein with prominent homology to human CLN5 (Holmberg et al., 2004). In addition, ovine CLN5 contains an N-terminal sequence, which undergoes proteolysis to become the mature form (Figure 3.8). Cleavage of the N-terminal signal peptides is also a characteristic feature of soluble lysosomal proteins. Therefore, taken together, all of the cross-species results imply that CLN5 is a soluble lysosomal glycoprotein, not a transmembrane-spanning protein as has been reported before (Savukoski et al., 1998).

When CLN5 was first discovered in a Finnish variant late infantile NCL, it was predicted to be a membrane bound protein, containing two type II transmembrane domains and cytoplasmic N and C termini (Savukoski et al., 1998). This later changed to having one transmembrane domain with a cytoplasmic N-terminal domain and an amphipathic helix (Mole et al., 2005; Larkin et al., 2013). These predictions were based on the results of the TMpred transmembrane prediction program. However, studies have shown that most of the transmembrane prediction programs perform poorly in distinguishing transmembrane proteins from soluble proteins, and the error rate for TMpred was shown to be 55% (Isosomppi et al., 2002; Moller et al., 2001). Another group also suggested that human CLN5 is a type II transmembrane protein (Jule et al., 2015, 2017) and their statements were based on the first methionine being the initiator sites of human CLN5. However, the true initiator site of human *CLN5* has been confirmed as being the third ATG (Frugier et al., 2008). This correct initiation site of human CLN5 aligned perfectly with ovine *CLN5* sequences and those from all the other species (Figure 2.18).

As mentioned before, the rabbit anti-CLN5 antibodies identified the mature glycosylated ovine CLN5 form with a molecular weight of 60 kDa and 35 kDa when unglycosylated by PNGase F. These results are consistent with the anticipated mass of the ovine CLN5myc protein, recognized by C-myc antibodies (Sleat et al., 2006b; Hughes et al., 2014) and the mass of the human CLN5 protein, detected by human CLN5 peptide antibodies (raised against aa 393-407) (Schmiedt et al., 2010). Another peptide antibody raised against human

CLN5 aa 258–273 also detected a mature protein in a human CLN5 expression study in BHK cells, and revealed a 60 kDa CLN5 band and a 38 kDa CLN5 polypeptide after PNGase F deglycosylation (Isosomppi 2002). A reported mouse peptide antibody recognized overexpressed mouse CLN5, detecting two bands of 48 and 50 kDa from CLN5 transfected cells and a reduced 34 kDa band after PNGase F treatment (Holmberg et al., 2004), indicating mouse CLN5 is slightly smaller than the CLN5 of sheep and human.

In contrast, some other reported human CLN5 antibodies, either commercially available or raised to include the N-terminal sequence detected protein bands of different molecular weights. A monoclonal CLN5 synthetic peptide antibody (abcam, ab170899), raised against human CLN5 aa 150-250, identified an endogenous 56 kDa proprotein and a mature form (De Silva et al., 2015). However, a search of this 100 aa peptide sequence against the universal data base (protein blast software, https://blast.ncbi.nlm.nih.gov/Blast.cgi?PAGE=Proteins) revealed that it also aligns 100% with two unnamed human protein products (NCBI, BAG64918 and BAG52069), so this antibody may select pick out proteins other than CLN5. Similarly, commercial polyclonal anti-CLN5 antibodies (sc-49928, Santa Cruz Biotechnology, Santa Cruz, CA), derived from the internal region of human CLN5 at aa 140-220, detected a soluble mature 50 kDa protein (Jules et al. 2017). This peptide sequence also aligns 100% with an unnamed human protein product (BAG64918), thus these antibodies may also select a different protein indicating that they are not specific to CLN5. In addition, an N-terminal peptide antibody (corresponding to human CLN5 aa 1-75, Figure 1.1) detected an apparently uncleaved CLN5 proprotein with a molecular weight of 47 kDa (Vesa et al., 2002). This is unlikely to be CLN5 because of the usage of a CLN5 antibody which started from an incorrect codon.

5.2.3.2 Adenoviral derived anti-CLN6 antibodies

The rabbit anti-CLN6 antibodies detected ovine CLN6 from the overexpressed CLN6 cells at a molecular weight of 27 kDa on Western blotting, consistent with the anticipated mass of human and mouse CLN6 proteins, recognized by a human CLN6 or a mouse CLN6 peptide antibodies (Heine et al., 2004, 2007; More et all, 2004). However, CLN6 has also been reported to form a homodimer (60 kDa) in cell extracts (Heine et al., 2007), but was found by SDS-PAGE of overexpressing cells (Figure 3.5).

Polyclonal CLN6 synthetic peptide antibodies (Eurogentech, Seraing, Belgium, Germany), raised against human CLN6 aa 155-168 and 281-293, revealed a single prominent

immunoreactive band of 27 kDa in cell extracts of CLN6 transfected BHK21 cells (Heine et al., 2004). However, these peptide antibodies are not specific to CLN6 alone, because comparison of the two peptide sequences against the universal database revealed that both align 100% with the integrin alpha-11 protein of the Chinese hamster (NCBI, EGW04330) and also an unnamed human protein product (NCBI, BAG56737.1). In addition, these antibodies detected a CLN6 band in both CLN6 affected and control sheep, indicating that they are not specific for ovine CLN6 (Dr. Lucy Barry, personal communication).

Similar results can be seen with another transmembrane NCL protein. Immunoblot experiments showed that all available anti-CLN3 antibodies lack specificity, as they detect the same protein bands in controls and CLN3 affected mouse tissues, the latter of which should not contain CLN3 proteins (Nelson et al., 2017). These data provide evidence that immunization against a transmembrane protein with a low to medium expression level does not necessarily generate specific antibodies because of the possible cross-reactivity with other proteins. Another two polyclonal anti-CLN6 antibodies (Eurogentech, Seraing, Belgium, Germany), produced by immunizing rabbits with synthetic polypeptides corresponding to aa 1-15 and 28-39 of human CLN6, detected a protein band of approximately 30 kDa in HEK293 cells and human fibroblasts by Western blotting (Mole et al., 2004). Consequently, human CLN6 was suggested to form a homodimer with a molecular weight of 60 kDa (Heine et al., 2004; Mole et al., 2004). However, these peptide antibodies are not specific to CLN6, because comparison of the two peptide sequences against the universal database revealed that both aligned 100% with an unnamed human protein product (NCBI, BAG55226.1), and not with CLN6.

5.2.4 Lysosomal trafficking of the CLN5 protein

Western blotting analysis described in Chapter 3 detected CLN5 bands in both solubilised CLN5 overexpressing cells and cell media (Figure 3.2 and Figure 3.5), and the secreted glycosylated CLN5 in cell media containing both high-mannose and complex type glycans, allowing CLN5 to be trafficked to lysosomes mainly via a mannose-6-phosphate (M6P)-dependent pathway (Hughes et al., 2014; Sleat et al., 2005, 2007) and to be secreted via exocytosis.

As soon as a CLN5 polypeptide is synthesized in the ER, the N-terminal signal peptide is cleaved, and the polypeptide receives oligosaccharide side chains which undergo a series of

post-translational modifications for proper folding and trafficking. The study described in Chapter 3 found eight N-glycosylation consensus sites (Asn – X – Ser/Thr) are present and confirmed that six Asn sites are N-glycosylated, at positions N180, 205, 257, 273, 283 and 355. Whether or not the other two Asn residues, at positions N132 and 145, are real N-glycosylation sites and function in CLN5 post-translation modification is still not clear (Figure 3.8). *In vivo* studies have determined that all eight human CLN5 Asn residues are utilized for N-glycosylation, and seven of eight sites are conserved among mammalian species (Moharir et al., 2013; Sleat et al., 2005, 2006, 2007). The five residues on human CLN5, corresponding to N132, 205, 257, 273 and 283 of ovine CLN5, are essential for proper protein folding (Isosomppi et al., 2002; Lebrun et al., 2009; Moharir et al., 2013). Loss of these N-glycosylation specific sites on human CLN5 leads to mis-localisation of CLN5 to the Golgi membranes. The two residues on human CLN5 corresponding to N145 and 180 of ovine CLN5 have been suggested to be crucial for functionality of the CLN5 protein in lysosomes (Moharir et al., 2013). The last human CLN5 glycosylation site, corresponding to N355 of ovine CLN5, is not present in the mouse protein (Moharir et al., 2013). However, this special N355 glycosylation site is essential for lysosomal localisation of human CLN5. Without it, CLN5 accumulates in the Golgi and is then secreted into the media. Therefore, the M6P modification on N355 is a major determinant marking human CLN5 to the M6P lysosomal trafficking pathway and six of the confirmed N-glycosylation sites on ovine CLN5 are likely have similar functions to the corresponding sites on human CLN5.

The properly folded CLN5 is translocated from the ER to the *cis*- and *trans*-Golgi complex where different types of glycans are generated, containing both high mannose-type and complex-type oligosaccharides bound to Asn residues (Figure 1.4 and Figure 5.1). The deglycosylation study of secreted ovine CLN5 revealed that both high mannose-type and complex-type oligosaccharides of CLN5 are present in both cell media (Figure 3.7) and cells (Hughes et al., 2014). These results are in agreement with previous N-deglycosylation studies of human and mouse CLN5 (Lyly et al., 2008; Sleat et al., 2005, 2006, 2007). As mentioned before, CLN5 contains multiple glycosylation binding sites, some for high mannose-type oligosaccharides and some complex-type oligosaccharides.

Glycosylated CLN5 with high mannose-type sugars, sensitive to Endo H, is trafficked via the M6P-dependent pathway (Figure 5.1, indicated in black solid arrows). The glycans are phosphorylated to form M6P which bind to M6P receptors, are then sorted and moved on to

the late endosome, where the M6P receptors disassociate as the pH reduces from 6.5 to 5.5 (Beck, 2007). Next the CLN5 molecules are dephosphorylated and transported to lysosomes, while the M6P receptors are recycled to the *trans*-Golgi network or to the plasma membrane (Ghosh et al., 2003). A fraction of phosphorylated CLN5 that misses intracellular M6PRs in the Golgi apparatus is enclosed into secreted protein budding vesicles, and secreted into the media via exocytosis (Figure 5.1, indicated in black dashed arrows). These secreted CLN5 molecules can be taken up into the cells by binding to plasma membrane M6P receptors, transported to the early and late endosomes and finally to lysosomes (Futerman and van Meer, 2004, Hughes et al., 2014a).

All CLN5 proteins are likely to contain both Endo H sensitive high mannose and PNGase F sensitive complex sugars (Figure 3.9). Transient expression may exceed the capacity of the phosphotransferase and oligosaccharides may be processed further to complex forms which are resistant to Endo H, but sensitive to PNGase F (Isosomppi et al., 2002).

5.2.5 The cellular and regional localisations of ovine CLN5 and CLN6

Evidence for the lysosomal intracellular localisation of ovine CLN5 was obtained by co-localisation of CLN5 and the lysosomal associated membrane protein LAMP1 in transfected 293FT LVMNDCLN5 cells (Figure 4.3). This is in the agreement with reports that mouse CLN5 protein co-localised with LAMP1 and overexpressed human CLN5 protein co-localised to lysosomes in transfected cells (Isosomppi et al., 2002; Vesa et al., 2002; Holmberg et al., 2004; De Silva et al., 2015).

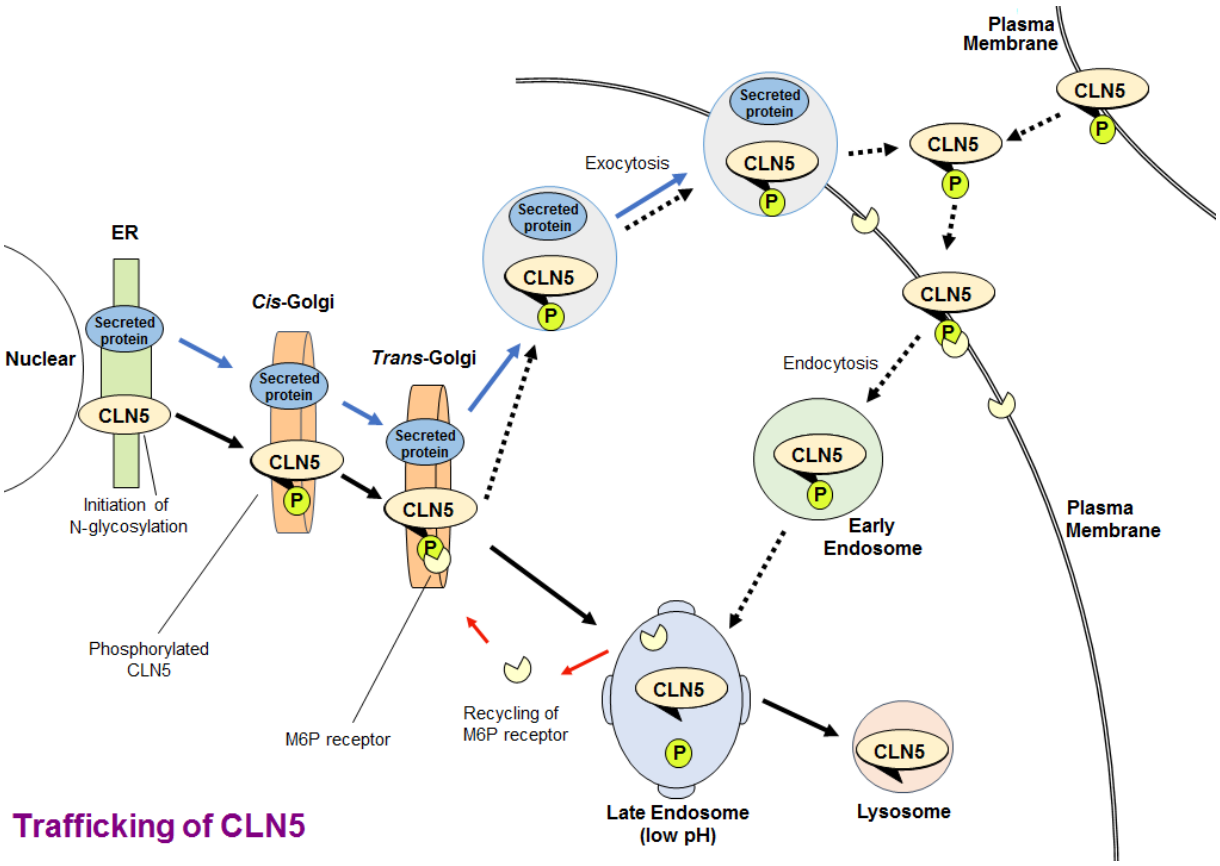

Figure 5.1 The predicated trafficking process of CLN5

The signal peptide is removed from the pre-proform of CLN5 in the ER and high mannose-type residues are added. CLN5 is transported to the Golgi apparatus where complex-type sugars are added and some mannose residues are phosphorylated at carbon 6. CLN5 is then transported through the early endosome and trafficked to lysosomes via the M6P-dependent pathway (indicated by solid black arrows). A small amount of CLN5 protein also joins the secretory pathway (indicated by solid blue arrows) and is secreted into the media via exocytosis. It can be taken up via M6P receptor-mediated endocytosis and transported to the early and late endosomes and finally to the lysosomes (indicated by dashed black arrows).

None of the published human or mouse antibodies detected endogenous human CLN5 (Isosomppi 2002; Holmberg et al., 2004; Schmiedt et al., 2010), however the rabbit anti-CLN5 antibodies were detected endogenous CLN5 expression throughout the sheep brain. The most prominent expression detected in pyramidal cells of the cerebral cortex, Purkinje and basket cells of the cerebellum as well as the hilus, granule cells of the dentate gyrus and the pyramidal cells of the normal sheep hippocampus, particularly in the CA3 and CA2 regions (Figure 4.5). In late stage human CLN5 disease, cerebellar Purkinje cells and thalamic neurons are nearly all lost, and some cerebral cortical neurons are obliterated (Tyynelä J et al., 1997; Kopra et al., 2004). The rabbit anti-CLN5 antibodies also detected CLN5 expression in normal human brain sections, in the hippocampus, cortex and cerebellum (Figure 4.6),

particularly in the granule cells and Purkinje cell bodies and axons of the human cerebellum (Figure 4.6 B). CLN5 immunostaining of the hippocampal pyramidal cells, Purkinje cells of cerebellum and pyramidal cells in the cortex in sheep and human brains is similar to that recorded in the mouse brain (Holmberg et al., 2004; Fabritius et al., 2014; Minye et al., 2016). The ovine CLN5 protein was also expressed in some reticular cells in the thalamus and some interneurons in the striatum, frontal and visual cortices. Tepper and co-workers (2010) also used three GABAergic interneuron markers to co-label CLN5 neurons in the mouse striatum. A large amount of *CLN5* mRNA was detected in qPCR studies of the normal sheep hippocampus, and some in the thalamus, frontal and occipital cortex (Tepper et al., 2010), consistent with these observations.

Evidence for the ER intracellular localisation of ovine CLN6 was revealed by co-staining with the rabbit anti-CLN6 antibodies and the ER marker PDI in transfected 293FT LVMNDCLN6 cells (Figure 4.4), supporting previous suggestions which implied that the CLN6 protein is localized to the ER (Mole et al., 2004; Heine et al., 2004; Kurze et al, 2010). Endogenous CLN6 expression has been studied by Dr. Nadia Mitchell using the rabbit anti-CLN6 antibodies on ovine brain tissues for immunohistochemistry. These antibodies detected CLN6 throughout the normal sheep brain, predominantly in the hippocampus, hypothalamus, cerebral cortex and cerebellum, but this required lower serum dilution than that used for CLN5 (Mitchell, 2016). Control CLN6 expression was 10 fold less than CLN5 expression in qPCR studies of sheep brains suggesting an extremely low level of CLN6 expression in sheep brains not easily detected by the CLN6 antibodies (Palmer et al., 2017). The small amounts of trypsin digested CLN6 peptide fragments in the gel band identified by rabbit anti-CLN6 antibodies and detected by mass spectrometry (Chapter 3, Table 3.2 and Figure 3.9) fits with this observation.

5.2.6 Interactions between NCL gene products

NCL patients with diseases caused by mutations in different genes have similar clinical, pathological and biochemical phenotypes. Many NCL proteins are trafficked through the ER-Golgi network and located in lysosomes, suggesting that they may share common cross-linked pathways, where different dysfunctions resulted in similar pathologies (Lyly et al., 2009; Getty and Pearce 2011; Palmer et al., 2015). NCL protein interactions have been described in a number of *in vitro* experiments, which suggest that the mutated growth of

patient cell lines were reversed by transfecting functional NCL proteins (Vesa et al., 2002; Persaud-Sawin et al., 2007; Lyly et al, 2009).

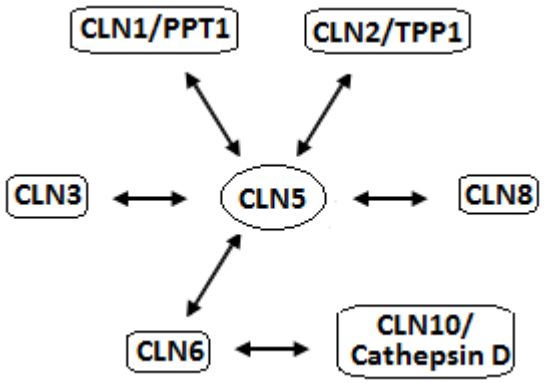

Figure 5.2 Schema of potential NCL protein-protein interactions Arrows indicate reported CLN5 interactions (Lyly et al., 2009; Vesa et al., 2002; von Schantz et al., 2009) and CLN6 interactions (this study; Palmer et al., 2015).

CLN5, a lysosomal protein, may have a central role. It has been suggested to interact with several other NCL proteins *in vitro*, including PPT1/CLN1, TPP1/CLN2, CLN3, CLN6 and CLN8 (Vesa et al., 2002; Lyly et al., 2009; von Schantz et al., 2009; Getty and Pearce 2011; Palmer et al., 2015). Interactions between CLN5 and CLN2 have been reported to occur after the proteins have left the ER (von Schantz, 2009), possibly in lysosomes or late endosomes (Vesa et al., 2002). CLN5 and CLN1 were suggested to share the same pathway, from the ER to the lysosome, in the CLN5 and CLN1 knockout mice brains (von Schantz et al., 2008; Lyly et al., 2009). Lyly and the co-workers (2009) found that co-expression of CLN1/PPT1 in cell culture could restore CLN5 in the overexpressed COS cells transfected with mutated mouse CLN5. Trafficking of CLN3 was partially affected by the simultaneous expression of mutated CLN5, possibly suggesting that CLN5 and CLN3 proteins interact in the ER (von Schantz, 2009). CLN5 and CLN8 have also been suggested to be related (Haddad et al., 2012).

CLN6, resident in the ER, has been suggested to play a role in protein trafficking pathways (Heine et al., 2004), especially in a network involving other NCL associated proteins (Figure 5.2). An investigation has tested whether mutated ovine CLN6 affected the activity of CLN1, CLN2 and CLN10 proteins (Palmer et al., 2015, 2017). This study indicated that the CLN6 mutation did not disrupt the trafficking of CLN1/PPT1 and CLN2/TPP1 to the lysosome, but CLN10/Cathepsin D enzyme activity in lysosomes was decreased.

Some studies have suggested that CLN5 and CLN6 are likely to interact in the CNS (Lyly et al., 2009; Warrier et al., 2013). Despite having mutations in different genes and having different cellular localisations, the development of clinical and neuropathological disease in CLN5 and

CLN6 affected sheep is very similar. They both result in the accumulation of lysosome-derived storage bodies containing large amounts of the c subunit of ATP synthase, retinal degeneration, seizures and pre-mature death, and follow a similar time-course. Affected sheep brains of both genotypes appear to be normally developed at birth. The masses of CLN5 and CLN6 affected sheep brains peak at 4 months of age, falling behind normal controls at this stage by 11% and 19% respectively, marking the start of progressive brain atrophy (Mitchell, 2016). This similarity is unexpected as the *CLN5* and *CLN6* genes and mutations are different and unrelated. CLN5 disease is caused by an intronic splice-site mutation resulting in deletion of exon 3 from the mRNA for a soluble lysosomal protein, while CLN6 defects result from a 5'UTR-exon 1 deletion from the gene for an ER membrane bound protein.

Gene therapies provided to small and large animals have shown persistent transgene expression (Jarraya et al., 2009; Lattanzi et al., 2010; Palmer et al., 2015). Affected soluble lysosomal proteins, such as CLN1, CLN2, CLN5 and CLN10, are considered potentially amenable to viral-mediated gene therapy by "cross-correction" when secreted proteins are taken up by adjacent or distal protein-deficient cells (Fratantoni et al., 1968). Promising results achieved from Western blotting and immunofluorescent studies showed that affected CLN5 foetal neural cells transduced with LV CLN5 expressed CLN5 *in vitro* (see Chapter 4, Figure 4.8). This is in agreement with the studies of *in vivo* AAV/lentiviral injections expressing CLN5 into CLN5 affected Borderdate sheep (Mitchell, 2016). Two years post-injection, the treated CLN5 affected sheep remained disease-free at 27 months of age, with the exception of delayed visual deficits. Compared with untreated animals, they benefited from an improvement in the quality of life, preservation of neurological function, and normalisation of brain structure and volume. Similarly, *in vivo* viral injections expressing CLN6 into CLN6 affected South Hampshire sheep were studied, but only 1 out of 6 treated animals had inhibited NCL neurobehavioural dysfunction and a normal brain structure at 27 months of age (Mitchell, 2016). The different outcomes to similar treatment by the CLN5 and CLN6 affected animals is likely due to the differences in the proteins. As mentioned before, CLN6 is an intracellular membrane protein that is not secreted like CLN5, and thus is unlikely benefit from extracellular cross-correction.

Co-transduction of LV CLN6 and LV CLN5 restored CLN5 expression in CLN6 affected cells (Figure 4.10), and increased CLN5 expression was seen in the CLN5 affected cells transduced

with both viruses compared with the cells transduced with LV CLN5 alone (Figure 4.9). These results could arise if CLN6 dysfunction caused ER associated protein degradation, therefore impeding the system of folding and glycosylation of CLN5 and preventing CLN5 from being exported out of the ER, or entering the CLN5 M6P trafficking pathway from the ER to lysosomes. Lack of CLN6 could also limit the endocytic pathway returning secreted CLN5 to cells, in agreement with the effect on the endocytic pathway of an exogenous protein, arylsulfatase A (ASA), in CLN6 affected cells (Heine et al., 2004).

Other studies are in agreement with these findings. Antibodies specific for the ovine CLN5 protein revealed very little CLN5 expression in CLN6 affected sheep and only intermediate staining in heterozygous CLN6 sheep (Mitchell, 2016). A further quantitative PCR study of brain samples revealed that full length *CLN5* mRNA expression was upregulated 3-4 fold in CLN6 affected brains of both South Hampshire and Merino sheep in previous studies, but this does not result in successful CLN5 protein expression (McIntyre, 2014; Palmer et al., 2017). These results indicate that the CLN5 and CLN6 protein and gene expressions may be cross-regulated. If CLN6 is required for the correct processing of the CLN5 protein, then it may be that the majority of the CLN5 protein may not reach the lysosome in its fully modified and folded mature form in CLN6 affected sheep, thus these CLN5 isoforms cannot function, and their related enzyme activity may be greatly reduced, resulting in an induced lysosomal CLN5 deficiency disease.

5.3 Final remarks

This thesis provided some promising methodology for overcoming the difficulties associated with amplification of the full length ovine *CLN5* gene sequence, which contains a large percentage of G/C bases in the exon 1 region. The studies have established methodology for lentiviral-mediated expression of CLN5 and CLN6 proteins in eukaryotic mammalian cells and proved the reliability of the generated adenoviral CLN5 and CLN6 antibodies.

These adenoviral CLN5 and CLN6 antibodies will be useful to further studies of the biological function of these two proteins and their trafficking as well. Further work to test the co-expression of CLN2, CLN3 and CLN5 in *CLN6*$^{-/-}$ cells, or co-expression of CLN2, CLN3 and CLN6 in *CLN5*$^{-/-}$ cells and to investigate whether CLN2 and CLN3 together with CLN5 and CLN6 could help restore or enhance CLN5 or CLN6 expression in affected cells, should be

considered. These studies will increase the possibility for therapies for human CLN5 and CLN6 patients.

Appendix A

A.1 Primers designed for the ovine *CLN5* genomic sequence

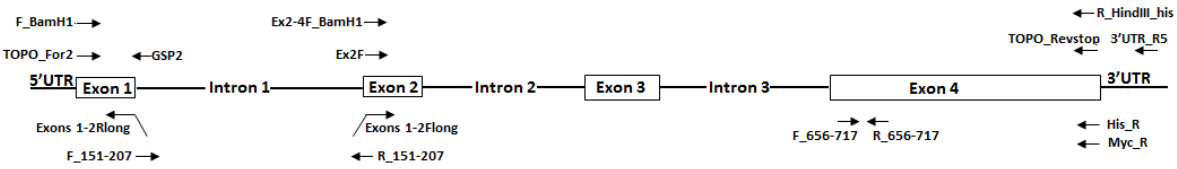

A.2 Ovine *CLN5* cloning into the pCR4-TOPO vector

5.3.1 A.2.1 pCR4-TOPO with the full *CLN5* insert (5153bp)

- Full length *CLN5* CDS (plus 109bp of 3'UTR insert, 1199 bp, red) without myc epitope
- The PCR product was A-tailed and then inserted between two *EcoR* I cut sites (underlined) for easy sub-cloning
- Start and stop codons in bold
- Plasmid DNA produced after ligation and confirmed by sequencing

AGCGCCCAATACGCAAACCGCCTCTCCCCGCGCGTTGGCCGATTCATTAATGCAGCTGGCCGACAGGTTTCCCGA
CTGGAAAGCGGGCAGTGAGCGCAACGCAATTAATGTGAGTTAGCCACTCATTAGGCACCCCAGGCTTTACACTTT
ATGCTTCCGGCTCGTATGTTGTGTGGAATTGTGAGCGGATAACAATTTCACACAGGAAACAGCTATGACCATGAT
TACGCCAAGCTCAGAATTAACCCTCACTAAAGGGACTAGTCCTGCAGGTTTAAACGAATTCGCCCTT

CACC**ATG**GCGCAGGCGGGGGGTGCCGGTGCGGGGGCCTGGGGTCGGCGGGGCGCGGGCGCAGGTGCGGGCCCGGA

GCGGGCGCCTTGGCGCTGGGCCCCCGCACTGCTCTGGCTGGCGGCGGCGACGGCGGCGGCGGCGGCGGCGGGCGA

CCCCTCCCGGCGCCAGTGGCCGGTGCCCTACAAACGCTTCTCCTTCCGTCCGGAACCAGATCCTTATTGTCAAGC

TAAATATACTTTCTGTCCCACTGGCTCCCCTATCCCGGTGATGAAGGATGACGATGTCATTGAAGTCTTTCGATT

ACAAGCCCCAGTGTGGGAATTTAAATATGGAGACCTCCTGGGACACTTGAAAATCATGCATGATGCCATTGGATT

CAGGAGTACTTTAACGGAGAAGAACTACACGATGGAATGGTATGAACTCTTCCAACTTGGAAACTGCACGTTTCC

CCATCTCCGACCTGAAATGAATGCCCCTTTCTGGTGTAATCAAGGAGCTGCCTGCTTTTTTGAAGGGATTGATGA

TAATCACTGGAAGGAAAATGGGACGTTAGTTCTAGTAGCAACCATATCAGGAGGCATGTTTAACAAAATGGCAAA

GTGGGTAAAACAGGACAATGAAACAGGGATTTATTATGAGACATGGACTGTCCAAGCCAGCCCGAAAAAGGAGGC

AGAGAAATGGTTTGAATCCTACGACTGCTCCAAATTTGTGTTAAGGACCTATGAGAAATTGGCTGAACTTGGAGC

AGACTTCAAGAAGATAGAAACCAACTATACAAGGATATTTCTTTACAGTGGAGAACCTACTTATCTGGGAAATGA

AACATCTGTTTTTGGGCCAACAGGAAACAAGACTCTTGCTTTAGCTATAAAAAAATTTTATTACCCTTTCAAACC

ACATTTGTCAACTAAAGAATTTCTGTTGAGTCTCTTGCAAATTTTTGATGCAGTGGTTATACACAGAGAGTTCTA

TTTGTTTTATAATTTTGAATATTGGTTTTTACCTATGAAATCCCCTTTTATTAAAATAACATATGAAGAAATCCC

TTTACCTAACAGAAAAAACAGAACACTCTCTGGTTTA**TAA**AACCTTAATTCTACTGCTTTTCTTTCTACCAGCAC

ATCAGTTTTTCAGGGAGTGGTTTTACAAGTGTGGGATTTCTTAGGCCTTTCTTCCTTGGGGCAGAAAGCTAACA

AAGGGCGAATTCGCGGCCGCTAAATTCAATTCGCCCTATAGTGAGTCGTATTACAATTCACTGGCCGTCGTTTTA
CAACGTCGTGACTGGGAAAACCCTGGCGTTACCCAACTTAATCGCCTTGCAGCACATCCCCCTTTCGCCAGCTGG
CGTAATAGCGAAGAGGCCCGCACCGATCGCCCTTCCCAACAGTTGCGCAGCCTATACGTACGGCAGTTTAAGGTT
TACACCTATAAAAGAGAGAGCCGTTATCGTCTGTTTGTGGATGTACAGAGTGATATTATTGACACGCCGGGGCGA
CGGATGGTGATCCCCCTGGCCAGTGCACGTCTGCTGTCAGATAAAGTCTCCCGTGAACTTTACCCGGTGGTGCAT

ATCGGGGATGAAAGCTGGCGCATGATGACCACCGATATGGCCAGTGTGCCGGTCTCCGTTATCGGGGAAGAAGTG
GCTGATCTCAGCCACCGCGAAAATGACATCAAAAACGCCATTAACCTGATGTTCTGGGGAATATAAATGTCAGGC
ATGAGATTATCAAAAAGGATCTTCACCTAGATCCTTTTCACGTAGAAAGCCAGTCCGCAGAAACGGTGCTGACCC
CGGATGAATGTCAGCTACTGGGCTATCTGGACAAGGGAAAACGCAAGCGCAAAGAGAAAGCAGGTAGCTTGCAGT
GGGCTTACATGGCGATAGCTAGACTGGGCGGTTTTATGGACAGCAAGCGAACCGGAATTGCCAGCTGGGGCGCCC
TCTGGTAAGGTTGGGAAGCCCTGCAAAGTAAACTGGATGGCTTTCTTGCCGCCAAGGATCTGATGGCGCAGGGGA
TCAAGCTCTGATCAAGAGACAGGATGAGGATCGTTTCGCATGATTGAACAAGATGGATTGCACGCAGGTTCTCCG
GCCGCTTGGGTGGAGAGGCTATTCGGCTATGACTGGGCACAACAGACAATCGGCTGCTCTGATGCCGCCGTGTTC
CGGCTGTCAGCGCAGGGGCGCCCGGTTCTTTTTGTCAAGACCGACCTGTCCGGTGCCCTGAATGAACTGCAAGAC
GAGGCAGCGCGGCTATCGTGGCTGGCCACGACGGGCGTTCCTTGCGCAGCTGTGCTCGACGTTGTCACTGAAGCG
GGAAGGGACTGGCTGCTATTGGGCGAAGTGCCGGGGCAGGATCTCCTGTCATCTCACCTTGCTCCTGCCGAGAAA
GTATCCATCATGGCTGATGCAATGCGGCGGCTGCATACGCTTGATCCGGCTACCTGCCCATTCGACCACCAAGCG
AAACATCGCATCGAGCGAGCACGTACTCGGATGGAAGCCGGTCTTGTCGATCAGGATGATCTGGACGAAGAGCAT
CAGGGGCTCGCGCCAGCCGAACTGTTCGCCAGGCTCAAGGCGAGCATGCCCGACGGCGAGGATCTCGTCGTGACC
CATGGCGATGCCTGCTTGCCGAATATCATGGTGGAAAATGGCCGCTTTTCTGGATTCATCGACTGTGGCCGGCTG
GGTGTGGCGGACCGCTATCAGGACATAGCGTTGGCTACCCGTGATATTGCTGAAGAGCTTGGCGGCGAATGGGCT
GACCGCTTCCTCGTGCTTTACGGTATCGCCGCTCCCGATTCGCAGCGCATCGCCTTCTATCGCCTTCTTGACGAG
TTCTTCTGAATTATTAACGCTTACAATTTCCTGATGCGGTATTTTCTCCTTACGCATCTGTGCGGTATTTCACAC
CGCATCAGGTGGCACTTTTCGGGGAAATGTGCGCGGAACCCCTATTTGTTTATTTTTCTAAATACATTCAAATAT
GTATCCGCTCATGAGATTATCAAAAAGGATCTTCACCTAGATCCTTTTAAATTAAAAATGAAGTTTTAAATCAAT
CTAAAGTATATATGAGTAAACTTGGTCTGACAGTTACCAATGCTTAATCAGTGAGGCACCTATCTCAGCGATCTG
TCTATTTCGTTCATCCATAGTTGCCTGACTCCCCGTCGTGTAGATAACTACGATACGGGAGGGCTTACCATCTGG
CCCCAGTGCTGCAATGATACCGCGAGACCCACGCTCACCGGCTCCAGATTTATCAGCAATAAACCAGCCAGCCGG
AAGGGCCGAGCGCAGAAGTGGTCCTGCAACTTTATCCGCCTCCATCCAGTCTATTAATTGTTGCCGGGAAGCTAG
AGTAAGTAGTTCGCCAGTTAATAGTTTGCGCAACGTTGTTGCCATTGCTACAGGCATCGTGGTGTCACGCTCGTC
GTTTGGTATGGCTTCATTCAGCTCCGGTTCCCAACGATCAAGGCGAGTTACATGATCCCCCATGTTGTGCAAAAA
AGCGGTTAGCTCCTTCGGTCCTCCGATCGTTGTCAGAAGTAAGTTGGCCGCAGTGTTATCACTCATGGTTATGGC
AGCACTGCATAATTCTCTTACTGTCATGCCATCCGTAAGATGCTTTTCTGTGACTGGTGAGTACTCAACCAAGTC
ATTCTGAGAATAGTGTATGCGGCGACCGAGTTGCTCTTGCCCGGCGTCAATACGGGATAATACCGCGCCACATAG
CAGAACTTTAAAAGTGCTCATCATTGGAAAACGTTCTTCGGGGCGAAAACTCTCAAGGATCTTACCGCTGTTGAG
ATCCAGTTCGATGTAACCCACTCGTGCACCCAACTGATCTTCAGCATCTTTTACTTTCACCAGCGTTTCTGGGTG
AGCAAAAACAGGAAGGCAAAATGCCGCAAAAAAGGGAATAAGGGCGACACGGAAATGTTGAATACTCATACTCTT
CCTTTTTCAATATTATTGAAGCATTTATCAGGGTTATTGTCTCATGACCAAAATCCCTTAACGTGAGTTTTCGTT
CCACTGAGCGTCAGACCCCGTAGAAAAGATCAAAGGATCTTCTTGAGATCCTTTTTTTCTGCGCGTAATCTGCTG
CTTGCAAACAAAAAAACCACCGCTACCAGCGGTGGTTTGTTTGCCGGATCAAGAGCTACCAACTCTTTTTCCGAA
GGTAACTGGCTTCAGCAGAGCGCAGATACCAAATACTGTTCTTCTAGTGTAGCCGTAGTTAGGCCACCACTTCAA
GAACTCTGTAGCACCGCCTACATACCTCGCTCTGCTAATCCTGTTACCAGTGGCTGCTGCCAGTGGCGATAAGTC
GTGTCTTACCGGGTTGGACTCAAGACGATAGTTACCGGATAAGGCGCAGCGGTCGGGCTGAACGGGGGGTTCGTG
CACACAGCCCAGCTTGGAGCGAACGACCTACACCGAACTGAGATACCTACAGCGTGAGCTATGAGAAAGCGCCAC
GCTTCCCGAAGGGAGAAAGGCGGACAGGTATCCGGTAAGCGGCAGGGTCGGAACAGGAGAGCGCACGAGGGAGCT
TCCAGGGGGAAACGCCTGGTATCTTTATAGTCCTGTCGGGTTTCGCCACCTCTGACTTGAGCGTCGATTTTTGTG
ATGCTCGTCAGGGGGGCGGAGCCTATGGAAAAACGCCAGCAACGCGGCCTTTTTACGGTTCCTGGCCTTTTGCTG
GCCTTTTGCTCACATGTTCTTTCCTGCGTTATCCCCTGATTCTGTGGATAACCGTATTACCGCCTTTGAGTGAGC
TGATACCGCTCGCCGCAGCCGAACGACCGAGCGCAGCGAGTCAGTGAGCGAGGAAGCGGAAG

5.3.2 A.2.2 pCR4-TOPO with the full *CLN5*myc insert (5074bp)

- Full length *CLN5* CDS (minus the *CLN5* stop codon) with myc epitope and new stop codon (1120 bp)
- The PCR product was A-tailed and then inserted between two *EcoR* I cut sites (underlined) for easy sub-cloning
- Start and stop codons in bold and the two restriction enzymes underlined
- Plasmid DNA produced after ligation and confirmed by sequencing:

AGCGCCCAATACGCAAACCGCCTCTCCCCGCGCGTTGGCCGATTCATTAATGCAGCTGGCCGACAGGTTTCCCGA
CTGGAAAGCGGGCAGTGAGCGCAACGCAATTAATGTGAGTTAGCCACTCATTAGGCACCCCAGGCTTTACACTTT
ATGCTTCCGGCTCGTATGTTGTGTGGAATTGTGAGCGGATAACAATTTCACACAGGAAACAGCTATGACCATGAT
TACGCCAAGCTCAGAATTAACCCTCACTAAAGGGACTAGTCCTGCAGGTTTAAAC<u>GAATTC</u>GCCCTT

CACC**<u>ATG</u>**GCGCAGGCGGGGGGTGCCGGTGCGGGGGCCTGGGGTCGGCGGGGCGCGGGCGCAGGTGCGGGCCCGGA

GCGGGCGCCTTGGCGCTGGGCCCCCGCACTGCTCTGGCTGGCGGCGGCGACGGCGGCGGCGGCGGCGGCGGGCGA

CCCCTCCCGGCGCCAGTGGCCGGTGCCCTACAAACGCTTCTCCTTCCGTCCGGAACCAGATCCTTATTGTCAAGC

TAAATATACTTTCTGTCCCACTGGCTCCCCTATCCCGGTGATGAAGGATGACGATGTCATTGAAGTCTTTCGATT

ACAAGCCCCAGTGTGGGAATTTAAATATGGAGACCTCCTGGGACACTTGAAAATCATGCATGATGCCATTGGATT

CAGGAGTACTTTAACGGAGAAGAACTACACGATGGAATGGTATGAACTCTTCCAACTTGGAAACTGCACGTTTCC

CCATCTCCGACCTGAAATGAATGCCCCTTTCTGGTGTAATCAAGGAGCTGCCTGCTTTTTTGAAGGGATTGATGA

TAATCACTGGAAGGAAAATGGGACGTTAGTTCTAGTAGCAACCATATCAGGAGGCATGTTTAACAAAATGGCAAA

GTGGGTAAAACAGGACAATGAAACAGGGATTTATTATGAGACATGGACTGTCCAAGCCAGCCCGAAAAAGGAGGC

AGAGAAATGGTTTGAATCCTACGACTGCTCCAAATTTGTGTTAAGGACCTATGAGAAATTGGCTGAACTTGGAGC

AGACTTCAAGAAGATAGAAACCAACTATACAAGGATATTTCTTTACAGTGGAGAACCTACTTATCTGGGAAATGA

AACATCTGTTTTTGGGCCAACAGGAAACAAGACTCTTGCTTTAGCTATAAAAAAATTTTATTACCCTTTCAAACC

ACATTTGTCAACTAAAGAATTTCTGTTGAGTCTCTTGCAAATTTTTGATGCAGTGGTTATACACAGAGAGTTCTA

TTTGTTTTATAATTTTGAATATTGGTTTTTACCTATGAAATCCCCTTTTATTAAAATAACATATGAAGAAATCCC

TTTACCTAACAGAAAAAACAGAACACTCTCTGGTTTAGAACAAAAACTCATCTCAGAAGAGGATCTG**TGA**

AAGGGCGAATTCGCGGCCGCTAAATTCAATTCGCCCTATAGTGAGTCGTATTACAATTCACTGGCCGTCGTTTTA
CAACGTCGTGACTGGGAAAACCCTGGCGTTACCCAACTTAATCGCCTTGCAGCACATCCCCCTTTCGCCAGCTGG
CGTAATAGCGAAGAGGCCCGCACCGATCGCCCTTCCCAACAGTTGCGCAGCCTATACGTACGGCAGTTTAAGGTT
TACACCTATAAAAGAGAGAGCCGTTATCGTCTGTTTGTGGATGTACAGAGTGATATTATTGACACGCCGGGGCGA
CGGATGGTGATCCCCCTGGCCAGTGCACGTCTGCTGTCAGATAAAGTCTCCCGTGAACTTTACCCGGTGGTGCAT
ATCGGGGATGAAAGCTGGCGCATGATGACCACCGATATGGCCAGTGTGCCGGTCTCCGTTATCGGGGAAGAAGTG
GCTGATCTCAGCCACCGCGAAAATGACATCAAAAACGCCATTAACCTGATGTTCTGGGGAATATAAATGTCAGGC
ATGAGATTATCAAAAAGGATCTTCACCTAGATCCTTTTCACGTAGAAAGCCAGTCCGCAGAAACGGTGCTGACCC
CGGATGAATGTCAGCTACTGGGCTATCTGGACAAGGGAAAACGCAAGCGCAAAGAGAAAGCAGGTAGCTTGCAGT
GGGCTTACATGGCGATAGCTAGACTGGGCGGTTTTATGGACAGCAAGCGAACCGGAATTGCCAGCTGGGGCGCCC
TCTGGTAAGGTTGGGAAGCCCTGCAAAGTAAACTGGATGGCTTTCTTGCCGCCAAGGATCTGATGGCGCAGGGGA
TCAAGCTCTGATCAAGAGACAGGATGAGGATCGTTTCGCATGATTGAACAAGATGGATTGCACGCAGGTTCTCCG
GCCGCTTGGGTGGAGAGGCTATTCGGCTATGACTGGGCACAACAGACAATCGGCTGCTCTGATGCCGCCGTGTTC
CGGCTGTCAGCGCAGGGGCGCCCGGTTCTTTTTGTCAAGACCGACCTGTCCGGTGCCCTGAATGAACTGCAAGAC
GAGGCAGCGCGGCTATCGTGGCTGGCCACGACGGGCGTTCCTTGCGCAGCTGTGCTCGACGTTGTCACTGAAGCG
GGAAGGGACTGGCTGCTATTGGGCGAAGTGCCGGGGCAGGATCTCCTGTCATCTCACCTTGCTCCTGCCGAGAAA
GTATCCATCATGGCTGATGCAATGCGGCGGCTGCATACGCTTGATCCGGCTACCTGCCCATTCGACCACCAAGCG
AAACATCGCATCGAGCGAGCACGTACTCGGATGGAAGCCGGTCTTGTCGATCAGGATGATCTGGACGAAGAGCAT
CAGGGGCTCGCGCCAGCCGAACTGTTCGCCAGGCTCAAGGCGAGCATGCCCGACGGCGAGGATCTCGTCGTGACC
CATGGCGATGCCTGCTTGCCGAATATCATGGTGGAAAATGGCCGCTTTTCTGGATTCATCGACTGTGGCCGGCTG
GGTGTGGCGGACCGCTATCAGGACATAGCGTTGGCTACCCGTGATATTGCTGAAGAGCTTGGCGGCGAATGGGCT
GACCGCTTCCTCGTGCTTTACGGTATCGCCGCTCCCGATTCGCAGCGCATCGCCTTCTATCGCCTTCTTGACGAG
TTCTTCTGAATTATTAACGCTTACAATTTCCTGATGCGGTATTTTCTCCTTACGCATCTGTGCGGTATTTCACAC
CGCATCAGGTGGCACTTTTCGGGGAAATGTGCGCGGAACCCCTATTTGTTTATTTTTCTAAATACATTCAAATAT
GTATCCGCTCATGAGATTATCAAAAAGGATCTTCACCTAGATCCTTTTAAATTAAAAATGAAGTTTTAAATCAAT
CTAAAGTATATATGAGTAAACTTGGTCTGACAGTTACCAATGCTTAATCAGTGAGGCACCTATCTCAGCGATCTG
TCTATTTCGTTCATCCATAGTTGCCTGACTCCCCGTCGTGTAGATAACTACGATACGGGAGGGCTTACCATCTGG
CCCCAGTGCTGCAATGATACCGCGAGACCCACGCTCACCGGCTCCAGATTTATCAGCAATAAACCAGCCAGCCGG
AAGGGCCGAGCGCAGAAGTGGTCCTGCAACTTTATCCGCCTCCATCCAGTCTATTAATTGTTGCCGGGAAGCTAG
AGTAAGTAGTTCGCCAGTTAATAGTTTGCGCAACGTTGTTGCCATTGCTACAGGCATCGTGGTGTCACGCTCGTC
GTTTGGTATGGCTTCATTCAGCTCCGGTTCCCAACGATCAAGGCGAGTTACATGATCCCCCATGTTGTGCAAAAA
AGCGGTTAGCTCCTTCGGTCCTCCGATCGTTGTCAGAAGTAAGTTGGCCGCAGTGTTATCACTCATGGTTATGGC
AGCACTGCATAATTCTCTTACTGTCATGCCATCCGTAAGATGCTTTTCTGTGACTGGTGAGTACTCAACCAAGTC
ATTCTGAGAATAGTGTATGCGGCGACCGAGTTGCTCTTGCCCGGCGTCAATACGGGATAATACCGCGCCACATAG
CAGAACTTTAAAAGTGCTCATCATTGGAAAACGTTCTTCGGGGCGAAAACTCTCAAGGATCTTACCGCTGTTGAG
ATCCAGTTCGATGTAACCCACTCGTGCACCCAACTGATCTTCAGCATCTTTTACTTTCACCAGCGTTTCTGGGTG
AGCAAAAACAGGAAGGCAAAATGCCGCAAAAAAGGGAATAAGGGCGACACGGAAATGTTGAATACTCATACTCTT
CCTTTTTCAATATTATTGAAGCATTTATCAGGGTTATTGTCTCATGACCAAAATCCCTTAACGTGAGTTTTCGTT
CCACTGAGCGTCAGACCCCGTAGAAAAGATCAAAGGATCTTCTTGAGATCCTTTTTTTCTGCGCGTAATCTGCTG
CTTGCAAACAAAAAAACCACCGCTACCAGCGGTGGTTTGTTTGCCGGATCAAGAGCTACCAACTCTTTTTCCGAA
GGTAACTGGCTTCAGCAGAGCGCAGATACCAAATACTGTTCTTCTAGTGTAGCCGTAGTTAGGCCACCACTTCAA
GAACTCTGTAGCACCGCCTACATACCTCGCTCTGCTAATCCTGTTACCAGTGGCTGCTGCCAGTGGCGATAAGTC
GTGTCTTACCGGGTTGGACTCAAGACGATAGTTACCGGATAAGGCGCAGCGGTCGGGCTGAACGGGGGGTTCGTG
CACACAGCCCAGCTTGGAGCGAACGACCTACACCGAACTGAGATACCTACAGCGTGAGCTATGAGAAAGCGCCAC

GCTTCCCGAAGGGAGAAAGGCGGACAGGTATCCGGTAAGCGGCAGGGTCGGAACAGGAGAGCGCACGAGGGAGCT
TCCAGGGGGAAACGCCTGGTATCTTTATAGTCCTGTCGGGTTTCGCCACCTCTGACTTGAGCGTCGATTTTTGTG
ATGCTCGTCAGGGGGGCGGAGCCTATGGAAAAACGCCAGCAACGCGGCCTTTTTACGGTTCCTGGCCTTTTGCTG
GCCTTTTGCTCACATGTTCTTTCCTGCGTTATCCCCTGATTCTGTGGATAACCGTATTACCGCCTTTGAGTGAGC
TGATACCGCTCGCCGCAGCCGAACGACCGAGCGCAGCGAGTCAGTGAGCGAGGAAGCGGAAG

A.3 Expression of ovine CLN5 and CLN6 recombinant proteins

5.3.3 A.3.1 Attempted expression of CLN5 and CLN6 proteins with pRUN vectors

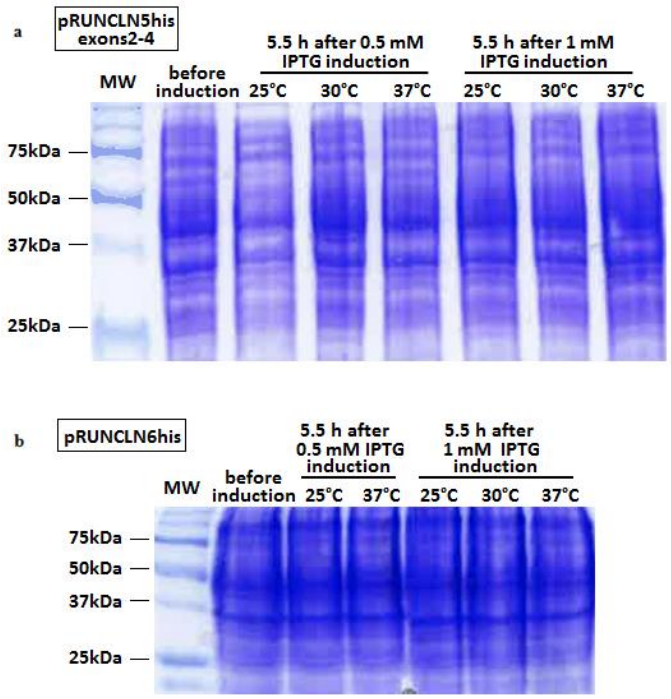

SDS-PAGE gel analysis of recombinant (a) CLN5 and (b) CLN6. Each protein sample, 30 µg, was run on 12% polyacrylamide gels which were stained with Commassie blue. C43 (DE3) cells containing CLN5 or CLN6 protein expression constructs pRUNCLN5his exons 2-4 and pRUNCLN6his were grown at 37°C and then induced with 0.5 mM or 1 mM IPTG and incubated at 25°C, 30°C or 37°C for 5.5 h. The samples for analysis were collected just before the induction and 5.5 h post-induction incubation. CLN5 soluble fractions and CLN6 insoluble fractions for collected samples were analysed. MW refers to Precision plus protein standard.

5.3.4 A.3.2 Attempted expression of CLN5 peptides by the Gateway system

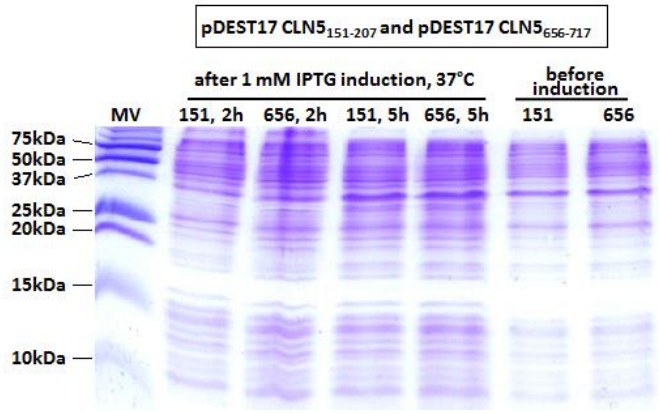

LDS-PAGE gel analysis of recombinant CLN5 polypeptides. 30 µg, was run on a 15% polyacrylamide gel. C43 (DE3) cells containing CLN5 protein expression constructs pDEST17 $CLN5_{151-207}$ and pDEST17 $CLN5_{656-717}$ were grown at 37°C, induced with 1 mM IPTG, incubated at 37°C for 5 h. The samples for analysis were collected just before the induction, 2 h and 5.5 h post-induction incubation.

A.4 Immunocytochemical optimisation CLN5 and CLN6 antibodies generated from adenoviral vectors

293FT LVMNDCLN5 and LVMNDCLN6 cells were fixed at a confluence of 70% and labelled with (i) rabbit anti-CLN5 (red, RαCLN5), (ii) rabbit anti-CLN6 (red, RαCLN6), (i) mouse anti-CLN5 (green, MαCLN5), and (iv) rabbit anti-CLN6 (green, MαCLN6) primary antibodies at concentrations of 1:500 and 1:1000. The scale bar represents 200 µM.

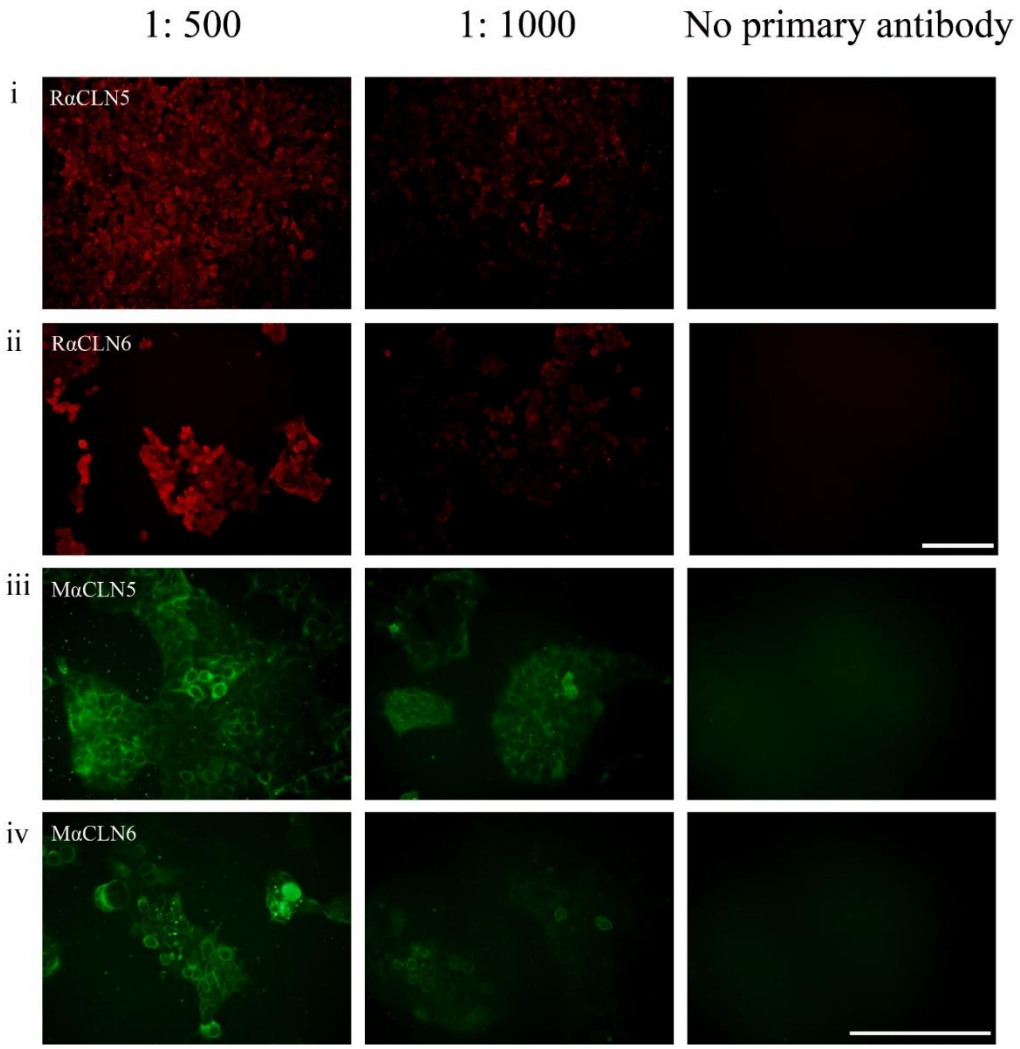

References

Abdelhak S, Louzir H, Timm J, Blel L, Benlasfar Z, Lagranderie M, Gheorghiu M, Dellagi K, Gicquel B. (1995) Recombinant BCG expressing the leishmania surface antigen Gp63 induces protective immunity against *Leishmania* major infection in BALB/c mice. *Microbiology*, 141: 1585-1592.

Akasaki K, Shiotsu K, Michihara A, Ide N, Wada I. (2014) Constitutive expression of a COOH-terminal leucine mutant of lysosome-associated membrane protein-1 causes its exclusive localisation in low density intracellular vesicles. *Journal of Biochemistry,* 156: 39-49.

Alroy J, Nraulke T, Cismondi IA, Cooper JD, Creegan D, Elleder M, Kitzmüller C, Kohan R, Kohlschütter A, Mole SE, Noher de Halac I, Pfannl R, Quitsch A, Schulz A. (2011) Chapter 10 CLN6. In: *The Neuronal Ceroid Lipofuscinoses (Batten Disease),* (2nd Edition). Mole S, William R, Goebel H. (Eds.), (pp. 159-175). Oxford, UK: Oxford University Press.

Anderson RD, Haskell RE, Xia H, Roessler BJ, Davidson BL. (2000) A simple method for the rapid generation of recombinant adenovirus vectors. *Gene Therapy,* 7: 1034-1038.

Andrade DM, Paton T, Turnbull J, Marshall CR, Scherer SW, Minassian BA. (2012) Mutation of the CLN6 gene in teenage-onset progressive myoclonus epilepsy. *Pediatric Neurology,* 47: 205-208.

Arsov T, Smith KR, Damiano J, Franceschetti S, Canafoglia L, Bromhead CJ, Andermann E, Vears DF, Cossette P, Rajagopalan S, McDougall A, Sofia V, Farrell M, Aguglia U, Zini A, Meletti S, Morbin M, Mullen S, Andermann F, Mole SE, Bahlo M, Berkovic SF. (2011) Kufs disease, the major adult form of neuronal ceroid lipofuscinosis, caused by mutations in CLN6. *American Journal of Human Genetics,* 88: 566-573.

Bailey R. (2017) Digestive system: nutrient absorption. *ThoughtGo*, https://www.thoughtco.com/digestive-system-nutrient-absorption.

Beck M. (2007) New therapeutic options for lysosomal storage disorders: enzyme replacement, small molecules and gene therapy. *Human Genetics*, 121: 1-22.

Bellizzi JJ, Widom J, Kemp C, Lu JY, Das AK, Hofmann SL, Clardy J. (2000) The crystal structure of palmitoyl protein thioesterase 1 and the molecular basis of infantile neuronal ceroid lipofuscinosis. *Proceedings of the National Academy of Sciences of the USA,* 97: 4573-4578.

Bessa C, Teixeira CA, Mangas M, Dias A, Sá Miranda MC, Ferreira JC, Guimarães A, Canas N, Cabral P, Ribeiro MG. (2006) Two novel CLN5 mutations in a Portuguese patient with vLINCL: insights into molecular mechanisms of CLN5 deficiency. *Molecular Genetic and Metabolism,* 89: 245-253.

Bessa C, Teixeira CA, Dias A, Alves M, Rocha S, Lacerda L, Loureiro L, Guimarães A, Ribeiro MG. (2008) CLN2/TPP1 deficiency: the novel mutation IVS7-10A>G causes intron retention and is associated with a mild disease phenotype. *Molecular Genetic and Metabolism,* 93: 66-73.

Bildfell R, Matwichuk C, Mitchell S, Ward P. (1995) Neuronal ceroid lipofuscinosis in a cat. *Veterinary Pathology,* 32: 485-488.

Boehme, DH, Cottrell, JC, Leonberg, SC, Zeman, W. (1971) A dominant form of neuronal ceroid-lipofuscinosis. *Brain,* 94: 745–760.

Bras J, Verloes A, Schneider SA, Mole SE, Guerreiro RJ. (2012) Mutation of the parkinsonism gene ATP13A2 causes neuronal ceroid-lipofuscinosis. *Human Molecular Genetics,* 21: 2646-2650.

Bronson RT, Donahue LR, Johnson KR, Tanner A, Lane PW, Faust JR. (1998) Neuronal ceroid lipofuscinosis (nclf): a new disorder of the mouse linked to chromosome 9. *Animal Journal of Medical Genetics,* 77: 289-297.

Brooks AI, Stein CS, Hughes SM, Heth J, McCray PM Jr, Sauter SL, Johnston JC, Cory-Slechta DA, Federoff HJ, Davidson BL. (2002) Functional correction of established central nervous system deficits in an animal model of lysosomal storage disease with feline immunodeficiency virus-based vectors. *Proceedings of the National Academy of Sciences of the USA,* 99: 6216-6221.

Broom MF, Zhou C, Broom JE, Barwell KJ, Jolly RD, Hill DF. (1998) Ovine neuronal ceroid lipofuscinosis: a large animal model syntenic with the human neuronal ceroid lipofuscinosis variant CLN6. *Journal of Medical Genetics,* 35: 717-721.

Brunda G, Sashidhar RB, Sarin RK. (2006) Use of egg yolk antibody (IgY) as an immunoanalytical tool in the detection of India cobra (*Naja naja naja*) venom in biological samples of forensic origin. *Toxicon,* 48: 183-194.

Byun SO, Fang Q, Zhou, H, Hickford, JG. (2009) An effective method for silver staining DNA in large numbers of polyacrylamide gels. *Analytical Biochemistry,* 385: 174-175.

Cannelli N, Nardocci N, Cassandrini D, Morbin M, Aiello C, Bugiani M, Criscuolo L, Zara F, Striano P, Granata T, Bertini E, Simonati A, Santorelli FM. (2007) Revelation of a novel CLN5 mutation in early juvenile neuronal ceroid lipofuscinosis. *Neuropediatrics,* 38: 46-49.

Cook RW, Jolly RD, Palmer DN, Tammen I, Broom MF, McKinnon R. (2002) Neuronal ceroid lipofuscinosis in Merino sheep. *Australian Veterinary Journal,* 80: 292-297.

Cooper JD, Russell C, Mitchison HM. (2006). Progress towards understanding disease mechanisms in small vertebrate models of neuronal ceroid lipofuscinosis. *Biochimica et Biophysica Acta*, 1762: 873–889.

Dahl M, Doyle A, Olsson K, Månsson J-E, Marques, AR, Mirzaian M, Aerts JM, Ehinger M, Rothe M, Modlich U, Schambach A, Karlsson S. (2015) Lentiviral gene therapy using cellular promoters cures type 1 Gaucher disease in mice. *Molecular Therapy*, 23: 835–844.

Daly TM. (2004) Overview of adeno-associated viral vectors. *Methods of Molecular Biology,* 246: 157-165.

Danthinne X, Imperiale MJ. (2000) Production of first generation adenovirus vectors: a review. *Gene Therapy*, 7: 1707-1714.

Das AK, Becerra CH, Yi W, Lu JT, Siakotos AN, Wisniewski KE, Hofmann SL. (1998) Molecular genetics of palmitoyl-protein thioesterase deficiency in the U.S. *Journal of Clinical Investigation*, 102: 361-370.

Dehay B, Ramirez A, Martinez-Vicente M, Perier C, Canron MH, Doudnikoff E, Vital A, Vila M, Klein C, Bezard E. (2012) Loss of P-type ATPase ATP13A2/PARK9 function induces general lysosomal deficiency and leads to Parkinson disease neurodegeneration. *Proceedings of the National Academy of Sciences of the USA,* 109: 9611-9616.

De Silva B, Adams J, Lee SY. (2015) Proteolytic processing of the neuronal ceroid lipofuscinosis related lysosomal protein CLN5. *Experimental Cell Research*, 338: 45-53.

Doccini S, Sartori S, Maeser S, Pezzini F, Rossato S, Moro F, Toldo I, Przybylski M, Santorelli FM, Simonati A. (2016) Early infantile neuronal ceroid lipofuscinosis (CLN10 disease) associated with a novel mutation in CTSD. *Journal of Neurology*, 263: 1029-1032.

Dong H, Nilsson L, Kurland CG. (1995) Gratuitous overexpression of genes in *Escherichia coli* leads to growth inhibition and ribosome destruction. *Journal of Bacteriology,* 177: 1497–1504.

Doronina V. (2012) How to amplify difficult PCR substrate? In PCR & real-time PCR, Blog Article, *Bitesize Bio*, https://bitesizebio.com/9331/tips-for-amplifying-difficult-pcr-substrates/.

Drickamer K, Taylor ME. (2006) *Introduction to Glycobiology*, (2nd Edition). Oxford University Press, USA.

Dumon-Seignovert L, Cariot G, Vuillard L. (2004) The toxicity of recombinant proteins in *Escherichia coli*: a comparison of overexpression in BL21 (DE3), C41 (DE3), and C43 (DE3). *Protein Expression and Purification,* 37: 203-206.

Eaton SL, Wishart TM. (2017) Bridging the gap: large animal models in neurodegenerative research. *Mammalian Genome*, 28: 324-337.

Fabritius A-L, Vera J, Minye HM, Nakano I, Kornblum H, Peltonen L. (2014) Neuronal ceroid lipofuscinosis genes, CLN2, CLN3 and CLN5 are spatially and temporally co-expressed in a developing mouse brain. *Experimental and Molecular Pathology,* 97: 484-491.

Falcón-Pérez JM, Nazarian R, Sabatti C, Dell'Angelica EC. (2005) Distribution and dynamics of Lamp1-containing endocytic organelles in fibroblasts deficient in BLOC-3. *Journal of Cell Science,* 118: 5243-5255.

Farhan SM, Murphy LM, Robinson JF, Wang J, Siu VM, Rupar CA, Prasad AN; FORGE Canada Consortium, Hegele RA. (2014) Linkage analysis and exome sequencing identify a novel mutation in KCTD7 in patients with progressive myoclonus epilepsy with ataxia. *Epilepsia*, 55: e106-111.

Faruq M, Narang A, Kumari R, Pandey R, Garg A, Behari M, Dash D, Srivastava AK, Mukerji M. (2014) Novel mutations in typical and atypical genetic loci through exome sequencing in autosomal recessive cerebellar ataxia families. *Clinical Genetics,* 86: 335-341.

Fisk R, Storts RW. (1988) Neuronal ceroid-lipofuscinosis in Nubian goats. *Veterinary Pathology*, 25: 171-173.

Fratantoni JC, Hall CW, Neufeld EF. (1968) Hurler and Hunter syndromes: mutual correction of the defect in cultured fibroblasts. *Science*, 162: 570-572.

Frugier T, Mitchell NL, Tammen I, Houweling PJ, Arthur DG, Kay GW, van Diggelen OP, Jolly RD, Palmer DN. (2008) A new large animal model of CLN5 neuronal ceroid lipofuscinosis in Borderdale sheep is caused by a nucleotide substitution at a consensus splice site (c.571 + 1G>A) leading to excision of exon 3*. Neurobiology of Disease* 29: 306-315.

Fuller M, Merikle P, Hopwood JJ. (Eds.) (2006) *Epidemiology of lysosomal storage disease: An overview.* Oxford, UK: Oxford PharmaGenes.

Futerman AH, van Meer G. (2004) The cell biology of lysosomal storage disorder. *Nature Reviews Molecular Cell Biology*, 5: 554-565.

Gaillet B, Gilbert R, Broussau S, Pilotte A, Malenfant F, Mullick A, Garnier A, Massie B. (2010) High-level recombinant protein production in CHO cells using lentiviral vectors and the cumate gene-switch. *Biotechnology Bioengineering,* 106: 203-215.

Gao H, Boustany RMN, Espinola JA, Cotman, SL, Srinidhi L, Antonellis K A, Gillis T, Qin X, Liu S, Donahue LR, Bronson RT, Faust JR, Stout D, Haines JL, Lerner TJ, MacDonald ME. (2002) Mutations in a novel CLN6-encode transmembrane protein cause variant neuronal ceroid lipofuscinosis in man and mouse. *American Journal of Human Genetics,* 70: 324-335.

Getty AL, Pearce DA. (2011) Interactions of the proteins of neuronal ceroid lipofuscinosis: clues to function. *Cell Molecular Life Science*, 68: 453-474.

Ghosh P, Dahms NM, Kornfeld S. (2003) Mannose 6-phosphate receptors: new twists in the tale. *Nature Review of Molecular Cell Biology*, 4: 202-212.

Gilliam D, Kolicheski A, Johnson GS, Mhlanga-Mutangadura T, Taylor JF, Schnabel RD, Katz ML. (2015) Golden Retriever dogs with neuronal ceroid lipofuscinosis have a two-base-pair deletion and frameshift in CLN5. *Molecular Genetics and Metabolism*, 115: 101–109.

Goebel HH, Schochet SS, Jaynes M, Brück W, Kohlschütter A, Hentati F. (1999) Progress in neuropathology of the neuronal ceroid lipofuscinoses. *Molecular Genetics and Metabolism,* 66: 367–372.

Graham FL, Smiley J, Russell WC, Naim R. (1977) Characteristics of a human cell line transformed by DNA from human adenovirus type 5. *Journal of General Virology,* 36: 59-74.

Haddad SE, Khoury M, Daoud M, Kantar R, Harati H, Mousallem T, Alzate O, Meyer B, Boustany RM. (2012) CLN5 and CLN8 protein association with ceramide synthase: biochemical and proteomic approaches. *Electrophoresis*, 33: 3798-3809.

Hafner S, Flynn TE, Harmon BG, Hill JE. (2005). Neuronal ceroid-lipofuscinosis in a Holstein steer. *Journal of Veterinary Diagnostic Investigation*, 17: 194–197.

Haltia M. (2003) The neuronal ceroid-lipofuscinoses. *Journal of Neuropathology and Experimental Neurology*, 62: 1–13.

Haltia M. (2006) The neuronal ceroid-lipofuscinosis: from past to present. *Biochimica et Biophysica Acta,* 1762: 850-856.

Haltia M, Goebel HH. (2013) The neuronal ceroid-lipofuscinoses: A historical introduction. *Biochimica et Biophysica Acta,* 1832: 1795-1800.

Harper PA, Walker KH, Healy PJ, Hartley WJ, Gibson AJ, Smith JS. (1988) Neurovisceral ceroid-lipofuscinosis in blind Devon cattle. *Acta Neuropathologica,* 75: 632-636.

Haskell RE, Hughes SM, Chiorini JA, Alisky JM, Davidson BL. (2003) Viral-mediated delivery of the late-infantile neuronal ceroid lipofuscinosis gene, TPP-I to the mouse central nervous system. *Gene Therapy,* 10: 34-42.

Hegde RS, Bernstein HD. (2006) The surprising complexity of signal sequences. *Trends in Biochemical Sciences,* 31: 563-571.

Heine C, Koch B, Storch S, Kohlschütter A, Palmer DN, Braulke T. (2004) Defective endoplasmic reticulum-resident membrane protein CLN6 affects lysosomal degradation of endocytosed arylsulfatase A. *The Journal of Biological Chemistry,* 279: 22347–22352.

Hersheson J, Burke D, Clayton R, Anderson G, Jacques TS, Mills P, Wood NW, Gissen P, Clayton P, Fearnley J, Mole SE, Houlden H. (2014) Cathepsin D deficiency causes juvenile-onset ataxia and distinctive muscle pathology. *Neurology*, 83: 1873-1875.

Hoffman J. (1956) Pigmentary retinal lipoid neuronal heredodegeneration (Spielmeyer-Vogt disease); the neuro-ophthalmologic considerations. *American Journal of Ophthalmology*, 42: 15-21.

Holmberg V, Jalanko A, Isosomppi J, Fabritius AL, Peltonen L, Kopra O. (2004). The mouse ortholog of the neuronal ceroid lipofuscinosis CLN5 gene encodes a soluble lysosomal glycoprotein expressed in the developing brain. *Neurobiology of Disease,* 16: 29-40.

Holopainen JM, Saarikoski J, Kinnunen PK, Järvelä II. (2001) Elevated lysosomal pH in neuronal ceroid lipofuscinoses (NCLs). *European Journal of Biochemistry*, 268: 5851-5856.

Houweling PJ, Cavanagh JA, Palmer DN, Frugier T, Mitchell NL, Windsor PA, Raadsma HW, Tammen I. (2006) Neuronal ceroid lipofuscinosis in Devon cattle is caused by a single base duplication (c.662dupG) in the bovine CLN5 gene. *Biochimica et Biophysica Acta,* 1762: 890-897.

Hughes SM, Hope KM, Xu JB, Mitchell NL, Palmer DN. (2014a) Inhibition of storage pathology in perinatal CLN5-deficient sheep neural cultures by lentiviral gene therapy. *Neurobiology and Disease,* 62: 543-550.

Hughes SM, Palmer DN, Schoderboeck L, Mitchell NL, Mclntyre K, Haskell RE, Anderson RD, Wicky HE, Xu JB. (2014b) New antibodies predict an interaction between CLN5 and CLN6. 14th International Conference on Neuronal Ceroid Lipofuscinoses (Batten disease). Hotel Sheraton, Cordoba, Argentina, 22 Oct 2014 - 26 Oct 2014, *Medicina, 74* (Supl II, O-49), 23.

Imperiali B, O'Connor SE. (1999) Effect of N-linked glycosylation on glycopeptide and glycoprotein structure. *Current Opinion in Chemical Biology*, 3: 643–9.

Isosomppi J, Jouni V, Jalanko A, Peltonen L. (2002) Lysosomal localisation of the neuronal ceroid lipofuscinosis CLN5 protein. *Human Molecular Genetics,* 11: 885-891.

Jakobsson J, Ericson C, Jansson M, Björk E, Lundberg C. (2003) Targeted transgene expression in rat brain using lentiviral vectors. *Journal of Neuroscience Research*, 73: 876–885.

Jarraya B, Boulet S, Ralph GS, Jan C, Bonvento G, Azzouz M, Miskin JE, Shin M, Delzescaux T, Drouot X, Herad AS, Day DM, Brouillet E, Kingsman SM, Hantraye P, Mitrophanous KA, Mazarakis ND, Palfi S. (2009) Dopamine gene therapy for Parkinson's disease in a nonhuman primate without associated dyskinesia. *Science Translational Medicine*, 1: 2ra4.

Järvelä I, Schleutker J, Haataja L, Santavuori P, Puhakka L, Manninen T, Palotie A, Sandkuijl LA, Renlund M, White R, Aula P, Peltonen L. (1991) Infantile form of neuronal ceroid lipofuscinosis (CLN1) maps to the short arm of chromosome 1. *Genomics,* 9: 170-173.

Jensen MA, Fukushima M, Davis RW. (2010) DMSO and betaine greatly improve amplification of GC-rich constructs in *de novo* synthesis. *PLoS One*, 5: e11024.
Jolly RD, Arthur DG, Kay GW, Palmer DN. (2002). Neuronal ceroid lipofuscinosis in Borderdale sheep. *New Zealand Veterinary Journal,* 50: 199-202.

Jolly RD, Janmatt A, West DM, Morrison I. (1980) Ovine ceroid-lipofuscinosis: a model of Batten's disease. *Neuropathology and Applied Neurobiology,* 6: 195-209.

Jolly RD, Palmer DN, Stubbert V, Sutton R, Kelly W, Koppang N, Dahme G, Hartley WJ, Patterson J, Riis R. (1994) Canine ceroid-lipofuscinoses: a review and classification. *Journal of Small Animal Practice,* 35: 299-306.

Jolly RD, Shimada A, Dopfmer I, Slack PM, Palmer DN. (1989) Ceroid-lipofuscinosis (Batten's disease): pathogenesis and sequential neuropathological changes in the ovine model. *Neuropathology and Applied Neurobiology*, 15: 371–383.

Jolly RD, West DM. (1976). Blindness in South Hampshire sheep: a neuronal ceroidlipofuscinosis. *New Zealand Veterinary Journal*, 24: 123.

Jules F, Sauvageau E, Dumaresq-Doiron K, Mazzaferri J, Haug-Kroper M, Fluhrer R, Costantino S, Lefrancois S. (2017) CLN5 is cleaved by members of the SPP/SPPL family to produce a mature soluble protein. *Experimental Cell Research*, 357: 40-50.

Jurišić V, Obradović J, Tošić N, Pavlović S, Kulić M, Djordjević N. (2016) Effects of DMSO, glycerol, betaine and their combinations in detecting single nucleotide polymorphisms of epidermal growth factor receptor (EGFR) gene promoter sequence in non-small-cell lung cancer (NSCLC) patients. *Journal of Pharmaceutical and Biomedical Analysis*, 128: 275-279.

Kandel ER. (2000) Nerve cells and behavior. In: *Principles of neural science,* (4th Edition). Kandel ER, Schwartz JH, Jessell TM. (Eds.), (pp. 19-35). McGraw-Hill, New York.

Kane JF. (1995) Effects of rare codon clusters on high-level expression of heterologous proteins in *Escherichia coli*. *Current Opinion in Biotechnology*, 6: 494-500.

Kolicheski A, Johnson GS, O'Brien DP, Mhlanga-Mutangadura T, Gilliam D, Guo J, Anderson-Sieg TD, Schnabel RD, Taylor JF, Lebowitz A, Swanson B, Hicks D, Niman ZE, Wininger FA, Carpentier MC, Katz ML. (2016) Australian cattle dogs with neuronal ceroid lipofuscinosis are homozygous for a CLN5 nonsense mutation previously identified in Border Collies. *Journal of Veterinary Internal Medicine*, 30: 1149-1158.

Kollmann K, Uusi-Rauva K, Scifo E, Tyynelä J, Jalanko A, Braulke T. (2013) Cell biology and function of neuronal ceroid lipofuscinosis-related proteins. *Biochimica et Biophysica Acta*, 1832: 1866–1881.

Koppang N. (1962) Lipodystrophia Cerebri in the English setters. *9th Nordic Veterinary Congress,* 4-7.

Koppang N. (1970) Neuronal ceroid-lipofuscinosis in English setters. *Journal of Small Animal Practice,* 10: 639-644.

Kopra O, Vesa J, von Schantz C, Manninen T, Minye H, Fabritius AL, Rapola J, van Diggelen OP, Saarela J, Jalanko A, Peltonen L. (2004) A mouse model for Finnish variant late infantile neuronal ceroid lipofuscinosis, CLN5, reveals neuropathology associated with early aging. *Human Molecular Genetics*, 13: 2893-2906.

Kordower JH, Bloch J, Ma SY, Chu Y, Palfi S, Roitberg BZ, Emborg M, Hantraye P, Déglon N, Aebischer P. (1999) Lentiviral gene transfer to the nonhuman primate brain. *Experimental Neurology,* 160: 1-16.

Kousi M, Lehesjoki A-E, Mole SE. (2012) Update of the mutation spectrum and clinical correlations of over 360 mutations in eight genes that underlie the neuronal ceroid lipofuscinoses. *Human Mutation,* 33: 42-63.

Kurze AK, Galliciotti G, Heine C, Mole SE, Quitsch A, Braulke T. (2010) Pathogenic mutations cause rapid degradation of lysosomal storage disease-related membrane protein CLN6. *Human Mutation,* 31: E1163-1174.

Larkin H, Ribeiro MG, Lavoie C. (2013) Topology and membrane anchoring of the lysosomal storage disease-related protein CLN5. *Human Mutation*, 34: 1688-1697.

Lattanzi A, Neri M, Maderna C, di Girolamo I, Martino S, Orlacchio A, Amendola M, Naldini L, Gritti A. (2010) Widespread enzymatic correction of CNS tissues by a single intracerebral injection of therapeutic lentiviral vector in leukodystrophy mouse models. *Human Molecular Genetics*, 19: 2208-2227.

Lebrun AH, Storch S, Rüschendorf F, Schmiedt ML, Kyttälä A, Mole SE, Kitzmüller C, Saar K, Mewasingh LD, Boda V, Kohlschütter A, Ullrich K, Braulke T, Schulz A. (2009) Retention of lysosomal protein CLN5 in the endoplasmic reticulum causes neuronal ceroid lipofuscinosis in Asian sibship. *Human Mutation*, 30: E651-661.

Leonard CK, Spellman MW, Riddle L, Harris RJ, Thomas JN, Gregory TJ. (1990) Assignment of intrachain disulfide bonds and characterization of potential glycosylation sites of the type 1 recombinant human immunodeficiency virus envelope glycoprotein (gp120) expressed in Chinese hamster ovary cells. *The Journal of Biological Chemistry,* 265: 10373-10382.

Lerner TJ, Boustany RM, Anderson JW, D'Arigo KL, Schlumpf K, Buckler AJ, Gusella JF, Haines JL. (1995) Isolation of a novel gene underlying Batten disease, CLN3. The International Batten Disease Consortium. *Cell*, 82: 949-957.

Linterman KS, Palmer DN, Kay GW, Barry LA, Mitchell NL, McFarlane RG, Black MA, Sand MC and Hughes SM. (2011) Lentiviral-mediated gene transfer to the sheep brain: implications for gene therapy in Batten disease. *Human Gene Therapy,* 22: 1011-1020.

Liu J, Lu W, Reigada D, Nguyen J, Laties AM, Mitchell CH. (2008) Restoration of lysosomal pH in RPE cells from cultured human and ABCA4$^{-/-}$ mice: pharmacologic approaches and functional Recovery. *Investigative Ophthalmology & Visual Science,* 49: 772-780.

Lodish H, Berk A, Zipursky L. Matsudaira P, Baltimore D, Darnell J. (2000) Section 17. Protein glycosylation in the ER and Golgi complex. *Molecular Cell Biology*, (4th Edition). New York, Freeman WH.

Lonka L, Kyttälä A, Ranta S, Jalanko A, Lehesjoki AE. (2000) The neuronal ceroid lipofuscinosis CLN8 membrane protein is a resident of the endoplasmic reticulum. *Human Molecular Genetics,* 9: 1691-1697.

Luzio JP, Pryor PR, Bright NA. (2007) Lysosomes: fusion and function. *Nature Reviews Molecular Cell Biology*, 8: 622-632.

Lyly, A, von Schantz C, Heine C, Schmiedt M-L, Sipilä T, Jalanko A, Kyttälä A. (2009) Novel interactions of CLN5 support molecular networking between Neuronal Ceroid Lipofuscinosis proteins. *BMC Cell Biology*, 10: 83.

Mamo A, Jules F, Dumaresq-Doiron K, Costantino S, Lefrancois S. (2012) The role of ceroid lipofuscinosis neuronal protein 5 (CLN5) in endosomal sorting. *Molecular and Cellular Biology*, 32: 1855-1866.

Mancini C, Nassani S, Guo Y, Chen Y, Giorgio E, Brussino A, Di Gregorio E, Cavalieri S, Lo Buono N, Funaro A. (2015) Adult-onset autosomal recessive ataxia associated with neuronal ceroid lipofuscinosis type 5 gene (CLN5) mutations. *Journal of Neurology*, 262: 173-178.

Mao Q, Foster BJ, Xia H, Davidson BL. (2003) Membrane topology of CLN3, the protein underlying Batten disease. *FEBS Letters*, 541: 40-46.

Margraf LR, Boriack RL, Routheut AAJ, Cuppen I, Alhilali L, Bennet CJ, Bennet MJ. (1999) Tissue expressio and subcellular localisation of CLN3, the Batten disease protein. *Molecular Genetics and Metabolism*, 66: 283-289.

Marshansky V, Futai M. (2008) The V-type H+-ATP in vesicular trafficking: targeting, regulation and function. *Current Opinion in Cell Biology*, 20: 415-426.

McIntyre K. (2014) *Understanding Batten disease: CLN5 expression in CLN6 deficient ovine neural cultures*. (Bachelor of Biomedical Sciences with Honours Thesis). University of Otago. Retrieved from http://hdl.handle.net/10523/5235.

Melville SA, Wilson CL, Chiang CS, Studdert VP, Lingaas F, Wilton, AN. (2005) A mutation in canine CLN5 causes neuronal ceroid lipofuscinosis in Border collie dogs. *Genomics,* 86: 287-294.

Meyerrose TE, Roberts M, Ohlemiller KK, Vogler CA, Wirthlin L, Nolta JA, Sands MS. (2008) Lentiviral-transduced human mesenchymal stem cells persistently express therapeutic levels of enzyme in a xenotransplantation model of human disease. *Stem Cell,* 26: 1713-1722.

Minye HM, Fabritius AL, Vesa J, Peltonene. (2016) Data on characterizing the gene expression patterns of neuronal ceroid lipofuscinosis genes: CLN1, CLN2, CLN3, CLN5 and their association to interneuron and neurotransmission markers: Parvalbumin and Somatostatin. *Data in Brief*, 8: 741-749.

Mitchell NL. (2016) *Longitudinal studies and the development of gene therapy for ovine neuronal ceroid lipofuscinoses*. PhD thesis, Lincoln University, Lincoln, New Zealand.

Mitchison HM, Taschner PE, O'Rawe AM, de Vos N, Phillips HA, Thompson AD, Kozman HM, Haines JL, Schlumpf K, D'Arigo K. (1994) Genetic mapping of the Batten disease locus (CLN3) to the interval D16S288-D16S383 by analysis of haplotypes and allelic association. *Genomics,* 15: 465-468.

Miroux B, Walker JE. (1996) Over-production of proteins in *Escherichia coli*: mutant hosts that allow synthesis of some membrane proteins and globular proteins at high levels. *Journal of Molecular Biology,* 260: 289-298.

Moharir A, Peck SH, Budden T, Lee SY. (2013) The role of N-Glycosylation in folding, trafficking, and functionality of lysosomal protein CLN5. *PLOS ONE,* 8: e74299.

Mohd Ismail IF. (2014) *Identification of a novel mutation in the CLN6 gene causing neuronal ceroid lipofuscinosis in South Hampshire sheep*. PhD thesis, University of Sydney, Sydney, Australia.

Mole SE, Mitchison HM, Munroe PB. (1999) Molecular basis of the neuronal ceroid lipofuscinosis: mutations in CLN1, CLN2, CLN3, and CLN5. *Human Mutation*, 14: 199-215.

Mole SE, Michaux G, Codlin S, Wheeler RB, Sharp JD, Cutler DF. (2004) CLN6, which is associated with a lysosomal storage disease, is an endoplasmic reticulum protein. *Experimental Cell Research,* 298: 399-406.

Mole SE, Williams RE, Goebel HH. (2005) Correlations between genotype, ultrastructural morphology and clinical phenotype in the neuronal ceroid lipofuscinosis. *Neurogenesis,* 6: 107-126.

Mole SE, Williams RE, Goebel HH. (2011) *The neuronal ceroid lipofuscinosis (Batten disease).* (2nd Edition). Oxford, UK: Oxford University Press.

Molgaard S, Ulrichsen M, Boggild S, Holm ML, Vaegter C, Nyengarrd J, Glerup S. (2015) Immunofluorescent visualization of mouse interneuron subtypes. *F1000 Research,* 3: 242.

Munroe PB, Mitchison HM, O'Rawe AM, Anderson JW, Boustany RM, Lerner TJ, Taschner PE, de Vos N, Breuning MH, Gardiner RM, Mole SE. (1997) Spectrum of mutations in the Batten disease gene, CLN3. *American Journal of Human Genetics*, 61: 310-316.

Nelson T, Pearce DA, Kovacs AD. (2017) Lack of specificity of antibodies raised against CLN3, the lysosomal/endosomal transmembrane protein mutated in juvenile Batten disease. *Bioscience Report*, 37: 1-12.

Nibe K, Miwa Y, Matsunage S, Chambers Jk, Uetsuka K, Nakayama H, Uchida K. (2011). Clinical and pathologic features of neuronal ceroid-lipofuscinosis in a ferret (*Mustela putorius furo*). *Veterinary Pathology*, 48: 1185–1189.

Noskova L, Stranecky V, Hartmannova H, Pistoupilova, A, Baresova V, Ivanek R, Hulkova H, Jahnova H, van der Zee J, Staropoli JF, Sims KB, Tyynelä J, van Broeckhoven C, Nijssen PC, Mole SE, Elleder M, Kmoch S. (2011) Mutations in DNAJC5, encoding cysteine-string protein alpha, cause autosomal-dominant adult-onset neuronal ceroid lipofuscinosis. *The American Journal of Human Genetics,* 89:241-252.

Oswald MJ, Palmer DN, Kay GW, Shemilt SJA, Jonathan PR, Cooper JD. (2005) Glial activation spreads from specific cerebral foci and precedes neurodegeneration in presymptomatic ovine neuronal ceroid lipofuscinosis (CLN6). *Neurobiology of Disease*, 20: 49-63.

Palfi S, Gurruchaga, JM, Ralph GS, Lepetit H, Lavisse S, Buttery PC, Watts C, Miskin J, Kelleher M, Deeley S, Iwamuro H, Lefaucheur JP, Thiriez C, Fenelon G, Lucas C, Brugières P, Gabriel I, Abhay K, Drouot X, Tani N, Kas A, Ghaleh B, Le Corvoisier P, Dolphin P, Breen DP, Mason S, Guzman NV, Mazarakis ND, Radcliff PA, Harrop R, Kingsman SM, Rascol O, Naylor S, Barker RA, Hantraye P, Remy P, Cesaro P, Mitrophanous KA. (2014) Long-term safety and

tolerability of ProSavin, a lentiviral vector-based gene therapy for Parkinson's disease: a dose escalation, open-label, phase 1/2 trial. *Lancet*, 383: 1138–1146.

Palmer DN. (2015) The relevance of the storage of subunit c of ATP synthase in different forms and models of Batten disease (NCLs). *Biochimica et Biophysica Acta*, 1852 (10 Pt B): 2287-2291.

Palmer DN, Barry LA, Tyynelä J, Copper JD. (2013) NCL disease mechanisms. *Biochimica et Biophysica Acta*, 1832: 1882-1893.

Palmer DN, Chen J, Mitchell NL. (2017, September) *Cross-regulation of CLN5 and CLN6 gene expression in ovine Batten disease models*. Paper presented at the meeting of the 21st ESGLD workshop, Ecully (Lyon), France.

Palmer DN, Fearnley IM, Walker JE, Hall NA, Lake BD, Wolfe LS, Haltia M, Martinus RD, Jolly RD. (1992) Mitochondrial ATP synthase subunit c storage in the ceroid-lipofuscinoses (Batten disease). *American Journal of Medical Genetics*, 42: 561–567.

Palmer DN, Jolly RD, van Mil HC, Tyynel, J, Westlake VJ. (1997) Different patterns of hydrophobic protein storage in different forms of neuronal ceroid lipofuscinosis (NCL, Batten Disease). *Neuropediatrics,* 28: 45-48.

Palmer DN, Martinus RD, Cooper SM, Midwinter GG, Reid JC, Jolly RD. (1989) The major lipopigment protein and the lipid-binding subunit of mitochondrial ATP synthase have the same NH2-terminal sequence. *The Journal of Biological Chemistry,* 264: 5736-5740.

Palmer DN, Neverman NJ, Chen JZ, Chang C-T, Houweling PJ, Barry, LA, Tammen I, Hughes SM, Mitchell NL. (2015) Recent studies of ovine neuronal ceroid lipofuscinoses from BARN, the Batten Animal Research Network. *Biochimica et Biophysica Acta*, *1852*(10 Pt B): 2279-2286.

Palmer DN, Tammen I, Katz ML, Johnson GS, Drögemüller C. (2011). Large Animal Models. In: *The Neuronal Ceroid Lipofuscinoses (Batten disease)* (2nd Edition). Mole SE, Williams RE, Goebel HH. (Eds.) (pp: 284–320). Oxford, UK: Oxford University Press.

Palomares LA, Estrada-Mondaca S, Ramirez OT. (2004) Production of recombinant proteins: challenges and solutions. *Methods in Molecular Biology,* 267: 15-52.

Persaud-Sawin DA, Mousallem T, Wang C, Zucker A, Kominami E, Boustany RM. (2007) Neuronal ceroid lipofuscinosis: a common pathway? *Paediatric Research*, 61: 146-152.

Pinnapureddy AR, Stayner C, McEwan J, Baddeley O, Forman J, Eccles MR. (2015) Large animal models of rare genetic disorders: sheep as phenotypically relevant models of human genetic disease. *Orphanet Journal of Rare Diseases*, 10: 107.

Platt FM, Boland B, van der Spoel AC. (2012) Lysosomal storage disorders: The cellular impact of lysosomal dysfunction. *Journal of Cell Biology,* 199: 723-734.

Ranta S, Zhang Y, Ross B, Lonka L, Takkunen E, Messer A, Sharp J, Wheeler R, Kusumi K, Mole S, Liu W, Soares MB, Bonaldo MF, Hirvasniemi A, de la Chapelle A, Gilliam TC, Lehesjoki AE. (1999) The neuronal ceroid lipofuscinoses in human EPMR and mnd mutant mice are associated with mutations in *CLN8*. *Nature Genetics,* 23: 233-236.

Rein DT, Breidenbach M, Curiel DT. (2006) Current developments in adenovirus-based cancer gene therapy. *Future Oncology,* 2: 137-143.

Rider JA, Rider DL. (1988) Batten disease: past, present and future. *American Journal of Medical Genetics Supplement,* 5: 21-26.

Saftig P, Klumperman J. (2009) Lysosome biogenesis and lysosomal membrane proteins: trafficking meets function. *Nature Reviews Molecular Cell Biology,* 10: 623-635.

Savukoski M, Klockars T, Holmberg V, Santavuori P, Lander ES, Peltonen L. (1998) *CLN5*, a novel gene encoding a putative transmembrane protein mutated in Finnish variant late infantile neuronal ceroid lipofuscinosis. *Nature Genetics,* 19: 286-288.

Schmiedt ML, Bessa C, Heine C, Ribeiro MG, Jalanko A, Kyttala A. (2010) The neuronal ceroid lipofuscinoses protien CLN5: new sights into cellular maturation, transpoprt, and consequences of mutations. *Human Mutation*, 31: 356-365.

Shacka JJ. (2012). Mouse models of neuronal ceroid lipofuscinoses: useful pre-clinical tools to delineate disease pathophysiology and validate therapeutics. *Brain Research Bulletin*, 88: 43–57.

Sharp JD, Wheeler RB, Lake BD, Savukoski M, Järvelä IE, Peltonen L, Gardiner RM, Williams RE. (1997) Loci for classical and a variant late infantile neuronal ceroid lipofuscinosis map to chromosomes 11p15 and 15q21-23. *Human Molecular Genetics,* 6: 591-595.

Shental-Bechor D, Levy Y. (2009) Folding of glycoproteins: toward understanding the biophysics of the glycosylation code. *Current Opinion in Structural Biology*, 19: 524–533.

Siintola E, Lehesjoki AE, Mole SE. (2006) Molecular genetics of the NCLs – status and perspectives. *Biochimica et Biophysica Acta,* 1762: 857-864.

Siintola E, Partanen S, Strömme P, Haapanen A, Haltia M, Maehlen J, Lehesjoki AE, Tyynelä J. (2006b) Cathepsin D deficiency underlies congenital human neuronal ceroid-lipofuscinosis. *Brain,* 129: 1438-1445.

Siintola E, Topcu M, Aula N, Lohi H, Minassian BA, Paterson AD, Liu XQ, Wilson C, Lahtinen U, Anttonen AK, Lehesjoki AE. (2007) The novel neuronal ceroid lipofuscinosis gene *NFSD8* encodes a putative lysosomal transporter. *The American Journal of Human Genetics,* 81: 136-146.

Sinclair AM, Elliott S. (2005) Glycoengineering: the effect of glycosylation on the properties of therapeutic proteins. *Journal of Pharmaceutical Sciences,* 94: 1626–1635.

Sleat DE, Della Valle MC, Zheng H, Moore DF, Lobel P. (2008a) The mannose 6-phosphate glycoprotein proteome. *Journal of Proteome Research*, 7: 3010-3021.

Sleat DE, Donnelly RJ, Lackland H, Liu CG, Sohar I, Pullarkat PK, Lobel P. (1997) Association of mutations in a lysosomal protein with classical late-infantile neuronal ceroid lipofuscinosis. *Science,* 277: 1802-1805.

Sleat DE, El-Banna M, Solar I, Kim KH, Dobrenis K, Walker SU, Lobel P. (2008b) Residual levels of tripeptidyl-peptidase I activity dramatically ameliorate disease in late-infantile neuronal ceroid lipofuscinosis. *Molecular Genetics Metabolism,* 94: 222-233.

Sleat DE, Lackland H, Wang Y, Sohar I, Xia, G, Li H, Lobel P. (2005) The human brain mannose 6-phosphate glycoproteome: A complex mixture composed of multiple isoforms of many soluble lysosomal proteins. *Proteomics,* 5: 1520-1532.

Sleat DE, Sohar I, Lackland H, Majercak J, Lobel P. (1996) Rat brain contains high levels of mannose-6-phosphorylated glycoproteins including lysosomal enzymes and palmitoyl-protein thioesterase, an enzyme implicated in infantile neuronal lipofuscinosis. *Journal of Biological Chemistry*, 271: 19191-19198.

Sleat DE, Sun P, Wiseman JA, Huang L, Ei-Banna M, Zheng H, Moore DF, Lobel P. (2013) Extending the mannose 6-phosphate glycoproteome by high resolution/accuracy mass spectrometry analysis of control and acid phosphatase 5-deficient mice. *Molecular & Cellular Proteomics*, 12: 1806-1817.

Sleat DE, Wang Y, Sohar I, Lackland H, Li Y, Li H, Zheng H, Lobel P. (2006a) Identification and validation of mannose 6-phosphate glycoproteins in human plasma reveal a wide range of lysosomal and non-lysosomal proteins. *Molecular and Cellular Proteomics,* 5: 1942-1956.

Sleat DE, Zheng H, Qian M, Lobel P. (2006b) Identification of sites of mannose 6-phosphorylation on lysosomal proteins. *Molecular & Cellular Proteomics*, 5: 686-701.

Sleat DE, Zheng H, Lobel P. (2007) The human urine mannose 6-phosphate glycoproteome. *Biochimica et Biophysica Acta,* 1774: 368-372.

Smith KR, Dahl HH, Canafoglia L, Andermann E, Damiano J, Morbin M, Bruni AC, Giaccone G, Cossette P, Saftig P, Grötzinger J, Schwake M, Andermann F, Staropoli JF, Sims KB, Mole SE, Franceschetti S, Alexander NA, Cooper JD, Chapman HA, Carpenter S, Berkovic SF, Bahlo M. (2013) Cathepsin F mutations cause Type B Kufs disease, an adult-onset neuronal ceroid lipofuscinosis*. Human Molecular Genetics,* 22: 1417-1423.

Smith KR, Damiano J, Franceschetti S, Carpenter S, Canafoglia L, Morbin M, Rossi G, Pareyson D, Mole SE, Staropoli JF, Sims KB, Lewis J, Lin WL, Dickson DW, Dahl HH, Bahlo M, Berkovic SF. (2012) Strikingly different clinicopathological phenotypes determined by progranulin-mutation dosage. *The American Journal of Human Genetics,* 90: 1102-1107.

Stahl SM. (2008) *Stahl's Essential Psychopharmacology: Neuroscientific Basis and Practical Applications*. Cambridge University Press.

Stengel C. (1982) Account of a singular illness among four siblings in the vicinity of Roraas. In: *Ceroid-lipofuscinosis (Batten's Disease),* Armstrong D, Koppang N, & Rider JA (Eds). Elsevier Biomedical Press, Oxford.

Strien J, Sanft J, Mall G. (2013) Enhancement of PCR amplification of moderate GC-containing and highly GC-rich DNA sequences. *Molecular Biotechnology*, 54: 1048-1054.

Tammen I, Cook RW, Nicholas FW, Raadsma HW. (2001) Neuronal ceroid lipofuscinosis in Australian Merino sheep: a new animal model. *European Journal of Paediatric Neurology,* 5: 37-41.

Tammen I, Houweling PJ, Frugier T, Mitchell NL, Kay GW, Cavanagh JAL, Cook RW, Raadsma HW, Palmer DN. (2006). A missense mutation (c.184C > T) in ovine *CLN6* causes neuronal ceroid lipofuscinosis in Merino sheep whereas affected South Hampshire sheep have reduced levels of *CLN6* mRNA. *Biochimica et Biophysica Acta,* 1762: 898-905.

Tang Y, Garson K, Li L, Vanderhyden BC. (2014) Optimisation of lentiviral vector production using polyethylenimine-mediated transfection. *Oncology Letters,* 9: 55-62.

Tecedor L, Stein CS, Schultz ML, Farwanah H, Sandhoff K, Davidson BL. (2013) CLN3 loss disturbs membrane microdomain properties and protein transport in brain endothelia cells. *The Journal of Neuroscience,* 33: 18065-18079.

Tepper JM, Tecuapetla F, Koós T, Ibáñez-Sandoval O. (2010) Heterogeneity and diversity of striatal GABAergic interneurons. *Frontiers in Neuroanatomy,* 4: 150.

Thomas P, Smart TG. (2005) HEK293 cell line: a vehicle for the expression of recombinant proteins. *Journal of Pharmacological and Toxicological Methods,* 51: 187-200.

Trono D. (2000) Lentiviral vectors: turning a deadly foe into a therapeutic agent. *Gene Therapy,* 7: 20-23.

Tyynelä J, Palmer DN, Baumann M, Haltia M. (1993) Storage of saposins A and D in infantile neuronal ceroid-lipofuscinosis. *FEBS Letters,* 330: 8-12.

Tyynelä J, Sohar I, Sleat DE, Gin RM, Donnelly RJ, Baumann M, Haltia M, Lobel P. (2000) A mutation in the ovine cathepsin D gene causes a congenital lysosomal storage disease with profound neurodegeneration. *The EMBO Journal,* 19: 2786-2792.

Tyynelä J, Suopanki J, Santavuori P, Baumann M, Haltia M. (1997) Variant late infantile neuronal ceroid-lipofuscinosis: pathology and biochemistry. *Journal of Neuropathology and Experimental Neurology*, 56: 369–375.

Url A, Bauder B, Thalhammer J, Nowotny N, Kolodziejek J, Herout N, Furst S, Weissenbock H. (2001) Equine neuronal ceroid-lipofuscinosis. *Acta Neuropathologica,* 101: 410-414.

Van Bogaert P, Azizieh R, Désir J, Aeby A, De Meirleir L, Laes JF, Christiaens F, Abramowicz MJ. (2007) Mutation of a potassium channel-related gene in progressive myoclonic epilepsy. *Annals of Neurology*, 61: 579–586.

Van Diggelen OP, Thobois S, Tilikete C, Zabot MT, Keulemans JL, van Bunderen PA, Taschner PE, Losekoot M, Voznyi YV. (2001) Adult neuronal ceroid lipofuscinosis with palmitoyl-protein thioesterase deficiency: first adult-onset patients of a childhood disease. *Annals of Neurology,* 50: 269-272.

Vellodi A. (2005) Lysosomal storage disorders. *British Journal of Haematology*, 128: 413-431.

Vesa J, Chin MH, Oelgeschlager K, Isosomppi J, Dell Angelica EC, Jalanko, A, Peltonen L. (2002) Neuronal ceroid lipofuscinoses are connected at molecular level: interaction of CLN5 protein with CLN2 and CLN3. *Molecular Biology of the Cell,* 13: 2410-2420.

Vesa J, Hellsten E, Verkruyse LA, Rapola CJ, Santavuori P, Hofmann SL, Peltonen L. (1995) Mutations in the palmitoyl protein thioesterase gene causing infantile neuronal ceroid lipofuscinosis. *Nature,* 376: 584-587.

Vodicka MA. (2001) Determinants for lentiviral infection of non-dividing cells. *Somatic Cell and Molecular Genetics,* 26: 35-49.

Von Schantz C. (2009) *Animal model and molecular interactions of CLN5*. Academic Dissertation, University of Helsinki, Finland.

Von Schantz C, Kielar C, Hansen SN, Pontikis CC, Alexander NA, Kopra O, Jalanko A, Copper JD. (2009) Progressive thalamocortical neuron loss in Cln5 deficient mice: Distinct effects in Finnish variant late infantile NCL. *Neurobiology of Disease*, 34: 308–319.

Von Schantz C, Saharinen, J, Kopra O, Copper JD, Gentile M, Hovatta I, Peltonen L, Jalanko A. (2008) Brain gene expression profiles of *Cln1* and *Cln5* deficient mice unravels common molecular pathways underlying neuronal degeneration in NCL diseases. *BMC Genomics*, 9: 146.

Wang Y, Gupta A, Toledo-Rodriguez M, Wu CZ, Markram H. (2002) Anatomical, physiological, molecular and circuit properties of nest basket cells in the developing somatosensory cortex. *Cerebral Cortex*, 12: 395-410.

Warrier V, Vieira M, Mole SE. (2013) Genetic basis and phenotypic correlations so the neuronal ceroid lipofusinoses. *Biochimica et Biophysica Acta*, 1832: 1827-1830.

Way M, Pope B, Gooch J, Hawkins M, Weeds AG. (1990) Identification of a region in segment 1 of gelsolin critical for actin binding. *The EMBO Journal,* 9: 4103-4109.

Wheeler RB, Sharp JD, Mitchell WA, Bate SL, Williams RE, Lake BD, Gardiner RM. (1999) A new locus for variant late infantile neuronal ceroid lipofuscinosis-CLN7. *Molecular Genetics and Metabolism,* 66: 337-338.

Wheeler RB, Sharp JD, Schultz RA, Joslin JM, Williams RE, Mole SE. (2002) The gene mutated in variant late-infantile neuronal ceroid lipofuscinosis (CLN6) and in nclf mutant mice encodes a novel predicted transmembrane protein. *American Journal of Human Genetics,* 70: 537.542.

Whitney ER, Kemper TL, Rosene DL, Bauman ML, Blatt GJ. (2008) Calbindin-D28k is a more reliable marker of human Purkinje cells than standard Nissl stains: a stereological experiment. *Journal of Neuroscience Methods*, 168: 42-47.

Wurm FM. (2004) Production of recombinant protein therapeutics in cultivated mammalian cells. *Nature Biotechnology*, 22: 1393-1398.

Xin W, Mullen TE, Kiely R, Min J, Feng X, Cao Y, O'Malley L, Shen Y, Chu-Shore C, Mole SE, Goebel HH, Sims K. (2010) CLN5 mutations are frequent in juvenile and late-onset non-Finnish patients with NCL. *Neurology,* 74: 565-571.

Zeman W, Dyken P. (1969) Neuronal ceroid-lipofuscinoses (Batten's disease). Relationship to amaurotic family idiocy? *Pediatrics,* 44: 570-583.

Zhao C, Eisinger B, Gammie SC. (2013) Characterization of GABAergic neurons in the mouse lateral septum: a double fluorescence in situ hybridization and immunohistochemical study using tyramide signal amplification. *PLoS One,* 8: e73750.

Zhou H, Hickford JGH, Fang Q. (2006) A two-step procedure for extracting genomic DNA from dried blood spots on filter paper for polymerase chain reaction amplification. *Analytical Biochemistry,* 354: 159-161.

Zufferey R, Dull T, Mandel RJ, Bukovsky A, Quiroz D, Naldnini L, Trono D. (1998) Self-inactivating lentivirus vector for safe and efficient *in vivo* gene delivery. *Journal of Virology*, 72: 9873-9880.